Catalytic aerobic oxidation of bio-renewable chemicals

Gorbanev, Yury; Woodley, John; Riisager, Anders

Publication date:
2012

Document Version
Publisher's PDF, also known as Version of record

Catalytic aerobic oxidation of bio-renewable chemicals

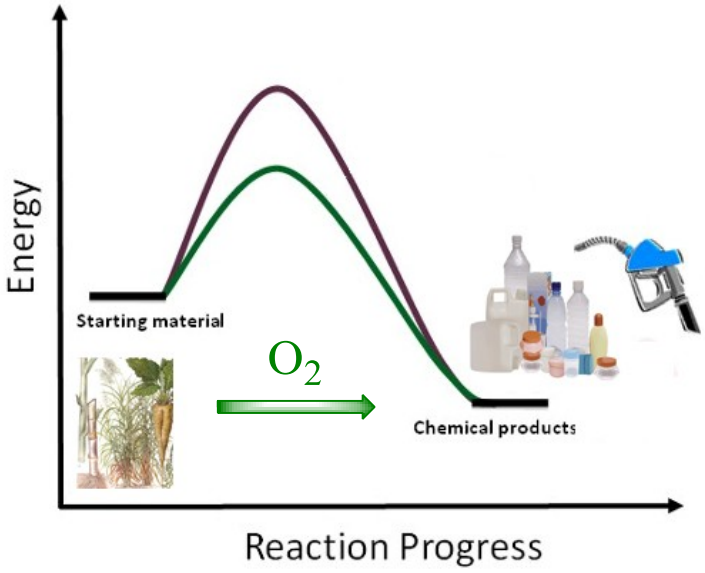

Yury Y. Gorbanev

Ph.D. thesis

September 2011

Centre for Catalysis and Sustainable Chemistry (CSC)

Department of Chemistry

Technical University of Denmark (DTU)

Centre for Catalysis and Sustainable Chemistry

Technical University of Denmark

Danmarks Tekniske Universitet

Abstract

This thesis covers the investigation of new catalytic systems for the aerobic oxidation of chemicals derived from bio-renewable sources. The effects of different factors and conditions on the reactions were examined. The employed catalysts were characterized by physisorption measurements, SEM, TEM, EDS, XRF and other methods.

Supported gold and ruthenium hydroxide catalyst systems were explored for the aerobic oxidation of 5-hydroxymethylfurfural (HMF) to 2,5-furandicarboxylic acid (FDA), a potential polymer building block for the plastic industry, or its dimethyl ester (FDMC). High product selectivities and yields were obtained under optimized conditions.

Heterogeneous catalysts consisting of Au nanoparticles on different supports were shown to efficiently oxidize HMF to FDA or FDMC in water or methanol, respectively. Additionally, the reaction conditions were shown to be adjustable for the exclusive production of intermediate products of the oxidation. Catalysts consisting of $Ru(OH)_x$ deposited on metal oxide supports, such as, for instance, CeO_2 and $MgAl_2O_4$, were employed in the aerobic oxidation of HMF in different ”green” reaction media, *e.g.* water and various ionic liquids, under base-free conditions. Moreover, a detailed study on the performance and stability of the ruthenium hydroxide catalysts on magnesium-containing supports under reaction conditions was conducted.

The aerobic oxidation of HMF to form another value-added chemical, 2,5-diformylfuran (DFF), was also investigated with supported $Ru(OH)_x$ catalysts in organic solvents. The examined catalyst systems and reaction conditions were also shown to be applicable for the efficient oxidation of other substituted furans. Furthermore, novel catalytic systems comprising vanadia supported on zeolites were investigated for the aerobic oxidation of HMF to DFF in organic solvents, and a lixiviation study was performed.

The oxidation of aliphatic alcohols over supported $Ru(OH)_x$ and RuO_x catalysts is also described. The highly selective and efficient oxidation of ethanol to acetic acid was shown with supported $Ru(OH)_x$ and highly dispersed RuO_x deposited on various metal oxides. Furthermore, this thesis presents the results of the catalytic aerobic oxidative degradation of higher alcohols over supported ruthenium hydroxide catalysts. A very efficient oxidative cleavage of *vic*-diols to form respective acids was also shown under examined conditions.

Thus, the oxidative transformations of biomass-derived chemicals over different gold and ruthenium-based catalyst systems with oxygen as the abundant oxidant were explored.

Dansk resumé

Denne afhandling undersøger nye katalytiske systemer til aerob oxidation af kemikalier udvundet fra biomasse. Forskellige faktorer og forsøgsbetingelsers indflydelse på reaktionen er blevet undersøgt. Katalysatorerne er blevet karakteriseret ved physisorptionsmålinger, SEM, TEM, EDS, XRF og andre metoder.

Supporteret guld og rutheniumhydroxid er blevet undersøgt som katalysatorer for aerob oxidation af 5-(hydroxymethyl)furfural (HMF) til 2,5-furandicarboxylsyre (FDA), som er en potentiel byggesten til fremstilling af plastik, og dens dimethylester (FDMC). Under optimerede betingelser blev der opnået høje selektiviteter og udbytter.

Heterogene katalysatorer bestående af Au-nanopartikler på forskellige bærematerialer var effektive til oxidation af HMF til FDA eller FDMC i henholdsvis vand og methanol. Reaktionsbetingelserne blev optimeret så en selektiv oxidation af HMF til intermediaterne 2,5-diformylfuran (DFF) og 2-hydroxymethyl-5-carboxylsyre kunne opnås ved anvendelse af forskellige opløsningsmidler. Katalysatorer bestående af $Ru(OH)_x$ på metaloxider såsom CeO_2 og $MgAl_2O_4$ blev ligeledes anvendt i aerob oxidation af HMF i "grønne" reaktionsmedier som vand og ioniske væsker uden tilsat base. Aktivitet og stabilitet af $Ru(OH)_x$-katalysatorer båret på magnesiumforbindelser blev undersøgt ved forskellige reaktionsbetingelser.

Oxidation af HMF til 2,5-diformylfuran (DFF) blev også undersøgt med supportet $Ru(OH)_x$ katalysatorer i organiske opløsningsmidler. De undersøgte katalysatorer kunne ydermere anvendes til oxidation af andre substituerede furaner under identiske betingelser. Endvidere blev zeolitbårne vanadiakatalysatorer undersøgt til aerob oxidation af HMF til DFF i organiske solventer og et udvaskningsstudium blev udført.

Oxidationen af alifatiske alkoholer over supporterede $Ru(OH)_x$ og RuO_x-katalysatorer er ligeledes undersøgt. Ethanol kunne selektivt oxideres til eddikesyre over $Ru(OH)_x$ og RuO_x katalysatorer båret på forskellige metaloxider. Anvendelse af højere alkoholer resulterede i produkter med kortere kulstofkædelængder pga. C-C-kløvning. *Vic*-dioler blev meget effektivt oxidativt kløvet til de respektive syrer.

Således er den oxidative omdannelse af kemikalier udvundet fra biomasse blevet undersøgt over forskellige guld- og rutheniumbaserede katalysatorer med ilt som rigelige oxidant.

Abbreviations

FAME	Fatty acid methyl ester
DOE	Department of energy
PTE	Polyethylene terephthalate
PTA	Purified terephthalic acid
HMF	5-Hydroxymethylfurfural
FDMC	2,5-Furandimethylcarboxylate
HMMF	Methyl 5-hydroxymethyl-2-furoate
MFF	Methyl 5-formyl-2-furoate
DFF	2,5-Diformylfuran
FDA	2,5-Furandicarboxylic acid
FFCA	5-Formyl-2-furancarboxylic acid
DHMF	2,5-Dihydroxymethylfuran
HMFCA	5-Hydroxymethyl-2-furancarboxylic acid
FA	Formic acid
LA	Levulinic acid
HT	Hydrotalcite
HAp	Hydroxyapatite
TFT	α,α,α-Trifluorotoluene
MIBK	Methyl isobutyl ketone
DMSO	Dimethylsulfoxide
DMF	*N*,*N*-Dimethylformamide
EtOH	Ethanol
*m*CPBA	*meta*-Chloroperoxybenzoic acid
NMR	Nuclear magnetic resonance
SEM	Scanning electron microscopy
TEM	Transmission electron microscopy
XR(P)D	X-ray (powder) diffraction
BET	Brunauer-Emmet-Teller (method)
EDS	Energy-dispersive X-ray spectroscopy

XRF	X-ray fluorescence spectroscopy
TPD	Temperature programmed desorption
TCD	Thermal conductivity detector
FID	Flame ionization detector
GC(-MS)	Gas chromatography(-mass spectrometry)
HPLC	High-performance liquid chromatography
XPS	X-ray photoelectron spectroscopy
EPR	Electron paramagnetic resonance
ICP	Inductively coupled plasma emission spectroscopy
NT	Nanotube
IL	Ionic liquid
[BMIm][BF_4]	1-Butyl-3-methylimidazolium tetrafluoroborate
[BMIm][PF_6]	1-Butyl-3-methylimidazolium hexafluorophosphate
[EMIm]Cl	1-Ethyl-3-methylimidazolium chloride
[BMIm]Cl	1-Butyl-3-methylimidazolium chloride
[EMIm][OAc]	1-Ethyl-3-methylimidazolium acetate
[EMIm][HSO_4]	1-Ethyl-3-methylimidazolium hydrogensulfate
[Bu_3MeN][$MeOSO_3$]	Tributylmethylammonium methylsulfate
[MMMPz][$MeOSO_3$]	1,2,4-Trimethylpyrazolium methylsulfate

Table of contents

1. *Scope of Thesis*

The present thesis is submitted in candidacy for the Ph.D. degree from the Technical University of Denmark (DTU). It represents part of the outcome of the three years work in the Centre for Catalysis and Sustainable Chemistry (CSC), Department of Chemistry from April 2008 to September 2011. The work was initially supervised by Professor Claus Hviid Christensen (until July 2008), and was continued under the supervision of Associate Professor Ander Riisager (CSC, DTU) and co-supervised by Professor John Woodley (PROCESS, Department of Chemical and Biochemical Engineering, Technical University of Denmark). The Ph.D. scholarship was funded by the Danish National Research Foundation and Novozymes A/S.

Along with the thesis, a number of publications in international peer-reviewed journals were prepared and are included as appendices (see list in Section 1.2.1 and Appendix). Additional miscellaneous manuscripts and poster presentations performed during the Ph.D. study are listed in Sections 1.3 and 1.4, respectively.

1.1. Acknowledgements

Throughout the whole work period, a great amount of input was obtained from collaboration with colleagues and friends at the Centre for Catalysis and Sustainable Chemistry. I am very grateful to all my friends and colleagues for making the last three years interesting and unforgettable.

I would like to thank Claus H. Christensen for giving me an opportunity to work at the Centre, and his inspiration and great enthusiasm in the fields of science and sustainable industry.

I would like to thank John Woodley for taking up responsibilities as my co-supervisor.

I would especially like to thank my supervisor Anders Riisager for his great influence on my research work and scientific development. His innovative spirit led to the contribution of an incredible number of ideas.

I would like to thank Susanne L. Mossin and Bodil F. Holten for their assistance with EPR and nitrogen physisorption measurements.

Also, I would like to thank Anders B. Laursen at the Center for Individual Nanoparticle Functionality (CINF), Department of Physics, DTU, for his assistance with TEM and EDS analysis and fruitful collaboration.

I would like to thank Anna Kulik, Guido Walther and Angela Köckritz, who helped and supervised me during my external stay at the Leibniz Institute for Catalysis (LIKAT), University of Rostock, Germany.

As part of my education, I have been fortunate to teach, supervise and attend courses with many very talented students. It was indeed a pleasure to work with you all.

I warmly thank all Ph.D. students, personnel and guests of the Department of Chemistry and Centre for Catalysis and Sustainable Chemistry who significantly contributed to my work and life, especially: Søren Kegnæs – for enormous amount of help and fruitful discussions; Tim Ståhlberg, Ester I. Eyjólfsdóttir and Irantzu Sádaba – for providing new ideas and collaboration, and for great get-togethers; Emily Corker and Anders T. Madsen – for their advices on writing this thesis; Anastasia A. Permyakova – for improving my central-Russian dialect; Christopher W. Hanning – for being a great friend and roommate.

Finally, I would like to thank Anne L. Thomsen for giving me her unlimited support and patience.

1.2. List of publications relevant for this thesis (see Appendix)

1.2.1. Manuscripts

- Y. Y. Gorbanev, S. K. Klitgaard, C. H. Christensen, J. M. Woodley, A. Riisager "Gold-Catalyzed Aerobic Oxidation of 5-Hydroxymethylfurfural in Water at Ambient Temperature", *ChemSusChem* **2009**, *2*, 672.
- A. Boisen, T. B. Christensen, W. Fu, Y. Y. Gorbanev, T. S. Hansen, J. S. Jensen, S. K. Klitgaard, S. Pedersen, A. Riisager, T. Ståhlberg, J. Woodley "Process integration for the conversion of glucose to 2,5-furandicarboxylic acid", *Chem. Eng. Res. Des.* **2009**, *87*, 1318.

- Y. Y. Gorbanev, S. Kegnæs, A. Riisager "Effect of support in heterogeneous ruthenium catalysts used for the selective aerobic oxidation of HMF in water", *Top. Catal.* **2011**, DOI: 10.1007/s11244-011-9754-2.
- Y. Y. Gorbanev, S. Kegnæs, A. Riisager "Selective aerobic oxidation of 5-hydroxymethylfurfural in water over solid ruthenium hydroxide catalysts with magnesium-based supports", *Catal. Lett.* **2011**, *accepted*.
- T. Ståhlberg, E. Eyjólfsdóttir, Y. Y. Gorbanev, A. Riisager "Aerobic Oxidation of 5-(Hydroxymethyl)furfural in Ionic Liquids with Solid Ruthenium Catalysts", **2011**, *submitted*.
- I. Sádaba, Y. Y. Gorbanev, S. Kegnæs, S. S. R. Putluru, A. Riisager "Aerobic oxidation of 5-hydroxymethylfurfural to 2,5-diformylfuran with zeolites-supported vanadia catalysts: A lixiviation study", **2011**, *submitted.*
- Y. Y. Gorbanev, S. Kegnæs, C. W. Hanning, T. W. Hansen, A. Riisager "Chemicals from renewable alcohols: Selective aerobic oxidation of aqueous ethanol into acetic acid over heterogeneous ruthenium catalysts", **2011**, *submitted*.
- A. B. Laursen, Y. Y. Gorbanev, F. Cavalca, A. Kleiman-Shwarsctein, A. Riisager, S. Kegnæs, I. Chorkendorff, S. Dahl "Highly dispersed ruthenium oxide as an aerobic catalyst for acetic acid synthesis", *manuscript in preparation.*

1.2.2. Books and book chapters

- S. K. Klitgaard, Y. Gorbanov, E. Taarning, C. H. Christensen "Renewable Chemicals by Sustainable Oxidations using Gold Catalysts", in *Experiments in Green and Sustainable Chemistry,* Eds. H.W. Roesky, D. Kennepohl, Wiley-VCH, **2009**, ISBN: 978-3-527-32456-7. (NOTE: This publication is not included in the Appendix. Please contact the publisher for the full text.)

1.3. Miscellaneous publications

- V. I. Simakov, Y. Y. Gorbanev, T. E. Ivakhnenko, V. G. Zaletov, K. A. Lyssenko, Z. A. Starikova, E. P. Ivakhnenko, V. I. Minkin "Synthesis, chemical properties, and

crystal structure of 2,4,6,8-tetra(*tert*-butyl)-9-hydroxyphenoxazin-1-one", *Russ. Chem. Bull. Int. Ed.* **2009**, *58*, 1361.

- M. Schau-Magnussen, Y. Y. Gorbanev, S. Kegnaes, A. Riisager "Magnesium and Nickel(II) 2,5-furandicarboxylate", *Acta Crystallogr., Sect. C: Cryst. Struct. Commun.* **2011**, *accepted*.

1.4. Poster presentations

- Y. Y. Gorbanev, S. K. Klitgaard, A. Boisen, A. Riisager "Green aerobic oxidation of HMF", *Annual meeting of the Danish Chemical Society*, Odense, Denmark, **2009**.
- Y. Y. Gorbanev, S. K. Klitgaard, A. Boisen, A. Riisager "Green Aerobic Oxidation of HMF", *6th World Congress on Oxidation Catalysis*, Lille, France, **2009**.
- Y. Y. Gorbanev, S. K. Klitgaard, E. Taarning, K. Egeblad, C. H. Christensen, A.Riisager "Gold-catalyzed formation of renewable building blocks for the plastic industry", *EuropaCat IX: Catalysis for a Sustainable World*, Salamanca, Spain, **2009**.
- Y. Y. Gorbanev, S. Kegnæs, J. M. Woodley, C. H. Christensen, A. Riisager "Renewable building block for plastic industry: Gold-catalyzed oxidation of HMF to FDA in water", *14th Nordic Symposium on Catalysis*, Elsinore, Denmark, **2010**.
- I. Sádaba, Y. Y. Gorbanev, S. S. S. R. Putluru, M. López Granados, A. Riisager "HMF oxidation with vanadia supported on zeolites: The search for a non-leaching catalyst", *First International Congress on Catalysis for Biorefineries,* Malaga, Spain, **2011**.

2. *Introduction*

The focus of a thesis with a title ”Catalytic aerobic oxidation of bio-renewable chemicals” implies that the research was aimed at exploring catalyst systems and conditions, which could be used for catalyzed aerobic oxidative transformations of the chemicals derived from biomass.

The first chapter of this thesis (Chapter 3) describes the basic concepts of catalysis and biomass usability, and highlights the importance of bio-renewables and bio-derived chemicals.

The following chapter (Chapter 4) reports the catalytic reactions of aerobic oxidation of 5-hydroxymethylfurfural (HMF) to 2,5-furandicarboxylicacid (FDA) and furan-2,5-dimethylcarboxylate (FDMC) with supported ruthenium and gold catalysts. The formation of FDA and its dimethyl ester is described in aqueous phase and methanol, respectively, with Au/TiO_2 catalyst at elevated pressures. The formation of FDA from HMF was also investigated with ruthenium hydroxide catalysts on different supports (*e.g.* oxides CeO_2, TiO_2, Al_2O_3, and magnesium-containing supports – MgO, hydrotalcite $Mg_6Al_2(CO_3)(OH)_{16}\cdot 4H_2O$ and spinel $MgAl_2O_4$) in aqueous solutions and ionic liquids at various temperatures and pressures.

Chapter 5 focuses on partial aerobic oxidation of HMF to 2,5-diformylfuran (DFF). HMF and other substituted furans were oxidized to respective carbonyl compounds in organic solvents (such as DMF, toluene, methyl isobutyl ketone, DMSO) with supported $Ru(OH)_x$ catalysts. Also, the study on the lixiviation of the active catalytic species from the V_2O_5/support employed in the aerobic oxidation of HMF to DFF in organic solvents is described.

In Chapter 6, the oxidation of alcohols over supported $Ru(OH)_x$ and RuO_x catalysts is presented. In particular, the oxidation of ”bio”-ethanol is described with supported $Ru(OH)_x$ catalysts supported on oxides CeO_2, TiO_2 and spinel. RuO_x catalysts deposited on various metal oxides and titanate nanotubes were also explored for the aforementioned reaction. Furthermore, the catalytic aerobic oxidative degradation of higher alcohols over supported ruthenium hydroxide catalysts. The oxidative degradation of *n*-propanol and the oxidative cleavage of vicinal diols with $Ru(OH)_x$ and RuO_x supported on CeO_2 and $MgAl_2O_4$ are presented.

3. *Background and basic concepts*

3.1. Sustainable chemical industry

3.1.1. Sustainable chemistry

Chemistry perpetually thrives on meeting the demands of the manufacturers, end users and, nowadays most importantly, the sustainability of chemical production processes. Contemporary chemistry is more than ever accentuated on minimizing the environmental footprint. At the same time, new demands arise constantly in the present day society in the fields of pharmaceutics, performance materials, and many others. Together, these factors lead to both consumers' and scientists' interest increase in sustainable chemistry.

Sustainable development is defined as the ''development that meets the needs of the present generation without compromising the ability of future generations to meet their own needs'' [1]. Thus, the aims of sustainable chemistry include many research areas, *e.g.* minimizing waste, avoiding hazardous substances, and especially utilization of renewable resources [2].

3.1.2. The renewable chemical industry

The drastic global population increase in the 2nd half of the 20th century created the resource challenge. For the majority of the existence of chemical industry, abundant fossil feedstock was available. Its continuous exploitation, however, together with an ever-increasing demand clearly indicates that the price of petroleum feedstock will greatly rise in the near future. This certainly affects the chemical industry, which shifts more and more towards renewable feedstocks [3]. Figure 1 presents the concepts of bio- and fossil refineries and shows the differentiation in roles of chemistry and biotechnology [4,5].

Biomass is the general term for energy sources which are renewable on an annual basis, and have biological origins (plant materials, agricultural crops, animal manure or other

waste, such as, *e.g.* fat) [6]. However, the term 'biomass' when used in literature generally refers to agricultural biomass [7]. Most common chemicals derived from biomass are the products of carbohydrates transformations. Furans, their derivatives and various organic acids have been defined by the U.S. Department of Energy (DOE) as the top twelve chemical opportunities from biomass [8,9]. Other important products obtained from biomass are bio-fuels: bio-alcohols and fatty acid methyl esters (FAMEs) [9-12].

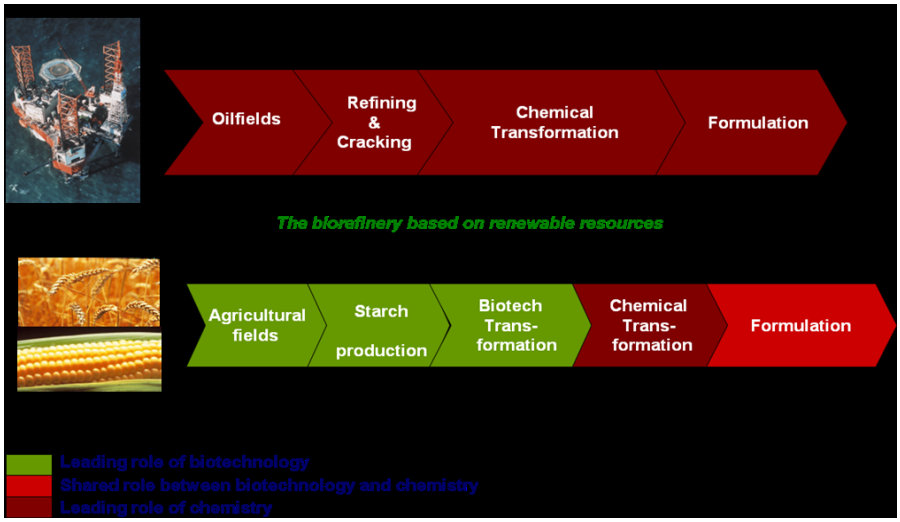

Figure 1. Fossil-based refinery versus renewable resources refinery.

Numerous reviews on the potential use of biomass have been published in the last decade [5,8,9,13-17], the most covering of which is probably the review by Corma *et al.* [15]. Figure 2 presents a partial, generalized product flow-chart for biomass feedstock with routes for production of chemicals [17].

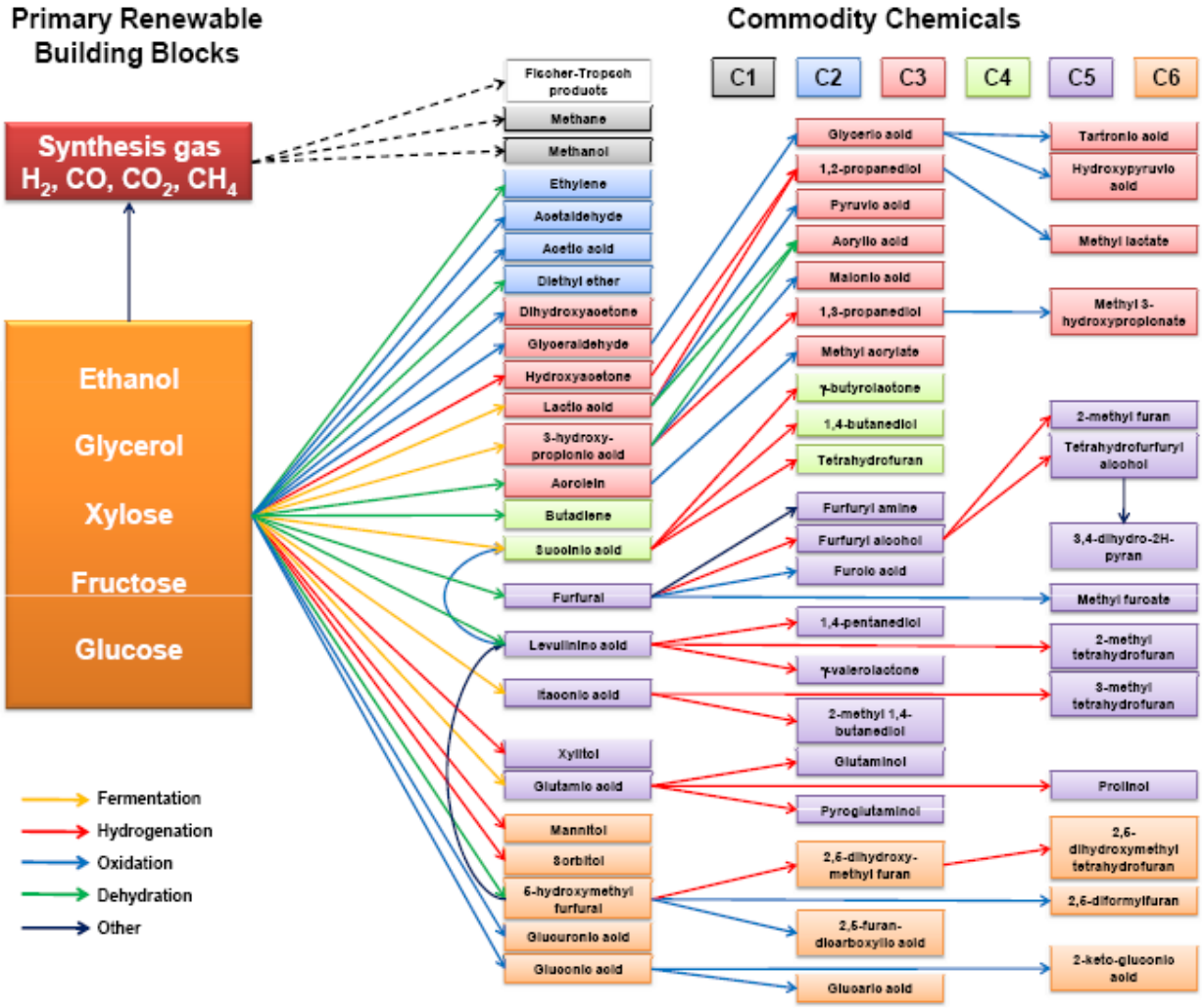

Figure 2. Partial product flow-chart for biomass feedstock [17].

Certainly, presently existing industrial processes are very cost-competitive when compared with new technologies. Figure 3 shows various commodity chemicals obtained from fossil and bio-renewable resources and their relative value [18].

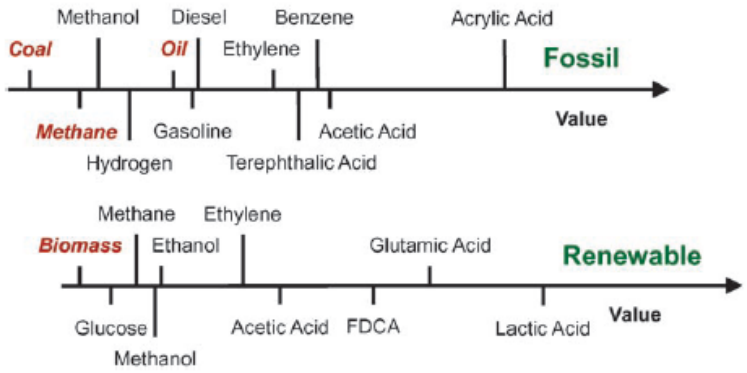

Figure 3. The fossil and renewable value chains indicate the value of different commodity chemicals relative to the feedstock [18].

Although the annual world-wide production of biomass is billions of tones [19], currently only 5 % of commodity chemicals are produced from renewable resources [20]. This, however, does not limit the possible usage or necessity for biorefineries, but rather stresses the importance and creates opportunity for researchers to develop innovative, efficient and sustainable pathways for producing value-added chemicals derived from biomass.

3.2. Catalysis and sustainability

As mentioned above, a sustainable process aims at optimizing the use of resources. Another important issue is to minimize the waste production. Catalysis is a tool for both cases; in other words, catalysis is a key to sustainability [21].

Catalysis has a huge impact on the industrial, agricultural and consumer sectors. Catalysts are used in a broad range of devices including sensors, fuel cells, exhaust gas converters and water purifiers. Development of new catalytic processes across the chemical, petroleum and new energies industries increases resource and energy utilization efficiencies, at the same reducing waste and overall environmental footprints. Thus, catalysis is one of the most promising tools for sustainable development and green chemistry [22].

Although numerous processes in organic synthesis are performed with homogenous catalysts, heterogeneous catalysis is gradually becoming more important, mostly due to possible industrial applications. The importance of heterogeneous catalysis for industry is defined by the ease of the catalyst separation and hence recyclability [23]. In fact, many ”classic” industrial processes, mainly in petrochemicals and bulk chemicals industry, such as ammonia synthesis (Haber-Bosch process), Fischer-Tropsch process and others, operate with heterogeneous catalysts [24]. Heterogeneous catalysis can also be useful in combination with enzymatic catalysis in the aforementioned biorefineries [17,25], as has already been proven plausible for the synthesis of fine chemicals and pharmaceuticals [22,25].

4. *Oxidation of 5-hydroxymethylfurfural to 2,5-furandicarboxylic acid*

4.1. Introduction

4.1.1. HMF – a precursor for commercial chemicals

As mentioned above, carbohydrates are one of the most important types of biomass feedstock. Sugars, in the form of mono- and disaccharides, are readily available from various biomass sources by, *e.g.* enzymatic hydrolysis and form a useful feedstock for the production of versatile chemicals (Figure 4). For example, hexose monosaccharides such as glucose and fructose can be catalytically dehydrated into 5-hydroxymethylfurfural (HMF) (Scheme 1) [26]. Presently, most research on saccharides conversion into HMF comprises dehydration of fructose, glucose or cellulose in water, high-boiling organic solvents or ionic liquids [26-33].

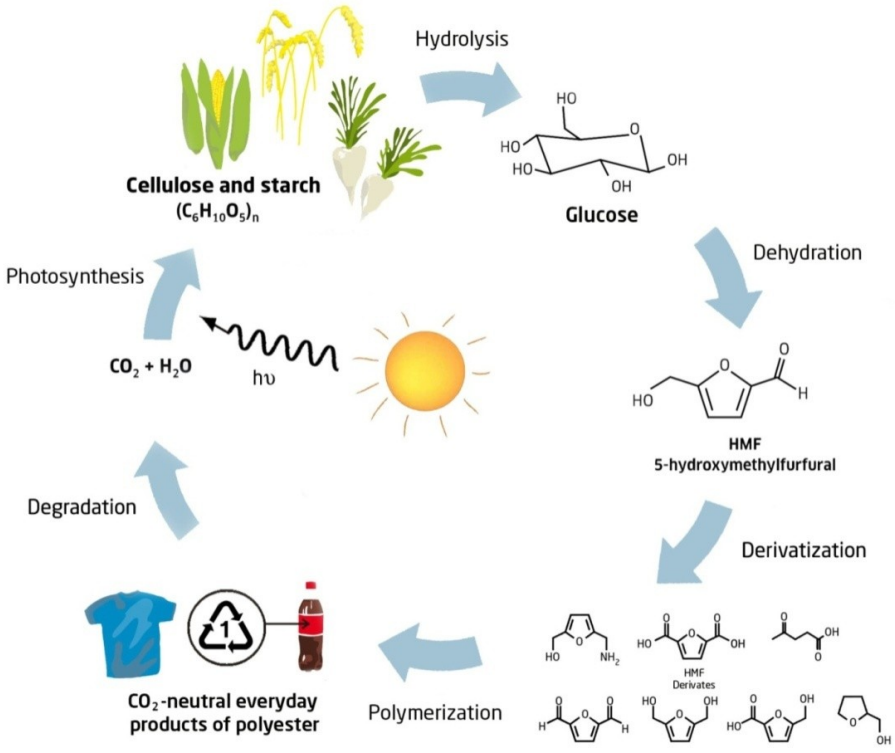

Figure 4. Reaction network and lifecycle of HMF as a renewable platform molecule.

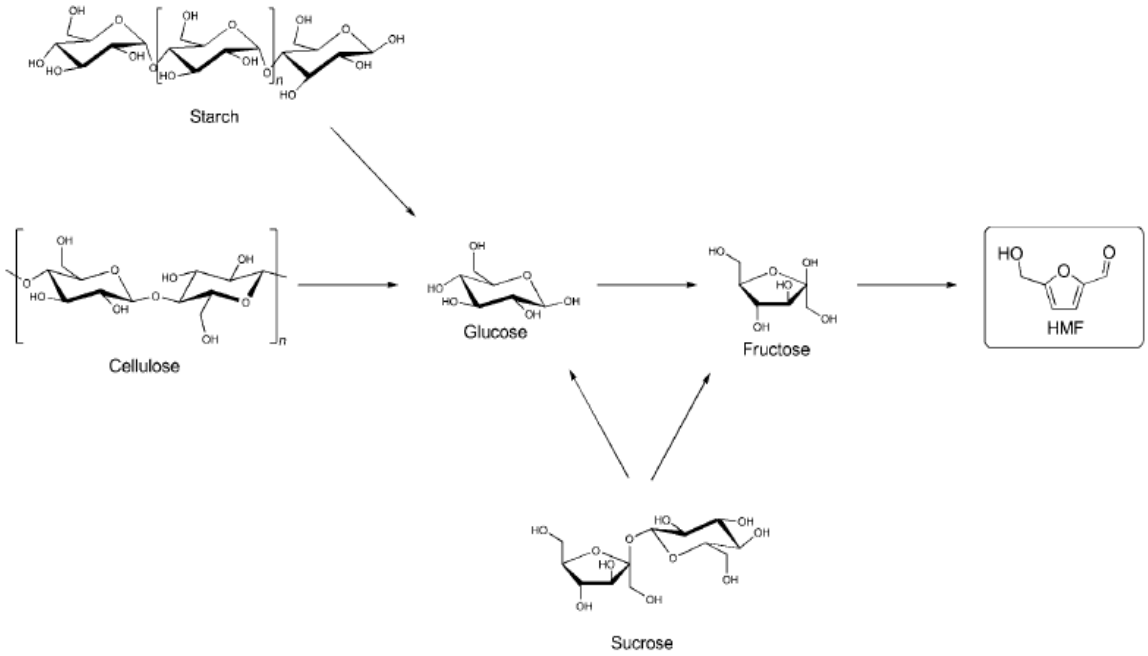

Scheme 1. The synthesis of HMF from carbohydrates [26].

HMF is listed as one of the 'top twelve' most important chemicals from biomass by the U.S. Department of Energy [8,9]. HMF has been extensively covered in several reviews [33,34] and is primarily considered to be a starting material for the production of other chemicals with important applications, such as monomers for plastics, solvents, or fuels (Scheme 2).

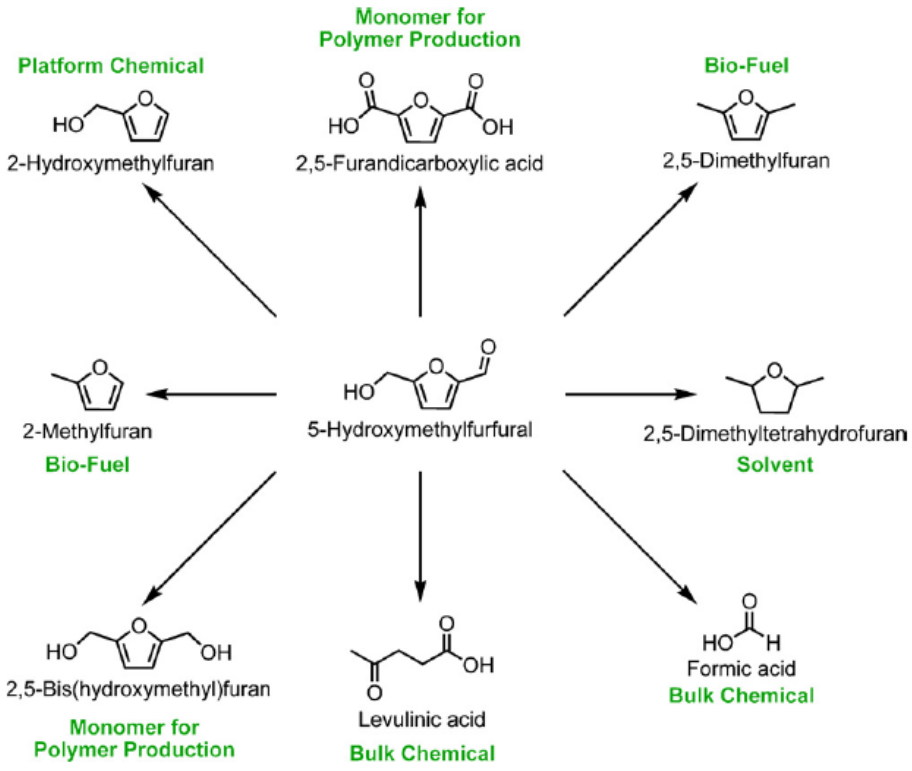

Scheme 2. 5-Hydroxymethylfurfural (HMF) as a precursor for a range of commercial chemicals.

As seen from Scheme 2, one of the chemicals obtained from HMF transformations is 2,5-furandicarboxylic acid. This chapter focuses further on the production of FDA and its dimethyl ester from HMF, specifically - *via* aerobic heterogeneously catalyzed oxidation.

4.1.2. FDA – a polymer building block

2,5-furandicarboxylic acid (FDA) has attracted great attention since being mentioned in U.S. DOE biomass program [8] together with its precursor, HMF. Due to the presence of the two carboxylic acid groups, FDA is considered to be a bio-renewable building block to form polymers from biomass and therefore become an alternative to terephthalic, isophthalic and adipic acids, which are all produced from fossil fuels [35]. Scheme 3 shows the structures of

terephthalic acid (PTA), used in the production of plastics, its polymer polyethyleneterephthalate (PET) and 2,5-furandicarboxylic acid (FDA).

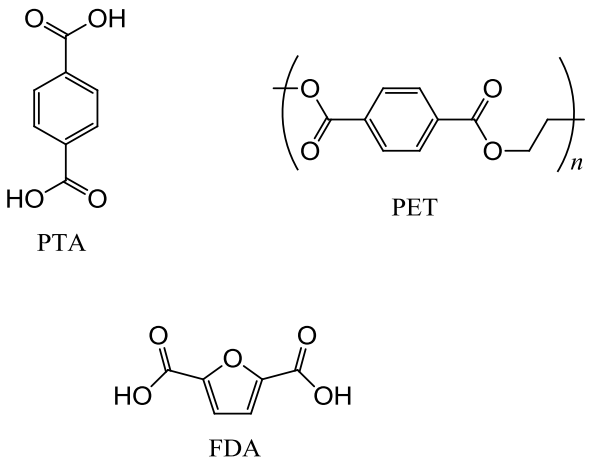

Scheme 3. (Purified) **T**erephthalic acid (PTA), polyethylene terephthalate (PET) and 2,5-furandicarboxylic acid (FDA).

HMF can be readily oxidized into FDA using a variety of routes and reaction types. Several reviews cover the topic of FDA production from HMF [34,36]. For instance, Lewkowski reports a vast variety of chemical methods for HMF oxidation to FDA, including electrochemical oxidation, the use of barium and potassium permanganates, nitric acid and chromium trioxide [36]. In this section focuses on some of the reported catalytic routes for the oxidation of HMF into FDA, including recent ones.

Partenheimer and Grushin [37] obtained FDA from HMF using metal bromide catalysts (Co/Mn/Zr/Br). The reactions were carried out in acetic acid at atmospheric pressure and also at 70 bar of air pressure; yields of FDA over 60 % were obtained. Cobalt as a catalyst was also used by Ribeiro and Schuchardt [38]. Using cobalt acetylacetonate as a bi-functional acidic and redox catalyst encapsulated in silica in an autoclave at 160^{o}C, they obtained FDA, from fructose *via* HMF formation, with 99 % selectivity to FDA at 72 % conversion of fructose. By *in situ* oxidation of HMF to FDA starting from fructose, Kröger *et al.* described a way of producing FDA *via* acid-catalyzed formation and subsequent oxidation of HMF in MIBK/water mixture using solid acids for fructose transformation and

PtBi-catalyst encapsulated in silicone and swollen in MIBK [39]. The reaction was carried out in a reactor divided with a PTFE-membrane in order to prevent the oxidation of fructose. However, though in principle the integration process has been described, the yields remain quite low. The resulting yield of FDA was 25 % based on fructose.

The efficient use of noble metals in the oxidation of HFM to FDA was first studied by Vinke *et al.* [40]. Here, mainly Pd, Pt or Ru supported on different carriers were used as aerobic oxidation catalysts. Although all the noble metals revealed catalytic activity, only Pt supported on Al_2O_3 remained stable, active and gave quantitative yields of FDA. The reactions were carried out in water at pH 9 using a reaction temperature of 60^{o}C and a partial oxygen pressure of 0.2.

In the last couple of years, several reports on novel methods for the oxidation of HMF to FDA have appeared in literature. As a good example of an innovative approach, Ruijssenaars *et al.* reported a whole-cell biotransformation of HMF into FDA. Here, 97 % yield of FDA was obtained from HMF using the whole-cell biocatalyst *Pesudomonas putida S12* with introduced *hmfH* gene [41]. However, a number of reports on heterogeneous catalyst systems for the oxidation of HMF to FDA were also published.

Lilga *et al.* have recently patented an industrially promising method to oxidize HMF to FDA in up to 98 % yield (100 % conversion; up to 98 % selectivity) at 100^{o}C and 1 MPa oxygen pressure using a Pt/ZrO_2 catalyst [42]. Later, the same group reported the oxidation of HMF in a fixed-bed continuous flow reactor [43]. Basic, neutral and acidic feeds of HMF were oxidized using Pt catalysts supported on carbon and ZrO_2. High yields of the oxidized derivatives of HMF were obtained, which allowed the authors to conclude that the process was industrially feasible.

Another way of oxidizing HMF to FDA that has attracted various research groups attention is the usage of supported gold nanoparticle catalysts. Corma *et al.* performed the aerobic oxidation of HMF in aqueous solutions with added base [44]. Gold nanoparticles supported on iron oxide, titania, ceria and carbon were tested for the oxidation of HMF in water at different concentrations of NaOH. Quantitative yields of FDA were obtained in the temperature range of 25-130^{o}C at different oxygen pressures. Au/TiO_2 and Au/CeO_2 catalysts proved to be most effective for HMF oxidation to FDA. At the optimized conditions of 403 K, 1000 kPa O_2 and 4:1 ratio NaOH : HMF, >99 % yield of FDA was obtained after 8 hours of reaction time over Au/CeO_2.

Davis *et al.* [45] performed a comparative study of Pt, Pd and Au catalysts for the aerobic oxidation of HMF at high pH in a semibatch reactor (with continuous oxygen feed). The authors found the rate of oxidation of HMF over Au catalysts to be an order of magnitude greater under the standard conditions of 295 K, 690 kPa O_2, 0.15 M HMF and 0.3 M NaOH. However, the rapid conversion of HMF over the Au catalysts was to the intermediate product 5-(hydroxymethyl)furancarboxylic acid (HMFCA) (*vide infra*), formed by oxidation of the aldehyde group of HMF. Under identical conditions, Pt and Pd were shown to provide high yields of FDA, indicating that Pt and Pd can activate the alcohol side chain of HMFCA whereas Au cannot. Thus, gold catalysts required high pressures of O_2 and high concentrations of base to efficiently oxidize HMF to FDA.

A very recent communication by Ebitani *et al.* showed the possibility of aqueous HMF oxidation with no added homogeneous base [46]. Gold nanoparticles supported on hydrotalcite provided quantitative yield of FDA in the aerobic oxidation of HMF in water at 368 K under an ambient oxygen pressure.

Another approach to the oxidation of HMF, which leads with the formation of furan-2,5-dimethylcarboxylate (FDMC) was first reported by our group (Taarning *et al.*; [47]). The authors oxidized HMF in methanol solutions to form furan-2,5-methyldicarboxylate (FDMC) with Au/TiO_2 catalyst under 4 bar of dioxygen pressure at 130^{o}C to provide the isolated yield of FDMC of 60 %. A reaction pathway with relative step velocities was proposed (Scheme 4).

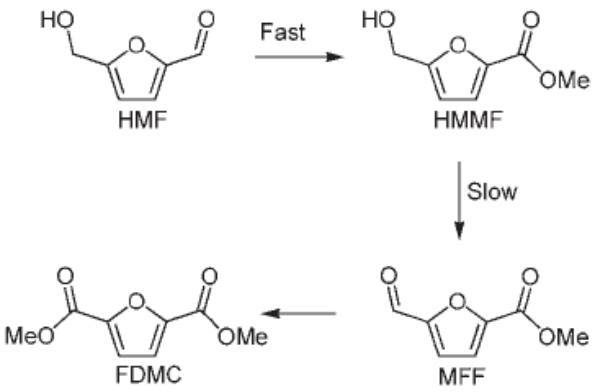

Scheme 4. Proposed reaction pathway for the aerobic oxidation of HMF in methanol (hemiacetal intermediates are omitted for clarity) according to Taarning *et al.* [47].

Subsequently, Corma *et al.* [49] reported the oxidation-esterification of HMF in various alcohols over catalysts comprising gold nanoparticles supported on carbon and iron, cerium, titanium oxides. A Au/CeO_2 catalyst was shown to be an efficient catalyst for the oxidation of HMF to FDMC without added base at different oxidant pressures and temperatures. Under optimized conditions, 100 % yields of FDMC were obtained. Also, the effect of adding water to the reaction was found to be negative for the oxidation towards FDMC.

The following section presents a research on the gold-catalyzed oxidation of HMF prior to the works published by Corma *et al.* [44,48], Davis *et al.* [45] and Ebitani *et al.* [46].

4.2. Gold-catalyzed aerobic oxidation of HMF

4.2.1. Introduction

The inertness of gold has been known since ancient times. It has led chemists to believe that gold was also catalytically inert being too unreactive. In fact, it started attracting attention from 1973, when Wells *et al.* applied gold for hydrogenation of olefins [49]. Since then, gold has been applied for a various chemical reactions. The broad range of the reactions catalyzed by gold is excellently covered in several recent reviews, *e.g.* by Hutchings *et al.* and Garcia *et al.* [50,51].

Aerobic oxidations have attracted increased attention over recent years [52,53]. Air or molecular oxygen are used as oxidants, producing water as the only by-product, thus they are considered "green" oxidants. Unlimited accessibility and low cost of air makes it an attractive reactant also from an economic point of view.

First aerobic oxidation reaction catalyzed by gold was reported by Haruta *et al.*, where carbon monoxide was oxidized over supported gold catalysts [54]. Following the discovery by Haruta *et al.*, a great variety of other aerobic oxidation reactions was discovered. For example, gold nanoparticles were used in the oxidation of alcohols to aldehydes and esters, oxidation of aldehydes to esters, in epoxidation of olefins, in the oxidation of amines to amides, and very recently - formation of imines from the oxidative coupling of alcohols and amines [55-70]. Importantly, gold has also been found to be an excellent catalyst for the oxidation of both aromatic and aliphatic alcohols to their corresponding acids or esters with oxygen as the oxidant under benign conditions [71–78].

The recent development on gold-catalyzed oxidation of HMF to FDA and its derivatives have already been mentioned in the previous section [44-48].

In this section, the results of the research on gold-catalyzed aerobic oxidation of HMF to FDA in water and the oxidation of HMF to FDMC in methanol (Scheme 5) are presented.

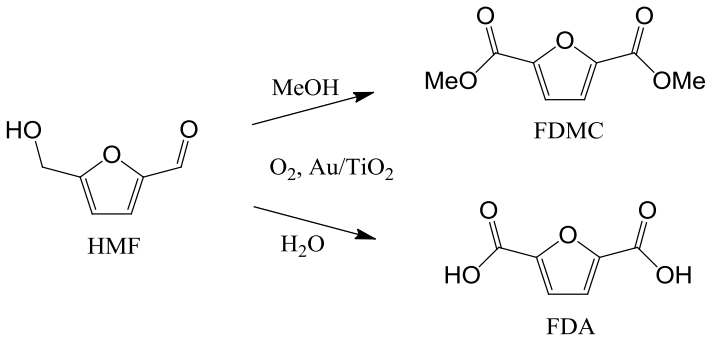

Scheme 5. Aerobic oxidation of HMF in water or methanol to produce FDA or FDMC, respectively.

4.2.2. Experimental

Materials: 5-Hydroxymethylfurfural (>99 %), anisol (99%), sodium methoxide (*ca.* 30 wt% solution in methanol), methanol (≥99.5 %), potassium carbonate (≥99.0 %), potassium bicarbonate (≥99.5 %), levulinic acid (98 %), formic acid (98 %), hydrogen tetrachloroaurate(III) trihydrate ($H[AuCl_4]\cdot 3H_2O$) (99.9 %), sodium hydroxide (>98%), potassium hydroxide (>98 %) , anisole (99 %) and triethylamine (≥99 %) were acquired from Sigma–Aldrich. Methyl isobutyl ketone (MIBK) (≥98.0 %) was purchased from Fluka. Cerium(IV) oxide (99.5%) was purchased from Alfa Aesar. Magnesium oxide (p.a.) was purchased from Riedel-de Haën AG. 2,5-furandicarboxylic acid (>99 %) and 5-hydroxymethyl-2-furancarboxylic acid (>99 %) were purchased from Toronto Research Chemicals Inc. and dioxygen (99.5 %) was obtained from Air Liquide Denmark. All chemicals were used as received.

For the oxidation reactions a commercial 1 wt% Au/TiO_2 catalyst was used (Mintek, Brunauer–Emmett–Teller (BET) surface area 49 m^2/g), which by high-resolution transmission electron microscopy analysis (JEM 2000FX microscope, 300 kV; sample mounted on a 300 mesh copper grid coated with holey carbon film) was found to contain gold particles with an average size of 4–8 nm (Figure 5). Titania-supported platinum and paladium catalysts were prepared using the incipient wetness impregnation method from the solutions of nitrates of respective metals.

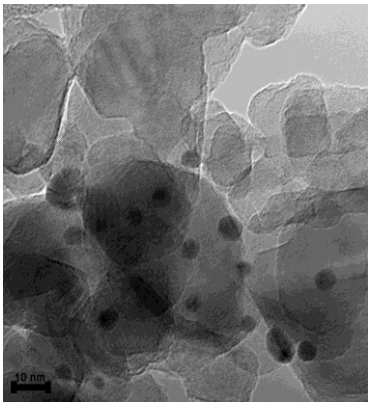

Figure 5. High-resolution TEM image of the 1 wt% Au/TiO_2 catalyst.

4.2.2.1. Oxidation in methanol

Oxidation reactions: High pressure oxidations were carried out in a Parr reactor autoclave (T316 steel, Teflon beaker insert, 325 mL) (Figure 8). The autoclave was charged with 0.504 g of HMF (4 mmol), methanol (12.65 mL, 300 mmol), anisol (internal standard; 44 μL, 0.4 mmol) and a solution of sodium methoxide in methanol (0.069 mL, 0.3 mmol base). Subsequently, 1 wt% Au/TiO_2 catalyst was added (0.25 g, 0.013 mmol Au) and the autoclave was equipped with a magnetic stirrer, flushed, pressurized with dioxygen (4 bar, *ca.* 52 mmol) and put in an oil bath at 130°C for 6 hours under stirring (800 rpm). After the reaction, the autoclave was cooled to room temperature (*i.e.*, 20°C) and after filtering off the catalyst a sample was taken out for GC analysis (Agilent Technologies 6890N with a flame ionizator detector (FID), HP-5 column (30 m x 0.320 mm x 0.25 μm, J&W Scientific) and/or GC-MS (GC Agilent Technologies 6850 coupled with MS Agilent Technologies 5975C, column HP-5MS (J & W Scientific, 30 m × 0.25 mm × 0.25 μm, 5 mol% phenylmethylpolysiloxane), flow gas He).

FDMC was isolated by the removal of methanol under reduced pressure. The remaining beige solid was sublimed at 1 atm and 170°C to afford colourless crystals (Figure 6).

Figure 6. Sublimation of 'crude' FDMC from the oxidation reaction of HMF in methanol to afford colourless crystals of pure FDMC.

NMR spectra were recorded on a Varian Mercury 300 MHz instrument. Chemical shifts were determined relative to that of chloroform. NMR spectroscopy confirmed that the product was FDMC: ^{1}H NMR (300 MHz, $CDCl_3$, 295 K): δ=3.92 (6H), 7.21 ppm (2H); ^{13}C NMR: δ=52.39, 118.46, 146.57, 158.37.

Open flask experiments were conducted in a two-necked round bottom flask equipped with a water-cooled reflux condenser, a magnetic stirrer, and an oil bath with a thermocontrol. Reactions were carried out similarly to described above. A solution of HMF (0.504 g, 4 mmol) in methanol (12.65 mL, 300 mmol) or MIBK/methanol (12.65 mL, 1:4), was put into a flask, then the internal standard (anisol, 4 μL, 0.4 mmol), base and a 1 wt% catalyst were added in the reaction. All bases and catalysts are listed in Table 1. All reactions were carried out under the flow of oxygen (1 atm) at 25^{o}C with *ca.* 0.3 mol% of the 1 wt% catalyst.

Table 1. Reaction conditions for the open flask aerobic oxidations reactions of HMF.

Entry	Catalyst	Solvent	Base	
1	Au/TiO2	CH_3OH	CH_3ONa	0.069 mL (8 mol%)
2			$(C_2H_5)_3N$	0.045 mL (8 mol%)
3			K_2CO_3	2.5 g
4			$KHCO_3$	2 g
5	Au/TiO_2	MIBK/CH_3OH (1:4)	CH_3ONa	0.069 mL (8 mol%)
6			K_2CO_3	2.5 g
7	Pd/TiO_2	CH_3OH	CH_3ONa	0.069 mL (8 mol%)
8	Pt/TiO_2	CH_3OH	CH_3ONa	0.069 mL (8 mol%)

4.2.2.2. Oxidation in water

Catalyst preparation: The formation 1 wt% Au on CeO_2 and MgO was performed using deposition-precipitation method. In a 25 mL beaker, 0.02 g of $H[AuCl_4]\cdot 3H_2O$ and 5 mL of water were added and mixed with stirring resulting in a pale yellow solution. A saturated solution of $KHCO_3$ (~20 drops) was added to the suspension until pH 9. Immediately after, 0.95 g of a support was added to the solution. After that the suspension was stirred at 50°C for approximately 1 hour. During this time the aqueous solution gradually shifts from yellow to clear as $Au_2O_3\cdot xH_2O$ precipitates onto the support. After 1 h, the suspension was filtered and the catalyst was washed with distilled water until no Cl^- ions were detected. The presence of Cl^- ions was tested by addition of $AgNO_3$ solution to the washing water. Finally, the recovered material was dried and calcined in a muffle furnace for 2 hours at 350°C with a heating ramp of 5°C/min. The resulting powder had a dark purple colour.

Oxidation reactions: High pressure oxidations were carried out in a stirred Parr minireactor autoclave equipped with internal thermocontrol (T316 steel, Teflon beaker insert, 25 mL) (Figure 8). A typical experiment was as follows: the autoclave was charged with 126 mg of HMF (1 mmol) and a solution of alkali hydroxide (0.1–0.8 g, 2.5–20 mmol) in 10 mL of water. Subsequently, 1 wt% Au catalyst was added (0.394-0.197 g, 0.01-0.02 mmol Au) and the autoclave was flushed and then pressurized with dioxygen (10–30 bar, *ca.* 4–12 mmol) and maintained at respective temperature for a given period under stirring (800 rpm). After the reaction, the autoclave was cooled to room temperature (*i.e.*, 20°C) and after filtering off the catalyst a sample was taken out for HPLC analysis (Agilent Technologies 1200 series, Aminex HPX-87H column from Bio-Rad, 300 mm x 7.8 mm x 9 mm, flow 0.6 mL/min, solvent 5 mM H_2SO_4, temperature 60°C). A typical chromatogram is presented on Figure 7.

Open flask experiments were conducted in a two-necked round bottom flask equipped with a water-cooled reflux condenser, a magnetic stirrer, and an oil bath with a thermocontrol. Reactions were carried out similarly to described above. A solution of HMF (0.126 g, 1 mmol) in water (8 mL) was put into a flask, then 1 M solution of sodium hydroxide (2 mL, 2 mmol) and the 1 wt% Au/TiO_2 catalyst (0.02-0.157 g, 1-8 μmol Au),

were added in the reaction. Reactions were carried out under the flow of oxygen (1 atm) at 25 and 50°C.

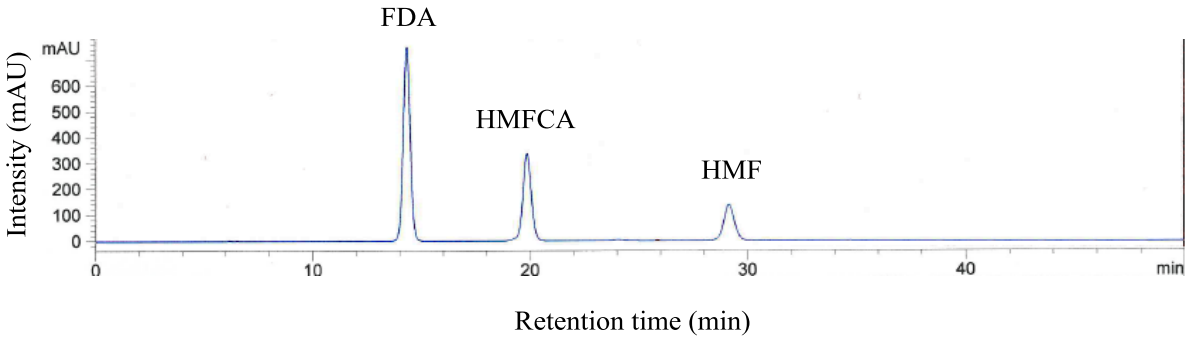

Figure 7. A typical chromatogram obtained by the HPLC analysis of the post-reaction mixture in the experiments of aqueous HMF oxidation. Compounds (left to right): 2,5-furandicarboxylic acid, 5-hydroxymethylfurancarboxylic acid, 5-hydroxymethylfurfural.

Reference samples were used to quantify the products. Reported results are averaged data (<7 % absolute error) obtained from 2–3 separate reactions with an apparent carbon mass balance of >90 % (no CO_2 product observed by TCD GC analysis). ICP analysis (Perkin–Elmer ELAN 6000 with cross-flow nebulizer and argon plasma) was performed on the diluted post-reaction mixture and quantified with an ICP standard solution (1.000 g/L, Fluka).

Figure 8. Parr Instruments reactor autoclaves used for the oxidation of HMF to FDMC in methanol (top) and HMF to FDA in water (bottom).

4.2.3. Results and discussion

4.2.3.1. Oxidation of HMF in methanol

The research on the oxidation of HMF to FDMC was carried out as a continuation of the results reported from our group by Taarning *et al.* [78]. Here, we present the improved isolated yield of FDMC and optimized reaction conditions, such as the use of lower amount of methanol and added base (Scheme 6).

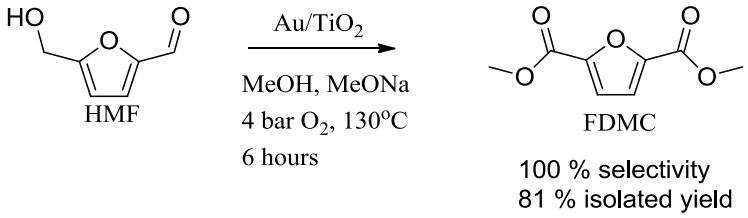

Scheme 6. Oxidation of HMF in methanol to form FDMC with a supported gold catalyst at 4 bar of the oxidant pressure at elevated temperature with added base.

In a typical high pressure experiment, HMF dissolved in methanol (1:75 molar ratio) was oxidized to FDMC with a catalytic amount of 1 wt% titania-supported gold catalyst (*ca.* 0.3 mol%). Reactions were carried out with an addition of base (sodium methoxide, 7.5 mol%), as base enhances the reaction rate of the oxidative esterification [62].

The crude product FDMC was subsequently purified by sublimation under atmospheric pressure at 170°C (see Figure 6) to provide a total isolated yield of FDMC of 81 %.

Additionally to the oxidation of methanol solutions of HMF in the autoclave reactors under high pressures, a set of experiments in an open flask was performed, in which different bases and catalysts were screened to oxidize HMF to FDMC (see Table 1).

Firstly, we attempted to perform the reaction with a different added base. For that, four reactions were carried out (Table 1, entries 1-4). In each reaction, 4 mmol of HMF were dissolved in 12.65 mL of methanol, and internal standard (anisol) was added to the reaction

mixture. Subsequently, 0.15 g of 1 wt% Au/TiO_2 catalyst was added. Figure 9 shows the product yields plotted against reaction time in the oxidation reactions when CH_3ONa and triethylamine were used as bases (Table 1, entries 1-2).

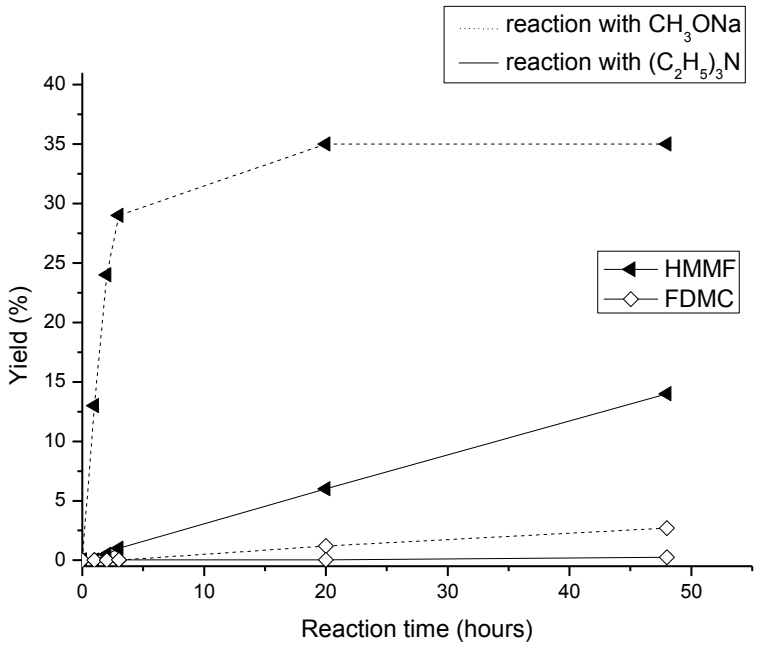

Figure 9. Product formation in HMF oxidation with dioxygen in methanol solution using 1 wt% Au/TiO_2 catalyst as a function of reaction time. Reaction conditions: 0.504 g HMF, 12.65 mL methanol, 44 μL anisole, 0.15 g of 1 wt % Au/TiO_2, O_2 flow (1 atm), 25°C, 8 mol% base.

Considering that the reaction proceeds *via* the formation of intermediate product 5-hydroxymethyl methylfuroate (HMMF) to the further oxidation to FDMC [47], it is seen from Figure 9 that the product yields in cases when the reaction was carried out at room temperature are significantly lower than those at elevated temperature and pressure. In fact, when sodium methoxide was substituted with $(C_2H_5)_3N$, the yield of FDMC constituted less than 1 % after 48 hours of reaction time, thus suggesting that Lewis base is less efficient in the gold-catalyzed oxidation reaction. Additionally, triethylamine itself could have undergone oxidation [70], although oxidation products such as acetaldehyde or acetic acid were not observed using GC-MS.

The usage of potassium salts ('as is' or dried prior to reaction) as solid bases for the oxidation of HMF in methanol, as well as platinum and palladium based catalysts (Table 1,

entries 3, 4 and 7, 8), under applied reaction conditions did not result in the formation of the oxidation products in the observed period of time. Also, the use of MIBK/methanol solvent mixture as a reaction medium did not result in any drastic change of product yields or HMF conversion when CH_3ONa was used as a base. However, when the solid base K_2CO_3 was employed, the reaction resulted in an almost quantitative yield of the oxidative condensation product (Scheme 7) according to GC-MS.

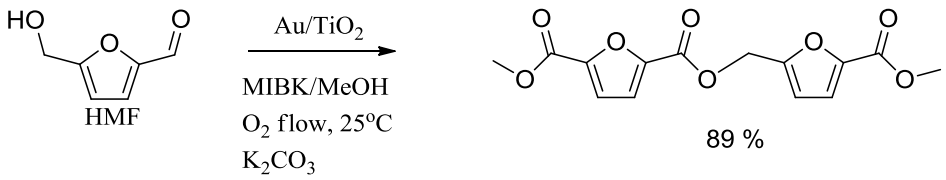

Scheme 7. The formation of oxidation/dimerisation product in the oxidation of HMF in MIBK/methanol mixture with Au/TiO_2 catalyst. Reaction conditions: 0.504 g HMF, MIBK/MeOH (12.65 mL, 1:4), 0.15 g of 1 wt% Au/TiO_2, O_2 flow, 25°C, 2.5 g K_2CO_3.

4.2.3.2. Oxidation of HMF in water

Initially, the oxidation of HMF was performed with 20 equivalents of sodium hydroxide at 20 bar dioxygen pressure (*ca.* 8 mmol) at 30°C (Scheme 8). The oxidation reaction was followed by measuring the concentration of the reaction products using HPLC (with acidic eluent to obtain FDA). In Figure 10 the measured yields of all observed reaction products are plotted against the reaction time (HMF was fully converted).

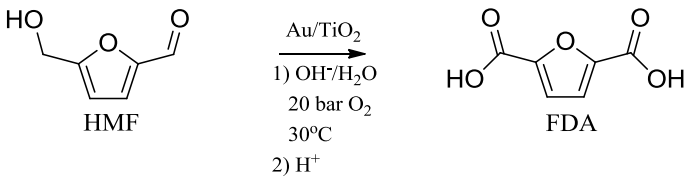

Scheme 8. Oxidation of HMF to form FDA with a supported gold catalyst at ambient temperature with added base and 20 bar dioxygen pressure.

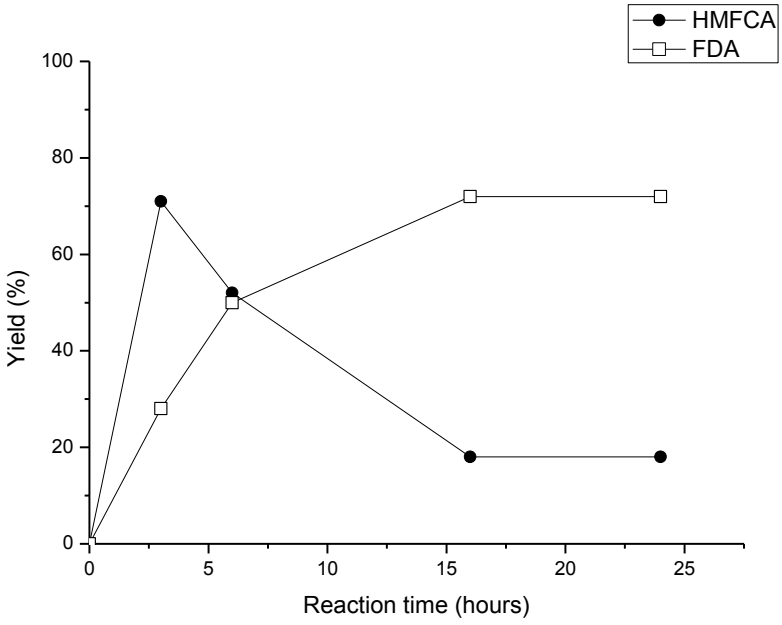

Figure 10. Product formation in HMF oxidation with dioxygen in aqueous solution using 1 wt% Au/TiO_2 catalyst as a function of reaction time. Reaction conditions: 20 equivalents of NaOH, 20 bar O_2, 30°C.

As seen from the data, HMF initially underwent relatively fast oxidation to 5-hydroxymethyl-2-furancarboxylic acid (HMFCA) before being further oxidized to FDA (*vide infra*), as was also previously found in methanol solution (see Scheme 4; [47]). Thus, no indication supporting a reaction route involving initial oxidation of the HMF alcohol group under these reaction conditions, due to stabilizing electron effects of the furan ring and formyl group, was found (as claimed by Vinke *et al.* [40]).

An 18 hour control reaction conducted under an inert nitrogen atmosphere in the absence of dioxygen (but with all other reaction conditions unchanged) also resulted in full HMF conversion, but with product yields of 51 % HMFCA, 38 % 2,5-dihydroxymethylfuran (DHMF) and 11 % levulinic acid (LA), respectively. This result suggested that by-products form under the generally applied reaction conditions partly by the Cannizzaro reaction (disproportionation of HMF to HMFCA and DHMF) [43,44] and partly by HMF degradation, thereby limiting the available FDA yield. Hence, under optimized conditions a maximum FDA yield of 71 % was obtained after 18 hours of reaction. Interestingly, HMF degradation resulted apparently in LA formation in the absence of oxidant, whereas traces of formic acid (FA) were exclusively formed in the presence of dioxygen.

HMF was also oxidized with various amounts of NaOH added to the reaction mixture. The dependence of product formation on the amount of the introduced base is shown in Figure 11. The use of aqueous KOH gave identical results.

In reactions with low amounts of added sodium hydroxide base (2.5 equivalents) the yield of the intermediate oxidation product (HMFCA) was comparatively high relative to FDA, resulting in only moderate yield of FDA at full HMF conversion. In contrast, the conversion of HMF was only 13 % (corresponding to 12 % and 1 % yield of HMFCA and FDA, respectively) without added base, suggesting gold catalyst deactivation by the initially formed acids, as was previously reported by Christensen *et al.* for alcohol oxidation in a methanol solution [77]. Additionally, precipitation of the formed FDA onto the catalyst surface may also have hampered the reaction significantly in the absence of base, where the solubility of FDA is quite low [43,45].

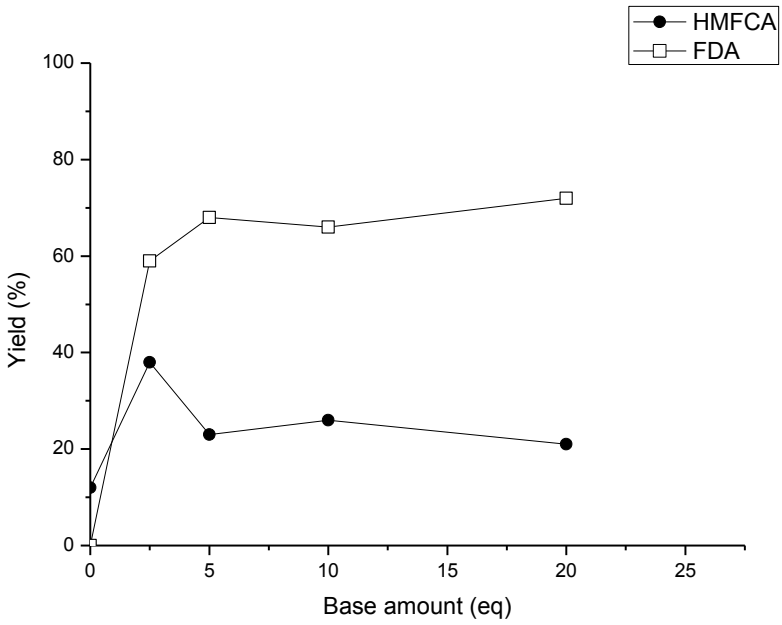

Figure 11. Product formation in HMF oxidation with dioxygen in aqueous solution using 1 wt% Au/TiO_2 catalyst as a function of the introduced NaOH amount. Reaction conditions: 20 bar O_2, 30°C, 18 hours.

The formation of by-products was largely avoided at all examined base concentrations (for both NaOH and KOH), with only traces of up to 3 % FA being observed at the higher base concentrations examined along with about 70 % and 25 % yield of FDA and HMFCA, respectively. Unexpectedly, LA was not observed, in contrast to what is usually found when HMF is degraded by rehydration [15,36]. Moreover, no conversion was observed when LA was introduced as a substrate in place of HMF under applied reaction conditions. This suggests that the trace of FA was generated from HMF degradation *via* a route which did not involve LA formation. In this connection a possible route could involve the *in situ* generated peroxide from oxygen, which has also been found to induce by-product formation by C-C bond cleavage in gold-catalyzed aerobic oxidation of aqueous glycerol [71,72]. This would also explain why FA was not formed in the absence of dioxygen.

In addition to the reactions described under 20 bar of oxygen, reactions were also examined with added sodium hydroxide under both lower and higher oxygen pressures of 10 and 30 bars respectively (Figure 12).

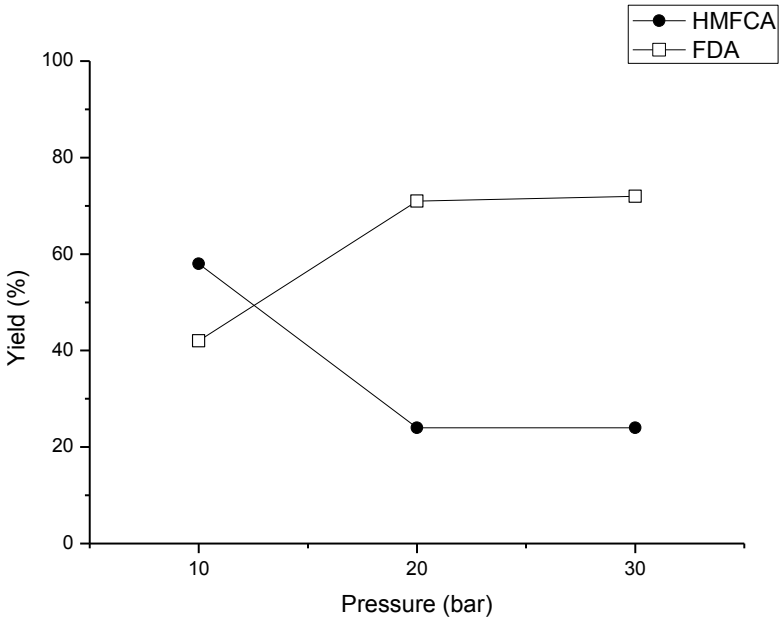

Figure 12. Product formation in aerobic HMF oxidation in aqueous solution using 1 wt% Au/TiO_2 supported catalyst as a function of the oxidant pressure. Reaction conditions: 20 equivalents NaOH, 30^{o}C, 18 hours.

As shown in Figure 12, an initial increase in the oxygen pressure from 10 to 20 bar (or 30 bar) increased the formation of FDA markedly relative to HMFCA (from 43 % to 71 %), whereas full HMF conversion was achieved at all pressures. This confirms that the aldehyde moiety of HMF is more easily oxidized than the hydroxymethyl group (thereby leading to initial formation of HMFCA), in accordance with previous findings for analogous oxidation performed in methanol [78]. As no intermediate DFF product was observed during the reaction, it further implies the final aldehyde oxidation step to FDA to be faster than the initial oxidation to aldehyde, as shown in Scheme 9.

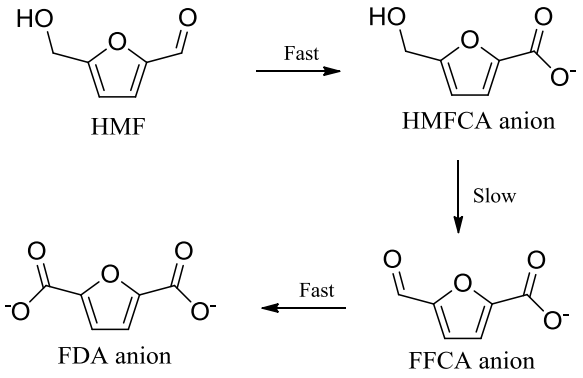

Scheme 9. Possible route for the HMF oxidation reaction *via* initial oxidation of the formyl group.

The catalyst, utilized in the reaction at 20 bars with 20 equivalents of added base, upon re-use (after filtration and drying) revealed lower activity towards the oxidation, resulting in a 5-10 % lower HMFCA conversion at comparable reaction times. ICP analysis of the post-reaction mixture confirmed this to correlate well with gold leaching (corresponding to <4 % of the original metal inventory).

Further, the oxidation reactions were performed at different temperatures in order to elucidate the temperature effect on the reaction progress. Also, gold nanoparticles supported on other oxides, *i.e.* magnesium and cerium oxides, were also briefly screened for this catalytic reaction. Selected results of these investigations are presented in Table 2.

Table 2. The yield of FDA in the oxidation of HMF in water at ambient pressure.[a]

Entry	1 wt% catalyst	Temperature, °C	Catalyst amount, mol% to HMF	NaOH, equivalents	Reaction time, hours	FDA yield, %
1		120	1	10	2	52
2		130	1	10	1	50
3	Au/TiO_2	130	1	10	2	57
4		130	1	10	18	72
5		140	1	10	2	58
6	Au/MgO	30	1	0	18	11
7		30	2	0	18	14
8		30	1	0	18	1
9	Au/TiO_2	30	2	0	18	2
10		30	1	10	18	44
11		30	2	10	18	99
12	Au/CeO_2	30	2	10	18	99

[a]Reaction conditions: 10 mL of 0.1 M solution of HMF in H_2O, 10 bar O_2. Yields of other products are not presented.

Here, firstly the temperature effect was investigated by performing the reaction at 120, 130 and 140°C (Table 2, entries 1-5). It is seen that the yields of FDA after 2 hours of reaction time are quite close at all three applied temperatures (*ca.* 55 %; Table 2, entries 1, 3, 5) (with complete HMF conversion in all experiments). Alas, the formation of formic acid was observed, *e.g.* increasing from 6 % to 8 % after 1 and 2 hours of reaction time at 130°C, respectively. By extending the reaction time at 130°C a 72 % yield of FDA was obtained (entry 4); however in this case the second major product was found to be formic acid (*ca.* 25 % yield), as also was later found by Corma *et al.* [44].

Furthermore, gold nanoparticles were deposited on magnesium oxide and applied in the aerobic oxidation of aqueous HMF (Table 2, entries 6-7). The goal here was to

investigate the possibility of avoiding the usage of homogeneous base (NaOH) by introducing a catalyst supported on basic oxide (MgO). As can be seen from the obtained results, a minor formation of FDA was observed under applied conditions (with *ca.* 50 % of HMF remaining unconverted). Increasing the catalyst amount from 1 to 2 mol% did not significantly increase the yield of FDA (HMF was fully converted, and the main product was found to be formic acid with the yield of *ca.* 40 %).

For comparison, experiments under similar conditions in the absence of added base were conducted with titania-supported gold catalyst (Table 2, entries 8-9). Yields of FDA here constituted 1 and 2 % for 1 and 2 mol% of the catalyst introduced in the reaction, respectively. Thus, gold nanoparticles deposited on a basic support exhibited higher activity in the oxidation of HMF to FDA compared to the TiO_2 supported ones.

The increase of the catalyst amount twice (entries 10-11) resulted in the FDA yield of 99 %. The same result was observed for CeO_2-supported gold catalyst (Table 2, entry 12).

Analogously to the examined oxidation of HMF in methanol, several experiments aimed at the investigation of the possibility of HMF oxidation in water at ambient pressure were conducted. Here, a comparison of the product distribution in time was made by performing the oxidation reaction at 25 and 50^{o}C under ambient pressure of oxygen with 0.157 g (8 μmol Au) of the 1 wt% Au/TiO_2 catalyst. In Figure 13, selected product yields (HMFCA formation at 50^{o}C not shown) are plotted against reaction time; HMF was fully converted after 24 hours.

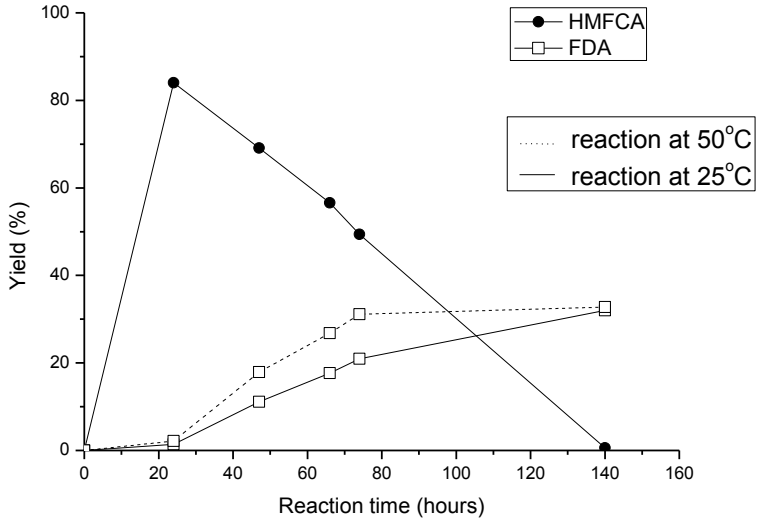

Figure 13. Product formation in aerobic HMF oxidation in aqueous solution using 1 wt% Au/TiO_2 supported catalyst as a function of reaction time. Reaction conditions: 10 mL of 0.1 M solution of HMF, 20 equivalents NaOH, O_2 flow (1 atm), 0.157 g of 1 wt% Au/TiO_2 catalyst.

It can be seen from the obtained data that the increase in temperature from 25 to 50°C increased the speed of FDA formation. Indeed, the yield of FDA after 72 hours of reaction time constituted 20 % and 30 % at 25 and 50°C, respectively.

Furthermore, as an attempt to perform the reaction with decreased amounts of base and catalyst, HMF was oxidized in water at 25°C with 2.5 equivalents of added sodium hydroxide and 0.02-0.079 g (1-4 μmol Au) of 1 wt% Au/TiO_2 catalyst. Table 3 shows the product yields in the respective reactions.

Table 3. Product yields in the oxidation of HMF in water at ambient pressure.[a]

Entry	Catalyst amount, g	Yield, %		
		FDA	HMFCA	FA
1	0.02	2	95	2.5
2	0.079	20	77	2

[a]Reaction conditions: 10 mL of 0.1 M solution of HMF in H_2O, 2.5 equivalents of NaOH, 25°C, O_2 flow (1 atm), 48 hours.

It is clearly seen from the obtained data that in the HMF oxidation under the atmospheric pressure of dioxygen under applied conditions after 24 hours of reaction time with 0.157 g of 1 wt% Au/TiO_2 and 20 equivalents of NaOH, and after 48 hours with 0.02 g of 1 wt% Au/TiO_2 and 2 equivalents of NaOH the major product was HMFCA (Figure 13; Table 3, entries 1-2). Moreover, increasing the amount of the introduced catalyst times four (Table 3, entry 2), as expected, facilitated further oxidation of HMFCA to FDA, thus increasing the selectivity towards FDA within the observed time period. The obtained data supports the hypothesis of HMF oxidation occurring in two steps, with a slow step of HMFCA formation *via* the initial oxidation of the aldehyde functionality (Scheme 9), as was previously shown for the oxidation of HMF in methanol under ambient pressure and temperature [47].

4.2.4. Conclusions

In conclusion, the oxidation of aqueous HMF to FDA and HMF to FDMC in methanol solutions with heterogeneous supported gold catalysts and oxygen in the presence of base have been investigated. Under optimized reaction conditions, a supported 1 wt% Au/TiO_2 catalyst was found to oxidize HMF in methanol into FDMC in 100 % yield (with 81 % isolated yield) at 130°C in 6 hours with 4 bar of oxygen. A procedure for the purification/isolation of FDMC was developed.

Additionally, the oxidation of HMF at ambient oxygen pressure and temperature was shown to lead almost exclusively to a formation of HMMF. The use of different bases and other titania-supported noble metals catalysts did not produce better results. Noteworthy, oxidation of HMF at similar conditions in MIBK/methanol mixture yielded in the formation of the product of oxidative dimerisation.

Aerobic oxidation of HMF in aqueous solutions was studied with gold catalysts supported on titania, magnesia and ceria. Pressure, temperature and base amount effects were investigated. Under optimized conditions, quantitative yields of FDA were obtained. Observed traces of formic acid were proposed to originate, in part, from peroxide degradation of the reagents and/or products, while base prevented deactivation of the gold catalyst and possibly also stabilized the FDA product in its anionic form.

Application of lower pressure and temperature afforded almost exclusive formation of the intermediate oxidation product HMFCA.

The reaction procedure introduced in this chapter involves HMF oxidation at ambient (in water) or elevated temperature (in water and methanol) using an abundant and environmentally friendly oxidant and solvent. Combined, these features make the protocol an interesting alternative to oxidation reactions based on stoichiometric amounts of heavy metal oxidants (*e.g.* chromium and manganese oxygenates), which traditionally have been applied to the oxidation of substrates with similar functionalities [78].

4.3. Aerobic oxidation of HMF to FDA with supported ruthenium hydroxide catalysts

4.3.1. Introduction

Numerous reactions known from literature are catalyzed by ruthenium [80-83]. Ruthenium-based catalysts are generally known for their aptitude in aerobic oxidation reactions [84-89], including applications for oxidation of alcohols to produce aldehydes or ketones. Hence, homogeneous Ru-complex catalysts have been found to generate aldehydes or ketones in almost quantitative yields when employed in organic solvents [90,91] or ionic liquids [92].

Recently, supported ruthenium hydroxide heterogeneous catalysts have recently been reported to be efficient catalysts for aerobic oxidation reactions. $Ru(OH)_x$ supported on ceria has been shown to oxidize alcohols to corresponding ketones, aldehydes and acids, and also aldehydes to acids with high yields at 80-140^{o}C at ambient air pressure [93], whereas a $Co(OH)_2$ co-promoted catalyst afforded high activity even at room temperature [94]. Kozhevnikov *et al.* [95] performed oxidation of primary alcohols to aldehydes using mixed Ru-Co oxide with 95 % yield in toluene at 110^{o}C under oxygen atmosphere. Similarly, a ruthenium-functionalized nickel hydroxide composite catalyst ($Ru/Ni(OH)_2$) has been used to oxidize alcohols quantitatively to aldehydes or ketones in organic solvents at 90^{o}C in the presence of molecular oxygen [96].

Additionally, Kaneda *et al.* [97,98] and Mizuno *et al.* [99-103] have reported selective aerobic oxidations of aromatic and aliphatic alcohols to aldehydes and ketones and amines to amides with $Ru(OH)_x$ supported by alumina, magnetite and hydroxyapatite. Alcohols and amines were oxidized to produce aldehydes/ketones and amides/nitriles, respectively, at 80-150^{o}C under ambient pressure of O_2 in toluene or $PhCF_3$ with yields above 99 %.

Also, alumina-supported ruthenium hydroxide has been used for oxidation of alcohols in a continuous multifunctional reactor [104]. Catalyst supports with basic functionalities like *e.g.* hydrotalcite and hydroxyapatite have recently been investigated further [105,106]. Synthetic Ru-Co-Al and Ru-Al-Mg hydrotalcites have been reported to catalyze aerobic oxidation of aliphatic and aromatic alcohols in toluene at 60^{o}C under ambient dioxygen

pressure, producing aldehydes and ketones in above 90 % yield. Ruthenium- and ruthenium-cobalt-promoted hydroxyapatite gave 99 % yields [107,108].

In this section the usage of heterogeneous $Ru(OH)_x$-based catalysts in the selective aerobic oxidation of HMF to FDA is presented. Several catalysts on various common supports (*e.g.* CeO_2, Al_2O_3, ZrO_2) were prepared with different supports, characterized by EPR, XRPD, nitrogen sorption (BET area), TEM and EDS and their catalytic activity compared. Notably, the oxidations were conducted in water or ionic liquid and without the addition of base (Scheme 10). Moreover, the aerobic oxidation reactions of HMF in water with $Ru(OH)_x$ catalysts supported on three different magnesium-containing supports: MgO (magnesium oxide), $MgAl_2O_4$ (spinel) and $Mg_6Al_2(CO_3)(OH)_{16}\cdot 4H_2O$ (hydrotalcite), were studied further. The effects of reaction time, pressure and temperature on the catalytic performance were studied and optimized to obtain near quantitative yield of FDA.

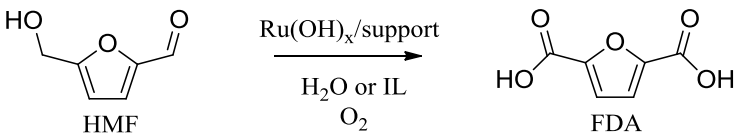

Scheme 10. Aerobic oxidation of HMF to FDA with supported $Ru(OH)_x$ catalyst in water or ionic liquid using oxygen as an oxidant with no added base.

4.3.2. Experimental

Materials: 5-Hydroxymethylfurfural (HMF) (>99 %), 2-furoic acid (98 %), levulinic acid (LA) (98 %), formic acid (FA) (98 %), ruthenium(III) chloride hydrate (purum, ~41 % Ru), hydrotalcite $Mg_6Al_2(CO_3)(OH)_{16}\cdot 4H_2O$ (HT), magnetite (Fe_3O_4) (>98 %), hydroxyapatite $Ca_5(PO_4)_3(OH)$ (HAp) (>97 %), spinel $MgAl_2O_4$, γ-aluminium oxide (>99.9 %), titanium oxide (anatase, 99.7 %), zirconium oxide (99 %), lantanum(III) nitrate hexahydrate (99.99 %), magnesium chloride (≥98 %) and sodium hydroxide (>98 %) were acquired from Sigma-Aldrich. Magnesium nitrate hexahydrate (p.a.) was obtained from Merck. Cerium(IV) oxide (99.5 %) and lanthanum(III) oxide (99.9 %) were purchased from Alfa Aesar. Magnesium oxide (p.a.) was purchased from Riedel-de Haën AG. 2,5-Diformylfuran (DFF) (98 %) was obtained from ABCR GmbH & Co. 2,5-Furandicarboxylic acid (FDA) (>99 %) and 5-hydroxymethyl-2-furan-carboxylic acid (HMFCA) (>99 %) were purchased from Toronto Research Chemicals Inc. and dioxygen (99.5 %) from Air Liquide Denmark. All chemicals were used as received.

The ionic liquids 1-ethyl-3-methylimidazolium dicyanamide ([EMIm][$(CN)_2$]) (98 %) and 1,3-dimethylimidazolium dimethyl phosphate ([MMIm][dmp]) (98 %) were purchased from Solvent Innovation, while all other ionic liquids (>95 %) were obtained from BASF. All ionic liquids were used as received.

Catalysts preparation: Magnesium-lanthanum oxide was prepared by co-precipitation and supported $Ru(OH)_x$ catalysts by deposition-precipitation procedures described elsewhere [100-103,109].

21.7 g (0.05 mol) $La(NO_3)_3\cdot 6H_2O$ and 38.4 g (0.15 mol) $Mg(NO_3)_2\cdot 6H_2O$ were dissolved in 250 mL water. Then 1 M solution of KOH was added in small portions to maintain pH around 12 over a time period of 8 hours. Hereafter, the formed precipitate was filtered, washed with water and calcined at 650°C for 6 hours.

4.876 g of support (*i.e.* TiO_2, Al_2O_3, Fe_3O_4, CeO_2, ZrO_2, MgO, $MgAl_2O_4$, HT, La_2O_3 or HAp) was added to 143 mL of 8.3 mM aqueous $RuCl_3$ solution (1.19 mmol Ru). After stirring for 15 minutes, 28 mL of 1 M NaOH solution was added and the mixtures were stirred for 18 hours. Then the catalysts were filtered off, washed thoroughly with water (colourless filtrates suggested absence of ruthenium ions) and dried at 140°C for 40 hours. A similar preparation procedure was applied for $MgO\cdot La_2O_3$ supported catalyst, except that no

base was added to the mixture. Approximately 4.9 g of each catalyst was obtained containing *ca.* 2.4 wt% Ru.

Catalyst characterization. XRPD patterns were recorded using a Huber G670 powder diffractometer (Cu-K_α radiation, λ = 1.54056 Å) in the 2θ interval 5-100^o.

EPR spectra (X band) were measured with a Bruker EMX-EPR spectrometer at room temperature with a rectangular 4102 ST cavity operating in the TE102 mode. The microwave source was a Bruker ER 041 XG Microwave bridge with frequencies around 9.22 GHz.

TEM images were recorded on a FEI Tecnai Transmission Electron Microscope at 200 kV with samples deposited on a carbon support. EDS analysis was performed with an Oxford INCA system.

Surface areas were determined by nitrogen sorption measurements at liquid nitrogen temperature on a Micromeritics ASAP 2020 pore analyzer. The samples were outgassed in vacuum at 150^{o}C for 4 hours prior to the measurements. The total surface areas were calculated according to the BET method.

ICP analysis was performed on a Perkin Elmer ELAN 6000 with cross-flow nebulizer and argon plasma.

4.3.2.1. Oxidations in water

Oxidation reactions. Oxidations were carried out in stirred Parr mini-reactor autoclaves equipped with internal thermocontrol (T316 steel, Teflon™ beaker insert, 100 mL). In each reaction the autoclave was charged with 63 mg of HMF (0.5 mmol) and 10 mL of water. Initial HMF concentration (0.05 M) solution was chosen based on experimental data on FDA solubility in water and extrapolation of this data to 140^{o}C values area. Subsequently, the supported 2.4 wt% $Ru(OH)_x$ catalyst was added (0.105 g, 0.025 mmol Ru). The autoclave was flushed and pressurized with dioxygen (1-40 bar, *ca.* 1.6-64 mmol) and maintained at 140°C for a given period of time under stirring (700 rpm). After the reaction, the autoclave was rapidly cooled with ice to room temperature. The reaction mixture was made basic with 1 mL of 1 M NaOH solution before filtering off the catalyst, or filtered directly without base,

followed by analysis using HPLC (Agilent Technologies 1200 series, Aminex HPX-87H column from Bio-Rad, 300 mm x 7.8 mm x 9 μm, flow 0.6 mL/min, solvent 5 mM H_2SO_4, temperature 60°C). In all figures where the product distribution is shown as a function of time each data point corresponds to an individual reaction run. ICP analysis was performed on diluted post-reaction mixtures and quantified with ICP standard solutions.

4.3.2.2. Oxidation in ionic liquids

Oxidation reactions: Catalytic oxidation experiments at ambient pressure were performed using a Radley Carousel 12 Plus Basic System, while high pressure oxidation reactions were carried out in stirred Parr autoclaves equipped with internal thermocontrol (T316 steel, Teflon™ beaker insert, 100 mL). All reaction samples were analyzed by HPLC.

In the catalytic screening experiments performed at ambient air pressure, catalyst (100 mg, 0.025 mmol Ru) and IL (1.0 g) were mixed in a 40 mL tube and stirred at 100-140°C for 10 minutes. HMF (70 mg, 0.56 mmol) was added and the mixture was stirred in an open flask for 24 hours. The reaction was subsequently cooled down to room temperature and diluted to 10 mL with 0.1 M NaOH. Finally, the catalyst was filtered off and the resultant solution analyzed by HPLC. In the high pressure oxidation reactions, catalyst (0.5 g, 0.125 mmol Ru), HMF (350 mg, 2.78 mmol) and IL (12.0 g) were mixed in a Parr autoclave, pressurized with dioxygen (10-30 bar) and stirred at 100-140°C for 5 hours. The reaction mixture was cooled down to room temperature and diluted to 100 mL with 0.1 M NaOH. Finally, the catalyst was filtered off and the resultant solution analyzed by HPLC.

Procedure for leaching test: Catalyst (100 mg, 0.025 mmol Ru) and [EMIm][OAc] (1.0 g) were mixed in a 40 mL tube and stirred at 100°C for 3 hours. The catalyst was filtered off affording a black colored liquid. HMF (70 mg, 0.56 mmol) was added to the liquid and the mixture was stirred in an open flask at 100°C for 24 hours. The mixture was cooled down to room temperature, diluted to 10 mL with 0.1 M NaOH, filtered and analyzed by HPLC.

4.3.3. Results and discussion

4.3.3.1. Screening of the supported $Ru(OH)_x$ catalysts for the oxidation of HMF in water

XRPD analysis of the prepared $Ru(OH)_x$ catalysts with TiO_2, CeO_2 or $MgO{\cdot}La_2O_3$ support (2.4 wt% Ru) did not reveal crystalline ruthenium oxide phases. However, at higherloading of catalytic material, corresponding to 40 wt% Ru, ruthenium dioxide was clearly found (diffractograms of $Ru(OH)_x/TiO_2$ materials are shown in Figure 14). This observation could indicate that amorphous ruthenium oxide might also be present in the 2.4 wt% Ru catalysts. Also, ruthenium content on the catalysts might have been too low to allow detection, thus revealing exclusively peaks originating from the respective supports.

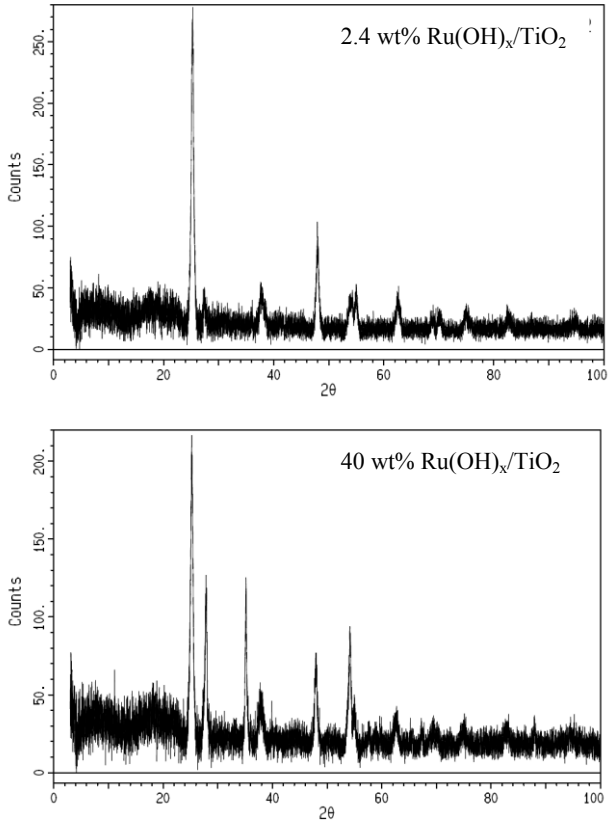

Figure 14. XRPD diffractograms of 2.4 wt% and 40 wt% $Ru(OH)_x/TiO_2$ catalysts.

In the recorded EPR spectra of the catalysts trace amounts of Ru(III) could only be identified in the hydrotalcite-supported 2.4 wt% catalyst. However, in the $Ru(OH)_X/TiO_2$ material with 40 wt% Ru, Ru(III) was also determined, thus suggesting that both Ru^{4+} and Ru^{3+} oxidation states are present in the ruthenium species [110], with Ru^{4+} as the major component.

TEM images of the prepared $Ru(OH)_x/TiO_2$ and $Ru(OH)_x/CeO_2$ catalysts are presented in Figure 15. Ruthenium species were not observed on the surface of titania, possibly due to their small size and the microscope resolution.

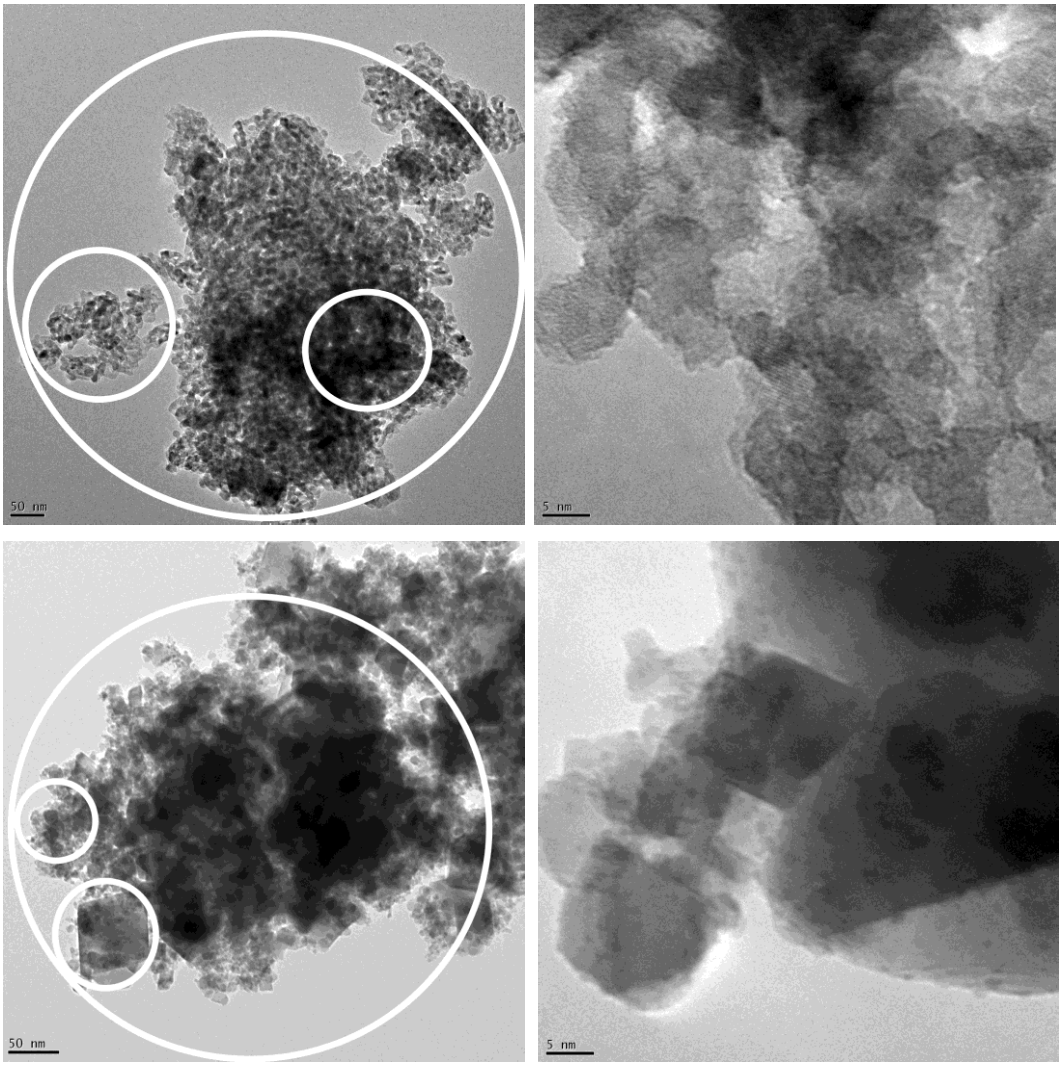

Figure 15. High-resolution TEM images of the 2.4 wt% $Ru(OH)_x/TiO_2$ catalyst (top) and 2.4 wt% $Ru(OH)_x/CeO_2$ catalyst (bottom). White circles represent the areas analyzed by EDS.

EDS analysis was performed on both whole catalyst samples and on random areas on the catalysts (see Figure 15). Atomic ratios of Ru:Ti and Ru:Ce were determined to be 1.8:98.2 and 3.7:96.3, respectively, on both the whole catalyst and random area measurements. Thus, the weight percentages of Ru on titania and ceria were found to be 2.32 and 2.26 wt%, respectively, which is in good accordance with the expected content calculated from the preparation procedure.

Previous sections describe the oxidation reaction of HMF to FDA in water or methanol solutions with added base using titania-supported gold nanoparticle catalyst. Here, the performance of $Ru(OH)_x/TiO_2$ as a catalyst in the HMF oxidation reaction in aqueous media without added base was initially investigated.

Firstly, experiments were carried out at 1 bar dioxygen pressure at 140^{o}C. After 2 hours of reaction most of the HMF remained unconverted under these reaction conditions with less than 1 % of FDA being formed. However, already at this reaction time he formation of formic acid (FA) was observed, resulting in a yield of 13.8 % which increased to 55.4 % after 20 hours of reaction, while FDA yield amounted to only 2.3 % after this reaction time. Formic acid, according to the literature, under base-free conditions may originate in acid-induced degradation of HMF and the oxidation products [36]. Thus, the yield of formic acid increases as the reaction propagates and the acidity increases.

Further, the reaction at increased oxygen pressures was investigated. The products formed in the oxidation reactions at 2.5 and 20 bar of dioxygen as a function of reaction time are presented in Figure 16a and 16b, respectively.

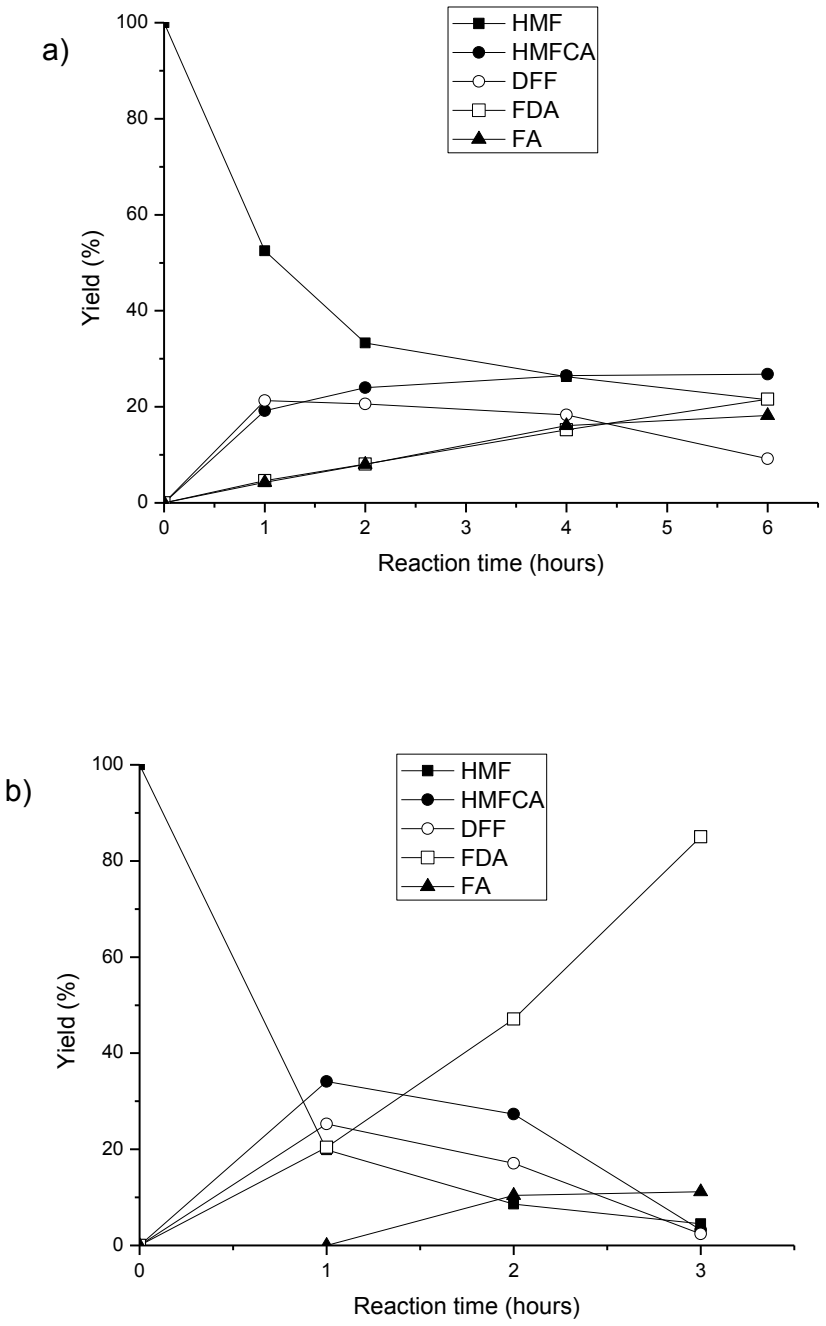

Figure 16. HMF oxidation with $Ru(OH)_x/TiO_2$ catalyst in water at (a) 2.5 bar O_2 and (b) 20 bar O_2. Reaction conditions: 10 mL of 0.05 M HMF in water, 140°C, 5 mol% Ru.

Two intermediate oxidation products were observed; 2,5-diformylfuran (DFF) and 2-hydroxymethyl-5-furancarboxylic acid (HMFCA), thus suggesting a competitive reaction

pathway for HMF oxidation with intermediate product formation of DFF and HMFCA, respectively, followed by oxidation to FDA (Scheme 11).

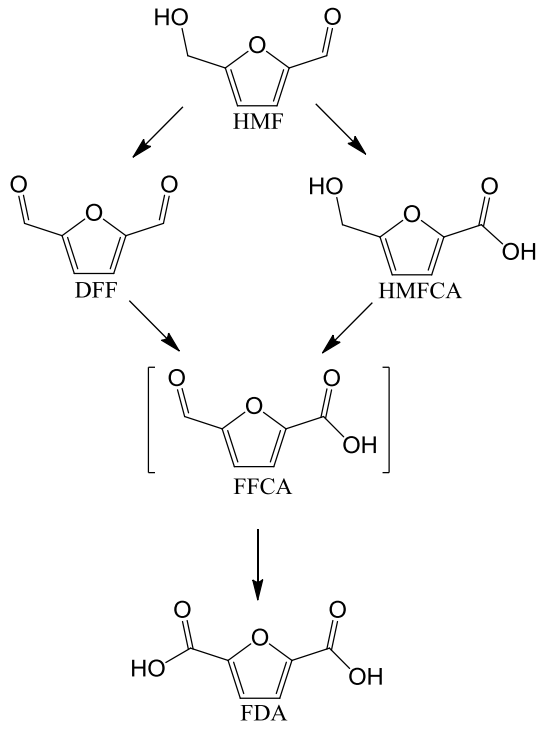

Scheme 11. Reaction pathway from HMF to FDA by aerobic oxidation *via* the competitive formation of the two intermediate products DFF and HMFCA

At both examined oxygen pressures high amounts of formic acid were formed, as was also found for Au/TiO_2-catalyzed oxidation in the presence of base. Nevertheless, at 20 bar of dioxygen the formation of FDA occured significantly faster than at 2.5 bar with the $Ru(OH)_x/TiO_2$ catalyst, whereas the reaction rate for degradation did not seem to increase. Thus, by performing oxidation of HMF in water solutions with $Ru(OH)_x/TiO_2$ catalyst at elevated pressure, it proved possible to obtain high selectivity towards 2,5-furandicarboxylic acid and high substrate conversion, while avoiding the formation of degradation by-products, such as formic (FA) and levulinic (LA) acids.

Subsequently, different metal oxide supports, spinel ($MgAl_2O_4$), hydrotalcite (HT; $Mg_6Al_2(CO_3)(OH)_{16}{\cdot}4(H_2O)$) and hydroxyapatite (HAp; $Ca_{10}(PO_4)_6(OH)_2$) were screened in

order to find a system with supported $Ru(OH)_x$ species that could provide high selectivity towards desirable oxidation products.

Characteristics of the screened supports and corresponding catalysts are compiled in Table 4. The surface areas of the catalysts were very much dependent on the choice of the metal oxide and, as expected, a small decrease in the surface areas was observed between the pure supports and the final catalysts.

The results obtained in HMF oxidation with the catalysts are shown in Figure 17.

Table 4. Supports applied for the oxidation of aqueous HMF to FDA with heterogeneous 2.4 wt% $Ru(OH)_x$ catalysts.

Catalyst support	Support surface area, m^2/g	Catalyst surface area, m^2/g	Reaction time, hours	pH after reaction
TiO_2	123	128	6	2
Al_2O_3	149	145	6	2
Fe_3O_4	44	45	6	2
ZrO_2	53	97	6	2
CeO_2	62	8	6	2
CeO_2 (blank)	62	-	18	3
MgO	30	27	6	10
La_2O_3	59	5	6	8
$MgAl_2O_4$	63	53	6	2
HT	8	6	6	7
HAp	17	25	6	3
$MgO{\cdot}La_2O_3$	30	68	6	8
w/o catalyst	-	-	18	1

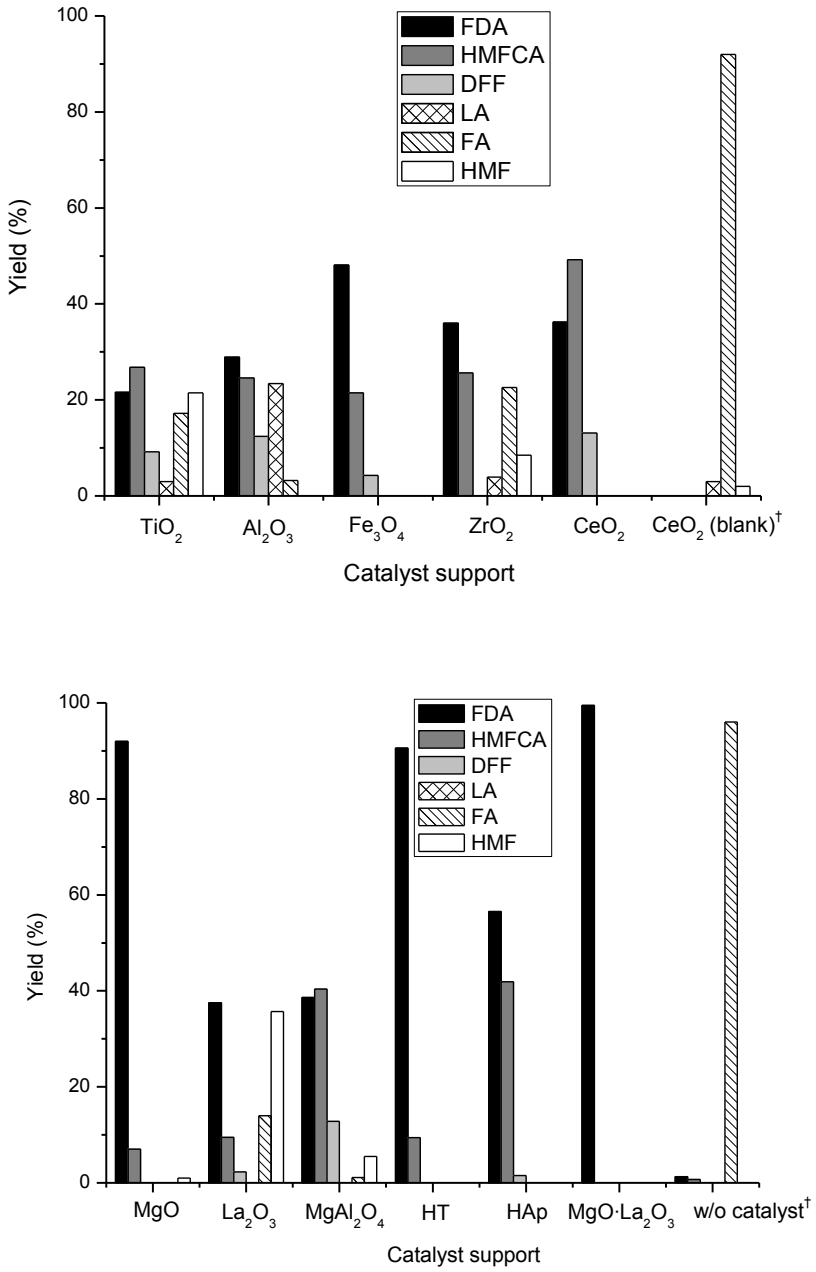

Figure 17. Product yields in HMF oxidation reaction with $Ru(OH)_x$/support catalysts. Reaction conditions: 10 mL of 0.05 M HMF, 2.5 bar O_2, 140°C, 6 hours, 5 mol% Ru. †Reaction time was 18 hours.

As seen in Figure 17, catalysts with basic magnesium-containing supports generally showed high efficiency in HMF to FDA oxidation, whereas the usage of other oxides (*e.g.* ZrO_2 and Al_2O_3) induced the formation of formic acid. Fe_3O_4- and hydroxyapatite-supported

$Ru(OH)_x$ catalysts revealed good selectivities towards FDA formation, however in both cases formation of solid humins was observed constituting approximately 30 % of the mass balance.

The supported catalysts with basic carrier materials, *i.e.* MgO, $MgO{\cdot}La_2O_3$ and HT gave excellent selectivities and substrate conversions resulting in FDA yields above 95 %. However, ICP analysis of the post-reaction solutions showed presence of magnesium ions, indicating that the support dissolved to a certain extent during reaction [111]. This was also confirmed by the relative high pH values measured in post-reaction mixtures with these supports, which was obtained from basic hydroxides formed upon dissolution of the support accompanied by formation of salts of the acid products.

The presence of magnesium, usually in an ionic form, is known to stabilize or even facilitate the activity several enzymes [112,113], including the enzyme that transforms glucose to fructose (glucose isomerase) [114]. Thus, an investigation of possibility of involving of magnesium ions in the oxidation of HMF to FDA has certain interest, since HMF can be produced from fructose, which in turn can be derived from glucose, as was mentioned above (see Scheme 1).

In order to elucidate the effect of the magnesium-containing supports, a control experiment was conducted in which $Ru(OH)_x/TiO_2$ catalyst was used together with two molar equivalents of $MgCl_2$. The reaction was carried out at reaction conditions identical to the support screening experiment conditions (10 mL of 0.05 M HMF, 2.5 bar of O_2, 140^{o}C, 6 hours). Although HMF was fully converted in the control experiment, only 3 % and 2 % of FDA and HMFCA were formed, respectively, while the rest constituted by formic acid. This strongly suggested that the support played an important role with respect to the catalyst performance, rather than simply providing magnesium ions.

A similar picture was also observed in a blank experiment when no catalyst was introduced into the reaction mixture. Here, formic acid was formed in 92 % yield, while yield of FDA and other oxidation products was less than 1 %.

More detailed investigation of the performance of the catalysts supported on MgO, spinel and hydrotalcite is described in the next section (4.3.3.2).

Apart from magnesium-containing supports, good oxidation performance was also observed for ceria-supported catalyst, as seen in Figure 17. Although selectivity towards FDA was only moderate in the time frame of 6 hours, no degradation products were

observed. Hence, $Ru(OH)_x/CeO_2$ was tested as a catalyst in the HMF oxidation at different pressures (Figure 18).

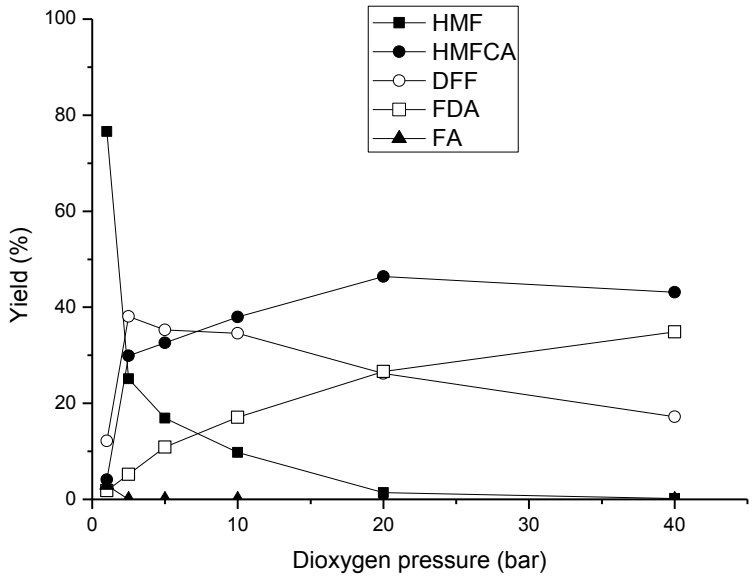

Figure 18. HMF oxidation with $Ru(OH)_x/CeO_2$ catalyst in water at different dioxygen pressures. Reaction conditions: 10 mL of 0.05 M HMF, 140°C, 1 hour, 5 mol% Ru.

The obtained data clearly suggested that it was possible to avoid formation of undesirable degradation products by use of elevated pressures, whereas ambient pressure (*i.e.* 1 bar of O_2) led to formation of 3 % formic acid after 1 hour of reaction. Therefore, with a desire to perform the reaction at lowest possible pressure, we investigated the product formation over time at 2.5 bar pressure. The results are presented on Figure 19.

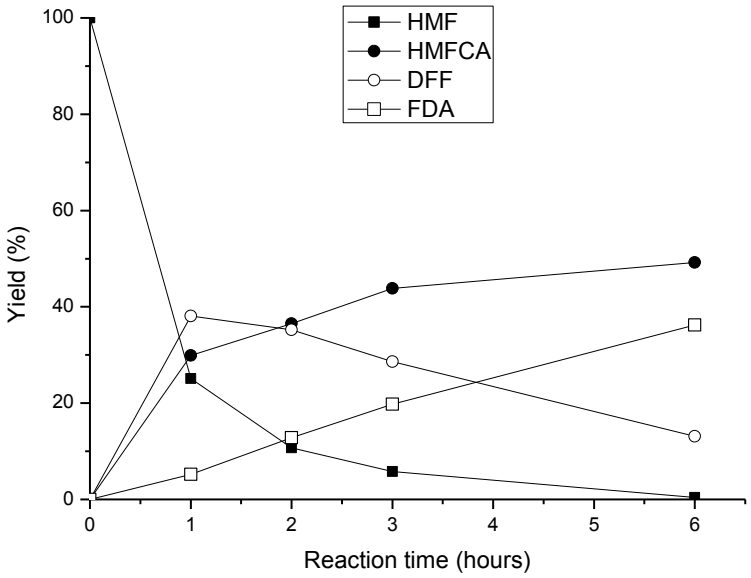

Figure 19. HMF oxidation with $Ru(OH)_x/CeO_2$ catalyst in water. Reaction conditions: 10 mL of 0.05 M HMF, 140°C, 2.5 bar O_2, 5 mol% Ru.

As observed from Figure 19, the FDA yield constituted 38 % under applied conditions after 6 hours, which is higher than the FDA yield observed when $Ru(OH)_x/TiO_2$ was used as the catalyst under the same reaction conditions (see Figure 16a). The yield of FDA increased to 60 % after 18 hours of reaction. However, HMFCA contributed 10 % to the mass balance, and neither formic acid nor levulinic acid were detected in the post-reaction mixture, possibly due to the degradation of the formed FA and LA at the extended reaction times.

Importantly, upon re-use the $Ru(OH)_x/CeO_2$ catalyst revealed no loss of activity, providing 38 % and 36 % yield of FDA after 6 hours of reaction in second and third runs, respectively. This clearly demonstrated the applicability of the ceria-supported catalyst system, and supported the study performed by Corma *et al.* [44], in which gold nanoparticles deposited on ceria showed superior performance in aerobic oxidations compared to Au/TiO_2 in the absence of base.

4.3.3.2. Ruthenium hydroxide catalysts with magnesium-based supports for the oxidation of HMF to FDA in water with no added base

As mentioned in the previous section, a more detailed study has been conducted for the catalysts deposited on three magnesium-based supports: MgO, $MgAl_2O_4$ and hydrotalcite (HT).

The BET surface areas of the applied support materials and the prepared catalysts are listed in Table 4 (see section 4.3.3.1). Representative high-resolution transmission electron microscopy (HR-TEM) images of the prepared catalysts are presented in Figure 20. Mainly agglomerated crystallites of the respective supports were observed on the TEM images with almost no noticeable ruthenium particles. EDS analysis of the catalyst samples (performed on the parts shown in white circles) revealed an uneven distribution of ruthenium species on the surfaces of the catalysts with highest basicity, *i.e.* magnesium oxide and HT. The measured Ru contents are compiled in Table 5.

Table 5. Ruthenium content of the supported $Ru(OH)_x$ catalysts.

Material	Ru content, wt%[a]
$Ru(OH)_x/MgO$	0.75 (1), 2.48 (2)
$Ru(OH)_x/MgAl_2O_4$	2.41 (1), 2.42 (2)
$Ru(OH)_x/HT$	0.25 (1), 7.55 (2)

[a]Based on Ru:Al atomic ratios provided by EDS. The values of (1) and (2) are related to the areas numbered 1 and 2 on Figure 20 for the respective support.

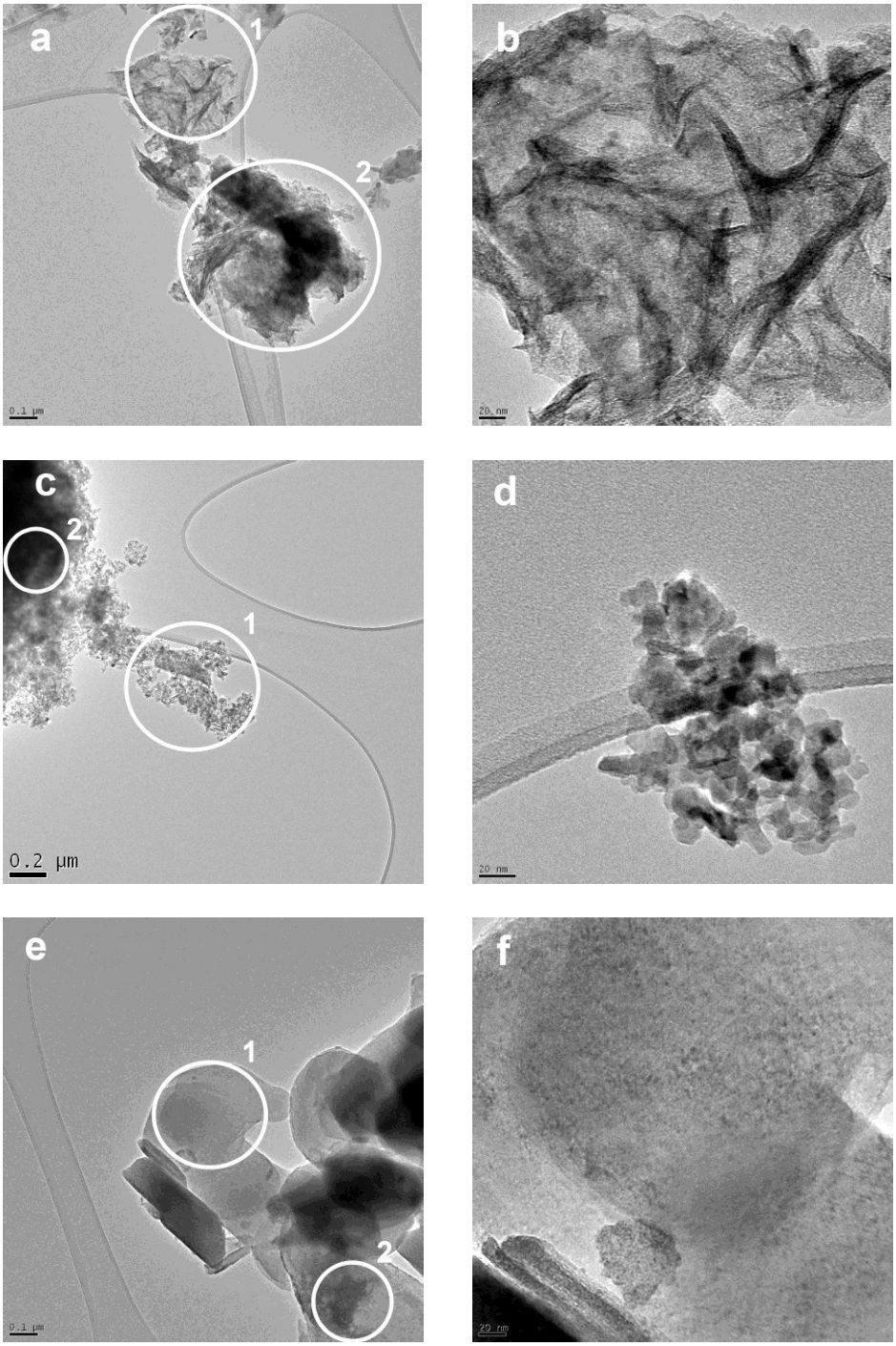

Figure 20. High-resolution TEM images of $Ru(OH)_x/MgO$ (a,b), $Ru(OH)_x/MgAl_2O_4$ (c,d) and $Ru(OH)_x$/HT (e,f) catalysts. White circles represent the areas analyzed by EDS.

Initially, the catalyzed oxidation of HMF to FDA was investigated with $Ru(OH)_x$/HT catalyst in water in the absence of added base at 1 bar dioxygen pressure and a reaction temperature of 140°C. In Figure 21 the formation of products is shown as a function of reaction time.

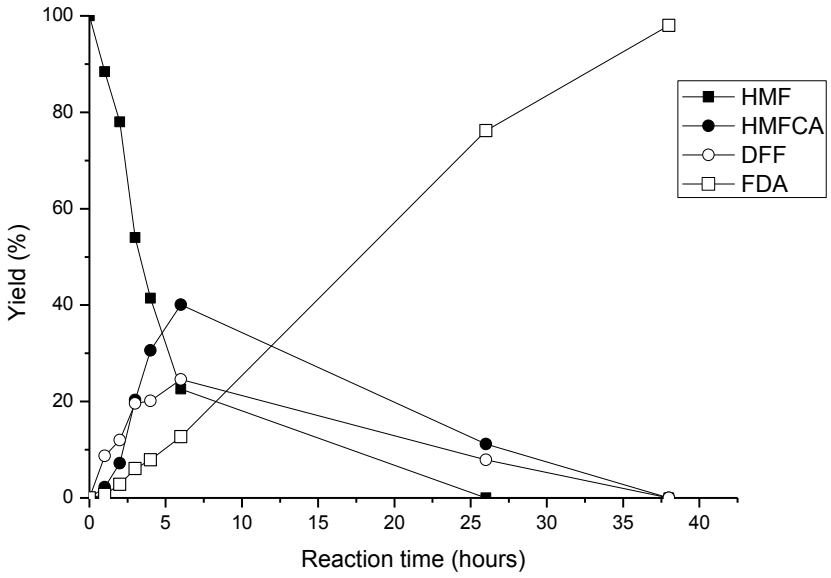

Figure 21. Product yields in HMF oxidation with $Ru(OH)_x$/HT catalyst in water under 1 bar of O_2. Reaction conditions: 10 mL of 0.05 M HMF, 140°C, 5 mol% Ru.

As seen in the figure, HMF was fully converted after 26 hours of reaction and a quantitative yield of FDA was obtained after a reaction time of 38 hours. Importantly, no product degradation was observed during the examined time period. Both rates of the formation and subsequent oxidation of HMFCA and DFF appeared to be similar under applied reaction conditions (i.e., 140°C and 1 bar of O_2 pressure).

Figure 22 shows the distribution of oxidation products obtained after oxidation of HMF for 1 hour with $Ru(OH)_x$/HT catalyst at oxygen pressures of 1-40 bar and constant reaction temperature of 140°C. As shown in the figure, it proved possible to get full conversion of HMF within one hour by increasing the pressure of oxygen. Moreover, it is evident from the low pressure results that the oxygen pressure effect was larger on DFF formation than on

HMFCA formation (*i.e.* higher reaction order of oxygen in the rate expression for DFF formation), resulting in a higher rate of oxidation of the alcohol moiety on HMF compared to the aldehyde group. When performing the reaction at 10 bar for 1 hour DFF was formed with a relatively high selectivity of about 75 %.

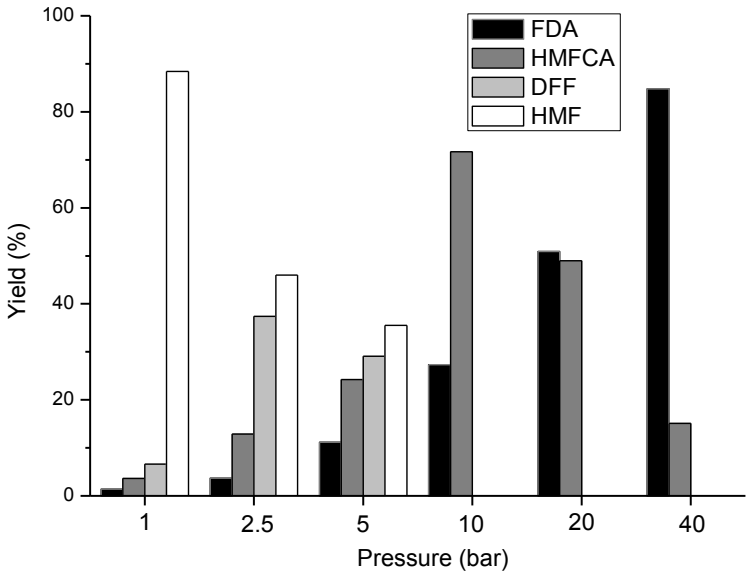

Figure 22. Product yields in HMF oxidation with $Ru(OH)_x$/HT catalyst in water. Reaction conditions: 10 mL of 0.05 M HMF, 1 hour, 140°C, 5 mol% Ru.

In order to elucidate the temperature effect on product formation, series of experiments were performed with $Ru(OH)_x$/HT catalyst with a reaction of 6 hours with 2.5 bar of oxygen at different reaction temperatures. The results are presented in Figure 23.

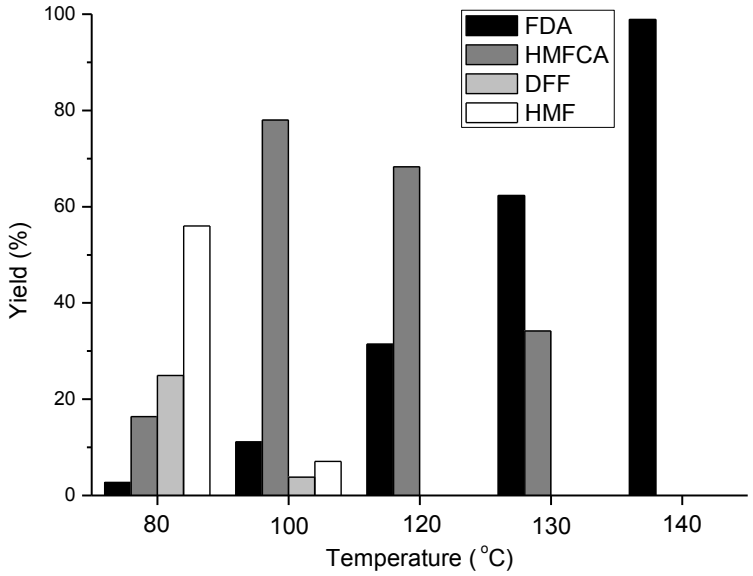

Figure 23. Product yields in HMF oxidation with $Ru(OH)_x$/HT catalyst in water. Reaction conditions: 10 mL of 0.05 M HMF, 6 hours, 2.5 bar O_2, 5 mol% Ru.

The reaction temperature drastically affected the performance of the catalyst which converted essentially all the HMF within 6 hours at 100°C and above. The major product formed at 100°C was HMFCA (*ca.* 80 % yield, with a selectivity of approximately 85 %) while only low amounts of FDA and DFF were formed (5-8 %). However, at higher temperature (140°C) only FDA was observed at almost quantitative yield. Here, the absence of DFF after 6 hours of reaction time is most likely a result of easier oxidation of the aldehyde functionality [75].

The stability of HMF under applied reaction conditions was confirmed by conducting an experiment with pure HT support. Here HMF remained essentially unconverted with only *ca.* 2 % of HMF been oxidized and converted to HMFCA (1.3 %) and FDA (0.7 %), respectively.

To examine the effect of the support on the catalytic activity for the ruthenium-catalyzed conversion of HMF to FDA, MgO- and $MgAl_2O_4$-supported $Ru(OH)_x$ catalysts were prepared and tested in the oxidation reaction (characteristics of the supports and catalysts are shown in Table 4). The performance of the catalysts was tested under 2.5 bar of

dioxygen and 140°C, which was shown to be optimal reactions conditions for the HT supported catalyst (see Figure 23). The obtained product yields as a function of reaction time are presented in Figure 24a-c.

The results in Figure 24 demonstrate that $Ru(OH)_x$ supported on MgO or HT under applied reaction conditions was able to convert almost all of HMF to FDA, as expected. However, for the $Ru(OH)_x/MgAl_2O_4$ catalyst (Figure 24c) the activity was lower, resulting in a yield of 60 % of FDA after 42 hours. Furthermore, a substantial amount (35 %) of formic acid was formed after 42 hours with this catalyst. Interestingly, no degradation products were observed when the more basic supports, magnesium oxide and hydrotalcite, were used. Recently, Corma and co-workers reported that usage of ceria-supported gold catalyst in HMF oxidation in basic aqueous media led to formation of both ring-opening degradation products and 2-furoic acid [44].

To increase the yield of FDA and limit the formation of formic acid when using $Ru(OH)_x/MgAl_2O_4$, the effect of dioxygen pressure on the HMF oxidation was further investigated. The product yields of the reactions performed at 140°C with a reaction time of 1 hour are shown on Figure 25.

Using the $Ru(OH)_x/MgAl_2O_4$ catalyst, the yield of HMFCA and FDA increased when the dioxygen pressure was increased, especially up to 5 bar as also found for the $Ru(OH)_x$/HT catalyst (see Figure 22). Notably, an increase in dioxygen pressure from 1 to 2.5 bar resulted in significantly lower formation of formic acid – from 15 to 0.1 %. Based on this observation, the time dependence experiment with the spinel-based catalyst was performed this time at 5 bar (Figure 7) instead of 2.5 bar (see Figure 24c) in order to minimize the byproduct.

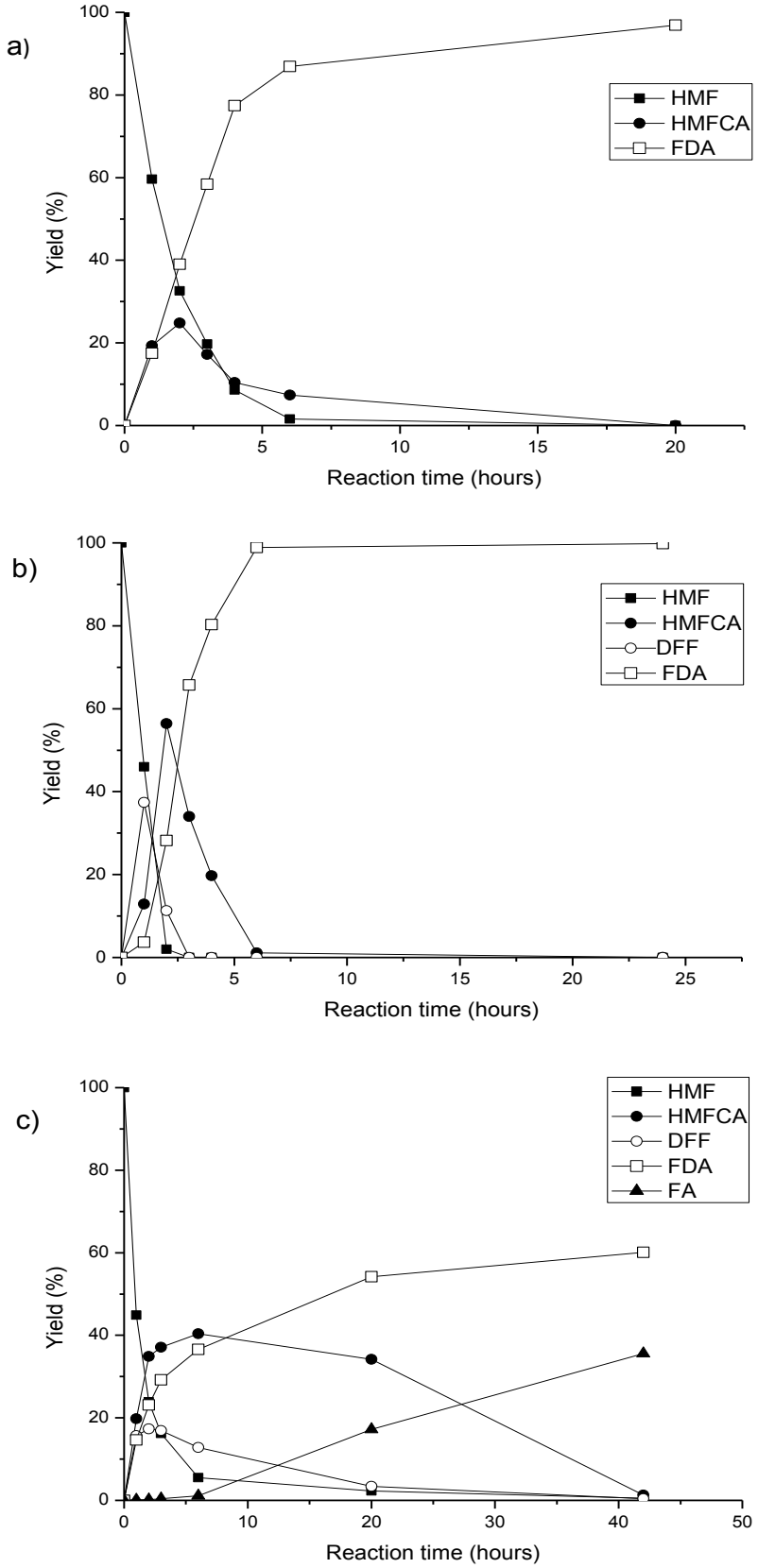

Figure 24. Product yields in HMF oxidation with $Ru(OH)_x$ catalysts in water supported on a) MgO, b) HT or c) $MgAl_2O_4$. Reaction conditions: 10 mL of 0.05 M HMF, 2.5 bar O_2, 140°C, 5 mol% Ru.

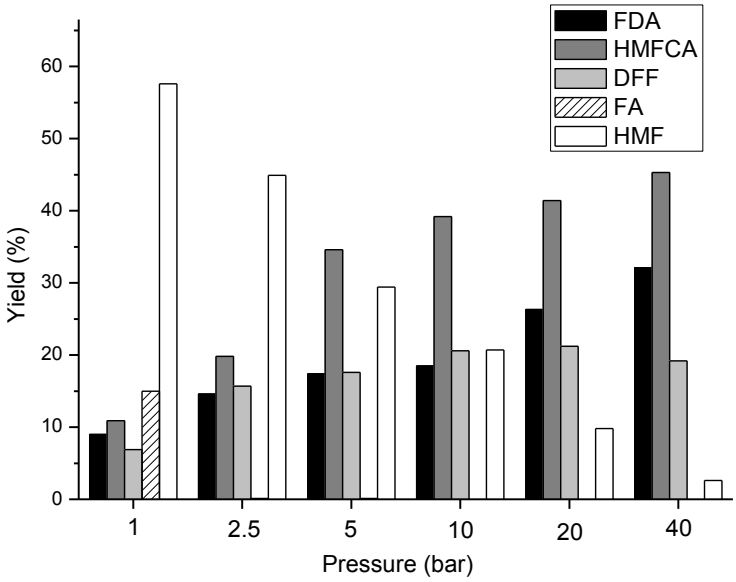

Figure 25. Product yields in HMF oxidation with $Ru(OH)_x/MgAl_2O_4$ catalyst in water. Reaction conditions: 10 mL of 0.05 M HMF, 1 hour, 140°C, 5 mol% Ru.

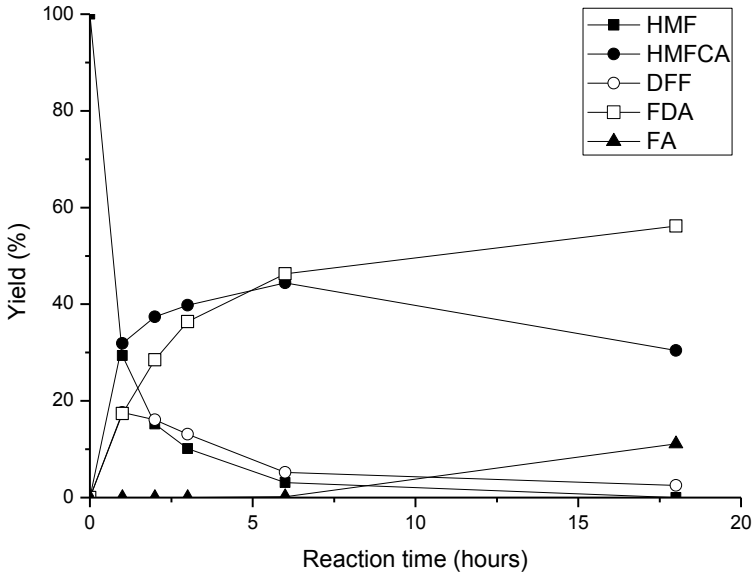

Figure 26. Product yields in HMF oxidation with $Ru(OH)_x/MgAl_2O_4$ catalyst in water under 5 bar O_2. Reaction conditions: 10 mL of 0.05 M HMF, 140°C, 5 mol% Ru.

From Figures 24c and 26 it is clear that at both 2.5 and 5 bar of dioxygen pressure formic acid formation initiated as the reaction progressed and high relative concentration of the products (*i.e.* HMFCA, DFF and FDA) accumulated. This indicated that a gradual increase in acidity of the media due to FDA formation could induce furan cycle decomposition. To understand these results in more detail, a control experiment with only $Ru(OH)_x/MgAl_2O_4$ catalyst and FDA (10 mL H_2O, 0.078 g (0.5 mmol) FDA, 2.5 bar O_2, 140°C, 16 hours) was performed to test the stability of FDA in the presence of the catalyst. The experiment revealed that 78 % of the initial amount of FDA remained unconverted after the 16 hours of reaction whereas partial degradation led to formation of 18 % formic acid. This clearly established the formic acid – at least partially – to originate from FDA, and possibly also from HMF or the intermediate products HMFCA and DFF. Accordingly, it is possible to limit the formation of formic acid in the reaction when using $Ru(OH)_x/MgAl_2O_4$ catalyst by applying short reaction time and high relative dioxygen pressure.

As was shown in the Figure 24, application of different magnesium-containing supports resulted in different amounts and distributions of products. To understand this difference post-reaction solutions from experiments with each of the catalysts were analyzed by ICP for magnesium and ruthenium content (Table 6).

Table 6. ICP analysis of the post-reaction solutions from the aerobic HMF oxidation using supported $Ru(OH)_x$ catalysts.[a]

Entry	Support	$[Mg^{2+}]$, g/L	Mg dissolved, %[c]	$[Ru^{n+}]$, mg/L	Ru dissolved, %[d]	pH[e]
1[b]	HT	0.980	26	0.030	0.013	7
2[b]	MgO	1.590	38	0.035	0.015	10
3[c]	$MgAl_2O_4$	0.157	0.9	0.046	0.020	2

[a]Reaction conditions: 10 mL of 0.05 M HMF, 2.5 bar O_2, 140°C, 5 mol% Ru. [b]Measured after 6 hours of reaction. [c]Measured after 42 hours of reaction. [d]Based on the overall element loading. [e]Measured pH values of the post-reaction solutions.

The ICP analysis confirmed presence of magnesium ions in all post-reaction solutions. Especially, for the HT- and MgO-supported catalysts (Table 6, entries 1 and 2) the amount of leached magnesium was high (26-38 %). Notably, the concentration of Mg^{2+}-ions leached from the HT-supported catalyst corresponded to approximately the amount (*i.e.* concentration) of FDA formed, thus indicating that the HT support acted as a solid base in the reaction and ionized the FDA to form a Mg-salt which most likely proved more stable towards degradation.

For the MgO support a similar tendency was also observed. The fact that HT dissolved during reaction and neutralized some of the formed FDA also explains the otherwise unexpected neutral pH value measured of the post-reaction solution. Similarly, the high pH value of 10 in the post-reaction solution with magnesium oxide support can be associated with its enhanced dissolution under the reaction conditions (Table 6, entry 2).

As the basicity of the respective support decreases in the order MgO>HT>$MgAl_2O_4$ [115], the absence of the DFF product in the HMF oxidation reaction with magnesium oxide support (Figure 24a) might be further explained by the highly basic media (Table 6), possibly facilitating Cannizzaro reaction of the dialdehyde.

The XRD analysis of the isolated Mg-FDA salt crystals showed it to be identical to the magnesium salt of FDA obtained from the dissolution of FDA in water with magnesium carbonate (see section 1.3).

In contrast to the HT and MgO supports, the spinel support remained significantly more stable under the reaction conditions permitting only a small amount (0.9 %) of the magnesium to dissolve in the acidic post-reaction solution. Accordingly, the formation of formic acid when using $MgAl_2O_4$ support can be rationalized to be related to lower stability and higher degradation of FDA and HMF in acidic media. In line with this, no degradation of substrate were observed in reactions with catalysts based on the HT and MgO supports, since the solutions here were maintained at high pH throughout the reactions due to partial dissolution of the supports. Additionally, the results of the XRPD analysis did not reveal any change in the spinel structure after the reaction (see Appendix).

In Table 6 the measured amounts of ruthenium in the post-reaction solutions are also reported. Importantly, only an extremely small amount (0.01-0.02 %) of the ruthenium metal on the catalysts was dissolved in the examined post-reaction solutions, thus making especially the $Ru(OH)_x/MgAl_2O_4$ catalyst prone for re-use. Hence, an experiment was

performed where this catalyst was recovered by filtration, washed with base and water (to remove any FDA precipitated on the surface of the catalyst after cooling down the reaction mixture) and re-used. Results are shown in Figure 27.

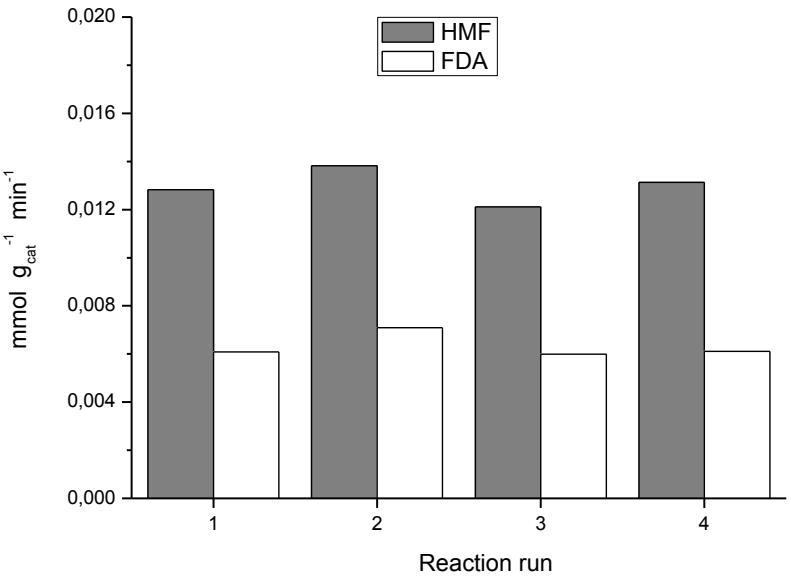

Figure 27. Rates of HMF conversion and FDA formation per gram of the catalyst in the recycling of $Ru(OH)_x/MgAl_2O_4$ catalyst in water. Reaction conditions: 0.05 M HMF, 5 bar O_2, 140°C, 5 mol% Ru, 6 hours of reaction time.

As seen from the results, the spinel-supported ruthenium catalyst preserved its initial activity even in the fourth catalytic cycle. Indeed, in the first run the conversion of HMF conversion and FDA yield constituted *ca.* 95 and 50 %, respectively. The rates of both substrate conversion and final product yield remained virtually the same in four catalytic cycles (Figure 27).

4.3.3.3. Oxidation of HMF to FDA with supported $Ru(OH)_x$ catalysts in ionic liquids

Ionic liquids (ILs) present an interesting alternative to conventional molecular solvents due to their negligible vapor pressure, redox stability, non-flammability and unique abilities for dissolving polar compounds [116]. The redox stability allowed oxidations in ILs to be widely studied for several applications, such as the oxidative Glaser coupling, oxidations of alcohols to aldehydes or ketones and the oxidation of alkanes [117-120]. Several examples of epoxidations of alkenes [121] and other functional group transformations in ILs are also found in literature [122-124]. In most cases, the applied oxidant is H_2O_2, however the usage of stoichiometric reagents such as NaOCl, Dess-Martin periodate, MnO_2 and *meta*-chloroperoxybenzoic acid (*m*CPBA) have also been reported. The most commonly employed ILs are 1-butyl-3-methylimidazolium tetrafluoroborate ([BMIm][BF_4]) and 1-butyl-3-methylimidazolium hexafluorophosphate ([BMIm][PF_6]).

The ideal oxidant for green chemical processes is molecular oxygen and aerobic oxidations with homogeneous catalysts in ILs have been reported in numerous studies [92,125–132].

The synthesis of HMF from sugars benefits particularly from using certain ILs as solvents, thus determining an overall process from HMF to FDA in ILs to be advantageous [26]. In addition, the exceedingly low solubility of FDA in water and other conventional solvents makes an oxidation process of HMF in ILs by the use of heterogeneous catalysts an attractive option [133]. In such a process the catalyst would be filtered off after the reaction, followed by the addition of water to the resulting IL/FDA mixture forcing FDA to precipitate. Water would then be evacuated and the IL recycled.

To the best of our knowledge, no investigation of heterogeneous catalysts for the aerobic oxidation of HMF in ILs has been reported. This section of the thesis presents a study, the objective of which was to investigate the possibility of performing the aerobic oxidation of HMF to FDA with heterogeneous $Ru(OH)_x$ catalysts on different supports in ILs, as well as catalysts' stability and performance. The reaction was studied at different reaction conditions and leaching tests of ruthenium were made to investigate the stability of the catalyst in ILs.

Previously it was shown by Riisager *et al.* that the ILs best suited for the synthesis of HMF from fructose or glucose were 1-ethyl-3-methylimidazolium chloride ([EMIm]Cl) and

1-butyl-3-methylimidazolium chloride ([BMIm]Cl) [26]. Hence, here [EMIm]Cl was initially applied for the screening of $Ru(OH)_x$ catalysts supported on different carriers for the HMF oxidation at ambient pressure. Relatively high temperature of 140°C was used to reduce the impact of viscosity of the mixture formed between the catalyst and IL. Since the screening was performed to allow comparison of the influence of the different types of catalyst supports, the reduced solubility of oxygen in the ILs at elevated temperature was disregarded. The results are presented in Table 7.

Table 7. HMF oxidation in [EMIm]Cl with $Ru(OH)_x$ catalysts on various supports.[a]

Entry	Catalyst support	Conversion, %	Yield, %	
		HMF	HMFCA	FDA
1	TiO_2	92	1	3
2	$MgAl_2O_4$	89	7	3
3	Fe_3O_4	99	14	5
4	ZrO_2	84	3	5
5	CeO_2	86	7	4
6	HAp	81	4	4
7	HT	>99	20	5
8	MgO	>99	20	2
9	La_2O_3	>99	25	1

[a]Reaction conditions: 1.0 g [EMIm]Cl, 68 mg (0.54 mmol) HMF, 0.1 g of 2.5 wt% $Ru(OH)_x$/support catalyst (5 mol% Ru), 140°C, 24 hours reaction time, air flow (1 atm).

As seen from Table 8, all catalysts were found to exhibit activity in [EMIm]Cl. Albeit the yields of FDA in all cases were low, the yields of an intermediate oxidation product HMFCA indicated which catalysts were the most promising candidates for further study. The catalysts providing high yields of HMFCA were found to be $Ru(OH)_x/Fe_3O_4$, $Ru(OH)_x$/HT, $Ru(OH)_x$/MgO and $Ru(OH)_x/La_2O_3$ (Table 7, entries 3, 7-9), with the yields of HMFCA in the range of 14-25 %. Interestingly, no DFF formation was observed in any of these experiments.

The study was expanded to include several other ILs. Notably, it did not include [BMIm][BF_4] and [BMIm][PF_6] which have been commonly employed in earlier oxidation studies in ionic liquids: these two ILs upon contact with moisture at elevated temperatures tend to form HF, which could be detrimental to reaction intermediates as well as catalyst [116,134]. The most promising catalysts from the first screening (see Table 7) were tested together with $Ru(OH)_x/CeO_2$ which had shown high activity in water (see section 4.3.3.1). Additionally, the catalyst precursor $RuCl_3 \cdot xH_2O$ was included for comparison.

Most of the reactions afforded very low yields of the different oxidation products and only a few provided results interesting for further studies. Selected results are summarized in Table 8.

Table 8. HMF oxidation in different ionic liquids with Ru(OH)x catalysts on various supports.[a]

Entry	Ionic liquid	Catalyst	Conversion, %	Yield, %		
			HMF	HMFCA	DFF	FDA
1	[EMIm][OAc]	$Ru(OH)_x/La_2O_3$	>99	30	0	10
2		$Ru(OH)_x$/HT	93	13	0	0
3		$Ru(OH)_x/MgAl_2O_4$	99	27	0	13
4		$Ru(OH)_x/CeO_2$	55	2	1	0
5		$RuCl_3$	>99	27	0	6
6	[EMIm][HSO_4]	$Ru(OH)_x/La_2O_3$	71	0	3	0
7		$Ru(OH)_x$/HT	99	0	1	19
8		$Ru(OH)_x/MgAl_2O_4$	55	0	3	0
9		$Ru(OH)_x/CeO_2$	77	1	9	0
10		$RuCl_3$	84	0	0	0
11	[Bu_3MeN][$MeOSO_3$]	$Ru(OH)_x/MgAl_2O_4$	64	0	12	0
12	[MMMPz][$MeOSO_3$]	$Ru(OH)_x/La_2O_3$	46	0	10	0
13		$Ru(OH)_x/MgAl_2O_4$	95	0	6	0

[a]Reaction conditions: 1.0 g IL, 68 mg (0.54 mmol) HMF, 0.1 g of 2.5 wt% $Ru(OH)_x$/support catalyst (5 mol% Ru), 140°C, 24 hours reaction time, air flow (1 atm).

As seen from the results presented in Table 9, the formation of FDA in 1-ethyl-3-methylimidazolium acetate ([EMIm][OAc]) was observed with $Ru(OH)_x/La_2O_3$ and $Ru(OH)_x/ MgAl_2O_4$ (Table 8, entries 1 and 3). A 6 % yield of FDA was also observed when using the homogeneous catalyst $RuCl_3$ (entry 5). Formation of HMFCA was also observed for all other catalysts in [EMIm][OAc], possibly indicating that the oxygen solubility was higher compared to other ILs. (Although no data on oxygen solubility in [EMIm][OAc] is available in literature, the solubility of O_2 is generally low in comparison to the solubility of other gases in ILs [135-137].)

Another IL that showed promising results was 1-ethyl-3-methylimidazolium hydrogen sulfate ([EMIm][HSO_4]) (Table 8, entries 6-10). It afforded 19 % yield of FDA when $Ru(OH)_x$/HT was introduced into the reaction (Table 8, entry 7). When employing $Ru(OH)_x/CeO_2$ in the same IL, DFF formation of 9 % was observed. No other oxidation products were observed along with a slightly lower conversion for HMF compared to $Ru(OH)_x$/HT (entry 7). The use of the catalyst precursor $RuCl_3$ did not result in any oxidation products in this solvent (entry 10).

Tributylmethylammoniummethylsulfate ([Bu_3MeN][$MeOSO_3$]) and 1,2,4-trimethylpyrazolium methylsulfate ([MMMPz][$MeOSO_3$]) provided DFF formation in combination with spinel-supported $Ru(OH)_x$ catalyst. Interestingly, HMF conversion was much higher in [MMMPz][$MeOSO_3$] with Ru(OH)x/spinel compared to the catalyst supported on lanthanum oxide – 95 and 46 %, respectively (Table 8, entries 12 and 13).

Riisager *et al.* have demonstrated that the use of [EMIm][OAc] as a solvent at hight temperatures had a detrimental effect on the HMF stability [28]. Accordingly, a set of experiments was carried out in order the investigate the effect of lower temperature on the reaction progress. Both [EMIm][HSO_4] and [Bu_3MeN][$MeOSO_3$] proved to be very viscous in combination with the catalyst at 100^{o}C, hence experiments with these liquids were eventually performed at lower temperature in autoclave with mechanical stirring in the subsequent high pressure experiments (see below).

The product distribution of the aerobic oxidation reaction of HMF over supported $Ru(OH)_x$ catalysts in [EMIm][OAc] is shown as a function of time in Figure 28.

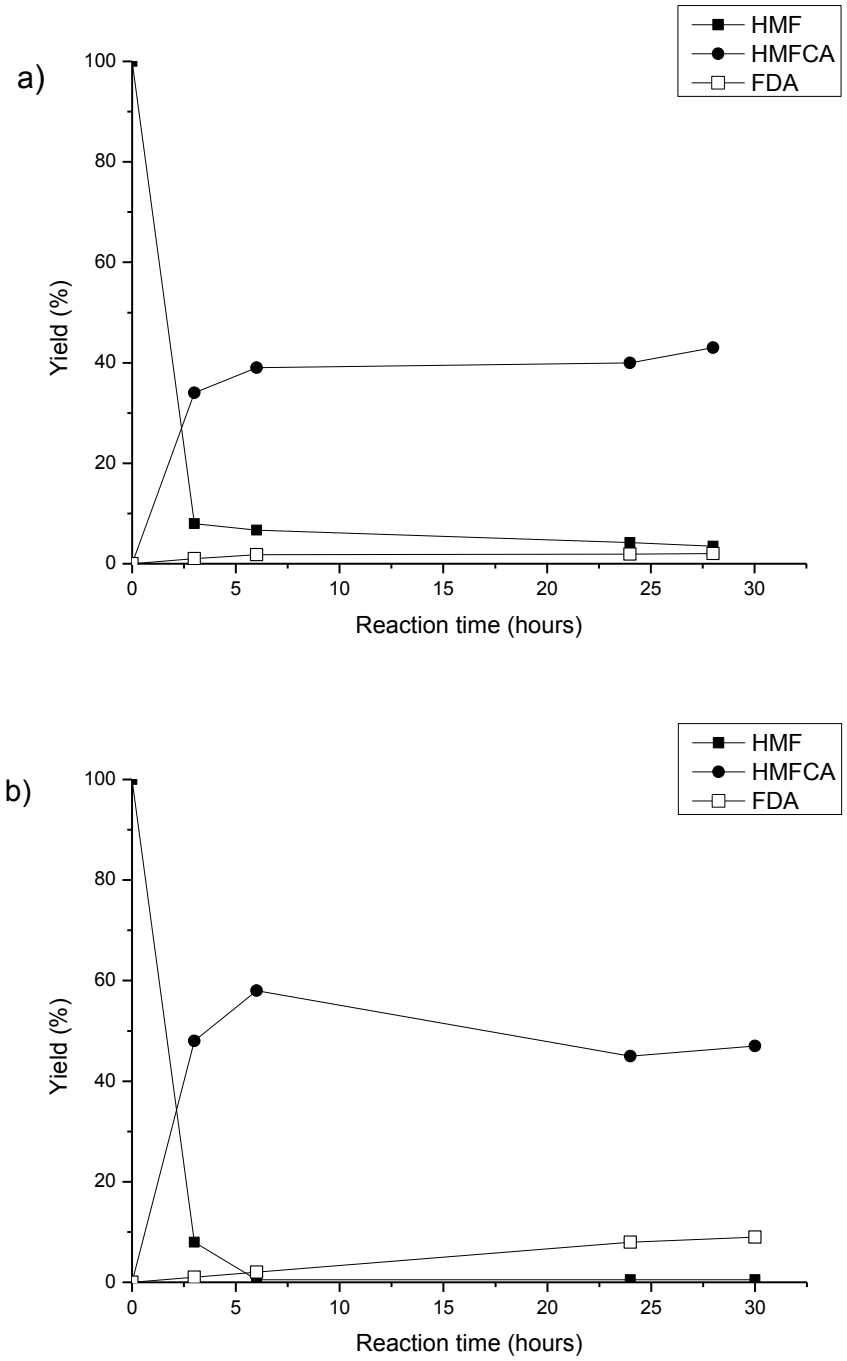

Figure 28. Product yields in the aerobic oxidation of HMF in [EMIm][OAc] with: a) $Ru(OH)_x/MgAl_2O_4$ catalyst; b) $Ru(OH)_x/La_2O_3$ catalyst. Reaction conditions: 1.0 g IL, 68 mg (0.54 mmol) HMF, 0.1 g of 2.5 wt% $Ru(OH)_x$/support catalyst (5 mol% Ru), 100°C, air flow (1 atm).

As seen in the figure, the final yield of FDA was lower than in the high temperature experiments (Table 8, entries 1-5) with no observed DFF formation, whereas the yield of HMFCA was higher and constituted *ca.* 50 %. The conversion of HMF remained high, thus accentuating the need of faster oxidation kinetics to avoid degradation. The best result at 100°C was obtained with La_2O_3 as catalyst support (Figure 28b). Here the HMF conversion reached a maximum already after 6 hours, corresponding to the HMFCA yield of 58 %. The amount of HMFCA then dropped slowly to form FDA which reached a yield of around 10 % after 30 hours of reaction time.

As in the above-described investigations of the aerobic HMF oxidation in water, similar research has been conducted on the possibility of improvement of the results obtained from the ambient pressure experiments. Although open flask experiments showed the potential of oxidizing HMF to HMFCA, the generally low solubility of molecular oxygen in ILs led to the assumption that pressures significantly higher than ambient were required to reach full conversion of HMFCA to FDA. The results are presented in Table 9.

Table 9. HMF oxidation in ionic liquids with the supported $Ru(OH)_x$ catalysts.[a]

Entry	Ionic liquid	Support	Temperature, °C	O_2 pressure, bar	Conversion, %	Yield, %			
					HMF	HMFCA	DFF	FDA	FA
1	[EMIm][HSO_4]	$MgAl_2O_4$	140	10	58	1	3	0	0
2	[EMIm][OAc]	MgA_2O_4	140	10	>99	4	0	14	0
3	[EMIm][HSO_4]	HT	100	10	32	3	18	0	0
4	[EMIm][OAc]	La_2O_3	100	10	97	34	0	23	31
5	[Bu_3MeN][$MeOSO_3$]	HT	100	30	60	16	26	1	0
6	[Bu_3MeN][$MeOSO_3$]	$MgAl_2O_4$	100	30	62	26	18	3	0
7	[EMIm][HSO_4]	HT	100	30	52	8	25	0	0
8	[EMIm][OAc]	La_2O_3	100	30	98	12	0	48	30

[a]Reaction conditions: 1.0 g [EMIm]Cl, 68 mg (0.54 mmol) HMF, 0.1 g of 2.5 wt% $Ru(OH)_x$/support catalyst (5 mol% Ru), 24 hours reaction time.

The results listed in Table 9 showed that formic acid formation was observed in some of the high pressure experiments, which was not the case in the oxidation under ambient pressure. The first set of autoclave experiments was conducted under 10 bar of dioxygen pressure at 140°C (the temperature was chosen to resemble the conditions of the oxidation reactions with supported ruthenium catalysts in water; see above) with a reaction time of 5 hours (Table 9, entries 1 and 2). Employing the $Ru(OH)_x$/ $MgAl_2O_4$ catalyst in [EMIm][HSO_4] (Table 9, entry 1) a very similar result to the open flask experiment at ambient pressure (see Table 8, entry 8) was obtained. Evidently, the increased pressure was in this case insufficient to impose an effect on the slow gas mass transfer. The use of the same catalyst in [EMIm][OAc] resulted in a decrease of HMFCA yield to 4 %, while the yield of FDA only increased to 14 % (as opposed to 27 and 13 % yields of HMFCA and FDA, respectively, at ambient pressure; Table 8, entry 3). This might indicate that high temperature in combination with an increased pressure most likely accelerated degradation of furan compounds in [EMIm][OAc], thus leading to lower yields than at ambient pressure.

Since it proved possible to improve the results by lowering the temperature in the open flask experiments (*vide supra*), the temperature for the high pressure experiments was subsequently chosen to be 100°C (Table 9, entries 3-8).

For $Ru(OH)_x$/HT in [EMIm][HSO_4] this resulted in a significant reduction of HMF conversion (from 99 to 32 %) while no FDA yield was observed, whereas HMFCA and DFF were obtained in 3 and 18 % yield, respectively (entry 3). The reduced substrate conversion was most likely a consequence of higher viscosity which made mixing more difficult, resulting in slower gas diffusion and accompanying mass transfer limitations. The same phenomenon appeared in the case of $Ru(OH)_x$/spinel in [Bu_3MeN][$MeOSO_3$] where the FDA yield was lowered drastically from 10 to 1 % (Table 8, entry 11; Table 9, entry 5). Improvement was observed at 100°C for $Ru(OH)_x/La_2O_3$ in [EMIm][OAc] where 23 % of FDA was formed along with 34 % of HMFCA (Table 9, entry 4). Clearly, the detrimental effect of [EMIm][OAc] on the HMF stability was reduced and selectivity towards the desired product was favored by decreasing the reaction temperature (compare with Table 8, entry 1).

The final adjustment made was to increase the dioxygen pressure even further to 30 bar. This gave a slight increase in HMF conversion from 32 to 52 % for $Ru(OH)_x$/HT in [EMIm][HSO_4], albeit still with no FDA being formed (entry 7). The best result was

obtained with $Ru(OH)_x/La_2O_3$ in [EMIm][OAc] which afforded 48 % of FDA and 12 % of HMFCA (entry 8). In addition to the desired products, 30 % of FA was formed, suggesting that some degradation was favored at elevated pressure in [EMIm][OAc]. Interestingly, high amount of formic acid (*ca.* 31 %) was formed when the oxidation reaction with the same solvent and catalyst was carried out at 10 bar O_2 at 100°C (entry 4). This suggests that the substrate and/or products might undergo the same degradation in the presence of protic acid (in this case, formed FDA), as was observed previously for the oxidation of HMF in water with spinel-supported ruthenium catalysts (see, for example, Figure 17, Figure 24).

It was shown above that hydrotalcite- and magnesium oxide-supported $Ru(OH)_x$ catalyst were found to be dissolving in the reaction medium (hot water). It is also known that heterogeneous catalysts can be sensitive to leaching of the active catalytic specie from the support which can be deceptive when interpreting experimental results. The reaction conditions for the performed oxidation experiments were such that leaching was not unlikely, and the experiments using the catalyst precursor $RuCl_3$ at ambient pressure had already confirmed that HMF oxidation could also proceed homogeneously. Accordingly, the two most promising catalysts ($Ru(OH)_x/La_2O_3$ and $Ru(OH)_x/MgAl_2O_4$) were tested toward leaching. This was made by stirring the catalysts in [EMIm][OAc] at 100°C for three hours, after which they were removed by hot filtration. In both cases the obtained filtrate had a black color, indicating presence of dissolved ruthenium species. To investigate if the black substance had a catalytic effect, the recovered IL was stirred in an open flask together with HMF for 24 hours. This afforded a substantial amount of HMFCA (44 %) as well as FDA (4 %) confirming that the solid catalysts had leached active catalytic material into the ionic liquid. Therefore, it is reasonable to conclude that the discussed catalytic oxidation proceeded, at least partly, homogeneously, thus making a direct re-use of the catalyst difficult.

4.3.4. Conclusions

A number of $Ru(OH)_x$/support catalysts were prepared and identified as highly efficient catalysts for aerobic oxidation of HMF to FDA under base-free and low to moderate oxygen pressures. Especially, ceria-, MgO- and HT-supported catalysts showed higher activities and selectivities compared to those based on TiO_2 as a support. More detailed investigation on the catalytic properties and differences of the catalysts supported on the three magnesium-based supports hydrotalcite (HT), magnesium oxide (MgO) and spinel ($MgAl_2O_4$) has been conducted. All three catalysts were found to effectively catalyze the oxidation of HMF. However, both HT and MgO supports dissolved partly under the reaction conditions liberating significantly amounts of Mg^{2+} ions, thus making the mixtures basic. This resulted in formation of Mg-FDA salts stabilized against further degradation. The spinel support, on the other hand, remained stable under the reaction conditions which allowed performing the oxidation reaction under base free conditions.

The reported data suggests that the reaction pathway for aerobic oxidation of HMF to FDA with the $Ru(OH)_x$ supported catalysts proceed *via* relatively slow initial competitive oxidation to DFF and HMFCA. The subsequent oxidations to form the product are fast since no other intermediates (*e.g.* 5-formylfuran-2-carboxylic acid) were observed.

Importantly, only very low amounts (<0.02 %) of the ruthenium metal inventory was found to dissolve from the catalysts (irrespectively of the support dissolution) under applied reaction conditions. Combined with the observation that $Ru(OH)_x/MgAl_2O_4$ preserved its activity upon re-use, makes this and analogous catalyst systems based on stable supports attractive alternatives to present aerobic HMF oxidation catalysts based on metal nanoparticles (*e.g.* gold catalysts), which often is less active upon re-use due to particle sintering [50].

In ionic liquids, the aerobic oxidation of HMF was investigated using solid ruthenium hydroxide catalysts supported on different carrier materials. The IL best suited for the oxidation was [EMIm][OAc], which afforded 48 % yield of FDA (30 bar of O_2, 100^{o}C) with $Ru(OH)_x$ deposited on La_2O_3 support. In the experiments with relatively high FDA yields, high yields of formic acid were also observed, which can originate, for instance, in the

detrimental effect of the IL on the HMF stability, and the appearance of the protic acid (formed FDA) and thus HMF degradation, as was shown for the HMF oxidation in water. The oxidation was shown to proceed, at least partly, homogeneously.

An apparent improvement of the yield was found when the temperature was lowered and the pressure was increased. Although [EMIm][OAc] is notorious in degrading HMF [28] and therefore not ideal as a solvent for HMF oxidation, it appeared to have a higher solubility of oxygen compared to other ILs, which made it the best solvent under applied reaction conditions. In several ILs the stirring was hindered due of high viscosity which most likely also had an impact on gas mass transfer and consequently on conversion and yield.

This work might provide valuable insights about the scope and limitations of aerobic oxidations in ILs using solid ruthenium hydroxide catalysts. The study also shows that the IL [EMIm][OAc] performed well as a solvent for aerobic oxidations making it attractive as a reaction media considering its unique dissolving properties.

5. *Oxidation of 5-hydroxymethylfurfural to 2,5-diformylfuran*

5.1. Introduction

Although production of FDA from HMF has been of a great interest in the last decade, numerous papers on the HMF oxidative transformation to form other oxidation products are found in literature. Some of the (potentially) important HMF derivatives were shown in section 4.1.1 (see Scheme 2). Here, different products of the oxidation of HMF, including the recently reported maleic anhydride [138], are presented in Scheme 12.

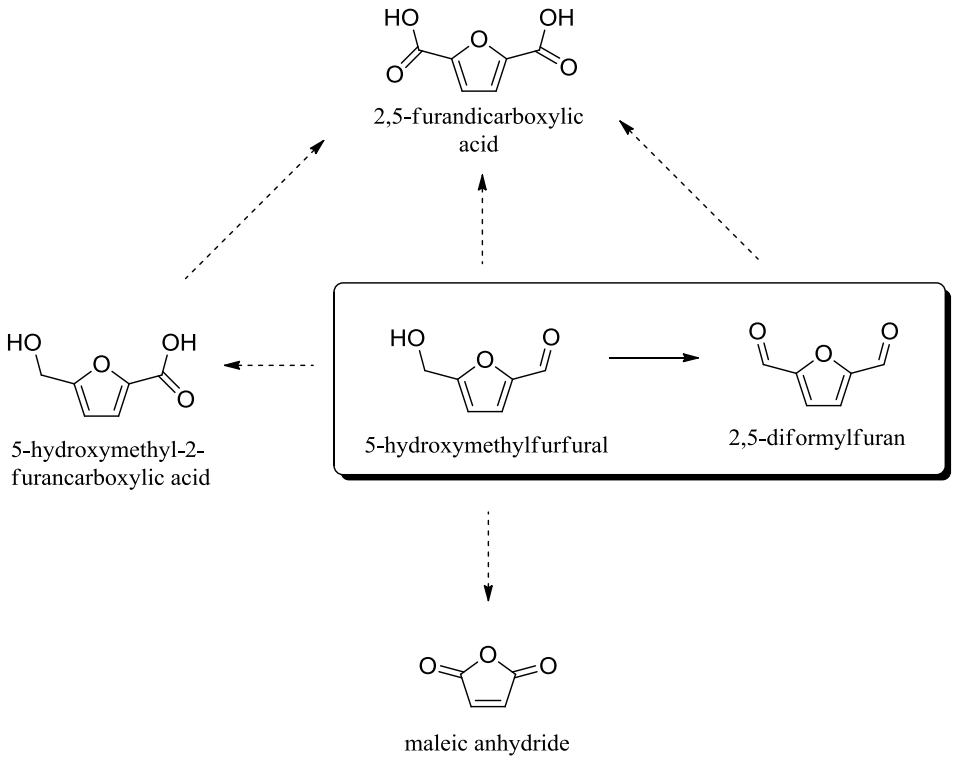

Scheme 12. Different oxidation products of HMF.

2,5-Diformylfuran (DFF) is a versatile compound, which, similarly to FDA, can be obtained by *e.g.* glucose dehydration to HMF and its subsequent oxidation [15,139]. It possesses many different applications in industry, for instance, it can be used as a monomer building block for resins, and as a starting material for the synthesis of adhesives, composites, foams, binders, sealants, solvents, antifungal agents, organic conductors and macrocyclic ligands [13,36,140-143].

Recently, a review was published by Li *et al.* [144] that covered the DFF production, also including early works utilizing the stoichiometric reagents as oxidants. Although such reactions are still investigated [145], in this subsection we will focus on the relatively recent reported aerobic catalytic oxidation reactions of HMF to DFF.

Grushin *et al.* [37] obtained DFF form the aerobic oxidation of HMF in acetic acid under 70 bar of air pressure at 50-75^{o}C over metal/bromide (Co/Mn/Br) catalyst with the yields and selectivity up to 63 and 78 %, respectively.

Halliday *et al.* have reported the oxidation of HMF to DFF with oxygen by using ion-exchange resins and vanadyl phosphate (VPO) catalysts as part of a direct *in situ* transformation of fructose to DFF (with yields up to 45 %) without isolation of the intermediate (HMF) [146]. Carlini *et al.* [147] reported that HMF, both as a starting reagent or produced one pot from fructose, was oxidized to the corresponding dialdehyde in water with methylisobutylketone (MIBK), as well as pure organic solvents, with vanadyl phosphate (VPO) based catalysts (Zr-, Nb-, Cr-, Fe-modified) as such or using a TiO_2 support at 75–200^{o}C and 1MPa. However, the reported yields were low (H_2O:MIBK = 0:30–5:30, HMF conversion 3–10 %, selectivity to DFF 100–60 %, respectively). Considering the oxidation as a stand-alone reaction and changing the solvents to less polar ones (benzene, toluene) better conversion rates and selectivity were obtained, and using MIBK as a solvent led to 98 % conversion with 50 % selectivity. However, in DMF the results were even better (at 150 ^{o}C), giving 84 % conversion and 97 % selectivity.

Chornet *et al.* performed the aerobic oxidation of HMF to DFF employing both homogeneous and immobilized vanadyl-pyridine complexes on polymeric and organofunctionalyzed mesoporous supports (*e.g.*, SBA-15) [148]. Here, the best result was obtained when the usage of poly(4-vinylpyridine)/$VO(acac)_2$ catalyst in α,α,α-trifluorotoluene (TFT) at 130^{o}C under 10 bar of air pressure afforded almost exclusively DFF (>99 % selectivity) at the HMF conversion over 80 %.

In a work reported by Pang *et al.* [143] the usage of $Cu(NO_3)_2$ with a co-catalyst vanadyl(IV) sulfate in acetonitrile under atmospheric oxygen pressure at room temperature provided the quantitative yields of DFF from HMF.

A one-pot two-step approach for the production of DFF directly from glucose was suggested by Hu *et al.* [149]. 18 % DFF yield from glucose was obtained with the $CrCl_3 \cdot 6H_2O/NaBr//NaVO_3 \cdot 2H_2O$ catalytic system in DMA at 110°C and air flow (1 atm) *via* a one-step approach, whereas a two-step approach with a change from a nitrogen to oxygen atmosphere for the dehydration and oxidation steps, respectively, and the separation of $CrCl_3 \cdot 6H_2O$ and NaBr provided the highest DFF yield of 55 %.

The aerobic oxidation of HMF with heterogeneous catalysts appears as a green process with a great perspective in biorefineries. Indeed, the catalytic process of DFF production has recently been studied from a techno-economic point of view to estimate the minimum selling prices [150], with the remarked importance of the price and performance of the solid catalyst in the feasibility of the process.

This chapter describes a research aiming on multiple goals (Scheme 13). First, a brief investigation on the possibility of performing a selective aerobic oxidation of HMF to DFF in different organic solvents employing heterogeneous $Ru(OH)_x$ catalysts deposited on different supports was performed. Second, activity of different titanate- and zeolite-supported vanadia catalysts was tested with a special attention to the homogeneous contribution arising from the lixiviated species, in an attempt to avoid the leaching of the active phase and to improve the stability and recyclability of the catalyst.

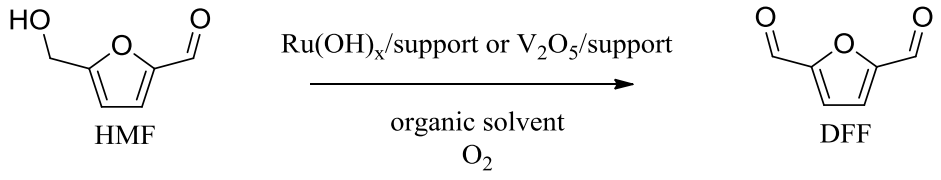

Scheme 13. Aerobic oxidation of HMF to DFF with supported ruthenium hydroxide or vanadia catalysts in organic solvents.

5.2. Experimental

Materials: 5-Hydroxymethylfurfural (HMF) (>99 %), lantanum(III) nitrate hexahydrate (99.99 %), titanium oxide (anatase, 99.7 %), spinel $MgAl_2O_4$, sodium and potassium hydroxides (>98 %), sodium nitrate (≥99 %), ruthenium(III) chloride (purum, ~41 % Ru), acetonitrile (≥99.9 %), toluene (anhydrous, 99.8 %), α,α,α-trifluorotoluene (TFT) (≥99 %), *N,N*-dimethylformamide (DMF) (≥99.9 %), ammonium metavanadate (≥99 %), oxalic acid (≥99 %), furfuryl alcohol (98 %), 5-methylfurfuryl alcohol (99 %) and anisole (99 %) were acquired from Sigma-Aldrich. Magnesium nitrate hexahydrate (p.a.) was obtained from Merck. Magnesium oxide (p.a.) was purchased from Riedel-de Haën AG. Cerium(IV) oxide (99.5 %) and lanthanum(III) oxide (99.9 %) were purchased from Alfa Aesar. Methyl isobutyl ketone (MIBK) (≥98 %) and dimethylsulfoxide (DMSO) (≥99 %) were obtained from Fluka. 2,5-Diformylfuran (DFF) (98 %) was obtained from ABCR GmbH & Co. Dioxygen (99.5 %) was purchased from Air Liquide Denmark. All NH_4-zeolites were obtained from Zeolyst International, USA. All chemicals were used as received.

5.2.1. Oxidation of HMF to DFF in organic solvents with $Ru(OH)_x$/support catalysts

$MgO{\cdot}La_2O_3$ and 2.4 wt% $Ru(OH)_x$/support catalysts were prepared as described above (see section 4.3.2). No other catalyst characterization was performed apart from that described above (see sections 4.3.3.1, 4.3.3.2).

Oxidation at ambient pressure: Experiments at ambient pressure were performed using a Radley Carousel 12 Plus Basic System. A typical experiment was as follows: a solution of HMF (0.126 g, 1 mmol), 5-methylfurfuryl alcohol (0.112 g, 1 mmol) or furfuryl alcohol (87 μL, 1 mmol) in 5-10 mL of solvent was put into a reaction *via*l with the internal standard (anisol, 11 μL, 0.1 mmol). Then 0.105-0.21 g of 1.2-2.4 wt% $Ru(OH)_x$/support catalyst was added in the reaction. Reactions were carried out under the flow of oxygen, nitrogen or air (1 atm) at 80-100^{o}C. During and after the reaction, samples of the reaction mixture were taken and after filtering off the catalyst analyzed by GC and/or GC-MS. Importantly, due to the relatively low solubility of the substrate (HMF) and even lower solubility of the product

(DFF) in some of the solvents (toluene, TFT) at temperatures below the reaction temperature, samples were diluted twice with the respective solvent.

High pressure oxidation reactions: Experiments were carried out in stirred Parr autoclaves equipped with internal thermocontrol (T316 steel, Teflon^{TM} beaker insert, 100 mL). Reaction mixture was as described above. The autoclaves were pressurized with 10-30 bar of oxygen and were kept stirring (600 rpm) at 80^{o}C. After the reaction, the autoclave was cooled to room temperature (*i.e.*, 20^{o}C) and after filtering off the catalyst a sample was taken out for GC and/or GC-MS analysis.

5.2.2. Oxidation of HMF to DFF in organic solvents with supported V_2O_5 catalysts

Catalyst preparation: Potassium titanate $K_2Ti_3O_7$ was prepared by hydrothermal treatment of TiO_2 with KOH. 1.92 g of the commercial TiO_2 anatase nanoparticles were suspended in 160 mL of aqueous 10 M KOH, followed by hydrothermal treatment at 150°C in a stainless Teflon-lined autoclave for 72 hours. The resulting powders were washed with large amounts of distilled water until neutral pH and dried at room temperature for 16 hours.

The protonated form of the titanate was obtained by ion exchange of the potassium titanate three times in acetic acid at 80°C.

Commercial NH_4-ZSM5 (Si:Al=15), NH_4-Beta (Si:Al=25), NH_4-Mordenite (Si:Al=10) and NH_4-Y (Si:Al=12) zeolites were initially calcined at 550ºC for 5 hours to obtain the H-ZSM5 (400 m^2/g), H-Beta (680 m^2/g), H-Mordenite (500 m^2/g) and H-Y (700 m^2/g) supports, respectively.

Surface areas of the catalysts were determined by nitrogen sorption measurements at liquid nitrogen temperature on a Micromeritics ASAP 2020 pore analyzer. The samples were outgassed in vacuum at 150^{o}C for 4 hours prior to the measurements. The total surface areas were calculated according to the BET method.

For the preparation of Na-Beta support, 10 g of NH_4-Beta were suspended in 300 mL of 1 M aqueous solution of $NaNO_3$. The mixture was heated to 80°C and stirred for 1 hour.

Afterwards, the zeoli5e was filtered and washed with distilled water. This procedure was repeated twice. Finally, the recovered Na-Beta material was dried and then calcined at 500°C for 5 hours.

Vanadia supported on titania, titanates and zeolites with 1–10 wt% V_2O_5 were prepared by wet impregnation of the supports with vanadium oxalate solution, as adopted from the literature [154]. *E.g.*, in a typical zeolite-supported catalyst preparation, 1.75 mL of NH_4VO_3/oxalic acid aqueous solution (0.378 M) (prepared from ammonium metavanadate and oxalic acid in the molar ratio 1:2 at 70ºC) was added to 1 g of the zeolite using incipient wetness impregnation technique. Once the incipient wetness impregnation was completed, the solids were dried at 120ºC for 8 hours and then calcined at 500ºC for 5 hours to afford 3 wt% V_2O_5/zeolite catalyst.

SEM-EDS analysis was done on a FEI Quanta 200 F SEM operated at 20 kV, using an Oxford Instruments X-max (51xmx0005) EDS running the INCA Suite v 4.15 software. Spectra were fitted using program standards and converted to atomic ratios. Samples were mounted on a carbon tape fitted to aluminium sample holders.

Oxidation at ambient pressure: Experiments were performed using a Radley Carousel 12 Plus Basic System. In a typical experiment, 0.1 g (*ca.* 0.8 mmol) of HMF, 0.01-0.1 g of the 1-10 wt% V_2O_5/support catalyst (0.7-1.4 mol% V) and 5 mL of the solvent (DMF, acetonitrile, MIBK, DMSO) were put into a 40 mL reaction *via*l. 11 μL of anisole were added as an internal standard and the *via*l was equipped with a magnetic stirrer (800 rpm). Reactions were carried out under a flow of oxygen (1 atm) at 100-150^{o}C. During and after the reaction, samples of the reaction mixture were taken and after filtering off the catalyst analyzed by GC and/or GC-MS.

In the homogeneous test experiments, the same procedure was applied. After 330 min the content of the reaction *via*l was filtered, the filtrate was recovered and used to conduct subsequent catalytic reaction.

In the recycling test, the catalyst was recovered after the reaction by filtration, washed with the solvent and ethanol and dried overnight at room temperature before being applied in another reaction run.

High pressure oxidation reactions: Experiments were carried out in stirred Parr autoclaves equipped with internal thermocontrol (T316 steel, Teflon^{TM} beaker insert, 100 mL). In a typical experiment, reactor was charged with 0.1 g HMF, 5 mL of solvent, 0.1 g of 1 wt% V_2O_5/H-Beta and 11 μL of anisole. The autoclave was then pressurized with 10-40 bar of oxygen and were kept stirring (800 rpm) at 100-150^{o}C. After the reaction, the autoclave was cooled to room temperature (*i.e.*, 20^{o}C) and after filtering off the catalyst a sample was taken out for GC and/or GC-MS analysis.

In the homogeneous test experiments, the same procedure was applied. After 180 min of reaction time under 10 bar of O_2 at 125^{o}C the catalyst was filtered off the solvent, the filtrate was recovered and used to conduct subsequent catalytic reaction.

5.3. Results and discussion

5.3.1. Oxidation of HMF and other substituted furans with supported Ru(OH)x catalysts

As was mentioned above, supported $Ru(OH)_x$ catalysts have attracted significant attention in the past years as efficient catalysts for the aerobic oxidation of alcohols to corresponding carbonyl compounds [93,97-103].

Here, the initial investigation on the oxidation of HMF to DFF was performed employing ruthenium hydroxide catalysts supported on CeO_2, TiO_2, MgO, La_2O_3, $MgO{\cdot}La_2O_3$ mixed oxide and $MgAl_2O_4$ in toluene (see Scheme 13). The results of this initial screening are shown in Table 10.

Table 10. Substrate conversion and product yield in the HMF aerobic oxidation in toluene with supported $Ru(OH)_x$ catalysts.[a]

Entry	Catalyst	HMF conversion, %	DFF yield, %
1	$Ru(OH)_x/TiO_2$	37	5
2	$Ru(OH)_x/MgO$	16	7
3	$Ru(OH_)_x/La_2O_3$	15	3
4	$Ru(OH)_x/MgO{\cdot}La_2O_3$	36	31
5	$Ru(OH)_x/CeO_2$	42	35
6	$Ru(OH)_x/MgAl_2O_4$	31	22
7	-	41	0

[a]Reaction conditions: 126 mg HMF, 5 mL toluene, 0.105 g of 2.4 wt% $Ru(OH)_x$/support catalyst (2.5 mol% Ru), 11 μL anisole, 80°C, O_2 flow, 26 hours.

It is seen from the obtained data that the said aerobic oxidation of HMF proceeded with all screened catalysts, albeit with relatively low HMF conversion and DFF yields. In fact, the usage of only three catalysts afforded DFF yields above 20 %: $Ru(OH)_x$ supported on CeO_2, $MgAl_2O_4$ and $MgO{\cdot}La_2O_3$ (Table 10, entries 4-6).

High conversion of HMF was also observed in cases when titania-supported catalyst was employed, as well as when reaction was performed in the absence of catalyst (Table 10, entries 1 and 7). Here, only 5 % yield of DFF was observed after 26 hours of reaction time with $Ru(OH)_x/TiO_2$ (entry 1), while the HMF conversion reached 37 %. As no other products were observed using the GC-MS analysis, this high conversion of HMF (similar to that when no catalyst was introduced into reaction) together with the dark brown colour of the post-reaction mixtures suggests possible formation of humins in both cases.

MgO- and La_2O_3-supported catalysts provided similarly low yields of DFF, however with higher selectivity (*i.e.*, lower HMF conversion). At the same time, the catalyst deposited on mixed magnesium-lanthanum oxide ($MgO{\cdot}La_2O_3$) exhibited superior activity in the reaction compared to the catalysts on respective simple oxides (Table 10, entry 4). Here, the use $Ru(OH)_x/MgO{\cdot}La_2O_3$ catalyst yielded in 34 % DFF at 39 % HMF conversion.

The mixed magnesium-lanthanum oxide was first reported to be an efficient catalyst for the aerobic oxidation of phenethyl alcohol to a respective aldehyde in organic solvents (*e.g.* toluene, trifluorotoluene, DMF) by Figueras *et al.* [151]. The authors related higher activity of the catalyst compared to $Ru(OH)_x/MgO$ and $Ru(OH)x/La_2O_3$ to the increased basicity of the mixed oxide [109,152]. Additionally, the usage of $MgO{\cdot}La_2O_3$ mixed oxide appears advantageous due to its high basicity: the precipitation of ruthenium species on it occurs without added homogeneous base [151].

To the best of our knowledge, no further research on the employment of the aforementioned catalyst has been reported in the literature so far. Hence, the aerobic oxidation of HMF with $Ru(OH)_x/MgO{\cdot}La_2O_3$ catalyst was investigated in more details. Here, reaction was conducted in different solvents at different temperatures, and with different amount of the introduced catalyst. The results are presented in Table 11.

Table 11. Substrate conversion and product yield in the aerobic oxidation of HMF in toluene with 2.4 wt% $Ru(OH)_x/MgO{\cdot}La_2O_3$ catalyst.[a]

Entry	Catalyst amount, mol%	Gas	Solvent	Temperature, °C	HMF conversion, %	DFF yield, %
1	2.5	O_2	Toluene	80	36	31
2	2.5	O_2	Toluene	90	34	28
3	2.5	O_2	Toluene	100	25	19
4	5	O_2	Toluene	80	55	41
5	10	O_2	Toluene	80	57	43
6	2.5	O_2	DMF	80	23	18
7	2.5	O_2	DMF	100	20	15
8	5	N_2	Toluene	80	11	1
9	0[b]	O_2	Toluene	80	2	1

[a]Reaction conditions: 126 mg HMF, 5 mL solvent, 0.105-0.42 g of 2.4 wt% $Ru(OH)_x/MgO{\cdot}La_2O_3$ catalyst, 11 μL anisole, gas flow, 26 hours. [b]Pure $MgO{\cdot}La_2O_3$ mixed oxide (0.105 g) was introduced into reaction.

The obtained results clearly indicate that the yield of DFF, as well as HMF conversion, in toluene decreased with the higher reaction temperature (Table 11, entries 1-3). That most likely originates in the lower solubility of oxygen in organic solvents at higher temperatures [153]. Interestingly, the substrate conversion and DFF yield did not change when the reaction was carried out in DMF (entries 6 and 7), possibly due to the fact that oxygen is only sparingly soluble in DMF even at low temperatures and its solubility doesn't change significantly with the temperature increase. However, both HMF conversion and DFF yield are similar in toluene and DMF when the reaction was performed at 80°C (entries 1, 6).

When higher amounts of catalyst (*i.e.* catalyst to substrate ratio) were introduced into reaction, expectedly higher conversion and yield were obtained within the reaction timeframe (Table 11, entries 1, 4, 5). Thus, HMF conversion and DFF yield increased from 36 and 31 % to 57 and 43 %, respectively, when the $Ru(OH)_x/MgO{\cdot}La_2O_3$ catalyst amount increased from 2.5 mol% to 10 mol%, while no change of selectivity towards DFF was

observed. Furthermore, only a very low DFF yield (1 %) at 11 % substrate conversion was observed when the reaction was conducted in the flow of nitrogen (Table 11, entry 8); introduction of pure support ($MgO{\cdot}La_2O_3$) with no deposited ruthenium species afforded equally low yield of the desired product (entry 9). It thus appeared that when a 'blank' basic support (*i.e.* with no catalytically active $Ru(OH)_x$ species) was used in the aerobic oxidation of HMF in toluene, HMF conversion remained low. Interestingly, similar picture was observed in the experiments employing MgO- and La_2O_3-supported catalysts: HMF conversion here was found to be approximately twice as low as the one with $Ru(OH)_x/TiO_2$ catalyst (see Table 11, entries 1-3). Thus, this suggests that the use of basic supports (when the catalyst on the respective support did not exhibit high activity in HMF oxidation, or when the pure support was used) induced the higher apparent stability of HMF in the toluene solution ($Ru(OH)_x/MgO$, $Ru(OH)_x/La_2O_3$, $MgO{\cdot}La_2O_3$), *i.e.* inhibited the formation of humins or other undesirable products.

Another catalyst that exhibited good activity in HMF aerobic oxidation to DFF was $Ru(OH)_x/CeO_2$ (Table 10, entry 5). Indeed, the highest selectivity towards DFF formation (*ca.* 83 %) at relatively high conversion of HMF was observed when 2.4 wt% $Ru(OH)_x/CeO_2$ was used. Therefore, the catalyst performance was further investigated. For comparison, ruthenium hydroxide catalyst supported on spinel was similarly employed. The product yield and substrate conversion are listed in Table 12.

As can be seen from the data, a tendency similar to discussed above was observed when the catalyst amount in the reaction was increased (Table 12, entries 1 and 2). The decrease of the substrate concentration by dissolving HMF in double amount of solvent (Table 12, entries 1 and 3) led to lower HMF conversion and DFF yield values, as was expected, whereas the selectivity towards DFF remained around 83 %. Changing the gas atmosphere to air or nitrogen afforded similar HMF conversion, however with only 4 and 2 % of DFF formed, respectively. Low, but not negligible yield of DFF (the oxidation product) in cases when reaction was performed with nitrogen (Table 11, entry 8; Table 12, entry 5) was observed probably due to oxygen absorbed on the surface of the catalyst.

Table 12. Substrate conversion and product yield in the HMF aerobic oxidation in organic solvents with supported $Ru(OH)_x$ catalysts.[a]

Entry	Catalyst	Solvent	V, mL	Catalyst amount, mol%	Gas flow	HMF conversion, %	DFF yield, %
1	2.4 wt% $Ru(OH)_x/CeO_2$	Toluene	5	2.5	O_2	42	35
2	2.4 wt% $Ru(OH)_x/CeO_2$	Toluene	5	5	O_2	49	41
3	2.4 wt% $Ru(OH)_x/CeO_2$	Toluene	10	2.5	O_2	34	28
4	2.4 wt% $Ru(OH)_x/MgAl_2O_4$	Toluene	10	2.5	O_2	28	21
5	2.4 wt% $Ru(OH)_x/CeO_2$	Toluene	10	2.5	N_2	31	1
6	2.4 wt% $Ru(OH)_x/CeO_2$	Toluene	10	2.5	air	30	4
7	2.4 wt% $Ru(OH)_x/CeO_2$	DMF	5	2.5	O_2	21	18
8	2.4 wt% $Ru(OH)_x/CeO_2$	DMF	10	2.5	O_2	19	16
9	2.4 wt% $Ru(OH)_x/CeO_2$	TFT	5	2.5	O_2	44	34
10	2.4 wt% $Ru(OH)_x/MgAl_2O_4$	TFT	5	2.5	O_2	32	28
11	2.4 wt% $Ru(OH)_x/CeO_2$	TFT	10	2.5	O_2	28	22
12	2.4 wt% $Ru(OH)_x/CeO_2$	MIBK	5	2.5	O_2	27	20
13	2.4 wt% $Ru(OH)_x/CeO_2$	MIBK	10	2.5	O_2	25	19
14	1.2 wt% $Ru(OH)_x/CeO_2$	Toluene	5	2.5	O_2	66	54
15	1.2 wt% $Ru(OH)_x/CeO_2$	DMF	5	2.5	O_2	25	22
16	1.2 wt% $Ru(OH)_x/CeO_2$	TFT	5	2.5	O_2	51	42
17	1.2 wt% $Ru(OH)_x/CeO_2$	MIBK	5	2.5	O_2	40	31
18	1.2 wt% $Ru(OH)_x/CeO_2$	Acetonitrile	5	2.5	O_2	34	26
19	1.2 wt% $Ru(OH)_x/MgAl_2O_4$	Acetonitrile	5	2.5	O_2	31	18

[a]Reaction conditions: 126 mg HMF, 0.105-0.21 g $Ru(OH)_x$/support, 11 μL anisole, 80°C, gas flow, 26 hours.

Interestingly, the use of MIBK and TFT has, in fact, resulted in lower DFF yields and selectivities. Here, reaction selectivity towards DFF was *ca.* 75 % (Table 12, entries 9, 11 and 12, 13), whereas the said selectivity did not decrease when the reaction was carried out in DMF (Table 12, entries 7, 8), albeit the obtained conversion and yield still were lower than those in toluene.

In order to investigate the effect of the ruthenium loading on the catalyst performance in the reaction, 1.2 wt% $Ru(OH)_x/CeO_2$ and 1.2 wt% $Ru(OH)_x/MgAl_2O_4$ catalyst were prepared and tested in the aerobic HMF oxidation in different solvents (Table 12, entries 14-

19). Here, a similar tendency to the performance of 2.4 wt% catalysts was observed, *e.g.* HMF conversion and DFF yield remained highest in toluene. The highest observed HMF conversion and DFF yield were found to be *ca.* 54 and 66 %, respectively (entry 14). The results of study on reaction progress are presented in Figure 29.

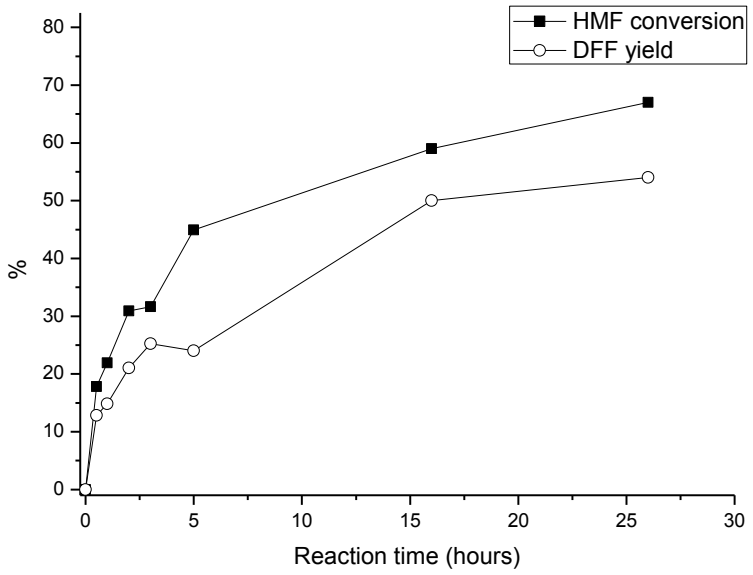

Figure 29. Product formation in aerobic HMF oxidation in toluene using $Ru(OH)_x/CeO_2$ catalyst as a function of reaction time. Reaction conditions: 126 mg HMF, 5 mL toluene, 11 μL anisole, 0.21 g of 1.2 wt% $Ru(OH)_x/CeO_2$, O_2 flow (1 atm), 80°C.

Importantly, substrate conversion and product yield were found to be higher in cases when 1.2 wt% catalysts were employed (compare, for instance, Table 12, entries 1 and 14), thus indicating higher aptitude of the ceria-supported ruthenium hydroxide catalysts with lower loading of the active species in the aerobic oxidation reactions. However, no further study on the effect of the active species loading was performed at this point. More detailed catalyst characterization and the discussion of the catalytic activity dependence on the $Ru(OH)_x$ species loading on the support are described further in this thesis (see section 6.3.1).

Notably, when the spinel-supported catalyst was used in the reaction in DMF, TFT or acetonitrile, the values of both HMF conversion and DFF yield were lower (Table 12, entries 4, 10, 19) compared to those when $Ru(OH)_x/CeO_2$ was introduced into reaction, which is in good accordance with the similar behavior of these catalysts, as described in other chapters of the present thesis (see, for example, sections 4.3.3.1, 6.3.1).

The results discussed above highlight the superior performance of the two catalysts, $Ru(OH)_x/CeO_2$ and $Ru(OH)_x/MgO{\cdot}La_2O_3$, for the aerobic oxidation of HMF. Following our previous research on the aerobic oxidation of HMF in water under both ambient and elevated pressures, a set of experiments was conducted in which HMF in toluene (126 mg HMF, 5 mL toluene) was introduced into aerobic oxidation reactions employing 1.2 wt% $Ru(OH)_x/CeO_2$ catalyst (0.21 g, 2.5 mol% Ru) at 10 and 30 bar of oxygen pressure. Respective DFF yield and HMF conversion are shown in Figure 30.

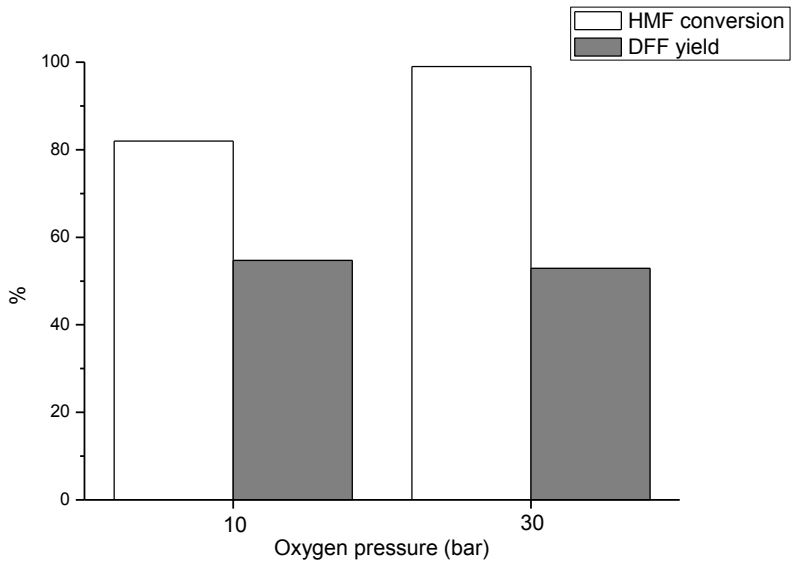

Figure 30. Substrate conversion and product yield in the aerobic oxidation of HMF at elevated pressures. Reaction conditions: 126 mg HMF, 5 mL toluene, 11 μL anisole, 0.21 g of 1.2 wt% $Ru(OH)_x/CeO_2$ catalyst (2.5 mol% Ru), 80°C, 26 hours.

The results presented in Figure 30 indicate that effectively no change in HMF yield was observed when the reaction was carried out at higher oxidant pressures. At the same

time, the reaction selectivity towards DFF was lowered. Indeed, HMF conversion increased from 67 % under ambient pressure to 82 and 98 % under 10 and 30 bar of O_2, respectively, whereas the yield of DFF remained around *ca.* 50 %. This might indicate the occurring product degradation or that HMF side-reactions were facilitated under elevated pressures.

As the results of preliminary screening revealed superior performance of the $Ru(OH)_x/CeO_2$ and $Ru(OH)_x/MgO{\cdot}La_2O_3$ catalysts in the aerobic oxidation of HMF in toluene (see Table 10, entries 4 and 5), these catalysts were tested for the oxidation of other substituted furans. Thus, furfuryl alcohol and 5-methylfurfuryl alcohol were oxidized in toluene and DMF with 2.4 wt% $Ru(OH)_x/CeO_2$ and $Ru(OH)_x/MgO{\cdot}La_2O_3$ catalysts (Scheme 14). Reactions were carried out under similar conditions as described above for the oxidation of HMF. The results are presented in Figures 31 and 32.

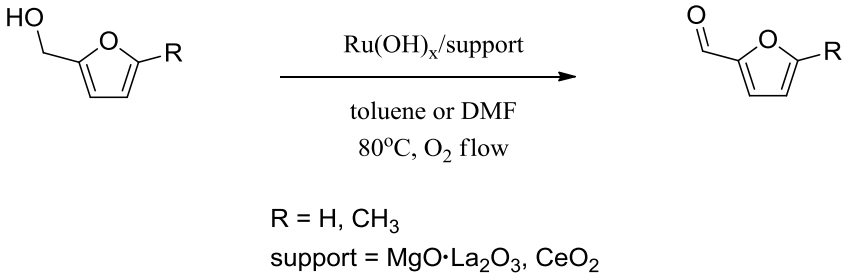

Scheme 14. Aerobic oxidation of furfuryl alcohol to furfural (R = H) and 5-methylfurfuryl alcohol to 5-methylfurfural (R = CH_3) with supported ruthenium hydroxide catalysts in organic solvents.

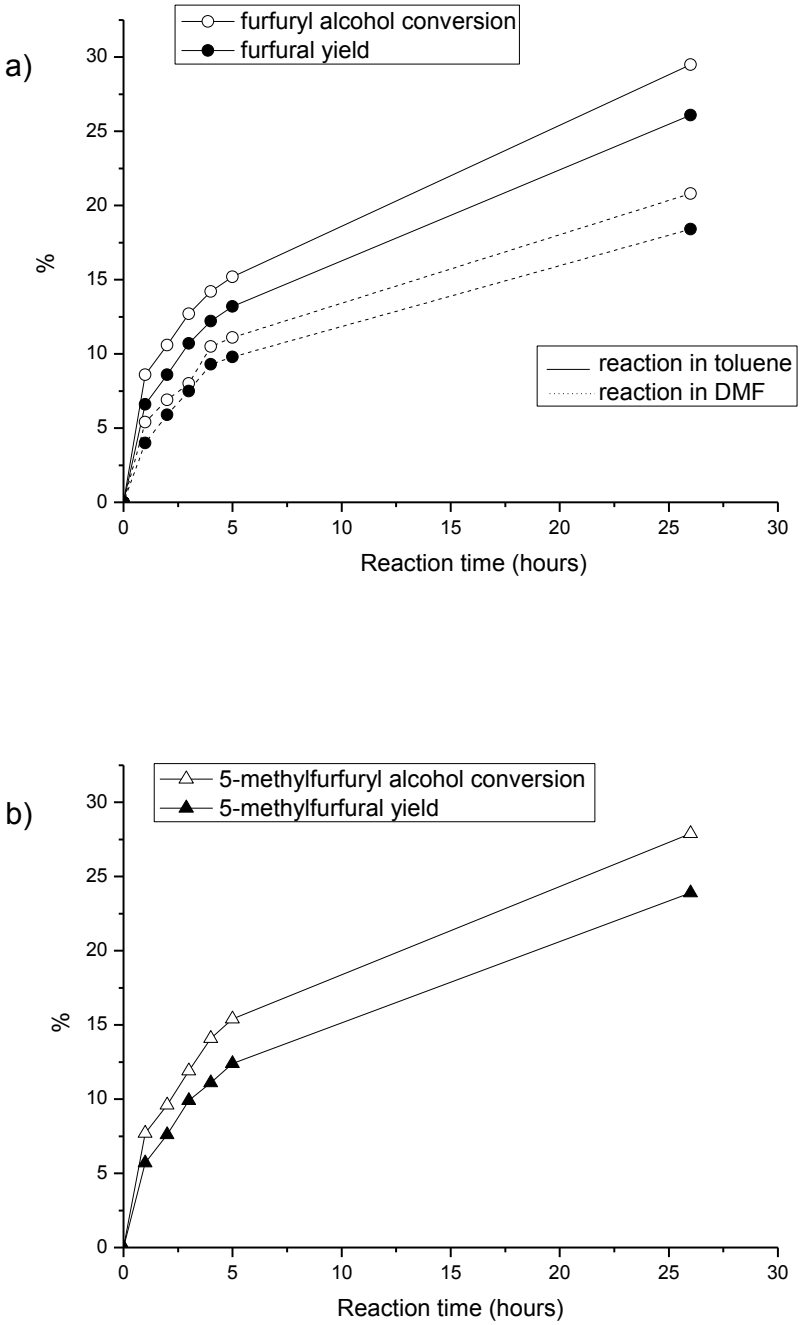

Figure 31. Substrate conversion and product formation in the aerobic oxidation of (a) furfuryl alcohol in toluene and DMF solutions and (b) 5-methylfurfuryl alcohol in toluene with 2.4 wt% $Ru(OH)_x/MgO{\cdot}La_2O_3$ catalyst as a function of reaction time. Reaction conditions: 1 mmol substrate, 5 mL solvent, 11 μL anisole, 0.105 g of 2.4 wt% $Ru(OH)_x/MgO{\cdot}La_2O_3$ catalyst, O_2 flow (1 atm), 80°C.

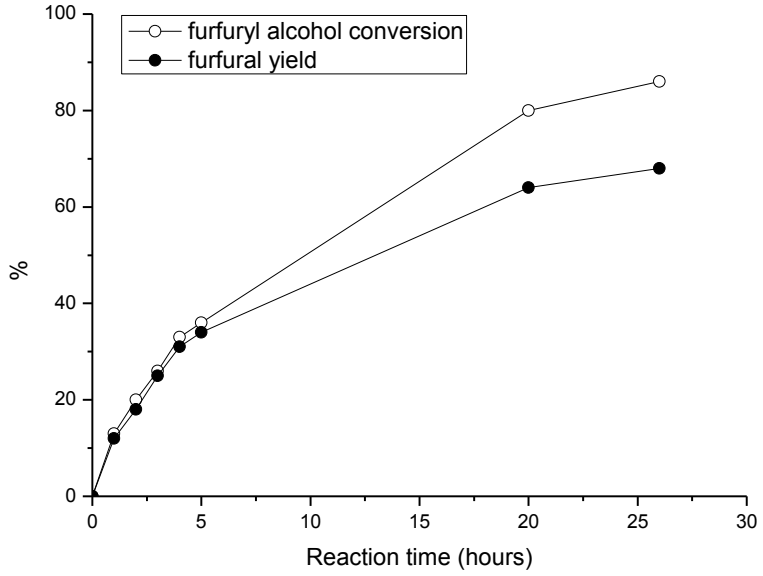

Figure 32. Substrate conversion and product formation in the aerobic oxidation of furfuryl alcohol in toluene with 2.4 wt% $Ru(OH)_x/CeO_2$ catalyst as a function of reaction time. Reaction conditions: 1 mmol furfuryl alcohol, 5 mL toluene, 11 μL anisole, 0.105 g of 2.4 wt% $Ru(OH)_x/CeO_2$, O_2 flow (1 atm), 80°C.

As seen from the presented results, the aerobic oxidation of furfuryl alcohol with $Ru(OH)_x/MgO{\cdot}La_2O_3$ catalyst was found to follow the same trend as was established for the oxidation of HMF. Both substrate conversion and product yield were lower in DMF compared to those in toluene (Figure 31a). Notably, however, the conversion values of the two investigated substrates (furfufyl alcohol, 5-methylfurfuryl alcohol) appeared to be almost the same after 26 hours of reaction (Figures 31a, 31b), resulting in approximately 30 % conversion (with 25 % product yield). At the same, higher reactivity was observed for HMF, where its conversion and DFF yield constituted 36 and 31 %, respectively (see Table 10, entry 4). This might indicate that the presence of the conjugated aldehyde functionality in HMF (see Scheme 2) facilitates the conversion of the hydroxymethyl group.

The usage of the $Ru(OH)_x/CeO_2$ catalyst for the aerobic oxidation of furfuryl alcohol in toluene afforded the subsrate conversion and furfural yield of 86 and 68 %, respectively (Figure 32), compared to *ca.* 30 % and 25 % when $Ru(OH)_x/MgO{\cdot}La_2O_3$ was used. This, again, supports the hypothesis of the superior performance of the $Ru(OH)_x$ catalysts supported on CeO_2 in the aerobic oxidation reactions. Also, the results of furfuryl alcohol aerobic oxidation with *e.g.* 2.4 wt% $Ru(OH)_x/CeO_2$ might suggest that the relatively low

HMF conversion and yield of DFF (Table 10, entry 5) with the latter catalyst was due to the low solubility of the product (see section 5.2.1), precipitation of which from the solution at higher concentrations (*i.e.* when the yield of DFF reaches certain amount) might block the active sites of the catalyst. Another possible reason could be a mass transfer limitation, which was not the case with the homogeneous mixture of two liquids, toluene and furfuryl alcohol.

5.3.2. Oxidation of HMF to DFF with supported V_2O_5 catalysts

Various methods and catalysts applied for the oxidation of HMF to DFF were described in section 5.1 of the present thesis, including those comprising the usage of different vanadium-based catalysts [143,147-149]. However, although reporting high selectivities and yields of DFF, none of the mentioned works presented any data to assess the heterogeneous character of the catalysts.

This work was aimed at testing the activity of different supported vanadia catalysts, paying special attention to the homogeneous contribution arising from the lixiviated catalytic species in an attempt to avoid the leaching of the active phase and improve the stability and recyclability of the catalyst.

One of the first HMF aerobic oxidation techniques involving heterogeneous V_2O_5/TiO_2 catalysts was reported by Moreau *et al.* [155]. Hence, in this work firstly the preliminary study on the activity and stability of the titania- and titanates-supported V_2O_5 catalyst was conducted. For that, three V_2O_5 catalysts supported on $K_2Ti_3O_7$, $H_2Ti_3O_7$ and TiO_2 were employed in the aerobic oxidation of HMF in *N,N*-dimethylformamide at 100°C under a flow of oxygen at ambient pressure (Scheme 15). The results are presented in Figure 32.

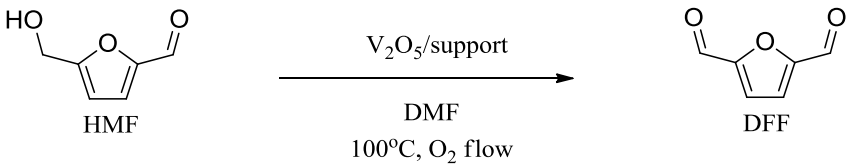

Scheme 15. Aerobic oxidation of HMF to DFF with supported vanadia catalysts in DMF.

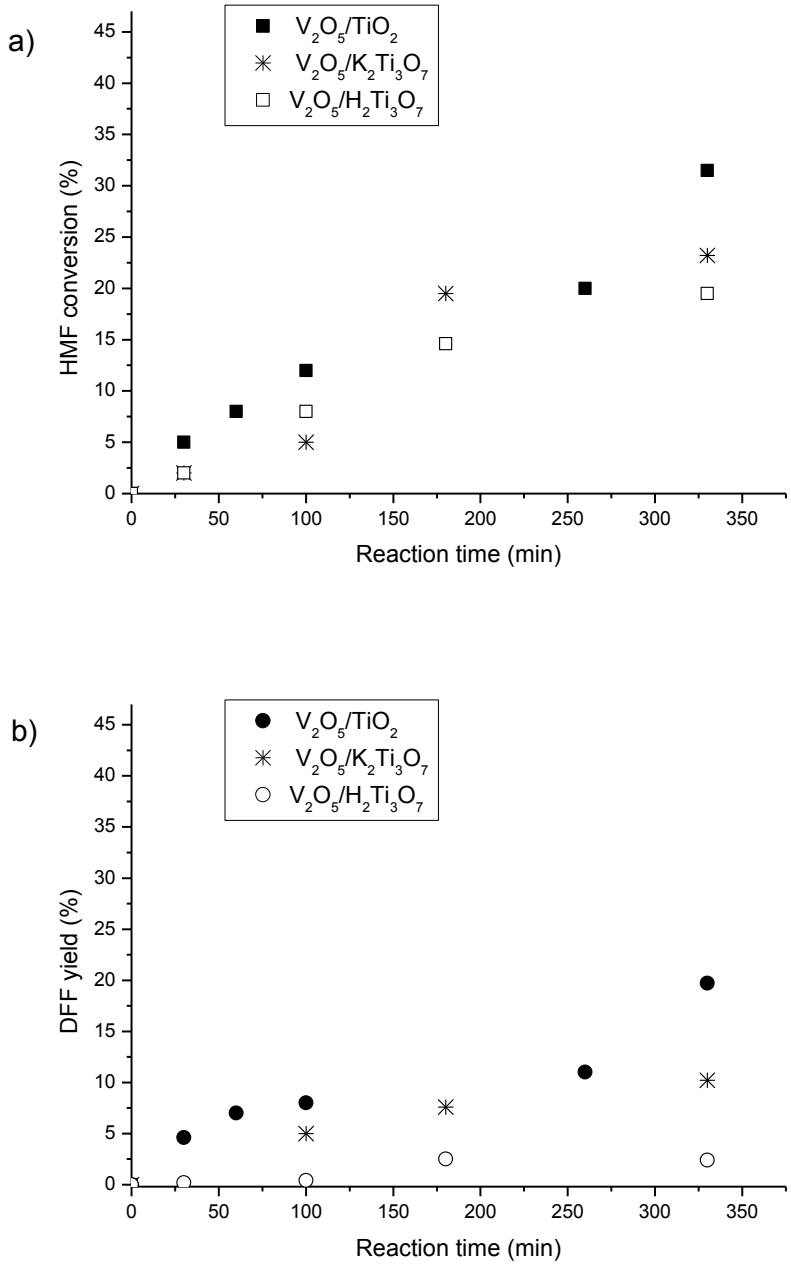

Figure 33. (a) HMF conversion and (b) DFF yield in the aerobic oxidation of HMF in DMF with supported V_2O_5 catalysts as a function of reaction time. Reaction conditions: 0.1 g HMF, 5 mL DMF, 11 μL anisole, 3.44-5 wt% V_2O_5/support catalyst (0.7 mol% V), O_2 flow (1 atm), 100°C.

It is seen from the obtained results that the best performance was exhibited by V_2O_5/TiO_2 catalyst. Here, after 330 min (5.5 hours) of reaction time the conversion of HMF and DFF yield reached *ca.* 32 and 20 %, respectively (Figures 33a,b). For comparison, the respective values in the reaction with $V_2O_5/H_2Ti_3O_7$ were found to be 19 % (HMF conversion) and 2 % (DFF yield). In fact, the latter catalyst afforded lowest selectivity towards the formation of DFF (*ca.* 11 %). This low DFF yield (at the value of HMF conversion comparable to the results obtained with other catalysts) probably was due to the enhanced acidity of $V_2O_5/H_2Ti_3O_7$ catalyst, which can facilitate HMF degradation.

As the highest selectivity towards DFF was observed in the aerobic oxidation of HMF in DMF with V_2O_5/TiO_2 catalyst, the said catalyst was further tested with the respect to the homogeneous contribution to the catalytic activity. Thus, an experiment was conducted where the catalyst was treated in DMF under the same reaction conditions as described above (see Figure 33) in the absence of substrate. After 330 min, the catalyst was filtered off, and the filtrate was re-used, this time with HMF as a substrate and without added solid catalyst. The results are presented in Figure 34.

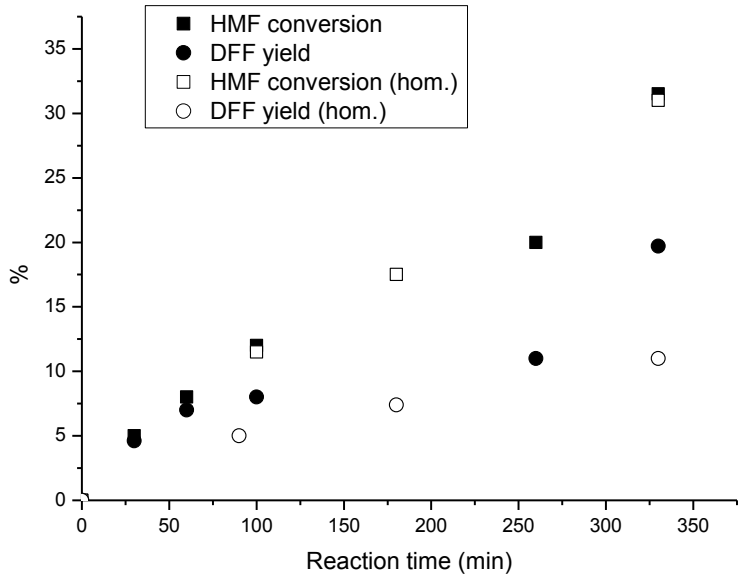

Figure 34. HMF conversion and DFF yield (full and contributed by lixiviated catalytic species) in the aerobic oxidation of HMF in DMF with 5 wt% V_2O_5/TiO_2 catalyst as a function of reaction time. Reaction conditions: 0.1 g HMF, 5 mL DMF, 11 μL anisole, 0.01 g of 5 wt% V_2O_5/TiO_2 (0.7 mol% V), O_2 flow (1 atm), 100°C.

Notably, the reaction performed without catalyst resulted in both the conversion of HMF and the yield of DFF of >2 % after 330 min of reaction time. Therefore, data presented in Figure 34 clearly indicated that the contribution of the lixiviated catalytic species to DFF yield constituted approximately 50 % (Figure 34). After 330 min, the performed reaction without added solid vanadia catalyst afforded the DFF yield of 10 %, compared to the 20 % yield in the reaction with the supported catalyst, at the same value of the HMF conversion (*ca.* 32 %), *i.e.* the selectivity of the reaction towards DFF formation decreased twice with the use of the solubilised catalytic species.

In a research conducted by Satsuma *et al.* [156] HMF was obtained from the dehydration of fructose using solid acids, such as, for instance, zeolites H-Y and H-Beta. Zeolites – crystalline microporous aluminosilicates – have found a multitude of industrial applications as, *e.g.* ion-exchangers, sorbents, etc. [157]. High thermal stability and remarkably high surface areas make zeolites attractive for catalytic applications [158,159]. Hence, the exploration of a dual function catalytic system comprised of a zeolite support (for fructose conversion to HMF) and vanadia aerobic catalyst (for the oxidation of HMF) may potentially present a possibility of a one-pot synthesis of DFF from fructose.

Although, as was mentioned above, SBA-type mesoporous supports were used for vanadyl-based catalyst in the oxidation of HMF to DFF [148], to date there are no reports in literature that can be used to assess the degree of lixiviation of catalytic species, and therefore the homogeneous contribution to the catalyst activity.

In this work, the prospects of using the vanadia catalysts supported on different microporous zeolites (H-Beta, H-ZSM5, H-Y and H-Mordenite) were explored. Some of the catalysts and supports characterization data, including XRPD diffractograms and SEM images of the catalysts, can be found in the Appendix. XRPD analysis of the prepared V_2O_5 catalysts with H-Beta zeolitic support (1, 3 and 10 wt% V_2O_5) revealed only the peaks of the support, indicating an amorphous structure and high dispersion of the deposited vanadium species.

Here, the results of the NH_3-TPD analysis of the zeolitic supports are shown in Table 13a. BET surface areas, the results of the EDS analysis and Raman spectroscopy of the 1, 3 and 10 wt% V_2O_5/H-Beta catalysts are presented in Table 13b.

Table 13a. Characteritics of the V_2O_5/H-Beta catalysts.

Entry	Zeolite	Surface area, m^2/g^a	Amount of absorbed ammonia, μmol/g[b]
1	H-Y	680	1138
2	H-Beta	532	1008
3	H-Mordenite	430	1418
4	H-ZSM5	437	1062

[a]Determined by nitrogen physisorption; calculated by BET method. [b]According to the results of NH_3-TPD analysis.

Table 13b. Characteritics of the V_2O_5/H-Beta catalysts.

Entry	Catalyst loading, wt%	Surface area, m^2/g^a	Experimental V_2O_5 content, wt%[b]
1	0	680	-
2	1	532	0.97
3	3	430	3.08
4	10	437	10.16

[a]Determined by nitrogen physisorption; calculated by BET method. [b]Provided by EDS analysis; calculated on the basis of atomic V:Si and V:Al ratios.

As can bee seen from the presented data, H-Beta zeolite possessed the lowest acidity of the four examined supports (Table 13a, entry 2).

The results of the EDS analysis were in good accordance with the desired weight loading of the prepared catalysts (Table 13b, entries 2-4). The surface areas of the catalysts decreased in order 0 > 1 wt% > 3 wt% catalyst (entries 1-3), as expected. However, when the catalyst weight loading was increased from 3 to 10 wt%, no change in surface area was observed (entries 3 and 4), possibly due to the formation of larger agglomerates of vanadium species without additional support surface coverage.

Initially, 10 wt% V_2O_5 catalysts deposited on zeolites were prepared as described in section 5.2.2 and employed in the aerobic oxidation of HMF in *N,N*-dimethylformamide. The substrate conversion and DFF yield plotted against the reaction time are presented in Figure 35. DFF yield plotted against HMF conversion is presented in Figure 36.

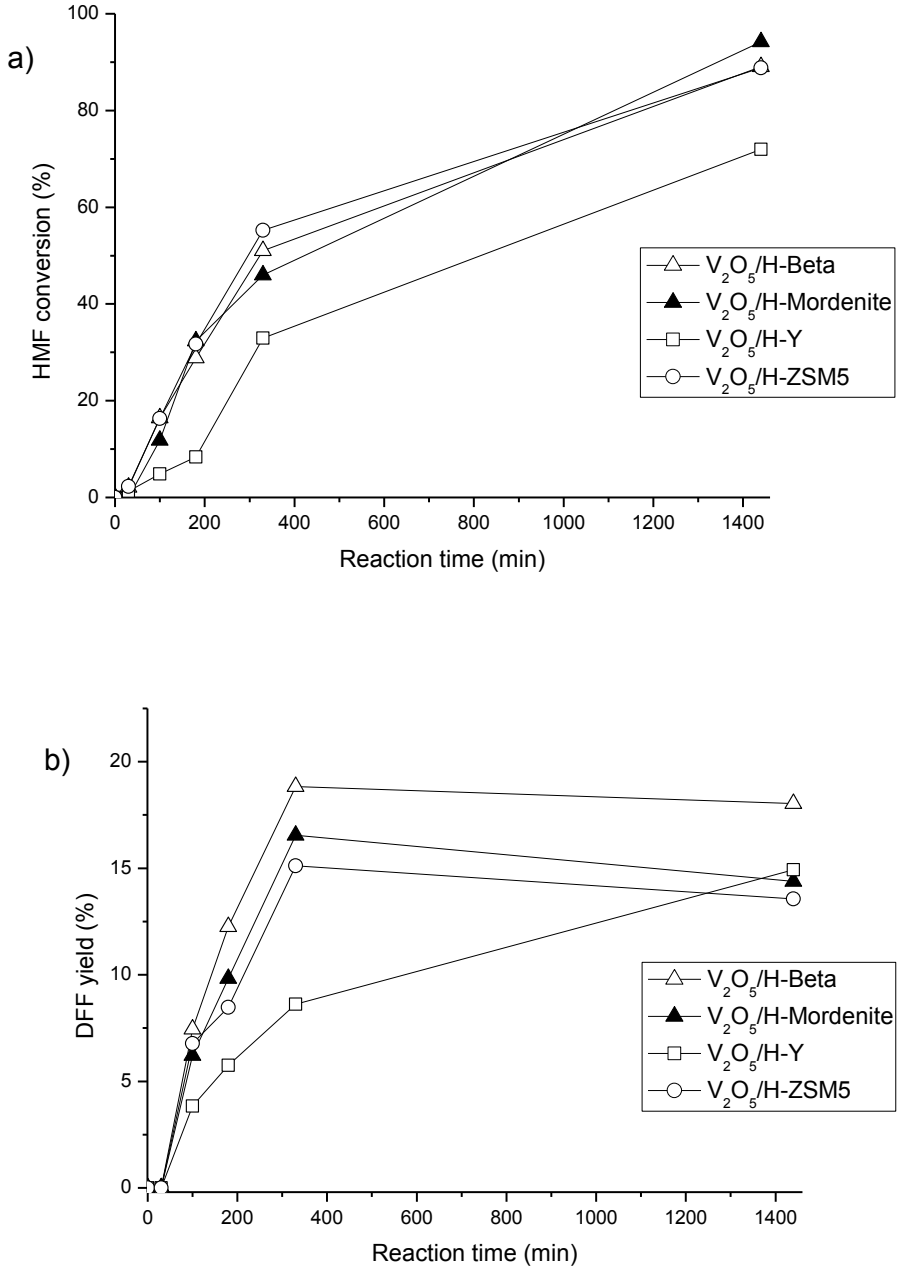

Figure 35. (a) HMF conversion and (b) DFF yield in the aerobic oxidation of HMF in DMF with 10 wt% zeolite-supported V_2O_5 catalysts as a function of reaction time. Reaction conditions: 0.1 g HMF, 5 mL DMF, 11 μL anisole, 0.01 g of 10 wt% V_2O_5/support catalyst (1.4 mol% V), O_2 flow (1 atm), 100°C.

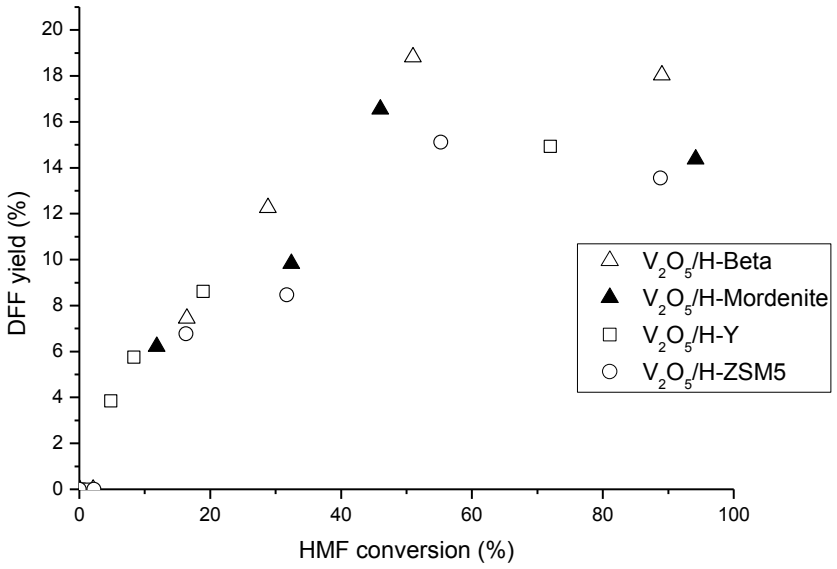

Figure 36. DFF yield in the aerobic oxidation of HMF in DMF with 10 wt% zeolite-supported V_2O_5 catalysts as function of the HMF conversion. Reaction conditions: 0.1 g HMF, 5 mL DMF, 11 μL anisole, 0.01 g of 10 wt% V_2O_5/support catalyst (1.4 mol% V), O_2 flow (1 atm), 100°C.

The reaction progress data showed the increasing HMF conversion within the examined timeframe (Figure 35a), whereas the yield of DFF decreased at the prolonged reaction time for at least three of the tested zeolites (Figure 35b). Here, for instance, when using the V_2O_5/H-Mordenite catalyst, the yield of DFF decreased from *ca.* 17 to 14 % after 5.5 hours (330 min) and 24 hours (1440 min) of the reaction, respectively. Similar tendency was observed when the vanadia catalysts supported on H-Beta and H-ZSM5 zeolites were employed. It was probably also the case in the reaction with the V_2O_5/H-Y catalyst, although at the compared reaction times (5.5 and 24 hours) the yield of DFF here appeared to increase. Nevertheless, the DFF yield plotted against HMF conversion in the mentioned reaction resembles the ones in the reactions where other zeolites were used as the catalysts supports (Figure 36).

The highest DFF selectivity at relatively high HMF conversion value was observed when V_2O_5/H-Beta was used (Figure 36). Notably, although all four tested zeolites were in H-form (*i.e.*, possessed Brønsted acidity detrimental for the stability of HMF), zeolite H-Beta had lower aluminium content compared to other tested zeolites (see section 5.2.2). It has been proposed by Zima *et al.* that the Lewis type surface acidity, usually associated with

the presence of coordinately unsaturated Al sites [160], can promote side reactions leading to undesired by-products [147]. This suggests that the observed difference in catalytic behaviour could possibly be related to the observed, although not drastic, difference in the acidity of the zeolitic supports (see Appendix).

Further, the homogeneous contribution to the activity of the four 10 wt% zeolite-supported catalysts was explored. Similarly to the respective tests for the titania-supported V_2O_5 catalyst (*vide supra*), the catalyst was kept under stirring in DMF for 330 min at 100°C under the flow of oxygen. After that, the catalyst was filtered off and the filtrate was tested for the aerobic oxidation of HMF. The conversion of HMF as found in these experiments is presented in Figure 37.

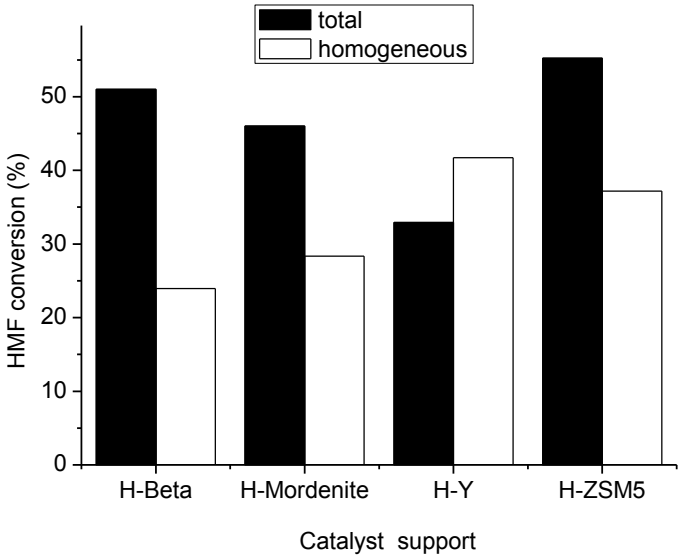

Figure 37. HMF conversion (total and contributed by lixiviated catalytic species) in the aerobic oxidation of HMF in DMF with 10 wt% V_2O_5/zeolite catalysts. Reaction conditions: 0.1 g HMF, 5 mL DMF, 11 μL anisole, 0.01 g of 10 wt% V_2O_5/zeolite catalyst (1.4 mol% V), O_2 flow (1 atm), 100°C, 330 min of reaction time.

Importantly, when the reaction was performed with pure H-Beta zeolite, both the conversion of HMF and the yield of DFF remained under 1 % after 5.5 hours (330 min) of reaction time. This clearly indicated that under applied reaction conditions HMF remained stable and therefore allowed to relate the conversion of HMF observed in the homogeneous test (as shown in Figure 37) to the dissolved catalytic species.

The obtained data showed that for V_2O_5/H-ZSM5 and V_2O_5/H-Mordenite catalysts over 60 % of the total catalyst activity was due to the catalytic species dissolved from the solid catalyst. Indeed, the use of *e.g.* V_2O_5/H-ZSM5 catalyst yielded in the total HMF conversion of 55 %, whilst HMF conversion of 37 % was contributed by the solubilised species (see Figures 35a, 37). The apparent higher homogeneously contributed HMF conversion with the V_2O_5/H-Y catalyst might suggest that the dissolution of vanadia from the H-Y support is generally longer than from the other examined. Therefore in the lixiviation test, where the catalytically active vanadium species have already been dissolved (Figure 37), the oxidation reaction proceeds faster than the reaction with the use of the solid catalyst (Figure 35a).

In the scope of the superior exhibited activity of V_2O_5/H-Beta catalyst in the HMF oxidation to DFF, and taking into consideration the lowest observed extent of the homogeneous contribution to the catalyst activity (*ca.* 45 %; Figure 37), this catalyst was chosen for further investigation.

Further, we explored the possible correlation between the leaching of the active phase and the vanadia content of the employed catalyst. 1 and 3 wt% V_2O_5/H-Beta catalysts were prepared as described above and their catalytic activity was investigated. For that, 1, 3 and 10 wt% V_2O_5/H-Beta catalysts were utilized in the aerobic oxidation of HMF. Importantly, the vanadia : substrate ratio remained the same in all experiments. Total HMF conversion and homogeneous contribution are presented in Figure 38.

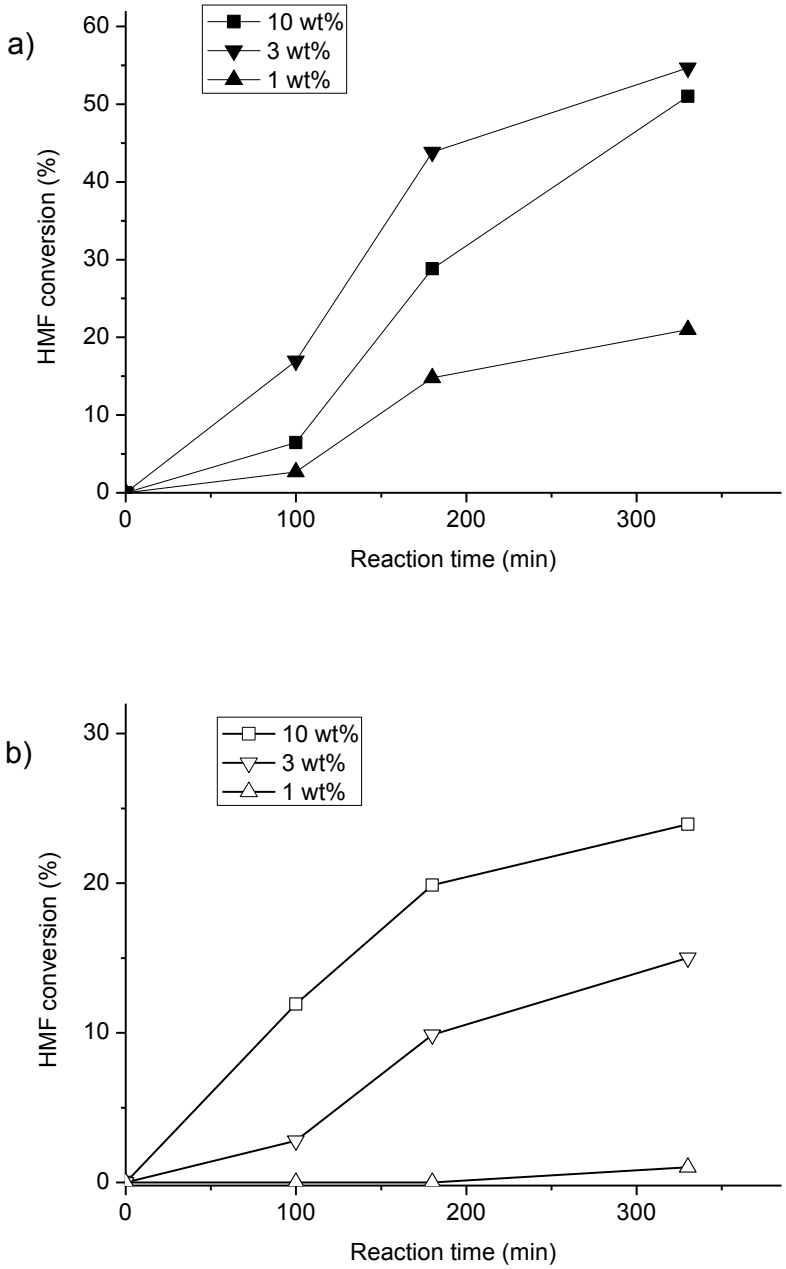

Figure 38. Substrate conversion in the aerobic oxidation of HMF in DMF with 1-10 wt% V_2O_5/H-Beta catalysts as a function of reaction time: (a) total and (b) contributed by lixiviated species. Reaction conditions: 0.1 g HMF, 5 mL DMF, 11 μL anisole, 1-10 wt% V_2O_5/H-Beta catalyst (1.4 mol% V), O_2 flow (1 atm), 100°C.

As it can be seen from the obtained data, the observed substrate conversion was found to be 51 % and 54 % for the 10 and 3 wt% catalysts, respectively, whilst the 1 wt% catalyst exhibited a lower activity (21 % HMF conversion) (Figure 38a). This is likely due the

presence of different vanadium species, corresponding to the different weight loading on a zeolitic support and hence the surface coverage [161].

Nonetheless, the homogeneous contribution to the total catalyst activity (related to the HMF conversion) decreased drastically with the decrease of the vanadium loading on the zeolite (Figure 38b). Indeed, in the case of the 1 wt% catalyst, the leaching of the active phase (and thus the activity of the dissolved species) was essentially avoided. This indicated that the activity of this catalyst was provided entirely by the solid phase and there was no lixiviation of the V_2O_5 induced by the reaction medium.

At the same time, the homogeneously catalysed HMF conversion with the 3 and 10 wt% V_2O_5/H-Beta catalysts was found to be *ca.* 15 and 25 % at 35 and 55 % total HMF conversion, respectively (Figures 37, 38a,b). In fact, the contribution of the lixiviated species constituted approximately half of the total activity for the 10 wt% V_2O_5/H-Beta, thus indicating that at 10 wt% loading the vanadium-containing species deposited on H-Beta zeolite are less prone to lixiviation from the surface of the support.

The previously obtained results of the HMF aerobic oxidation to DFF with $Ru(OH)_x$ supported catalysts (see section 5.3.1) suggested an employment of the V_2O_5/H-Beta catalyst in the HMF aerobic oxidation in other organic solvents, such as toluene, TFT, MIBK, acetonitrile and DMSO. The results are shown in Figure 39a,b. For comparison, the results of the HMF oxidation in DMF are also shown in Figure 39b.

Notably, HMF conversion of <2 % was observed when the reaction was performed in acetonitrile or DMSO at 100^{o}C under the flow of oxygen.

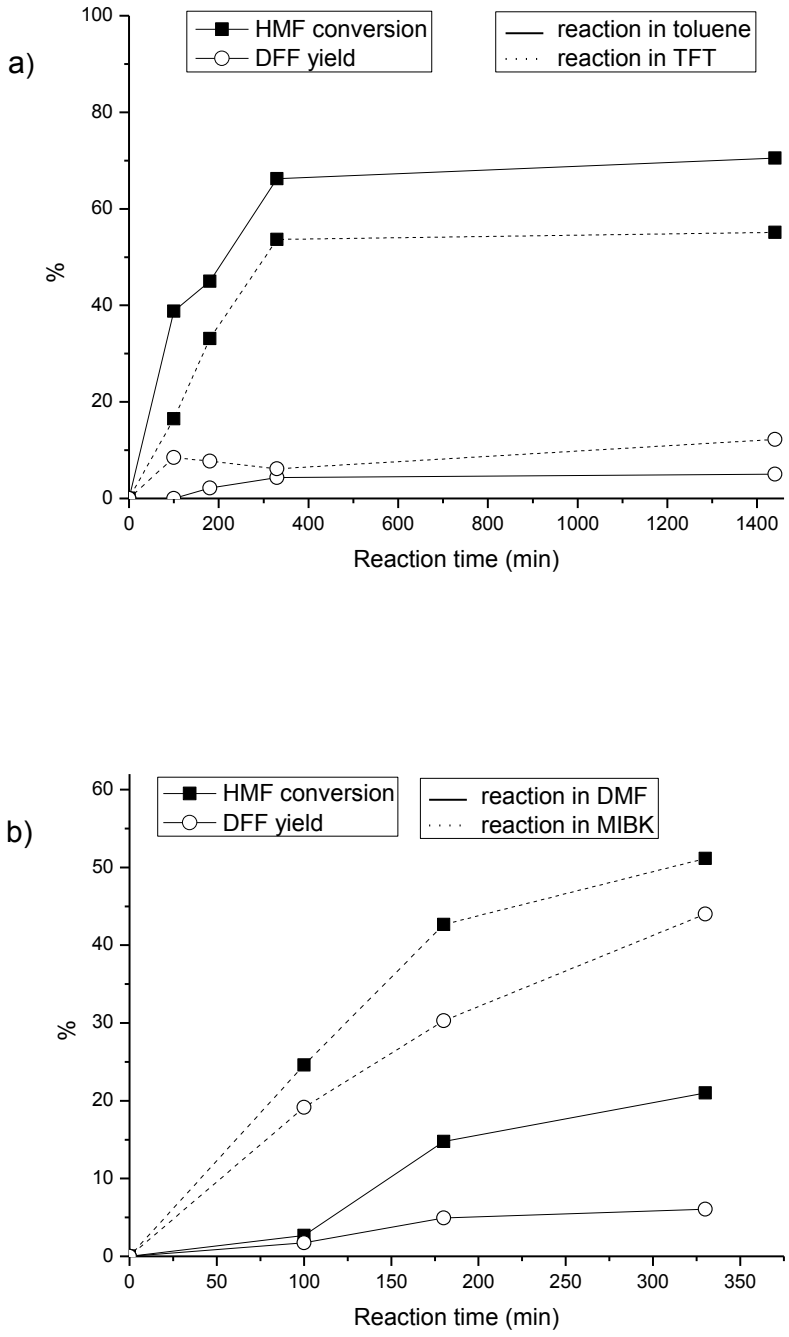

Figure 39. HMF conversion and DFF yield in the aerobic oxidation of HMF in a) toluene and TFT and b) DMF and MIBK with 1 wt% V_2O_5/H-Beta catalyst as a function of reaction time. Reaction conditions: 0.1 g HMF, 5 mL solvent, 11 μL anisole, 0.1 g of 1 wt% V_2O_5/H-Beta catalyst (1.4 mol% V), O_2 flow (1 atm), 100°C.

It can be seen from the results in Figure 39a that although the conversion of HMF reached *ca.* 70 % when the reaction was performed in toluene or TFT already after 330 min of reaction time, the yield of DFF remained 5-10 %. This was not the case in the previously investigated HMF oxidation with the 1.2 wt% Ru(OH)x/CeO_2, where after 26 hours at 80^{o}C the reaction afforded the DFF yield and HMF conversion of 54 and 66 %, respectively (see Figure 29).

In Figure 39b the reaction propagation for the HMF aerobic oxidation in DMF and MIBK is shown. It is seen that when MIBK was chosen as a solvent, HMF conversion proceeded to a much higher extent and constituted *ca.* 50 % after 330 min. At the same time, the yield of DFF was found to be high as well (45 %). Thus, the reaction selectivity to DFF and DFF yield were found to be significantly higher after 330 min of reaction time in MIBK compared to DMF. Also, it can be seen that the DFF selectivity did not decrease as drastically with the reaction progress as it did in DMF (Figure 39b).

It is generally assumed that solvent polarity affects the activity of the catalyst, although there is no general agreement regarding the effect that this phenomenon has on the conversion and selectivity [145,147,155]. When vanadium-based catalysts were used, the conversion of HMF appeared to increase with the increased polarity [147]. In our case, different solvents with increasing polarity were used: methyl isobutyl ketone (MIBK), acetonitrile, *N,N*-dimethylformamide (DMF) and dimethylsulfoxide (DMSO) with polarity indexes of 4.2, 5.8, 6.4 and 7.2, respectively [162]. Very low values of conversion (<5 %) were observed in acetonitrile and DMSO under applied conditions, while MIBK provided higher conversion and selectivity data compared to the previous runs in DMF. Besides, the selectivity to DFF was also improved by using MIBK as a solvent (Figure 39b). According to these results, the polarity of the solvent does not appear to have a distinct effect on the activity, but it is noticeable that the medium plays a role in the development of the reaction.

In a spotlight of the established negligible homogeneous contribution of the 1 wt% V_2O_5/H-Beta catalyst in DMF and the above-discussed acidity of the zeolitic support which can facilitate side-reactions of HMF leading to undesirable products, a catalyst comprised of V2O5 supported on Na-Beta zeolite was prepared *via* an ion exchange and used in the HMF oxidation in DMF (Figure 40).

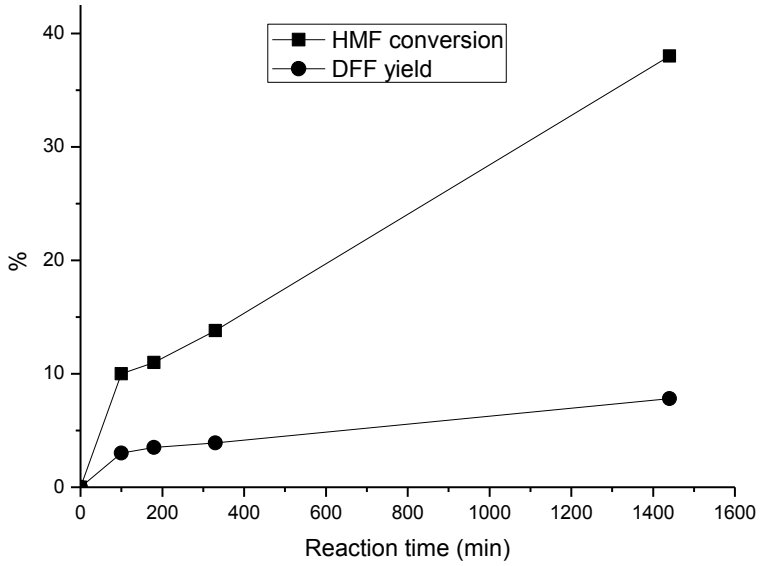

Figure 40. HMF conversion and DFF yield in the aerobic oxidation of HMF in DMF with 1 wt% V_2O_5/Na-Beta catalyst as a function of reaction time. Reaction conditions: 0.1 g HMF, 5 mL DMF, 11 μL anisole, 1 wt% V_2O_5/Na-Beta (1.4 mol% V), O_2 flow (1 atm), 100°C.

It is clearly seen form the results presented in the figure that the usage of 1 wt% V_2O_5/Na-Beta did not result in higher DFF selectivity compared to the reaction with 1 wt% V_2O_5/H-Beta (see Figure 39b). However, both HMF conversion and DFF yield decreased (14 % and 4 % after 330 min, respectively). This unambiguously indicated the effect of the support acidity on the activity of the catalysts (*i.e.*, Brønsted acidity enhanced the overall catalytic activity), and a dominant role of the Lewis acidity on the side-reactions of HMF (*i.e.*, on the DFF selectivity). Thus, an above-discussed observed difference in catalytic behaviour of the V_2O_5 supported on four different zeolites could possibly be related to the observed, albeit not drastic, difference in the Lewis acidity of the supports (see Table 13a).

Finally, the possibility of recycling the catalyst in two solvents, DMF and MIBK, was explored. Figure 41 shows the results of the recycling experiments of the 1 wt% V_2O_5/H-Beta catalyst.

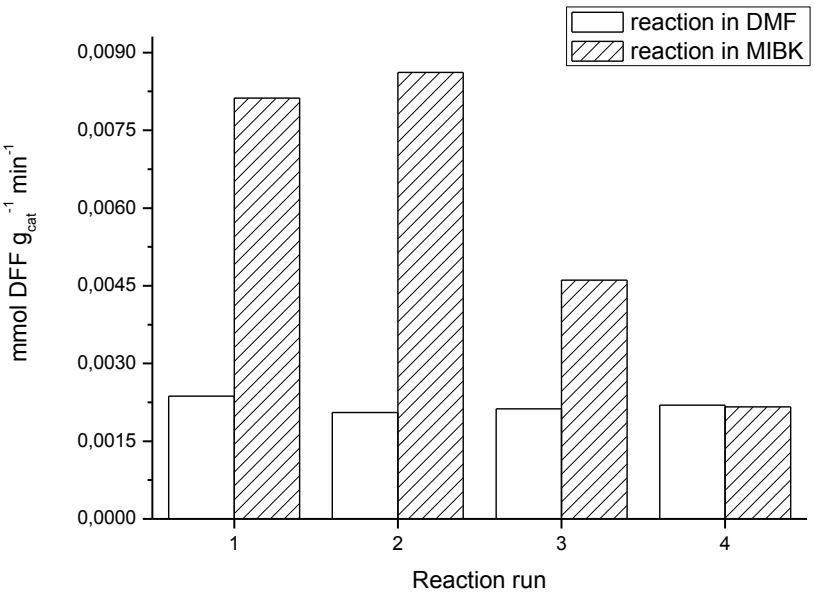

Figure 41. Rate of DFF formation per gram of the catalyst in the recycling of 1 wt% V_2O_5/H-Beta catalyst in DMF and MIBK. Reaction conditions: 0.1 g HMF, 5 mL solvent, 11 μL anisole, 0.1 g of 1 wt% V_2O_5/H-Beta catalyst (1.4 mol% V), O_2 flow (1 atm), 100^{o}C, 330 min reaction time.

It is seen from the results presented in Figure 41 that the rate of DFF production per gram of catalyst remained constant in DMF even after 4 catalytic cycles. In the case of MIBK, the apparent deactivation of the catalyst took place after the second run. This can be due to deposition of carbonaceous residues in the pores of the catalyst, blocking the access of the HMF to the active sites. (In fact, the colour of the catalyst darkened after use, and an increment of weight could be detected.) Furthermore, when the homogeneous contribution test was performed in MIBK, high DFF yield (60 %) was observed immediately after adding the substrate (HMF) to the reaction medium containing lixiviated vanadium species. Since this yield did not increase in time, it might possibly be attributed to a presence of very active oxidant species soluble in the medium, formed as a consequence of the interactions between the solvent and the catalyst.

Although under applied conditions reaction in DMSO resulted in a very low HMF conversion (see above), an attempt to improve the obtained results was performed by conducting the reaction at higher temperature (150^{o}C). The results are presented in Figure 42.

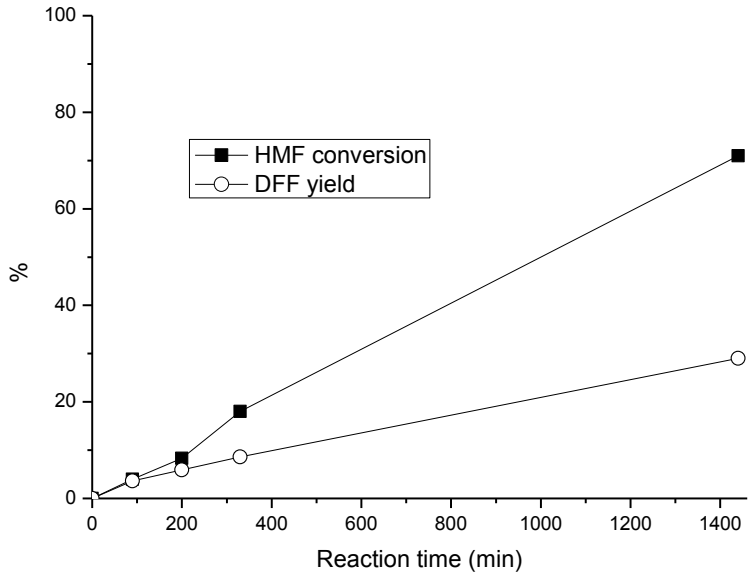

Figure 42. HMF conversion and DFF yield in the aerobic oxidation of HMF in DMSO with 1 wt% V_2O_5/H-Beta catalyst as a function of reaction time. Reaction conditions: 0.1 g HMF, 5 mL solvent, 11 μL anisole, 0.1 g of 1 wt% V_2O_5/H-Beta catalyst (1.4 mol% V), O_2 flow (1 atm), 150^{o}C.

As can be seen from the results shown in Figure 42, after 24 hours at 150^{o}C the reaction resulted in *ca.* 70 % HMF conversion and 30 % DFF yield. Therefore, it proved possible to oxidize HMF in DMSO with the 1 wt% H-Beta-supported vanadia catalyst, albeit with a low DFF selectivity under applied conditions.

These results, together with the proven durability and recyclability of the 1 wt% V_2O_5/H-Beta catalyst in DMF, let us investigate the possibility of improving the DFF yield and selectivity by performing the reaction at elevated pressures. Here, firstly the HMF aerobic oxidation was performed in DMF under 2.5 bar of dioxygen pressure at 100^{o}C. DFF yield and HMF conversion are shown in Figure 43.

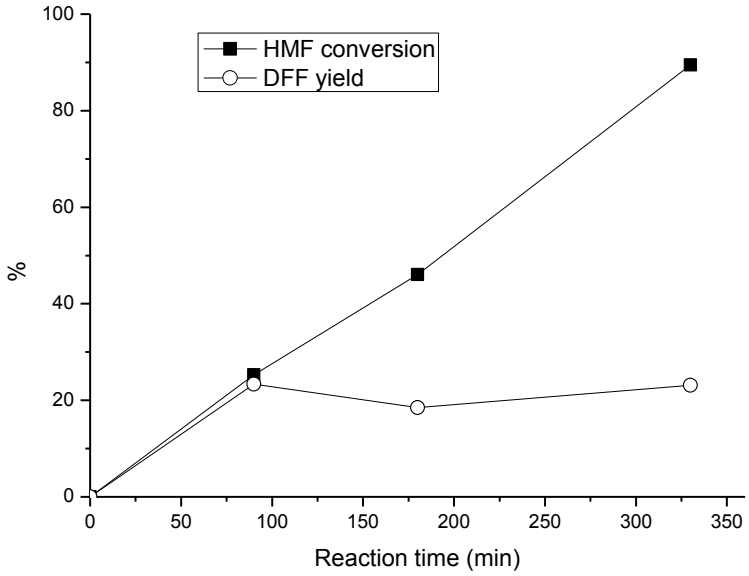

Figure 43. HMF conversion and DFF yield in the aerobic oxidation of HMF in DMF with 1 wt% V_2O_5/H-Beta catalyst as a function of reaction time. Reaction conditions: 0.1 g HMF, 5 mL solvent, 11 μL anisole, 0.1 g of 1 wt% V_2O_5/H-Beta catalyst (1.4 mol% V), 2.5 bar of O_2, 100°C.

It is clearly seen from the data in Figure 43 that both HMF conversion and DFF yield increased with the increase in the oxidant pressure. *Ca.* 90 % HMF conversion and 25 % DFF yield were obtained after 330 min at 2.5 bar of O_2, in contrast to 20 and 5 % under ambient pressure (see Figure 39a). Interestingly, the DFF selectivity did not change with the pressure increase, and remained around 25 % in both cases. However, the only product found by GC-MS and HPLC analysis was DFF, thus suggesting side-reactions leading to the formation of humins, which in fact could define the brown colour of the post-reaction mixture observed in all of these experiments.

Importantly, when a reaction under identical conditions was performed in MIBK (2.5 bar O_2, 100°C), already after 90 min of the reaction the results of the HPLC analysis revealed large amounts of formed formic acid (*ca.* 20 % yield at 90 % HMF conversion). At the same time, substantial amounts of formed HMFCA and FFCA were observed by using both GC-MS and HPLC, indicating low selectivity of the reaction in MIBK under elevated pressures. DFF yield here constituted only 5 %, which was not the case at ambient O_2 pressure (see Figure 39b).

Further, in order to explore the possibility of improving the obtained results, HMF oxidation experiments were conducted in DMSO and DMF at elevated pressures. The results are presented in Table 14.

Table 14. HMF conversion and DFF yield and selectivity in the aerobic oxidation of HMF in organic solvents with 1 wt% V_2O_5/H-Beta catalyst under elevated pressure.[a]

Entry	Solvent	O_2 pressure, bar	Temperature, °C	Reaction time, min	HMF conversion, %	DFF	
						yield, %	selectivity, %
1	DMF	10	60	330	8	7	90
2		10	80	330	55	23	41
3	DMSO	2,5	150	180	84	59	69
4		2,5	150	330	>99	68	69
5		10	150	180	91	67	74
6		10	100	180	13	13	>99
7		10	100	330	21	20	97
8		10	100	1200	77	62	80
9		10	125	180	84	82	98
10		10	125	240	94	70	75
11		10	125	330	>99	71	71
12		40	100	330	44	41	95
13		40	125	180	92	81	89

[a]Reaction conditions: 0.1 g HMF, 5 mL solvent, 0.1 g of 1 wt% V_2O_5/H-Beta catalyst (1.4 mol% V), 11 μL anisole.

The obtained data clearly indicates that the reaction in DMF resulted in much higher DFF selectivity at lower temperatures and higher oxidant pressure. Here, the selectivity of the reaction towards DFF formation was found to be 90 % and 41 %, when the reaction was carried out for 330 min at 60 and 80°C, respectively (Table 14, entries 1 and 2). For comparison, the DFF selectivity after 330 min constituted only *ca.* 26 % when the reaction was performed under 2.5 bar of O_2 at 100°C (see Figure 43). However, the DFF selectivity

decreased drastically (from 90 to 41 %) when the temperature was increased from 60 to 80^{o}C, whilst HMF conversion remained relatively low in both cases.

Furthermore, the reaction in DMSO at 150^{o}C afforded high yields and selectivities of DFF athigh values of the HMF conversion (Table 14, entries 3, 4). In fact, DFF yield and selectivity reached 68 and 69 %, respectively, at full HMF conversion already after 330 min of reaction time under 2.5 bar of O_2 (entry 4). In contrast, the respective values were found to be only ca. 9 and 19 % for the reaction under ambient pressure (Figure 42).

Taking into consideration these results together with the improved conversion and yield of the reaction in DMF under 10 bar pressure, the reaction in DMSO was investigated further in an attempt to obtain high DFF yield within a relatively reaction time. For that, the aerobic oxidation of HMF was conducted in DMSO under 10 bar of O_2 pressure for 180 min at different temperatures (Table 14, entries 5, 6, 9). It is seen from the data that the DFF selectivity decreased with the increase of temperature. Indeed, the selectivity was found to be *ca.* 99, 98 and 74 %, when the reaction was performed at 100, 125 and 150^{o}C, respectively. Notably, although providing high selectivity towards desired product, the reaction at 100^{o}C afforded only a very low HMF conversion (13 %) (Table 14, entry 6). However, at prolonged reaction times the increase in the HFM conversion and DFF yield were observed together with the decrease of the DFF selectivity (entries 6-8): from >99 % to 80 % after 3 and 20 hours, respectively (entries 6 and 8).

Similar tendency was observed when the progress of the reaction at 125^{o}C was explored. Here, DFF selectivity decreased with the reaction propagation from 98 after 180 min (84 % HMF conversion) to 71 % (>99 % HMF conversion) (Table 14, entries 9-11). In fact, the amount of DFF decreased in this case, suggesting a side-reaction leading to the gradual product degradation.

The increase of the oxidant pressure from 10 to 40 bar at 100^{o}C allowed to achieve higher, albeit less then 50 %, HMF conversion and DFF yield (entry 12) with approximately equal selectivity (*ca.* 95 %). At the same time, the reaction under 40 bar O_2 at 125^{o}C resulted in a lower DFF selectivity (89 %; entry 13) compared to that achieved under 10 bar (98 %; entry 9).

Furthermore, the homogeneous test similar to described above for the oxidation at ambient pressure was conducted for the reaction with the highest achieved values of both

substrate conversion and DFF selectivity (0.1 g HMF, 5 mL DMSO, 0.1 g of 1 wt% V_2O_5/H-Beta, 10 bar O_2, 125°C, 180 min of reaction time). The results are presented in Figure 44.

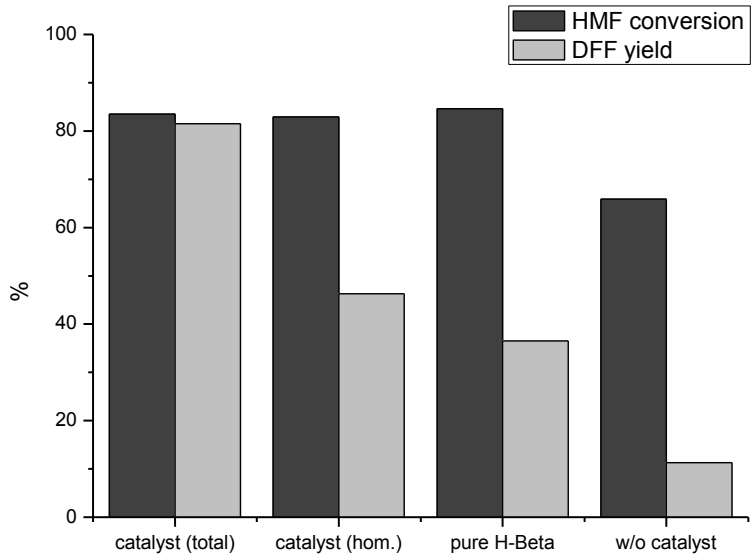

Figure 44. HMF conversion and DFF yield in the aerobic oxidation of HMF in DMSO with 1 wt% V_2O_5/H-Beta catalyst. Reaction conditions: 0.1 g HMF, 5 mL solvent, 11 μL anisole, 0.1 g of 1 wt% V_2O_5/H-Beta catalyst (1.4 mol% V), 10 bar of O_2, 125°C, 180 min reaction time.

The data in Figure 44 showed that an equally high extent of the HMF conversion (about 84 %) was reached in the oxidation reaction with the lixiviated catalytic species, as well as when pure H-Beta zeolite was introduced in the reaction instead of the catalyst. The yield of DFF remained highest when the solid catalyst was used (*ca.* 82 %), whereas the homogeneously contributed DFF yield was only 46 %. Interestingly, the use of pure zeolitic support afforded a 36 % DFF yield, whereas when the reaction was performed in DMF under ambient pressure at 100°C, it exhibited no catalytic activity (see above). In fact, a low but not negligible yield of DFF (10 %) was observed when the reaction was performed in the absence of catalyst, thus making a precise direct evaluation of the homogeneous contribution difficult. Nevertheless, the catalytic effect of the solubilised species was suggested by the difference in the DFF yield between the reactions with lixiviated catalyst and pure H-Beta support, as well as the difference in HMF conversion caused by the solubilised species and obtained in the absence of the catalyst.

5.4. Conclusions

First, an aerobic oxidation of HMF to DFF with supported $Ru(OH)_x$ catalysts in different organic solvents (*e.g.*, toluene, trifluorotoluene, MIBK, DMF, acetonitrile) under ambient oxidant pressure was investigated. An effect of the reaction medium was shown, with toluene having a supremacy towards higher HMF conversion DFF selectivity.

Ruthenium hydroxide catalysts supported on ceria and the mixed magnesium-lanthanum oxide were shown to have superior performance compared to those supported on titanium, magnesium, lanthanum oxides and spinel. An improvement in the catalytic activity of the CeO_2-supported catalyst was observed when the loading of the ruthenium species was reduced from 2.4 to 1.2 wt%. The effects of catalyst amount, substrate concentration, reaction temperature, oxidant pressure and gas atmosphere were shown. Under optimized conditions, a 54 % yield of DFF with 82 % selectivity was obtained with 1.2 wt% $Ru(OH)_x/CeO_2$ in toluene at 80^oC.

Additionally, the aerobic oxidation of other substituted furans, such as furfuryl alcohol and 5-methylfurfuryl alcohol was explored with $Ru(OH)_x/MgO{\cdot}La_2O_3$ and $Ru(OH)_x/CeO_2$ catalysts. Higher reactivity of HMF compared to other investigated furans was shown when $Ru(OH)_x$ supported on $MgO{\cdot}La_2O_3$ was used. The usage of $Ru(OH)_x/CeO_2$, however, afforded 86 and 68 % furfuryl alcohol conversion and furfural yield, respectively, possibly indicating that the oxidation of HMF under similar conditions was limited by the relatively low solubility of both substrate and product (DFF).

Second, a study on the homogeneous contribution to the total catalytic activity of the supported vanadia catalysts was performed. V_2O_5 catalysts supported on TiO_2, $K_2Ti_3O_7$, $H_2Ti_3O_7$, zeolites H-Beta, H-Y, H-Mordenite, H-ZSM5 and Na-Beta were used in the aerobic oxidation of HMF in different organic solvents (*e.g.*, DMF, toluene, TFT, acetonitrile, MIBK, DMSO). Significant extent of the lixiviation of catalytic species from catalyst in DMF was shown in case of V_2O_5 supported on titania and titanates.

Further, an investigation of the application of the new catalytic systems comprising vanadia supported on zeolites was conducted. V_2O_5 suppored on H-Beta zeolite exhibited better performance in the HMF oxidation in DMF. By exploring the homogeneous contribution of the 10, 3 and 1 wt% V_2O_5/H-Beta catalysts, it was established that the usage

of the 1 wt% V_2O_5/H-Beta produced almost no lixiviated catalytic species under applied reaction conditions. Furthermore, the effect of the reaction medium was discussed. The 1 wt% V_2O_5/H-Beta catalyst was also shown to be prone to re-use in DMF, whereas conducting of the reaction in MIDK caused the decrease in the activity of the catalyst.

Moreover, the employment of the 1 wt% H-Beta-supported V_2O_5 catalyst was investigated in the aerobic oxidation of HMF in DMF and DMSO under elevated pressures. Under optimized reaction conditions (125^{o}C, 10 bar O_2), the oxidation reaction with 1 wt% V_2O_5/H-Beta yielded in the 84 % conversion of HMF and 82 % DFF yield. However, under applied conditions the conversion of HMF to DFF yield was found to proceed to a certain extent even in the absence of catalyst thus making a direct assessment of the homogeneous contribution to the catalytic activity difficult.

6. *Aerobic oxidation of alcohols to acetic acid with supported ruthenium catalysts*

6.1. Introduction

The oxidation reaction of primary alcohols to aldehydes or especially carboxylic acids, and secondary alcohols to ketones is one of the key fundamental synthetic transformations in chemical industry [163]. Also, in the past years due to the increase of the demand of shift from massively used fossil feedstock towards bio-derived chemicals the catalytic transformations of alcohols gain new importance [62,164]. However, still many processes utilize environmentally unfeasible oxidants and low atom efficiencies [165]. Hence, the investigation of yet new ways of alcohols oxidation using benign solvents and oxygen as the oxidant remains an important task [88,165].

Acetic acid is a highly important organic bulk chemical with the current annual production of approximately 8.5 million tonnes and annual growth rate of roughly 1 % [166]. Traditionally, acetic acid has been derived from ethanol *via* fermentation, a production route that is still used today to make vinegar (*i.e.* aqueous acetic acid) [167]. Since the late 1990s, production of biomass-derived ethanol or 'bio-ethanol' has increased dramatically [168]. So far the main utilization of bio-ethanol has been as fuel additive, however, ethanol is a low value bulk chemical with potential to be a sustainable chemical feedstock when upgraded to other higher value products, *e.g.* bio-acetic acid [164]. Although such 'bio-acetic acid' only makes up a small volume of the total annual acetic acid production (*i.e.* 0.8 million tonnes per year) [168], this is still a significant volume positioning this production route in the lower end of the bulk chemical scale production.

As an alternative to fermentation of ethanol, various chemical pathways to aqueous acetic acid have already been shown in the literature. An obvious route is *via* the oxidation of an ethyl species using dioxygen [169], which has been demonstrated with ethane [170], ethanol and acetaldehyde [171] (Scheme 16).

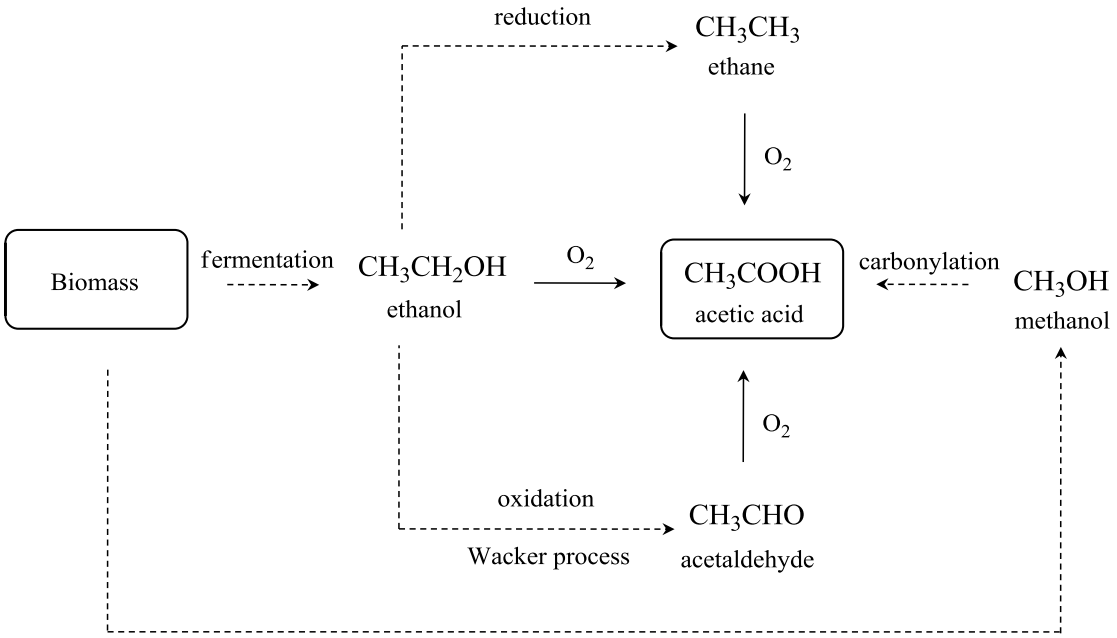

Scheme 16. Possible routes for the production of acetic acid from biomass.

All of these methods have, however, only been shown on a lab scale and not successfully scaled up to industrial levels [170], though the possibility of obtaining acetic acid from biomass *via* bio-ethanol would be an attractive route, that is not based on petrochemicals like the current large scale productions *via* methanol carbonylation [171] or the Wacker process of acetaldehyde oxidation [170].

For the oxidation of ethanol (not limited by aqueous conditions) studies have shown that supported gold [63,165,172,173], copper/copper-chromium oxides [174], molybdenum, vanadium, niobium mixed oxides [175], palladium [52,176,177], and platinum [178] catalysts can be used. Hence, Rajesh *et al.* [174] succeeded, by using either copper or copper-chromium catalysts supported on γ-alumina, to achieve yields of acetaldehyde up to 27 % by the oxidation of ethanol. Li *et al.* [175] were able to show that supported mixed oxides containing molybdenum, vanadium and niobium provided 100 % ethanol conversion combined with a 95 % selectivity towards acetic acid. ten Brink *et al.* demonstrated use of a homogeneous palladium catalyst in a biphasic system for the oxidation of both primary and secondary alcohols in an aqueous medium [52]. Here conversions of over 90 % for a large variety of substrates were obtained with isolated yields of the corresponding ketone,

aldehyde or carboxylic acid above 80 %. Nishimura *et al.* made use of supported palladium catalyst to perform the oxidation of primary and secondary alcohols to aldehydes and ketones [176]. Again, high conversions were combined with high isolated yields (>95 % and >85 %, respectively).

Gold catalysts supported on silica, titania, ceria, zinc and niobium oxides have been actively utilized by various research groups for the oxidation of ethanol in both liquid and gas phase, providing high conversion and selectivity towards acetic acid. Most of these results are summarized in the recent review by Haruta *et al.* [179].

In this chapter, $Ru(OH)_x$ and RuO_x catalysts on different supports including titanate nanotubes and various metal oxides, such as TiO_2, CeO_2 or $MgAl_2O_4$, were found to catalyze the aerobic oxidation of ethanol and 1-propanol to acetic acid in aqueous solutions with moderate to excellent yields (Scheme 17).

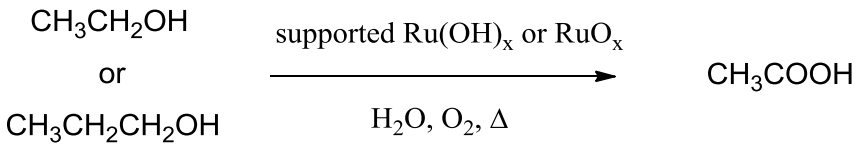

Scheme 17. Aerobic oxidation of aqueous ethanol to form acetic acid with supported ruthenium catalysts.

6.2. Experimental

Materials: Ethanol (99.9 %, Kemetyl A/S); acetaldehyde (>99.5 %, Sigma-Aldrich); acetic acid (99.8%, Riedel-de Haën AG); ruthenium(III) chloride (purum, ~41 % Ru, Sigma-Aldrich); titanium oxide (anatase, 99.7 %, Sigma-Aldrich); spinel $MgAl_2O_4$ (Sigma-Aldrich); cerium(IV) oxide (99.5 %, Alfa Aesar); sodium hydroxide, formic acid, 1,2-ethanediol (glycol), 1- and 2-propanol, propionaldehyde, propionic acid, glycerol, acetone (all ≥98-99 %, Sigma-Aldrich); 1,2- and 1,3-propanediol, 1- and 2-butanol, 2-methyl-2-propanol (*t*-butanol), 1,3-, 1,2- and 2,3-butanediol (all ≥99-99.7 %, Fluka); dioxygen (99.5 %, Air Liquide Denmark) were all used as received.

For the preparation of supported highly dispersed RuO_x catalysts, additional reagents and supports were used: $KMnO_4$ (p.a., Merck), dopamine chloride (98 %, Sigma-Aldrich), Degussa P25 TiO_2 (Degussa), hydrotalcite ($Mg_6Al_2(CO_3)(OH)_{16}\cdot 4H_2O$, synthetic, Sigma-Aldrich), spinel $MgAl_2O_4$ (courtesy of Haldor Topsøe A/S), ZnO (≥99 %, Sigma-Aldrich), γ-Al_2O_3 (Puralox TH100/150, Sasol), WO_3 (≥99 %, Sigma-Aldrich), CeO_2 (nanopowder, ≥99.9 %, Sigma-Aldrich), high surface area (hs) nanoparticulate CeO_2 and $CeZrO_4$ (AMR Technologies Inc.).

6.2.1. Ethanol oxidation with $Ru(OH)_x$/support catalysts

Catalyst preparation: 2.44, 4.88 or 9.76 g of support (*i.e.* CeO_2, $MgAl_2O_4$ or TiO_2) were added to 143 mL of 8.3 mM aqueous $RuCl_3$ solution (1.19 mmol Ru). After stirring for 15 min, 28 mL of 1 M NaOH solution was added and the mixtures were stirred for 18 hours. Then the catalysts were filtered off, washed thoroughly with water until neutral reaction (and dried at 140°C for 40 hours resulting in catalysts with optimally 4.7, 2.4, 1.2 wt% Ru, respectively.

For the study of heat treatment effects, catalysts were calcined at 170 and 450°C in still air for 18 hours.

Surface areas were determined by nitrogen physisorption measurements at liquid nitrogen temperature on Micrometrics ASAP 2020. The samples were outgassed in vacuum

at 150^{o}C for 6 hours prior to measurements. The total surface areas were calculated according to the BET method. For transmission electron microscopy (TEM) characterization, samples were dispersed on a lacy amorphous carbon support film. Images were acquired using a FEI Tecnai Transmission Electron Microscope operated at 200 kV. EDS analysis was performed using an Oxford INCA system. XRPD patterns were recorded using a Huber G670 powder diffractometer (Cu-K_α radiation, λ = 1.54056 Å) in the 2θ interval 5-100^{o}.

Oxidation reaction: Oxidations were carried out in stirred Parr autoclaves equipped with internal thermocontrol (T316 steel, Teflon™ beaker insert, 100 mL). In each reaction the autoclave was charged with 10 g of 2.5-50 wt% aqueous ethanol solutions.

The supported 1.2-4.7 wt% $Ru(OH)_x$ catalyst (weight percentage given on Ru metal basis) was added (0.05-0.21 g, 0.012-0.05 mmol Ru) to the solution and the autoclave was pressurized with dioxygen (10-30 bar, *ca.* 16-48 mmol) and maintained at 125-250^{o}C for a given period of time under stirring (500 rpm). After the reaction, the autoclave was rapidly cooled to room temperature (*i.e.* 20^{o}C). The reaction mixture was then filtered and analyzed using HPLC (Agilent Technologies 1200 series, Aminex HPX-87H column from Bio-Rad, 300 mm x 7.8 mm x 9 μm, flow 0.6 mL/min, solvent 5 mM H_2SO_4, temperature 60^{o}C) and/or GC-MS (GC Agilent Technologies 6850 coupled with MS Agilent Technologies 5975C, HP-5MS column from J & W Scientific, 30 m × 0.25 mm × 0.25 μm, 5 mol% phenylmethylpolysiloxane, flow gas He). In all figures where the product distribution is shown as a function of time each data point corresponds to an individual reaction run.

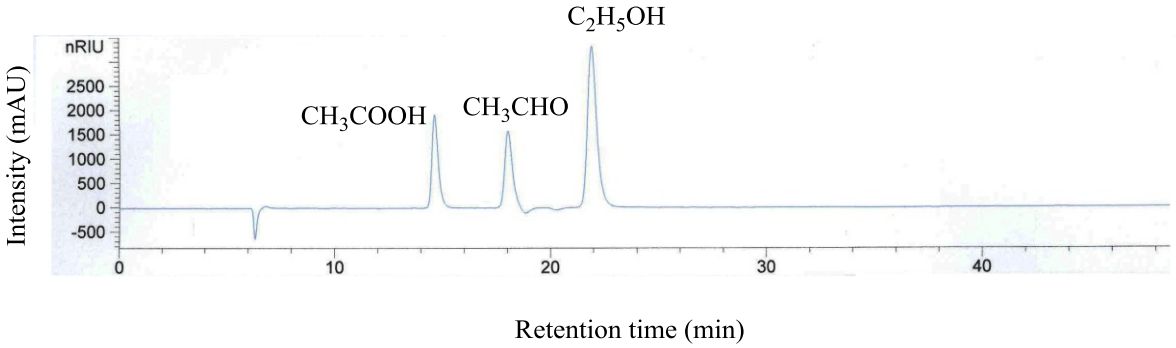

Figure 45. A typical chromatogram obtained by the HPLC analysis of the post-reaction mixture in the experiments of aqueous ethanol oxidation. Compounds (left to right): acetic acid, acetaldehyde, ethanol.

6.2.2. Ethanol oxidation with highly dispersed RuO_x/support catalysts

This research was conducted in collaboration with Anders B. Laursen (DTU CINF), who performed the synthesis of the highly dispersed ruthenium hydroxide catalysts.

Catalyst preparation: Sodium titanate support was prepared as described in literature [65]. Catalysts were prepared as reported by Laursen *et al.* [180]. For supports functionalization, 1 g of support was suspended in a 20 mM dopamine chloride solution in 30 % CH_3OH/H_2O by sonication for 30 min in a Branson 8510 ultrasonicator. The powder was recovered by centrifugation at 20000 rpm for 60 min. The liquid was removed by decantation, and the product was resuspended in water. The procedure was repeated 4 times. The resulting powder was dried at 95^{o}C overnight in air, yielding in *ca.* 0.9 g of the functionalized support.

RuO_x coating was performed as follows: 0.5 g of the functionalized support was placed in a glass tube (3 mm x 30 cm) between two Pyrex wool corks in both ends. The tube was placed through one septum inlet in a three-necked flask. The flask was charged with a solution of 40 mg $RuCl_3 \cdot xH_2O$ in 10 mL of water and the mixture was stirred for 5 min. Then a solution of 80 mg $KMnO_4$ in 10 mL of water was added to the flask. The flask was sealed and N_2 was bubbled through the solution. The flask is continuously stirred at 400 rpm throughout the deposition. Every hour the tube with the catalyst was rotated allowing an equal coating. After 4 hours the deposition was finished and the powder collected (yield *ca.* 0.84 g of RuO_x/support).

For the samples with lower and higher loadings of RuO_x the amounts of added $RuCl_3 \cdot xH_2O$ and $KMnO_4$ were reduced and increased respectively to the desired weight loading.

For the study of heat treatment effects, three samples of 1.8 wt% RuO_x/CeO_2 catalyst (0.3 g each) were calcined at 170, 200 and 450°C in still air for 18 hours.

BET surface areas of the catalysts were determined similarly to described above. X-ray fluorescent (XRF) analysis was performed on PAN'alytical MiniPal 3.

SEM images were obtained on a FEI Quanta 200 F Microscope (5 kV) for uncoated samples dropcast from ethanol suspension directly onto the sample holder. TEM images were obtained on FEI Titan 80-300ST TEM and FEI Tecnai T20 TEM microscopes (300 kV, sample mounted on a copper grid coated with holey carbon film).

Oxidation reactions: Experiments were carried out in stirred Parr mini-reactor autoclaves equipped with internal thermocontrol (T316 steel, Teflon™ beaker insert, 100 mL). In each reaction the autoclave is charged with 10 g of 5 wt% aqueous ethanol. Subsequently, the supported 0.9-3.4 wt% RuO_x catalyst (weight percentage given for Ru metal basis) was added (0.09-0.33 g, *ca.* 0.03 mmol Ru). The autoclave was then pressurized with O_2 (10 bar, *ca.* 16 mmol) and maintained at 150°C for a given period of time under stirring (500 rpm). After the reaction, the autoclave was rapidly cooled to room temperature. The reaction mixture was filtered and analyzed using HPLC. In all figures where the product distribution is shown as a function of time each data point corresponds to an individual reaction run.

6.2.3. Oxidation of higher alcohols with supported ruthenium catalysts

Oxidation reactions: Experiments were carried out in stirred Parr mini-reactor autoclaves equipped with internal thermocontrol (T316 steel, Teflon™ beaker insert, 100 mL). In each reaction the autoclave was charged with 10.13 mL of 0.107 M aqueous solution of substrate. In cases when the substrate was not water-soluble at room temperature, the autoclave was charged with a two-phase mixture substrate/H_2O with 10.8 mmol of substrate and the resulting volume of 10.13 mL. Subsequently, the supported 1.2-4.7 wt% $Ru(OH)_x$ catalyst (weight percentage given for Ru metal basis) was added (0.05-0.21 g, 0.012-0.05 mmol Ru). The autoclave was pressurized with dioxygen (5-20 bar, *ca.* 8-32 mmol) and maintained at 125-175°C for a given period of time under stirring (500 rpm). After the reaction, the

autoclave was rapidly cooled to room temperature (i.e. 20°C). The reaction mixture was filtered directly, followed by analysis using HPLC (Figure 46) (Agilent Technologies 1200 series, Aminex HPX-87H column from Bio-Rad, 300 mm x 7.8 mm x 9 μm, flow 0.6 mL/min, solvent 5 mM H_2SO_4, temperature 60°C) and/or GC-MS (GC Agilent Technologies 6850 coupled with MS Agilent Technologies 5975C, column HP-5MS (J & W Scientific, 30 m × 0.25 mm × 0.25 μm, 5 mol% phenylmethylpolysiloxane), flow gas He). In all figures where the product distribution is shown as a function of time each data point corresponds to an individual reaction run.

The gas phase analysis was performed by GC-TCD (Agilent GC 7890A, inlet gas N_2, split injection, 1st column FFAFP, 2nd column Plot Q, reference/make up gas He, reference flow 10 ml/min, make up flow 5 mL/min).

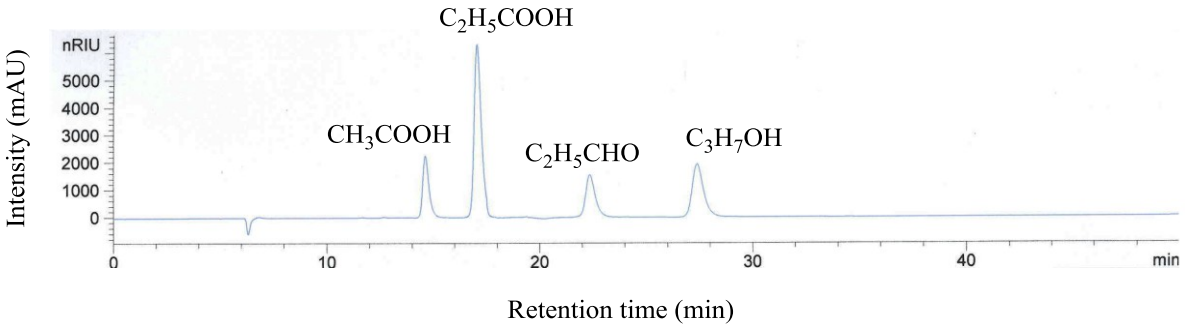

Figure 46. A typical chromatogram obtained by the HPLC analysis of the post-reaction mixture in the experiments of aqueous 1-propanol oxidation. Compounds (left to right): acetic acid, propionic acid, propionaldehyde, 1-propanol.

6.3. Results and discussion

6.3.1. Aerobic oxidation of aqueous ethanol into acetic acid over heterogeneous ruthenium hydroxide catalysts

BET surface areas of some of the catalysts and supports were shown in Table 4 (section 4.3.3.1). Here, The EDS analysis data and BET surface areas of all applied support materials and the prepared catalyst samples are listed in Table 15. TEM images of the 1.2, 2.4 and 4.7 wt% $Ru(OH)_x/CeO_2$ catalysts are presented in Figure 47.

Table 15. Characteristics of supports and supported $Ru(OH)_x$ catalysts.

Entry	Material	BET surface area, m^2/g	Ru content, wt%[a]	Particle size, nm[b]
1	TiO_2	123	-	-
2	2.4 wt% $Ru(OH)_x/TiO_2$	128	2.32	n/a
3	$MgAl_2O_4$	63	-	-
4	1.2 wt% $Ru(OH)_x/MgAl_2O_4$	54	1.35	0.5 – 2
5	2.4 wt% $Ru(OH)_x/MgAl_2O_4$	53	2.41	n/a
6	CeO_2	62	-	-
7	1.2 wt% $Ru(OH)_x/ CeO_2$	8	1.31	0.6 - 2
8	2.4 wt% $Ru(OH)_x/ CeO_2$	8	2.26	0.8 – 3.5
9	4.7 wt% $Ru(OH)_x/ CeO_2$	8	4.56	1.5 – 6

[a]Based on Ru:Ti, Ru:Al, Ru:Ce atomic ratios provided by EDS (average for the analyzed sample).
[b]Determined from TEM imaging.

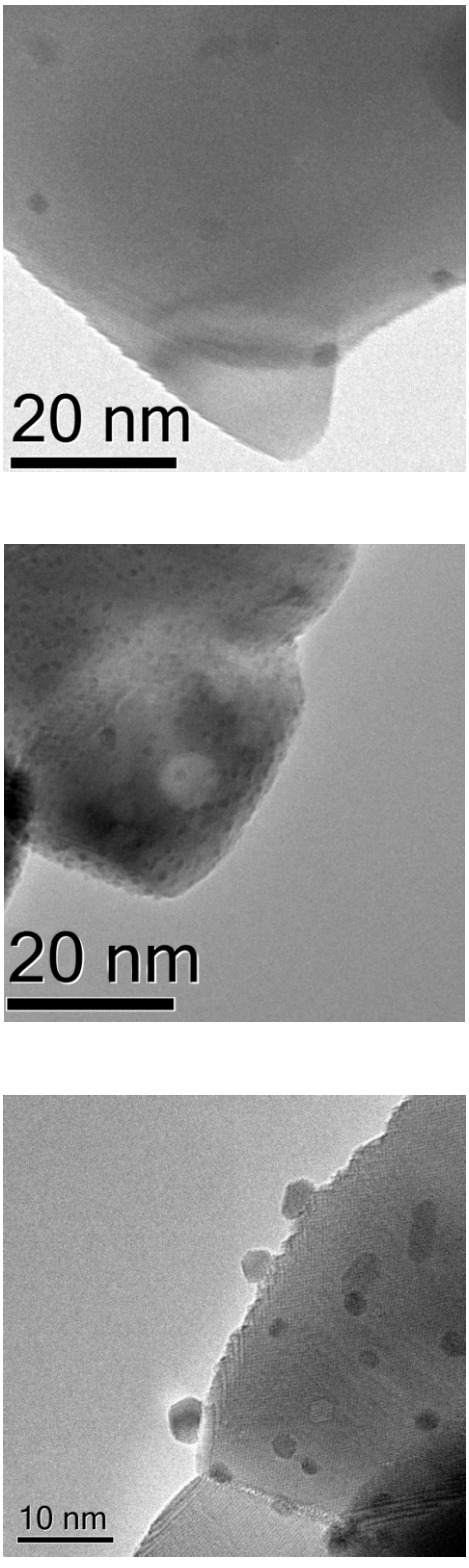

Figure 47. High-resolution TEM images of the 1.2 wt% (top), 2.4 wt% (center) and 4.7 wt% (bottom) $Ru(OH)_x/CeO_2$ catalysts.

As seen from the data, the experimental ruthenium contents determined by EDS were in good accordance with the calculated amounts. As was also shown previously, the nitrogen physisorption analysis revealed a moderate decrease in BET surface areas when the ruthenium species were deposited on $MgAl_2O_4$ support (Table 15, entries 3-5), as expected. Interestingly, the decrease in the BET surface area of $Ru(OH)_x$ catalysts supported on CeO_2 compared to pure CeO_2 was much more drastic (entries 6-9), suggesting a change in morphology. Notably, however, in the cases of both spinel and ceria the decrease of the surface area did not apparently correlate with the weight loading of ruthenium (entries 4-5 and 7-9).

The particle sizes of the deposit on 1.2, 2.4 and 4.7 wt% $Ru(OH)_x/CeO_2$ catalysts increased with increasing ruthenium loading (Table 15, entries 7-9). A few anomalously large agglomerates of ruthenium species were observed on the surface of cerium oxide. In contrast, the results from EDS analysis of the catalyst supported on spinel (entry 4) revealed small variation in the amount of determined ruthenium, thus suggesting an improved dispersion of active species on the surface of spinel. With respect to catalytic performance, the contribution of the agglomerates is expected to be negligible, since the surface area provided by these few large particles is insignificant compared to the collective surface area of the smaller particles.

First, the aerobic oxidation of ethanol in aqueous solutions with $Ru(OH)_x$ supported on spinel, titania and ceria as catalysts was investigated and the results are presented in Figure 48. Titania, ceria and spinel were chosen due to their stability which makes them attractive supports for various catalytic reactions. These supports were also applied in other investigations described in the previous chapters of the present thesis.

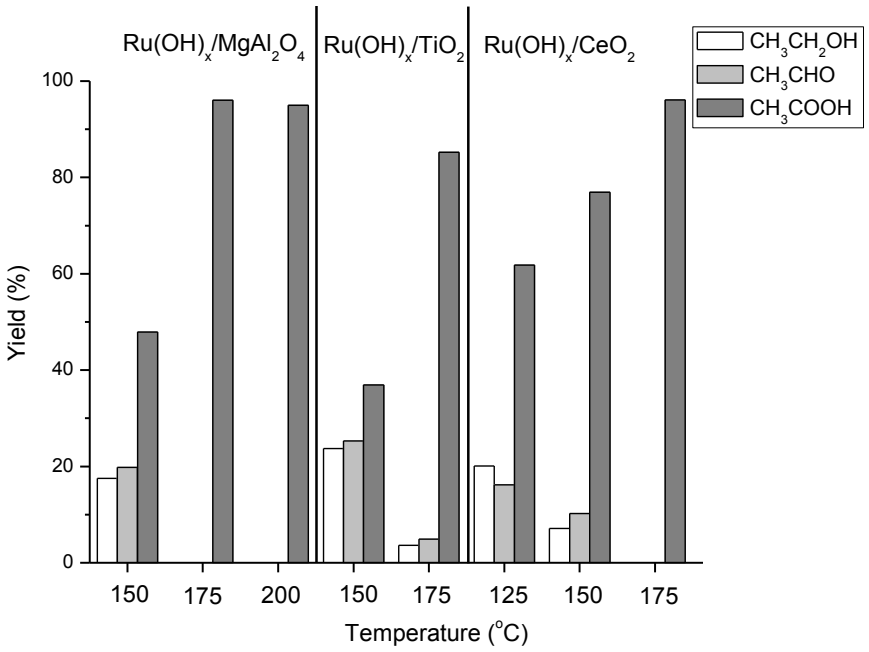

Figure 48. Product distribution in the aerobic oxidation of aqueous ethanol with supported 2.4 wt% $Ru(OH)_x$ catalysts at different temperatures. Reaction conditions: 10 g of 5 wt% ethanol/H_2O, 0.23 mol% Ru, 30 bar O_2, 3 hours reaction time.

As seen in Figure 48, all three tested supported catalysts exhibited high activity in the aerobic oxidation of ethanol, providing full conversion and yields above 90 % at 30 bar of oxygen after 3 hours of reaction. The efficiency of the spinel- and titania-supported catalysts proved to be comparable, although the TiO_2-supported catalyst was slightly less effective under applied reaction conditions. Notably, $Ru(OH)_x/CeO_2$ showed better catalytic performance in the oxidation reaction: even at the lower temperature (125°C) the product yields in the reaction when $Ru(OH)_x/CeO_2$ catalyst was applied were higher than the respective yields for TiO_2 and spinel at 150°C. This data supports the previously established superior performance of ceria-supported ruthenium hydroxide catalysts for aerobic oxidations (*vide supra*).

However, in order to investigate the effect of the support on the catalytic performance in the oxidation of ethanol, a decrease in the reaction operating temperature was performed for two catalysts (ceria and spinel) while running reactions long enough to achieve high yields under these conditions (Figure 49).

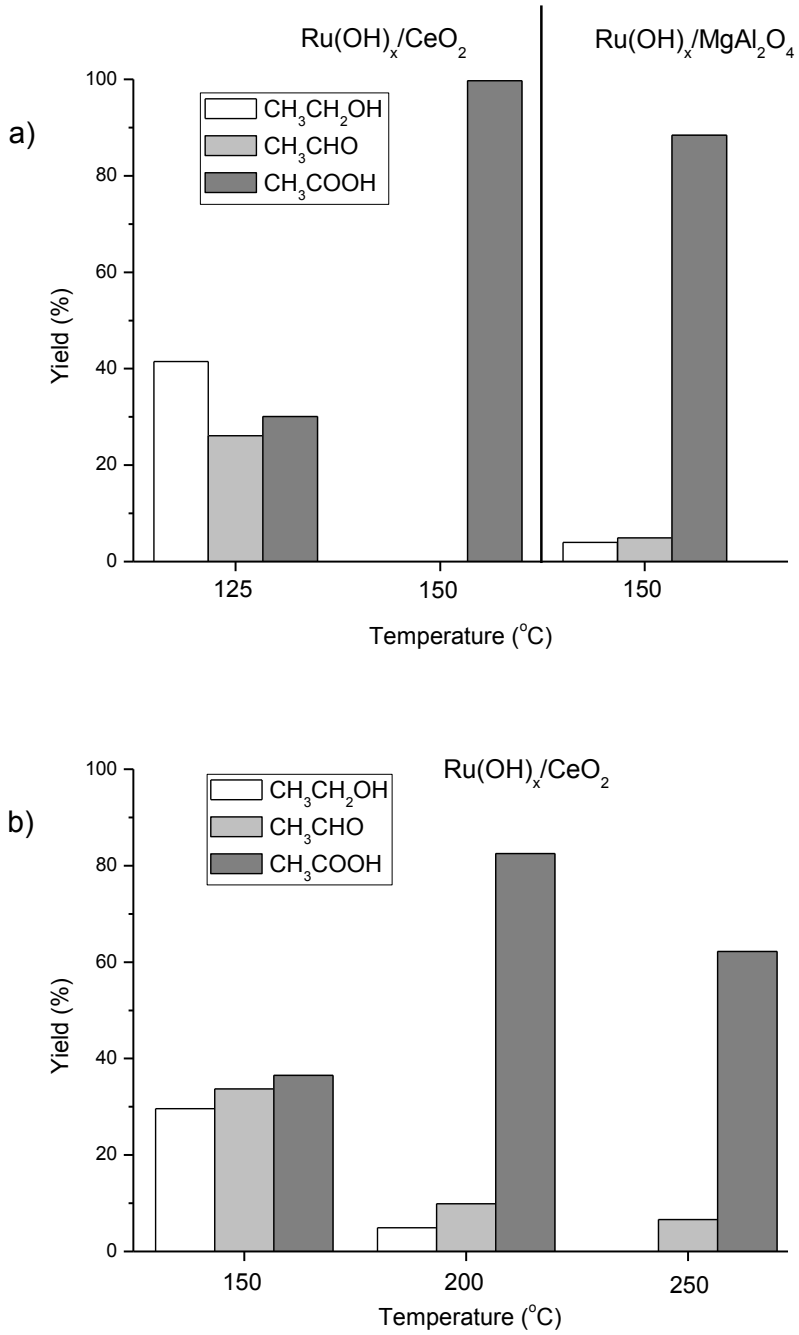

Figure 49. Product distribution in the aerobic oxidation of aqueous ethanol with the supported 2.4 wt% $Ru(OH)_x$ catalysts after (a) 20 hours and (b) 3 hours of reaction time. Reaction conditions: 10 g of 5 wt% ethanol/H_2O, 0.23 mol% Ru, 10 bar O_2.

The results presented in Figure 49a indicated that ceria-supported ruthenium catalyst performed more efficiently than $Ru(OH)_x/MgAl_2O_4$ at the same reaction conditions, *i.e.* 10 bar of dioxygen and 150°C. The results of the temperature variation (Figure 49b) showed that at 200°C an acetic acid yield above 80 % was already observed after only 3 hours of reaction time using the $Ru(OH)_x/CeO_2$ catalyst. However, an increased temperature of 250°C resulted in a lower yield of acetic acid (and lower overall carbon mass balance). This was likely due to the decomposition of aqueous acetic acid over ruthenium catalyst, similarly to reported by Imamura *et al.* [181], who performed the oxidation of acetic acid under 30 bar of O_2/N_2 mixture at 200°C over RuO_2 supported on CeO_2. Notably, in our work no significant over-oxidation to CO_2 or other product degradation seemed to occur with $Ru(OH)_x/CeO_2$ catalyst even at 200°C, where the carbon mass balance still was intact (*i.e.* >95 %).

Decreasing the temperature to 125°C affected the rate of the reaction, as expected, providing only *ca.* 40 % acetic acid yield at 70 % conversion of ethanol after 20 hours (Figure 49a).

Further, a time-yield dependence was investigated for the reaction utilizing $Ru(OH)_x/CeO_2$ catalyst at 150 and 200°C under 10 bar of oxygen (Figure 50). Full ethanol conversion and acetic acid yield above 90 % were achieved after 6 hours of reaction time at 200°C, whereas the reaction at 150°C occurred expectedly slower and a yield of *ca.* 75 % acetic acid was obtained after 12 hours of reaction time.

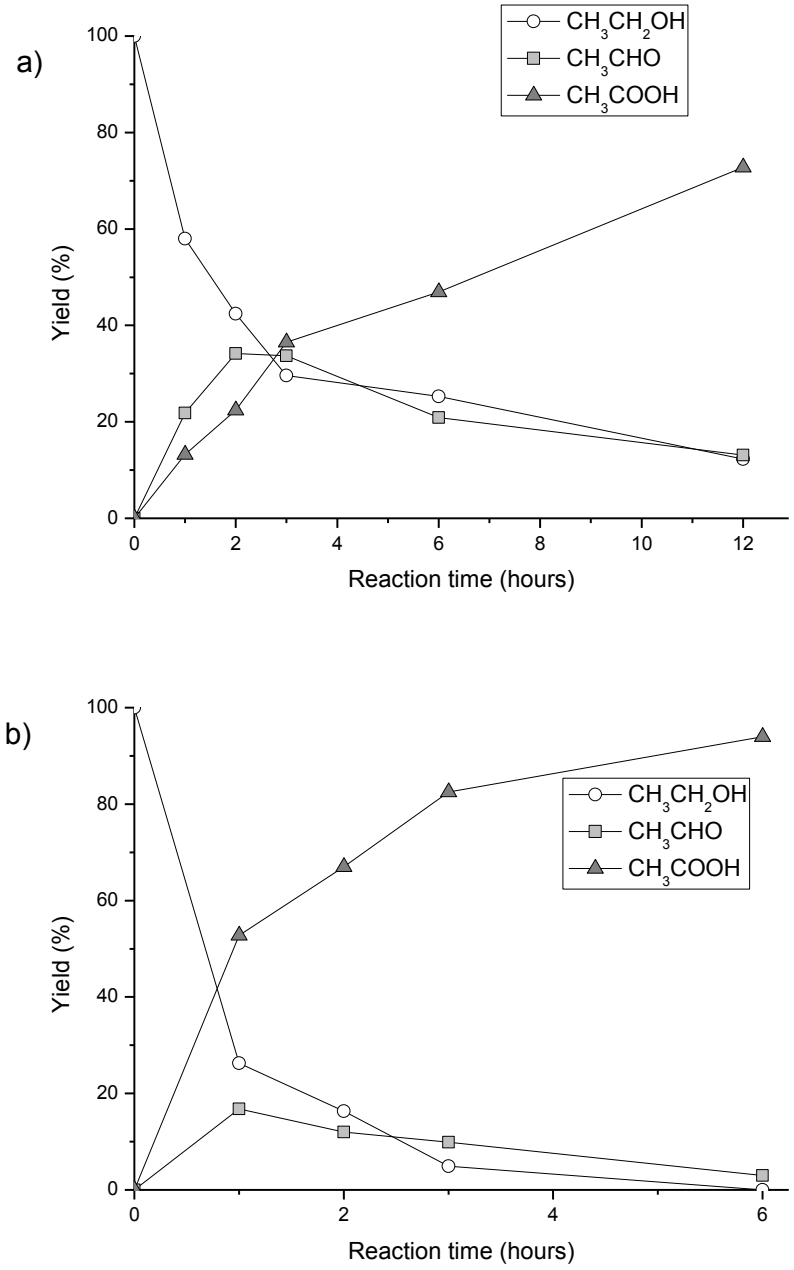

Figure 50. Product yields in the aerobic oxidation of aqueous ethanol with 2.4 wt% $Ru(OH)_x/CeO_2$ catalyst at (a) 150°C and (b) 200°C (10 g of 5 wt% ethanol/H_2O, 0.23 mol% Ru, 10 bar O_2).

The data compiled in Figure 50 clearly demonstrated that the initially formed acetaldehyde is oxidized into acetic acid as the reaction progresses. Notably, acetaldehyde is thus an intermediate oxidation product under these conditions, rather than a final product as

in the case reported by Iglesia *et al.* [182], where ethanol was oxidized to acetaldehyde at low temperatures using RuO_2 supported on tin, titanium, aluminium, zirconium oxides and silica. At 200°C the aldehyde oxidation occurred relatively faster than at 150°C, making acetic acid the major product already after 1 hour of reaction time.

In fact, a reaction pathway involving an initial formation of acetaldehyde is in good accordance with the mechanism of the alcohols oxidation to aldehydes and ketones over supported Ru(OH)x catalysts suggested by Mizuno and co-workers [102,103]. Here, the authors suggested a mechanism involving a formation of alkoxide species followed by β-hydride elimination.

In order to examine the influence of the ethanol concentration on the product formation, oxidation experiments with different initial concentrations (wt%) of ethanol in water were performed (Figure 51).

Interestingly, no significant difference in catalyst performance was observed when the concentration of ethanol was changed from 2.5 wt% to 50 wt% in water while the catalyst : substrate ratio was kept constant (Figure 51a). This clearly showed that the concentration did not affect the yield as much as the oxidant pressure or temperature, and possibly indicated that the reaction was not kinetically controlled under applied reaction conditions.

However, it is seen from Figure 51b that varying the concentration of the substrate effected the ethanol conversion and the product distribution within a certain period, *i.e.* after 3 hours of reaction time. In fact, a clear tendency of increased ethanol conversion and acetic acid yield in the order 2 wt%>5 wt%>10 wt% ethanol/water mixtures was observed. Obviously, this is correlated to the substrate : catalyst ratio, which decreased in the same order. Summarizing the results from Figures 51a and 51b, it is clear that the catalytic system is applicable for a wide range of alcohol concentrations, thus making it prone to be utilized for various applications, including fermented bio-ethanol oxidation.

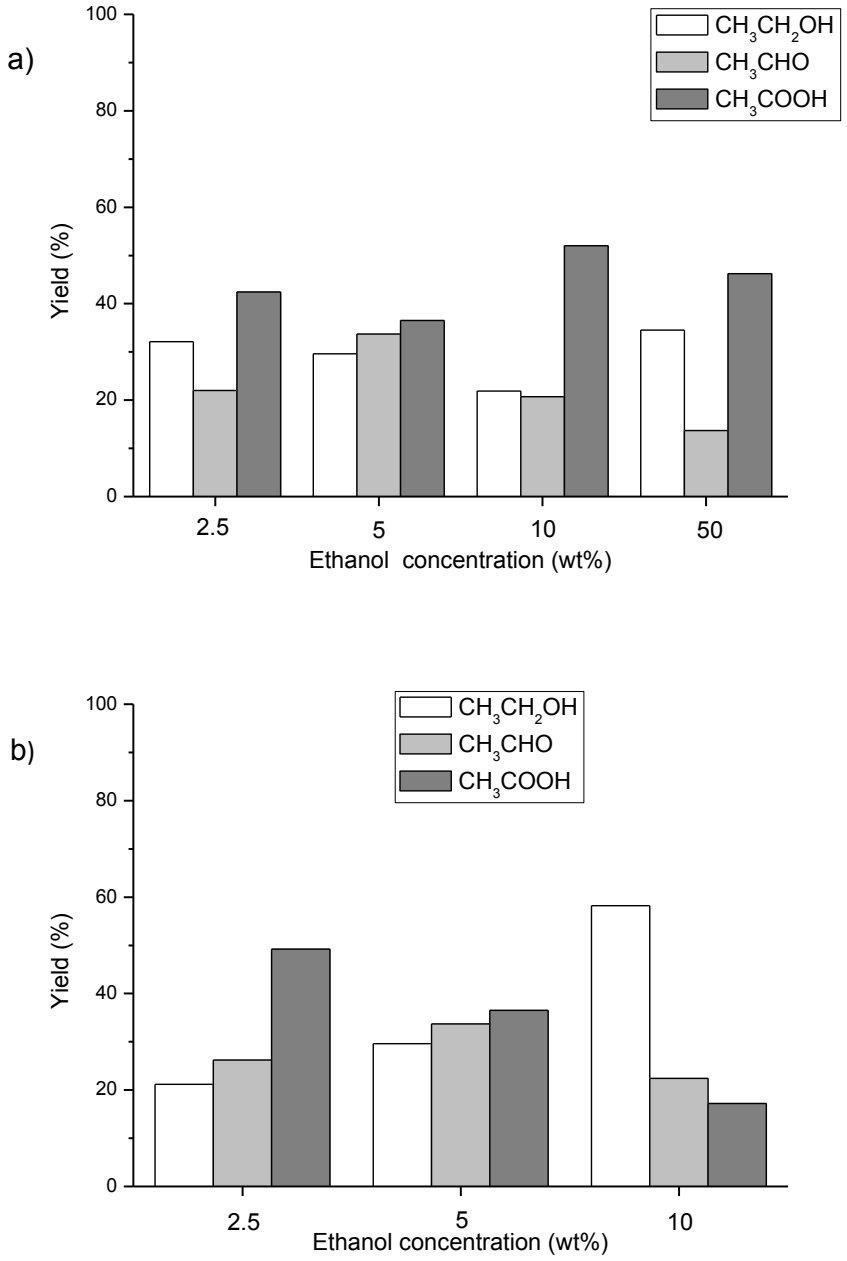

Figure 51. Product distribution in the aerobic oxidation of aqueous ethanol with 2.4 wt% $Ru(OH)_x/CeO_2$ catalyst (a) at constant catalyst : substrate ratio (0.23 mol%) and (b) with constant added amount (0.1 g) of the catalyst . Reaction conditions: 10 g of ethanol/H_2O solution, 10 bar O_2, 150^oC, 3 hours of reaction time.

Since in this case, as well as in HMF oxidation in aqueous medium and organic solvents (see above), cerium oxide-supported ruthenium catalyst exhibited improved activity compared to TiO_2 and spinel supports, additional experiments to investigate its performance were conducted and the results were summarized in Table 16.

Table 16. Product yields in the aerobic oxidation of aqueous ethanol with 2.4 wt% ruthenium catalysts.[a]

Entry	Catalyst	Reaction time, hours	Gas/pressure, bar	Conversion, %	Yield, %	
				CH_3CH_2OH	CH_3CHO	CH_3COOH
1	-	3	O_2/10	11	2	3
2	CeO_2	3	O_2/10	17	7	9
3	$Ru(OH)_x/CeO_2$	3	O_2/10	72	34	37
4	$Ru(OH)_x/CeO_2$	90	O_2/10	>99	0	97
5	$Ru(OH)_x/CeO_2$	3	Ar/10	13	4	4

[a]Reaction conditions: 10 g of 5 wt% ethanol/H_2O, 0.23 mol% Ru (entries 3-5), 150°C.

The results in Table 16 suggest that the support itself, *i.e.* pure CeO_2, had low but not negligible catalytic activity. Here, the conversion of ethanol after 3 hours of reaction time increased from 11 %, when no catalyst or support was introduced to the reaction (Table 16, entry 1), to *ca.* 17 % in presence of CeO_2 (entry 2), while the product formation increased accordingly. This can possibly be ascribed to the Ce^{4+}/Ce^{3+} redox interactions on the surface of cerium(IV) oxide [183-185].

In contrast, the oxidation in argon atmosphere (Table 16, entry 5) appeared to be negligible, as anticipated. The small amount of the formed oxidation product could possibly originate from the oxygen dissolved in water and ethanol, due to insufficient removal when saturated with argon prior to the experiment. Good catalytic activity was only observed with the catalyst containing ruthenium species (entry 3), thus suggesting that most of the catalytic activity originated from the metal inventory.

Additionally, to obtain information on the product stability under applied conditions, an experiment was carried out at prolonged reaction time (Table 16, entry 4). After 90 hours

of continuous reaction, the product (acetic acid) was exclusively formed and remained stable; the *ca.* 2.5 % difference between conversion and yield could possibly be related to the almost negligible acetic acid degradation.

In order to elucidate the effect of alteration of the loading of ruthenium on the surface of cerium oxide, 1.2 wt% and 4.7 wt% $Ru(OH)_x/CeO_2$ catalysts were also tested in the aerobic oxidation of ethanol. The results of the employment of 1.2, 2.4 and 4.7 wt% supported $Ru(OH)_x/CeO_2$ catalysts are listed in Table 17.

Table 17. Product yields in the aerobic oxidation of aqueous ethanol with supported $Ru(OH)_x$ catalysts.[a]

Entry	Catalyst[b]	Reaction time, hours	Conversion, %	Yield, %	
			CH_3CH_2OH	CH_3CHO	CH_3COOH
1	1.2 wt% $Ru(OH)_x/CeO_2$	6	86	9	77
2	2.4 wt% $Ru(OH)_x/CeO_2$	6	75	21	47
3	4.7 wt% $Ru(OH)_x/CeO_2$	6	63	25	30
4	1.2 wt% $Ru(OH)_x/CeO_2$	3	71	27	43
5	1.2 wt% $Ru(OH)_x/CeO_2$ (re-use)	3	70	24	42
6	1.2 wt% $Ru(OH)_x/MgAl_2O_4$	3	45	15	27
7	2.4 wt% $Ru(OH)_x/MgAl_2O_4$	3	41	14	22
8	0.6 wt% $Ru(OH)_x/CeO_2$	6	99	1	98
9[c]	1.2 wt% $Ru(OH)_x/CeO_2$, CeO_2	6	99	2	97
10[d]	4.7 wt% $Ru(OH)_x/CeO_2$, CeO_2	6	76	24	49
11[e]	2.4 wt% $Ru(OH)_x/CeO_2$, CeO_2	6	83	16	65

[a]Reaction conditions: 10 g of 5 wt% ethanol/H_2O, 0.23 mol% Ru, 10 bar O_2, 150°C. [b]The mass of the introduced catalyst was altered in different experiments, while the molar Ru:substrate ratio remained 0.23 mol% (entries 1-8). [c]0.21 g of 1.2 wt% $Ru(OH)_x/CeO_2$ with added 0.21 g of CeO_2. [d]0.053 g of 4.7 wt% $Ru(OH)_x/CeO_2$ with added 0.157 g of CeO_2.

It is seen that the change of the ruthenium loading from 1.2 to 4.7 wt% gradually decreased the activity of the catalyst (Table 17, entries 1-3). This may possibly be explained

by the different particle sizes found in the ceria-supported catalysts (see Table 15). Higher ruthenium loading resulted in larger particles, and hence in a decrease of the number of active sites, which in turn decreased the activity of the catalyst. Also, the extraordinary properties of ceria as surface oxygen capacitor [185] and the catalytic properties of CeO_2 in the oxidation of aqueous ethanol (as was shown in Table 16) might facilitate the oxidation as more ceria is introduced in the reaction when the same substrate to catalyst ratio is used (*e.g.*, 0.21 g of 1.2 wt% $Ru(OH)_x/CeO_2$ corresponds to 0.0525 g of 4.7 wt% $Ru(OH)_x/CeO_2$).

Interestingly, the decrease of the ruthenium loading on spinel did not significantly improve the results for the oxidation with spinel-supported $Ru(OH)_x$ catalysts (Table 17, entries 6 and 7). As was shown above, $MgAl_2O_4$, and especially with the deposited ruthenium, has higher surface area than CeO_2 (see Table 15, entries 3-9).

Further, when the results of an experiment with 0.42 g of 0.6 wt% $Ru(OH)_x/CeO_2$ (prepared similarly to 1.2-4.7 wt% catalysts as described in section 6.2.1) were compared to the results of the usage of 0.21 g of 1.2 wt% $Ru(OH)_x/CeO_2$ with added 0.21 g of CeO_2 (i.e., both Ru mol% and support amount remained constant at two different ruthenium loadings), no difference in the products yields was observed, supporting the suggested hypothesis that both ceria and $Ru(OH)_x$ contribute to the overall catalyst activity (Table 17, entries 8 and 9). However, when a similar comparison between the performance of 1.2 and 4.7 wt% $Ru(OH)_x/CeO_2$ catalysts (0.23 mol% Ru, overall mass 0.21 g) was performed (Table 17, entries 1 and 10), it was shown that both substrate conversion and product yields were significantly lower in case of 4.7 wt% catalyst, even with added CeO_2. A similar result was obtained when reactions with 1.2 and 2.4 wt% catalysts were compared (Table 17, entries 1 and 11).

Thus, the obtained results suggest that: *a)* a small variation in loading of the active species does not affect the particles size, which can explain similar performance for 1.2 and 2.4 wt% $Ru(OH)_x/MgAl_2O_4$; *b)* at least some of the improved performance of the $Ru(OH)_x/CeO_2$ catalyst with lesser $Ru(OH)_x$ loading originates in the increase of the support amount (as spinel is a redox inert support [62] in contrast to CeO_2); and *c)* when the performance of the CeO_2-supported catalysts with decreasing $Ru(OH)_x$ loading is compared, after reaching some optimal size (possibly corresponding to about 1 wt% $Ru(OH)_x$) the particle size effect becomes insignificant compared to the catalytic activity of the increased amount of CeO_2.

A catalyst re-use experiment was also conducted. Here, the reaction was first carried out with 1.2 wt% $Ru(OH)_x/CeO_2$ catalyst for 3 hours, then the catalyst was filtered off, washed with hot water, dried at 140°C for 2 hours and employed in another reaction (Table 17, entries 4 and 5). The obtained data showed that the catalyst was prone to re-use under applied reaction conditions, which was in good accordance with the previously found re-usability of *e.g.* 2.4 wt% $Ru(OH)_x/CeO_2$ catalyst for the oxidation of HMF in water at elevated temperatures and pressures (see section 4.3.3.1).

As the preliminary test showed that 1.2 wt% ceria-supported ruthenium catalyst exhibited superior performance compared to 2.4 wt% ceria- as well as 1.2 and 2.4 wt% spinel-supported catalysts (Table 17; see also section 5.3.1), the time study of the reaction with the former catalyst was conducted. The obtained results are shown in Figure 52.

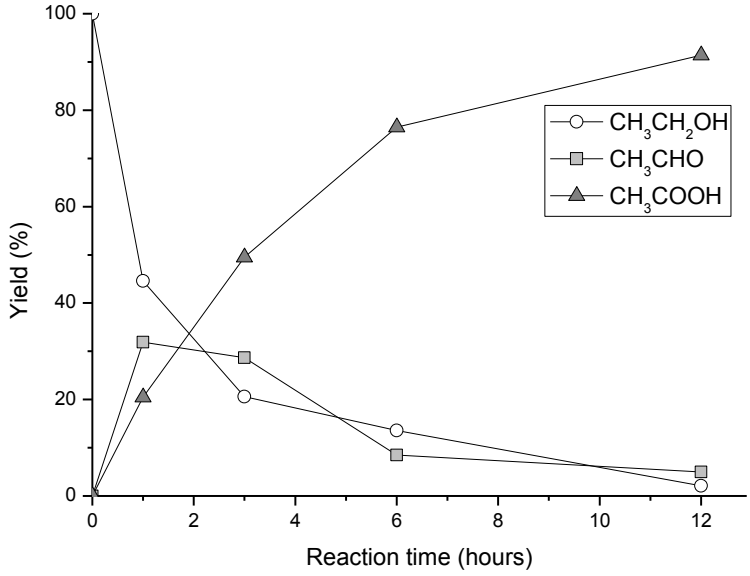

Figure 52. Product yields in the aerobic oxidation of aqueous ethanol with 1.2 wt% $Ru(OH)_x/CeO_2$ catalyst. Reaction conditions: 10 g of 5 wt% ethanol/H_2O, 0.23 mol% Ru, 10 bar O_2, 150°C.

It is clearly seen that the 1.2 wt% catalyst was more active than the 2.4 wt% catalyst under the same reaction conditions (see Figure 50a), allowing to obtain the yield of acetic acid above 90 % after 12 hours of reaction time.

Although the recovered catalyst proved to be re-usable under the applied reaction conditions, an experiment was conducted in order to elucidate the homogeneous contribution in the catalyzed reaction, examining whether the catalytically active ruthenium species remained heterogeneous or were dissolved from the catalyst. The reaction was carried out at 150°C under 10 bar of O_2 for 1 hour, then the catalyst was filtered off and the filtrate poured back into the autoclave. The autoclave was then re-pressurized with 10 bar O_2 and the reaction continued for 2 hours more. The results of this experiment are presented on Figure 53.

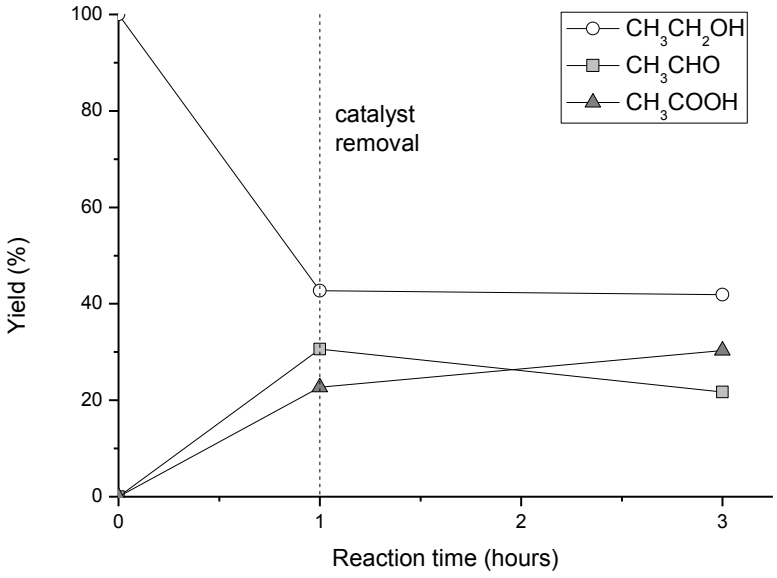

Figure 53. Product yields in the aerobic oxidation of aqueous ethanol with 1.2 wt% $Ru(OH)_x/CeO_2$ catalyst. Reaction conditions: 10 g of 5 wt% ethanol/H_2O, 0.23 mol% Ru, 10 bar O_2, 150°C.

As seen from the data in Figure 53, no substrate (ethanol) conversion occurred after the catalyst was removed (*i.e.* no catalytic species dissolved), while a certain amount of aldehyde was converted into acid. The latter reaction can however proceed without added catalyst [186], hence it is expected to occur under the reaction conditions as well. As an additional experiment, the oxidation reaction was performed at the same conditions with acetaldehyde as the substrate. 1.2 wt% $Ru(OH)_x/CeO_2$ (0.23 mol% Ru) catalyst was introduced to the reaction with 10 g of 5 wt% acetaldehyde solution in water at 150°C and 10

bar of O_2. After a reaction time of 3 hours, the yield of acetic acid constituted 86 % with 10 % of acetaldehyde remaining unconverted. This result, together with the data from Table 16 and Figures 52 and 53, clearly indicates the initial oxidation of ethanol to acetaldehyde to be the performance determining step in the reaction process.

To elucidate the effect of the calcination on the activity of the catalyst, the results of the aqueous ethanol oxidation reaction with the non-treated catalyst was compared to the catalysts calcined at different temperatures. The results are presented in Figure 54.

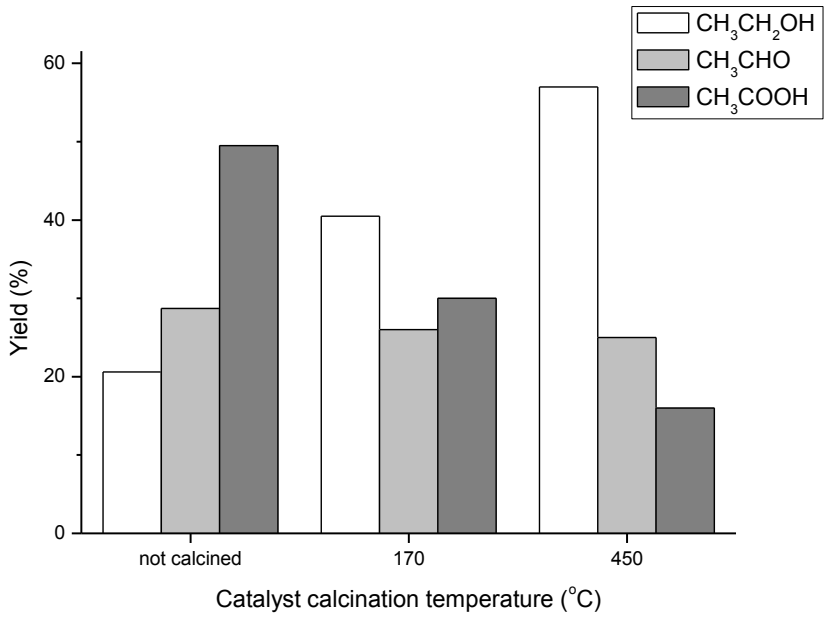

Figure 54. Product yields in the aerobic oxidation of aqueous ethanol with calcined 1.2 wt% $Ru(OH)_x/CeO_2$ catalysts. Reaction conditions: 10 g of 5 wt% ethanol/H_2O, 0.23 mol% Ru, 10 bar O_2, 150°C, 3 hours reaction time.

It is clearly seen from the presented results that the calcinations affected the activity of the catalyst. Indeed, within 3 hours of reaction time the usage of calcined catalysts resulted in decreased ethanol conversion and acetic yield, although the yield of acetaldehyde remained virtually the same (Figure 54). Moreover, both substrate conversion and acetic yield decreased with the increase of the catalyst calcination temperature. This was in good accordance with the results reported by Yang *et al.* [187], where a decrease in the aerobic catalyst activity was observed when hydrated ruthenium oxide catalytic species were annealed in N_2 at high temperatures. Interestingly, an increase in the catalyst heat-treatment

temperature only to 170°C (compared to the catalyst drying temperature of 140°C) resulted in approximately 20 % decrease of ethanol conversion and acetic acid yield.

Another possible reason for the loss of the catalytic activity is heat-induced particle sintering accompanied by the formation of crystalline ruthenium species from the initially amorphous $Ru(OH)_x$. Further discussion on this matter can be found in the following section (6.3.2).

This might also indicate that higher reaction temperatures (*e.g.* 200, 250°C) could eventually cause catalyst deactivation, though within the reaction timeframe (3-6 hours, see Figures 48, 49b, 50b) these effects were not clearly revealed. However, the above-discussed overoxidation of acetic acid at 250°C (see Figure 49b) was possibly due to the presence of crystalline RuO_2, in accordance with the results reported by Imamura *et al.* [181]. Nonetheless, it must be mentioned here that although the reaction conditions of *e.g.* 250°C were discussed above (see Figure 49b), the said reaction was carried out in aqueous solution, thus making an evaluation of the possible temperature effect on the catalyst deactivation difficult.

6.3.2. Aerobic oxidation of aqueous ethanol with highly dispersed supported RuO_x catalysts

As was mentioned above, in a study performed by Iglesia *et al.* [182] the authors demonstrated that RuO_2 supported on SnO_2 and SiO_2 had high activity for the selective oxidation of ethanol to acetaldehyde and diethoxyethane at 100°C and 0.02-0.5 bar pressure in a flow reactor. Recently, a new procedure for the preparation of coated metal oxide supports with RuO_x nanoparticles has been investigated by Laursen *et al.* [180]. The co-catalyst comprised of RuO_x supported on TiO_2 or WO_3 was prepared according to this procedure exhibited an improved water oxidation activity compared to the pristine semiconductor. The nanoparticle coating was shown to consist of thin and homogeneous layers.

Hence, in a work presented in this section we have elaborated the research demonstrated above (section 6.3.1) to employ the supported highly dispersed RuO_x catalysts in the aerobic oxidation of aqueous ethanol (see Scheme 17). For this, highly dispersed RuO_x catalysts supported on titania, hydrotalcite, spinel, sodium titanate nanotubes, zinc and tungsten oxides, alumina, cerium and cerium-zirconium oxides were prepared as described above (see section 6.2.2).

Full information on the catalysts characterization, including SEM and TEM images, is available in the Appendix. Here, a short catalysts description will have to suffice. Importantly, although the performed analysis could not provide the information on the hydration state ($RuO_x \cdot zH_2O$) of the catalytic species, it was assumed that the it was relatively lower compared to $Ru(OH)_x$ catalysts prepared by the forced ruthenium species precipitation with hydroxide.

The results of the SEM and TEM analysis (see Appendix) have revealed three types of catalysts morphology: porous particle agglomerates (TiO_2, spinel, HT, ZnO, WO_3, CeO_2, hs-CeO_2 and $CeO_2 \cdot ZrO_2$), porous web-like agglomerates ($Na_2Ti_6O_{13}$-NTs), and rod-like agglomerates (γ-Al_2O_3). The morphology of all examined materials was found to be homogeneous, indicating the absence of large agglomerates of RuO_x. The results of the XRF analysis and the particle size distribution obtained from TEM images are presented in Table 18.

Table 18. Characteristics of supported RuO_x catalysts.

Entry	Catalyst support	Ru content, wt%[a]	BET surface area, m^2/g	Particle size, nm[b]
1	TiO_2	4.9	54	n/a
2	HT	1.5	5	0.5-1.5
3	$MgAl_2O_4$	1.5	89	0.5-1.0
4	$Na_2Ti_6O_{13}$-NTs	1.5	214	0.8
5	ZnO	1.3	9	n/a
6	Al_2O_3	1.6	151	0.6-1.5
7	WO_3	1.3	2	0.8-1.0
8	CeO_2	0.9	62	0.5
9	CeO_2	1.8	58	0.5-1.2
10	CeO_2	3.4	60	0.6-0.8
11	hs-CeO_2	2.3	122	0.8-1.5
12	$CeZrO_4$	0.9	127	1.0-1.5

[a]Provided by XRF analysis. [b]Determined from TEM imaging.

As can be seen from the data in Table 18, generally the size distribution of the RuO_x deposits on a support was quite narrow, thus indicating that the applied preparation method allowed a highly uniform and highly dispersed catalyst deposition. It also clearly indicated that the amount of RuO_x deposited by the applied procedure strongly depended on the support, as the same amount of Ru precursor was allowed to react with all supports (except Table 18, entries 8 and 10). The difference in loading then could possible be related to a difference in the dopamine coverage (the dopamine molecule was previously demonstrated to be a key participant in the RuO_x loading [180]).

The results of the XRD analysis have revealed the amorphous state of RuO_x; XPS measurements demonstrated a presence of both Ru^{6+} and Ru^{3+} oxidation states, however the peak of the latter one might also be ascribed to the hydrated RuO_2 [180].

Further, the initially prepared catalysts were tested in the aerobic oxidation of aqueous ethanol under the reaction conditions similar to those used for the oxidation with supported $Ru(OH)_x$ catalyst. The catalysts performance was compared on the basis of the yield of acetic acid in the reaction. As the weight loading of ruthenium was different on different supports, the amount of the introduced catalysts was the same in every reaction (*ca.* 0.3 mol% Ru) to allow a comparison of the obtained results (Figure 55).

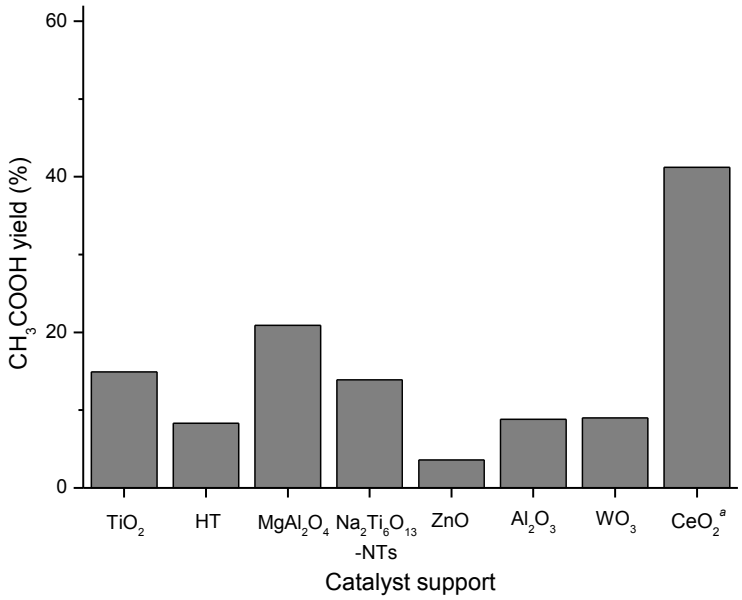

Figure 55. Acetic acid yields in the aerobic oxidation of ethanol with supported RuO_x catalysts. Reaction conditions: 10 g of 5 wt% ethanol/H_2O, 10 bar O_2, 150°C, *ca.* 0.3 mol% Ru, 3 hours of reaction time. [a]1.8 wt% RuO_x/CeO_2.

It can be seen from the obtained data that the best catalytic performance (corresponding to the highest acetic acid yield) was exhibited by ceria-supported RuO_x catalyst, which was in good accordance with the observed results with $Ru(OH)_x/CeO_2$ catalyst (see section 6.3.1). It might appear that the yield of CH_3COOH was lower than that afforded by the use of 1.2 wt% $Ru(OH)_x/CeO_2$ and approximately the same with the one provided by 2.4 wt% $Ru(OH)_x/CeO_2$ catalyst (*ca.* 40 %; see Figures 50a, 51). However, a direct comparison here is difficult since the amount of the introduced catalyst in the experiments with RuO_x and $Ru(OH)_x$ was 0.3 and 0.23 mol%, respectively.

Reactions with some of the catalysts (supported on ZnO, WO_3, HT, spinel, TiO_2) resulted in the observed significant loss of carbon mass balance, possibly indicating a complete oxidation to CO_2 or formation of other products unidentified by HPLC. Interestingly, this was not the case when $Ru(OH)_x$ supported on TiO_2 and $MgAl_2O_4$ were employed in the reaction (see above).

As was mentioned in the previous section, a mixed $RuO_2{\cdot}CeO_2$ oxide was previously demonstrated by Imamura *et al.* [181] to completely oxidize organic compounds such as, for instance, acetic acid and *n*-propanol, in aqueous solutions. In contrast, in this work both RuO_x/CeO_2 and $Ru(OH)_x/CeO_2$ catalytic systems were shown to be efficient catalysts for the production of acetic acid from ethanol (see also section 6.3.1) and propanol (*vide infra*; section 6.3.3) under applied conditions.

Nonetheless, since the use of ceria-supported catalyst clearly provided best results, the RuO_x/CeO_2 catalyst system was explored further. The product distribution of the aerobic oxidation of ethanol with the aforementioned catalyst is plotted against reaction time in Figure 56.

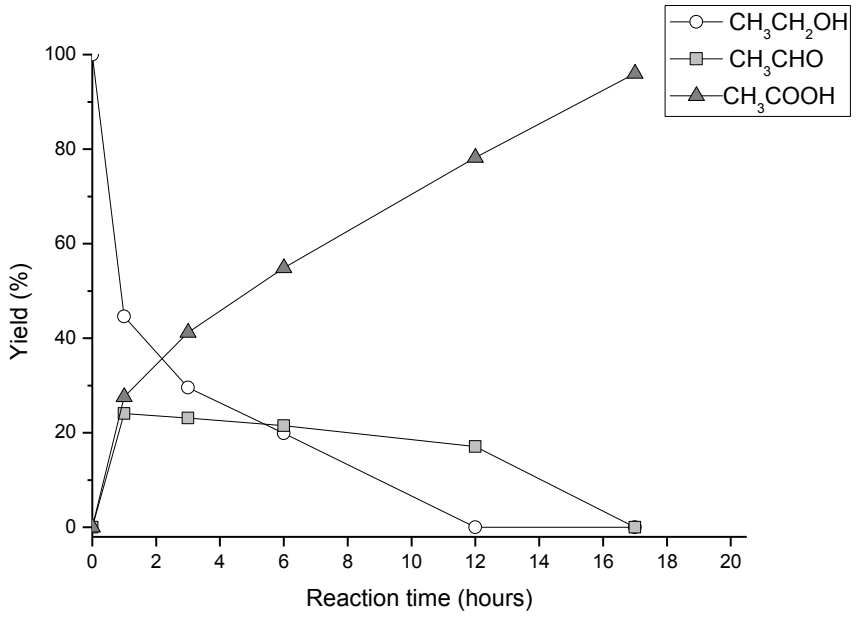

Figure 56. Product yields in the aerobic oxidation of aqueous 1-propanol with 1.8 wt% RuO_x/CeO_2 catalyst. Reaction conditions: 10 g of 5 wt% ethanol/H_2O, 0.3 mol% Ru, 10 bar O_2, 150^oC.

It was shown above (see section 6.3.1) that for the oxidation of ethanol in aqueous solutions under applied reaction conditions with supported $Ru(OH)_x$ the reaction propagates in two steps, with the initial oxidation of ethanol to acetaldehyde and the subsequent oxidation of the latter compound to acetic acid. This is also likely to be the case with the supported RuO_x catalysts. Additionally, it is seen from the obtained results that as the reaction progresses, after approximately 1 hour of reaction time the yield of CH_3CHO remained almost constant in time (approximately 20 %), resembling a steady state-like situation (Figure 56). After 12 hours, when all the substrate (ethanol) was converted, the amount of acetaldehyde decreased, and its conversion to CH_3COOH was completed after *ca.* 18 hours of reaction time. In contrast, when the reaction was performed with SnO_2- and SiO_2-supported RuO_2 catalysts [182], no formation of acetic acid was observed. Although most likely this was defined by the difference in the reaction conditions (0.5 bar at 100^{o}C and 10 bar at 150^{o}C), another possible reason for this discrepancy is the difference in particle size or particle crystallinity and/or oxidation state. For the RuO_2/SnO_2 catalyst, a decrease in the particle size caused a reduction in a turnover frequency in the reaction of the partial oxidation of methanol [182]. In fact, for the gold-catalyzed oxidation reactions an optimal performance was observed with particle sizes of less than 10 nm [188,189]. Thus, in order to elucidate the effect of particle size in the RuO_x/CeO_2 catalytic system on the reaction progress, the loading of the coating RuO_x particles was varied and the catalysts with 0.9 wt% and 3.4 wt% Ru were obtained (see Table 18, entries 8-10). Additionally, RuO_x catalysts supported on high surface-CeO_2 (hs-CeO_2) and mixed cerium-zirconium oxide were prepared (Table 18, entries 11 and 12). Figure 57 represents the results of the reaction of the aerobic oxidation of ethanol with these catalysts.

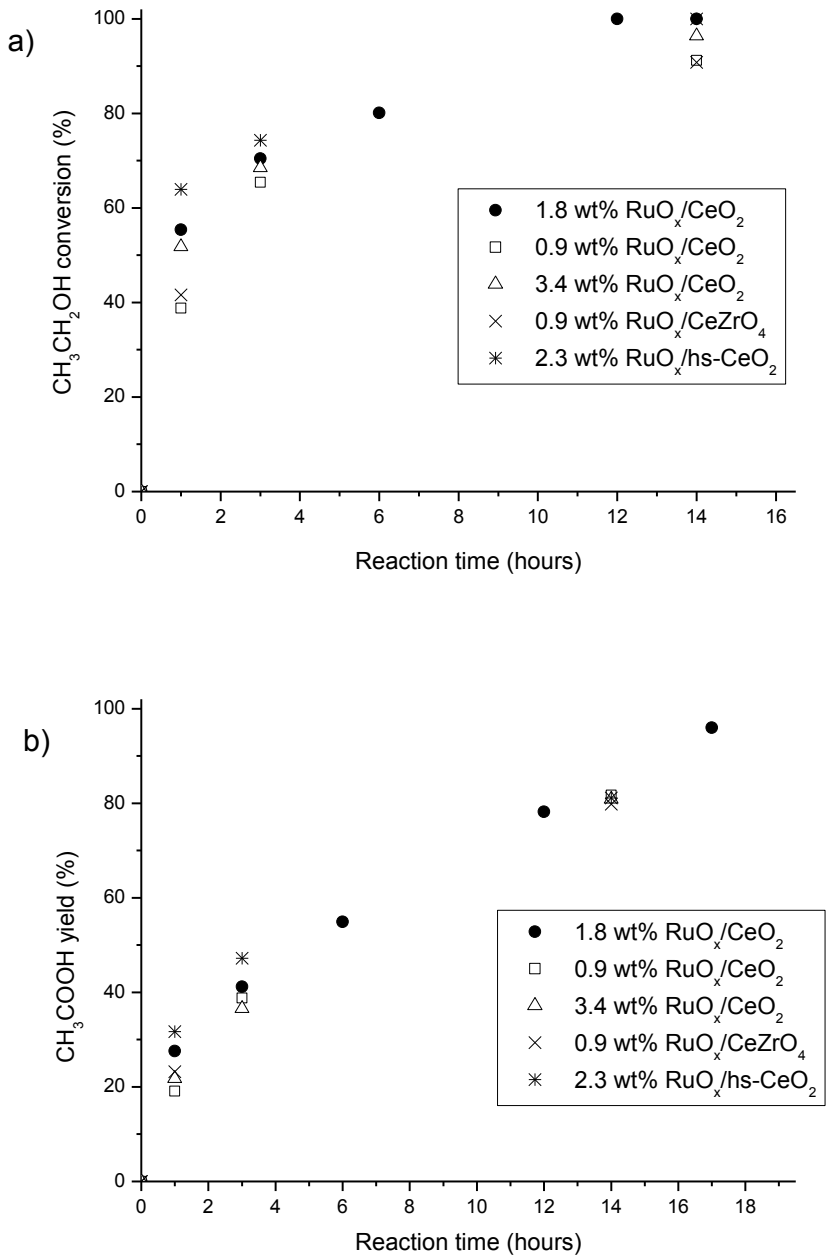

Figure 57. (a) Ethanol conversion and (b) acetic acid yield in the aerobic oxidation of ethanol with supported RuO_x catalysts. Reaction conditions: 10 g of 5 wt% ethanol/H_2O, 10 bar O_2, 150^oC, 0.3 mol% Ru.

From the data presented in Figure 57 it is seen that, within the experimental uncertainty, already after *ca.* 3 hours of reaction time no drastic difference in the catalytic activity was observed with the ceria-supported catalysts possessing different RuO_x loading (0.9, 1.8 and 3.4 wt% RuO_x/CeO_2), yielding in *ca.* 70 % CH_3CH_2OH conversion (Figure 57a) and *ca.* 40 % CH_3COOH yield (Figure 57b). It was shown above that the particle size of RuO_x/CeO_2 catalysts did not change significantly with the variation in ruthenium loading (see Table 18, entries 8-10), in contrast to what have been found for CeO_2-supported $Ru(OH)_x$ catalysts prepared by wet impregnation, where particle size increased at higher $Ru(OH)_x$ loadings causing a decrease in the catalyst activity (see Table 15, entries 7-9; Table 17, entries 1-3). Thus, the absence of a ”loading-size” dependence makes the deposition method utilized here advantageous: a catalyst material can be produced with low to high catalytic metal basis while particle size remains almost constant. This presents an excellent feature for a potential industrial process.

The results of the ethanol oxidation with the catalyst comprised of RuO_x supported on cerium oxide with high surface area (pristine hs-CeO_2: 122 m^2/g, pristine CeO_2: *ca.* 60 m^2/g) are also shown in Figure 57. However, generally no significant difference in catalytic activity between the two catalysts, 1.8 wt% RuO_x/CeO_2 and 2.3 wt% RuO_x/hs-CeO_2, was observed (although hs-CeO_2-supported catalyst performed slightly better). This supported the hypothesis that the catalyst preparation method presented here was indeed suitable for obtaining catalysts with a high dispersion and high loading of catalytic species regardless of the surface area of the starting support material.

The mixed cerium-zirconium oxide is know in literature to have an improved oxygen storage effect [190,191], which hypothetically might contribute to the performance of the aerobic catalyst supported on this material. Thus, a $RuO_x/CeZrO_4$ catalyst was prepared and utilized in the aerobic oxidation of ethanol (see Figures 56a,b). Again, slightly better performance of the aforementioned catalyst was observed compared to RuO_x/CeO_2 catalyst, however this difference faded as the reaction progressed. Here, after 14 of reaction time the yield of acetic acid obtained using the two compared catalysts constituted *ca.* 80 % (Figure 57b).

It was found by Laursen *et al.* [180] that the heat treatment of the amorphous RuO_x deposited on TiO_2 at temperatures above 250°C led to a reduction of ruthenium from the mixed oxide of Ru^{6+} and Ru^{3+} (or hydrated RuO_2) into a mixed (possibly hydrated) oxide of $RuO_2 \cdot Ru_2O_3$. This reduction was accompanied by sintering into larger particles, as was determined using a combination of XPS and TEM analysis. It has been suggested in literature that three factors might influence the catalytic activity of the RuO_x catalysts: the degree of hydration [187], particle size [182] and the presence of high-valence state Ru^{6+} [192]. Therefore, in order to assess the heat-treatment effect on the catalyst performance, a set of experiments was conducted with the CeO_2-supported RuO_x catalysts calcined at different temperatures. In Figure 58 the performance of the catalysts calcined at 170, 200 and 450°C is compared to the non-treated 1.8 wt% RuO_x/CeO_2.

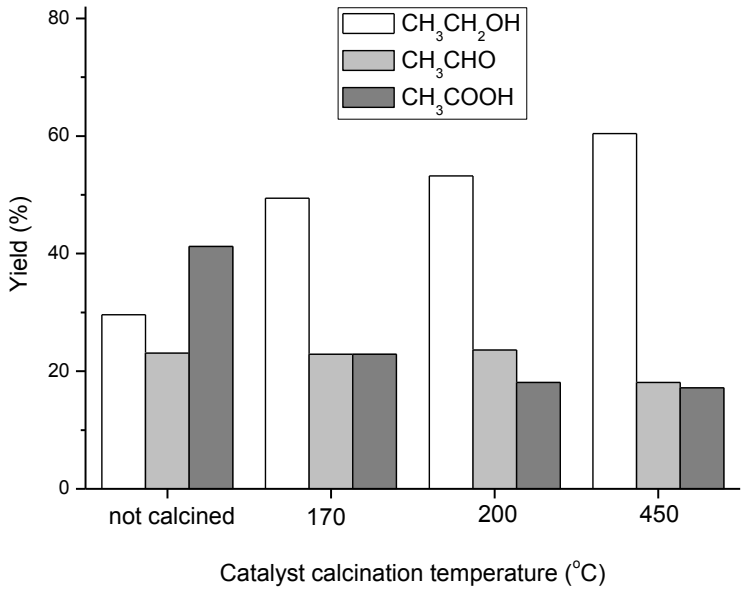

Figure 58. Product yields in the aerobic oxidation of aqueous ethanol with calcined 1.8 wt% RuO_x/CeO_2 catalysts. Reaction conditions: 10 g of 5 wt% ethanol/H_2O, 0.3 mol% Ru, 10 bar O_2, 150°C, 3 hours of reaction time.

It is clearly seen form the presented results that the calcinations affected the activity of the catalyst. Indeed, within 3 hours of reaction time the usage of calcined catalysts resulted in decreased ethanol conversion and acetic yield, although the yield of acetaldehyde

remained virtually constant (Figure 57). Moreover, both substrate conversion and acetic yield decrease with the increase of the catalyst calcination temperature. Since the XPS analysis could not reveal the difference between Ru_2O_3 and hydrated RuO_2 [180], it is likely that most of the initially amorphous (possibly hydrated) catalytic species annealed in N_2 at high temperatures were transformed into crystalline RuO_2 [187]. These results, together with the heat treatment-caused reduction of the gas-phase deposited Ru^{6+} [180] and the results of the calcination of the $Ru(OH)_x/CeO_2$ catalyst (see Figure 54, section 6.3.1), suggest that the oxidation to acetic acid occurs more readily on the amorphous mixed oxide containing Ru^{6+} and Ru^{3+} oxidation states (or, as in case of supported Ru(OH)x catalysts, Ru^{3+}), amorphous rather than crystalline and preferably with a high extent of hydration.

6.3.3. Oxidative degradation of higher alcohols with supported ruthenium-based catalysts

Previous sections of this chapter described the formation of acetic acid *via* the aerobic oxidation of ethanol with supported $Ru(OH)_x$ and RuO_x catalysts. Here, partial degradation of C-chain in the oxidation of C2-, C3- and C4-alcohols and diols and dominating formation of acetic acid in the oxidation reaction of 1-propanol is presented.

Biomass-derived alcohols (or "bio-alcohols") are not limited by ethanol. Higher alcohols, for example, propanol and butanols, are also available form biomass through fermentation; one of the existing technologies for such conversion is the MixAlco process [193].

Results presented in section 6.3.1 of this thesis described the superior performance of the 1.2 wt% $Ru(OH)_x/CeO_2$ catalyst in the aerobic oxidation of aqueous ethanol. Hence, here firstly an oxidation of 1-propanol with the aforementioned catalyst was investigated. Reaction conditions similar to those used for the oxidation of ethanol were applied: 150°C, 10 bar O_2, 10.13 mL of *ca.* 1.07 M aqueous alcohol solution (corresponding to 10 g of 5 wt% ethanol/H_2O). The product yields plotted against reaction time are presented in Figure 59.

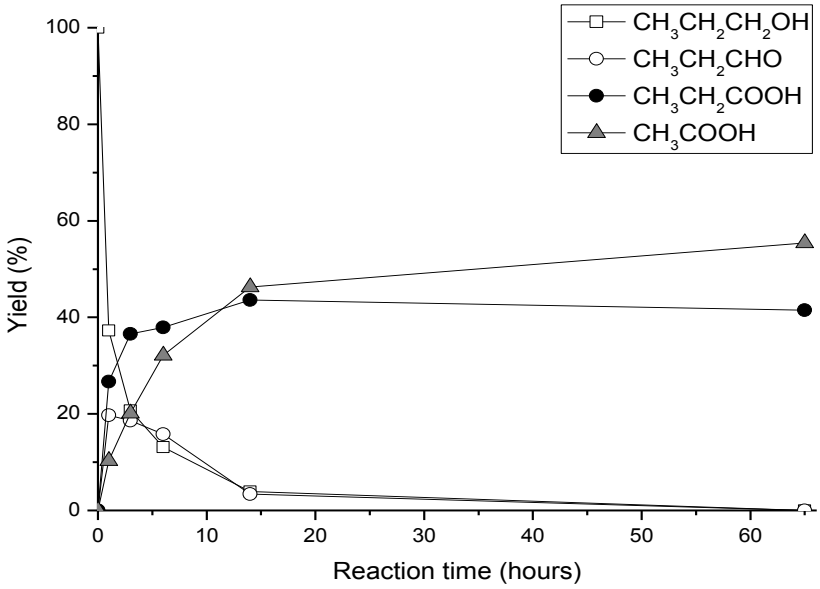

Figure 59. Product yields in the aerobic oxidation of aqueous propanol with 1.2 wt% $Ru(OH)_x/CeO_2$ catalyst. Reaction conditions: 10.13 mL of 1.07 M 1-propanol/H_2O solution, 10 bar O_2, 150°C, 0.23 mol% Ru.

As seen from the results, the oxidation of 1-propanol resulted in high yields of acetic acid (Figure 59). In fact, after 14 hours the reaction resulted in *ca.* 46 % of acetic acid, whereas the yield of propionic acid constituted 43 %. Notably, acetaldehyde was not observed at any point of the reaction (see *e.g.* Figure 46), thus suggesting that either the degradation route did not involve its formation or it was immediately oxidized into acetic acid.

In order to elucidate the possible origin of acetic acid, experiments were conducted in which propionic acid, propionaldehyde and 1-propanol were used as substrates in the aerobic oxidation with and without an introduced catalyst. The results are presented in Table 19.

Table 19. Product yields in the aerobic oxidation reaction of 1-propanol (C_3H_7OH), propionic acid (C_2H_5COOH) and propionaldehyde (C_2H_5CHO) in aqueous solutions.[a]

Entry	Substrate	Catalyst	Time, hours	Yield, %			
				C_3H_7OH	C_2H_5CHO	C_2H_5COOH	CH_3COOH
1	C_3H_7OH	-	3	96	0	0	0
2		CeO_2	3	77	12	6	1
3[b]		$Ru(OH)_x/CeO_2$	16	2	2	45	48
4	C_2H_5CHO	-	3	-	22	66	9
5		CeO_2	3	-	0	85	10
6[b]		$Ru(OH)_x/CeO_2$	3	-	0	71	24
7[b]		$Ru(OH)_x/CeO_2$	16	-	0	66	28
8	C_2H_5COOH	-	3	-	-	98	0
9		CeO_2	3	-	-	97	0
10[b]		$Ru(OH)_x/CeO_2$	3	-	-	81	13
11[b]		$Ru(OH)_x/CeO_2$	16	-	-	74	22
12[b]	C_3H_7OH	$Ru(OH)_x/CeO_2$ (re-use)	16	2	3	46	47
13[c]		RuO_x/CeO_2	3	30	20	33	14
14[b]		$Ru(OH)_x/MgAl_2O_4$	3	35	18	22	18
15[d]		$Ru(OH)_x/CeO_2$	3	46	19	16	13

[a]Reaction conditions: 10.8 mmol susbstrate in a total volume of 10.13 mL reaction mixture, 0.23 mol% Ru (*b*,*c*,*d*), 10 bar O_2, 150°C. [b]1.2 wt% $Ru(OH)_x$/support. [c]1.8 wt% RuO_x/CeO_2. [d]4.7 wt% $Ru(OH)_x/CeO_2$.

As seen from the obtained results, 1-propanol remained practically unconverted under the applied reaction conditions in the absence of catalyst (Table 19, entry 1), thus clearly indicating that the formation of oxidation products (see Figure 57) can be fully ascribed to the catalytic activity of supported $Ru(OH)_x$. In the presence of cerium dioxide, however, propanol conversion reached 33 % after 3 hours. This was in accordance with the previously found contribution of CeO_2 to the overall catalytic activity of the supported $Ru(OH)_x/CeO_2$ catalysts in the aerobic oxidation of ethanol.

The data presented in Table 19 also suggests that acetic acid originated at least partially in the degradation of propionic acid (entries 8-11). However, the yield of acetic acid constituted only 22 % after 16 hours of reaction time when propionic acid was used as a substrate (entry 11), whereas the direct oxidation of propanol resulted in 48 % acetic acid (entry 3). Additionally, the degradation of propionic acid over pristine CeO_2 was almost negligible (entry 9), whereas the reaction with propionaldehyde (entry 5) resulted in 10 % of acetic acid, revealing a higher stability (towards C-chain degradation) of C_2H_5COOH compared to C_2H_5CHO under applied conditions.

The results of the GC-TCD analysis of the post-reaction gas mixture (Figure 60) revealed the presence of CO_2 formed in the reaction, thus suggesting that the degradation of propionic acid was a decarboxylation [194-196]. The available analysis method, however, did not allow a quantification of CO_2 in the gas mixture (Figure 60), as its peak interlapped with a similar peak of CO. (Due to the instrument specifics, CO is always present in the GC-TCD analysis system.)

The results of the oxidation of propionaldehyde with ceria-supported ruthenium catalyst, ceria and in the absence of catalyst are compared in Table 19, entries 4-7. After 3 hours, the reaction with the introduced 1.2 wt% $Ru(OH)_x/CeO_2$ catalyst afforded a 24 % yield of acetic acid (Table 19, entry 6), which is similar to the result obtained for direct propanol oxidation (see Figure 59). This yield, however, did not increase significantly after 16 hours of reaction time (28 %; Table 19, entry 7) when compared to the respective acetic acid yield of *ca.* 43 % in the propanol oxidation reaction, as was shown in Figure 58. In fact, the conversion of propionaldehyde into propionic acid occurred even in the absence of a catalyst: after 3 hours of the reaction time, the conversion or C_2H_5CHO reached approximately 78 % at 66 and 9 % yields of propionic and acetic acid, respectively (Table 19, entry 4).

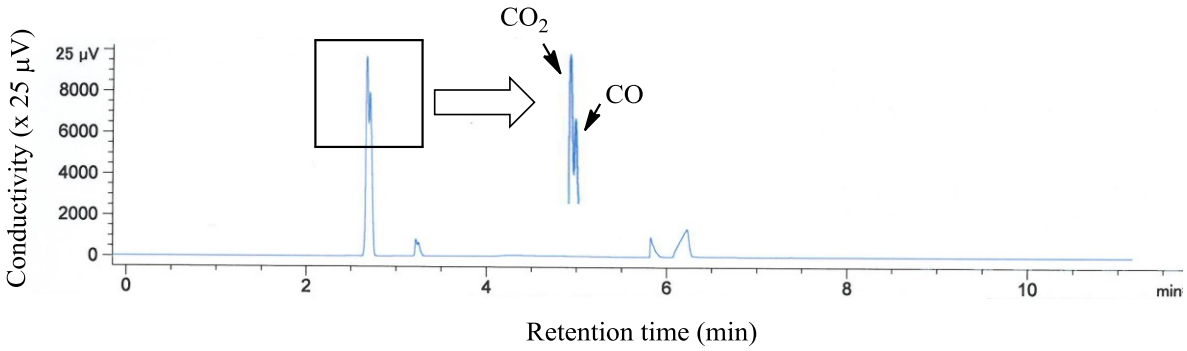

Figure 60. Typical GG-TCD chromatogram of the propanol oxidation post-reaction gas mixture. Unnamed peaks on the figure represent (left to right) methylacetate, water and methanol, always present in the GC instrument system.

These results suggested that the partial degradation of the carbon chain of 1-propanol was facilitated during the direct oxidation of propanol, compared to the oxidation of propionaldehyde.

Importantly, reaction conditions that proved to be suitable for the formation and stability of acetic acid were at the same time detrimental for propionic carbonyl compounds, resulting in a C-chain degradation.

Additionally, following the promising results of the ethanol oxidation with $Ru(OH)_x$ supported on spinel (see section 6.3.1) and RuO_x supported on CeO_2, experiments with these catalysts were conducted. Both substrate conversion and product yields were lower in these reactions compared to the reaction with 1.2 $Ru(OH)_x/CeO_2$ (Table 19, entries 13 and 14), similarly to the previously obtained results for the oxidation of ethanol. Also, the reaction with 4.7 wt% $Ru(OH)_x/CeO_2$ catalyst resulted in lower levels of conversion and yields (entry 15), as anticipated.

Further, the effects of altering oxygen pressure and reaction temperature have been investigated. The results are presented in Figure 61.

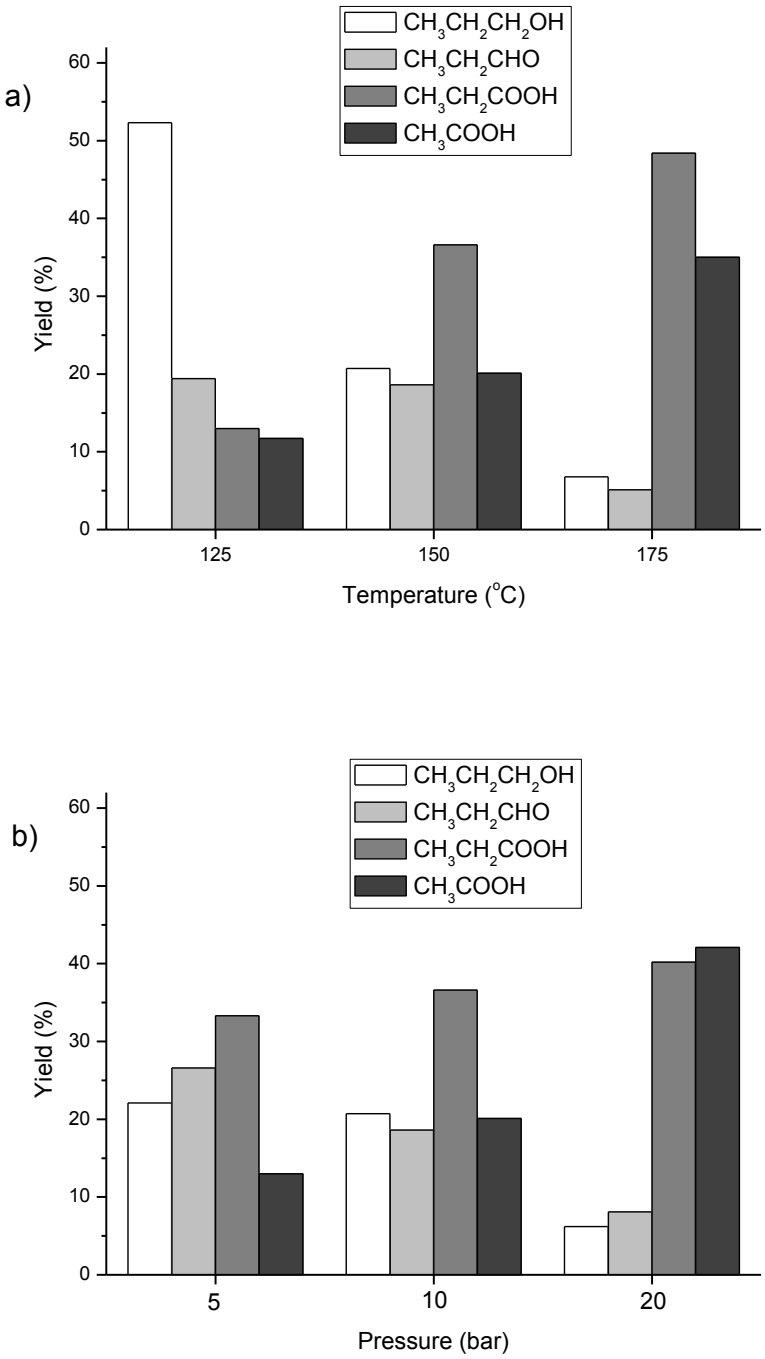

Figure 61. Product yields in the aerobic oxidation of aqueous propanol with 1.2 wt% $Ru(OH)_x/CeO_2$ catalyst: (a) under 10 bar O_2 and (b) at 150°C. Reaction conditions: 10.13 mL of 0.107 M 1-propanol/H_2O solution. 0.23 mol% Ru, 3 hours reaction time.

It is clearly seen from the obtained results that the higher substrate conversion was achieved at increased temperature (and lower – at decreased temperature, respectively) (Figure 61a), in good accordance with the results of the aerobic oxidation of ethanol (see, for example, Figure 49b). In fact, the yields of both carboxylic acids - acetic and propionic - increased as well. Also, at 175^{o}C after 3 hours of reaction time the apparent reaction selectivity towards acetic acid was higher compared to the results of the reactions at 125 and 150^{o}C. Similar tendency was observed for varied applied pressure. Here, propanol conversion increased in the order 5 bar < 10 bar < 20 bar of O_2 pressure (Figure 61b). Acetic acid selectivity also increased. These results clearly indicated that the partial decomposition of the C3-products of propanol oxidation to form acetic acid was more efficient at increased temperatures and pressures.

Following the promising results of acetic acid formation from propanol, the reaction conditions explored for ethanol and propanol (150^{o}C, 10 bar O_2) were applied for the aerobic oxidation of other higher aliphatic alcohols. The results of these oxidation reactions with the accent on the formation of acetic and propionic acids are presented in Table 20.

Yields of other products are not presented in the table; however, it is worth mentioning that those were found to be ‘‘simple’’ expected oxidation products (aldehydes, ketones, carboxylic acids) of respective alcohols. For instance, in the case of 2-propanol (Table 20, entry 2) the major product was found to be acetone (54 % yield); the oxidation of 1-butanol (Table 20, entry 6) resulted in formation of butyraldehyde (*ca.* 30 %) and butanoic acid (*ca.* 40 %).

The data from Table 20 showed that all screened alcohols or their oxidation products underwent the C-C bond cleavage to a certain extent, leading eventually to the formation of acetic acid. This, again, was probably a decarboxylation, as was suggested above for the degradation of propionic acid. Hence, for 1-butanol oxidation products (entry 6) several consecutive decarboxylation reactions would lead from butanoic acid *via* propionic to acetic acid, whereas a degradation pathway of some of the alcohols remains unclear, as was for example in the case of 2-propanol, 2- and *tert*-butanol (entries 4, 7, 8).

Table 20. Alcohols conversion and acetic and propiopnic acids yield in the aerobic oxidation reactions of higher aliphatic alcohols in water with 1.2 wt% $Ru(OH)_x/CeO_2$ catalyst.

Entry	Substrate	Reaction time, hours	Alcohol conversion, %	Yield, %	
				CH_3CH_2COOH	CH_3COOH
1	1-Propanol	16	98	45	48
2	2-Propanol	16	>99	5	30
3	1,2-Propanediol	3	39	0	37
4	1,3-Propanediol	16	74	5	60
5	Glycerol	16	>90	3	15
6	1-Butanol	3	>90	8	4
7	2-Butanol	3	78	1	8
8	*t*-Butanol	3	88	1	16
9	1,3-Butanediol	3	48	0	14
10	1,3-Butanediol	16	81	0	20
11	2,3-Butanediol	3	59	1	58[b]
12	2,3-Butanediol	16	91	0	88[b]
13	1,4-Butanediol	3	42	2	0
14[c]	2,3-Butanediol	3	>99	0	>99[b]
15[d]	2,3-Butanediol	3	9	0	0
16[e]	2,3-Butanediol	3	4	0	1
17[f]	2,3-Butanediol	3	2	0	0

[a]Reaction conditions: 10.13 mL of 1.07 M aqueous alcohol solution, 0.23 mol% Ru, 10 bar O_2, 150°C, 3 hours reaction time. [b]Halved amount, based on the assumption that 1 mol of substrate produces 2 mol of acetic acid. [c]Reaction under 20 bar O_2. [d]Reaction under 10 bar Ar. [e]0.21 g of pure CeO_2. [f]W/o catalyst.

Although the major product of the 1-butanol oxidation (entry 6) was found to be butanoic acid (see above), the results obtained from the oxidation of 2,3-butanediol (Table 20, entries 11, 12, 14-17) suggest that the substrate underwent cleavage as the vicinal aliphatic diol, possibly following the pathway *via* the formation of an aldehyde product

[197,198], in this case - acetaldehyde, which was further oxidized into acetic acid (Scheme 18a). This can explain high yields of acetic acid and low or absent yields of propanoic acid in these experiments. However, acetaldehyde was not detected at any point of the reaction, suggesting that either it was immediately oxidized into acetic acid or that the pathway leading to acetic acid did not involve the formation of an aldehyde.

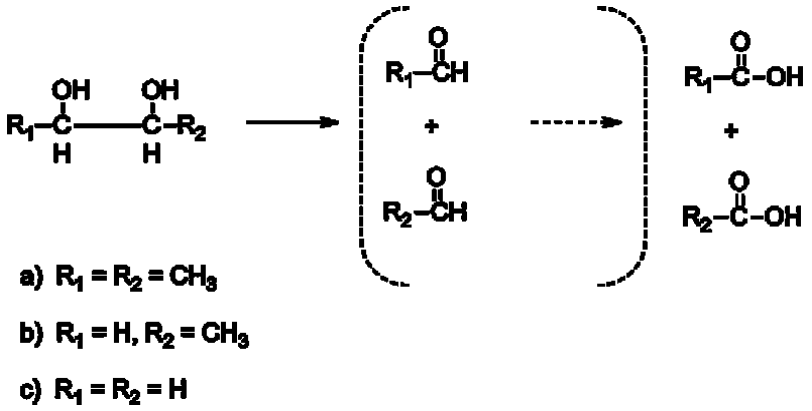

Scheme 18. The pathway of the oxidative cleavage of vicinal diols with $Ru(OH)_x/CeO_2$ catalyst, probably involving a formation of aldehydes.

In literature, oxidative cleavage of compounds containing vicinal hydroxyl groups has been reported with ruthenium tetroxide [199,200], ruthenium-bismuth and ruthenium-lead pyrochlore oxides (both electrooxidation [201] and aerobic oxidation in the presence of base [197,202]) and aerobic oxidation with $Ru(PPh_3)_3Cl_2$ on activated carbon [198]. It is however notable that diols cleavage did not occur with RuO_2, indicating its inactivity under the conditions reported by Ishii *et al.* (TFT, 60°C, 1 atm of O_2) [198].

Nevertheless, to the best of our knowledge to date there are no reports on selective oxidative cleavage of *vic*-diols utilizing supported aerobic $Ru(OH)_x$ catalyst.

Similarly to the oxidation of ethanol, a mechanism involving the initial formation of aldehydes (Scheme 18) would be in accordance with the reaction mechanism for the alcohols oxidation over $Ru(OH)_x$ supported catalysts. However, the possible reaction mechanism and computational model proposed by Mizuno *et al.* [102,103,203] did not consider aqueous media. Also, the *ab initio* calculations [202] focused on a catalyst model comprised only of Ru^{3+} oxidation state. A possibility of fitting the cleavage of *vic*-diols into the proposed model

also remains unclear, although for $Ru(PPh_3)_3Cl_2$/C catalyst Ishii *et al.* [198] suggested that the reaction proceeded through a six-membered alkoxide transition state. Most importantly, the fact that acetaldehyde was not observed at any point of the reaction (as mentioned above) might indicate a different reaction mechanism/pathway. Further investigations are required to clearify the reaction mechanism of the vicinal diols cleavage over $Ru(OH)_x$ catalysts.

In the oxidation of 1,2-propanediol the high yield and selectivity of acetic acid were also obtained (Table 20, entry 3). Here, another observed product was formic acid, in accordance with the pathway shown in Scheme 18b. Indeed, when a test experiment of the oxidation of glycol was performed (0.0107 mol of 1,2-ethanediol (glycol) in 10.13 mL solution, 1.2wt% $Ru(OH)_x/CeO_2$ (0.23 mol% Ru), 10 bar O_2, 150^{o}C), *ca.* 50 % substrate conversion and no acetic acid formation was observed after three hours of the reaction time, whereas the yield of formic acid (the only observed product) constituted 14 %. Importantly, in an experiment at the same conditions with formic acid as the substrate, after 3 hours of the reaction time only 45 % of formic acid remained unconverted, evidently indicating its degradation: either overoxidation to carbon dioxide or dehydration to CO [204,205]. This supports the hypothesis of the *vic*-diols cleavage reaction, suggesting the oxidative cleavage of glycol *via* the formation of 2 molecules of formic acid (Scheme 18c), which are further degraded into CO or CO_2. However, due to the instrument specifics, the applied analysis methods did not allow to observe formed CO and/or quantify CO_2 (see above; Figure 60).

Additionally, the results of the 2,3-butanediol oxidation under 20 bar of O_2 (Table 20, entry 14) and under 10 bar of Ar (entry 15) indicated the aerobic nature of the C-C bond cleavage. As observed from the data, when the reaction was performed under increased oxidant pressure (20 bar of O_2) a quantitative yield of acetic acid was obtained already after 3 hours of reaction time (entry 14). Accordingly, a reaction under 10 bar of Ar (entry 15) resulted in only *ca.* 9 % substrate conversion with >99 % selectivity to 3-hydroxy-2-butanone (*i.e.*, no products of the oxidative cleavage were observed). A reaction with the introduced 'blank' CeO_2 (entry 16) yielded in 4 % alcohol conversion and 1 % acetic acid yield, whereas a reaction in the absence of the catalysts resulted in negligible 2,3-butanediol conversion (entry 17). This clearly demonstrated the stability of the substrate under applied conditions, allowing to ascribe the formation of the oxidation products to the catalytic activity of $Ru(OH)_x/CeO_2$, as was the case in the oxidation of 1-propanol and ethanol.

6.4. Conclusions

Highly selective and efficient aerobic oxidation of aqueous ethanol (2.5-50 wt%) to acetic acid with supported ruthenium hydroxide catalysts at elevated temperatures and oxygen pressures is reported. The performance of catalysts based on different supports increased in the order $Ru(OH)_x/TiO_2 < Ru(OH)_x/MgAl_2O_4 < Ru(OH)_x/CeO_2$. An enhanced activity of the $Ru(OH)_x/CeO_2$ catalyst was found to originate in a combination of the catalytic activity of support (CeO_2) and $Ru(OH)_x$ species.

Furthermore, the activity of the CeO_2-supported $Ru(OH)_x$ catalysts was found to be dependant on the ruthenium species loading on the surface of the support and hence the particle size. The optimal performance was suggested to correspond to approximately 1 wt% $Ru(OH)_x$ loading with a particle size of 0.6 - 2 nm. Here, the increase in loading resulted in a decrease of the catalytic activity contributed by ruthenium species, and a decrease in ruthenium loading did not improve $Ru(OH)_x$ catalytic activity.

Moreover, the detrimental effect of heat-treatment of the $Ru(OH)_x/CeO_2$ catalyst was shown. The effects of the substrate concentration and reaction temperature were also demonstrated. Importantly, the oxidation of aqueous ethanol solutions of high concentrations is shown to proceed with similar efficiency, thus providing opportunity for utilization of the catalyst systems in bio-ethanol upgrading.

The aerobic oxidation of ethanol was also investigated with supported highly dispersed RuO_x catalysts. It was demonstrated that the novel gas-phase synthesis for ruthenium oxide nanoparticles coating of various metal oxides produced active catalysts for the selective aerobic oxidation of ethanol to acetic acid. RuO_x particles were deposited on TiO_2, hydrotalcite, spinel, sodium titanate nanotubes, ZnO, Al_2O_3, WO_3, CeO_2 and mixed oxide $CeZrO_4$ supports. Similarly to what was shown for $Ru(OH)_x$ supported catalysts, RuO_x/CeO_2 was found to be the most active aerobic catalyst.

In order to gain additional insight into the support effect, RuO_x was deposited on a support comprised of a mixed cerium-zirconium oxide, known to have an increased redox activity in three-way catalysts. Notably, no promoting affect of the support was observed compared to CeO_2-supported catalyst.

An examination of the heat-treatment effect on the catalytic activity revealed a decrease in the catalyst's performance, similarly to the $Ru(OH)_x$ catalysts. This was suggested to be due the decrease in the Ru valence state and hydration level in the as-deposited Ru oxide.

Most importantly, it was demonstrated that the loading of RuO_x deposited by the gas-phase reaction did not affect the catalytic activity when the compared reactions were normalized to the RuO_x content. This clearly demonstrated that the nanoparticles deposited on CeO_2 by this novel method were equally active regardless of the support porosity and ruthenium species loading. In general, this present a possibility of catalysts production with a very wide range of the active species loadings, a remarkable feature for potential industrial applications.

An oxidative degradation of higher alcohols to form acetic acid was also shown with supported ruthenium catalysts. In particular, the oxidation of 1-propanol with $Ru(OH)_x$ and RuO_x deposited on CeO_2 resulted in high yields of acetic acid. The latter product was shown to originate at least partially in the degradation of propionic acid.

Additionally, a reaction of the oxidative cleavage of vicinal diols was investigated with the ruthenium catalysts. Supported $Ru(OH)_x/CeO_2$ catalyst was shown to be a very efficient catalyst for the aerobic oxidation of *vic*-diols, such as 1,2-propanediol and 2,3-butanediol, to form respective carboxylic acids. Interestingly, no carbonyl-containing products were observed in the reactions, thus making an applicability of a pathway involving the formation of aldehydes unclear. Additional investigations are required to clearify a possible reaction mechanism.

7. *Concluding remarks*

In this thesis, oxidative catalytic transformations of different biomass-derived compounds for the production of value-added chemicals have been investigated. The investigated processes have the potential for being a part of future chemical industries based on bio-renewables. It can't be predicted whether this future scenario will emerge, however one thing remains certain, and that is the continuing depletion of fossil resources. Massive changes and investments in the chemical industry are needed to enable a switch to new energy sources. Future scientific research must be combined with already existing technologies to allow such a shift.

The research presented in this thesis was comprised of, firstly, the oxidation of 5-hydroxymethylfurfural (HMF) to form 2,5-furancarboxylic acid (FDA) and 2,5-diforrmylfuran (DFF), chemical compounds of great industrial potential. FDA is considered to be a substitute building block for the plastics industry, in place of the contemporarily used terephtalic acid, which is commonly obtained from fossil resources. DFF has the potential to become a starting material for various medicinal and cosmetic chemical productions.

The oxidation of alcohols to produce acetic acid was also investigated. Acetic acid is an important food and industrial product with a great number of applications. In this work, ethanol and higher alcohols were shown to be readily oxidized (in case of propanol and 2,3-butanediol – undergo oxidative degradation) to selectively form acetic acid in high yields.

All investigations were performed by the means of heterogeneous catalysis, one of the key components of the contemporary chemical industry. Reactions leading to the production of FDA and acetic acid were explored in an environmentally friendly or "green" media (water or ionic liquids) using an abundant and inexhaustible oxidant (oxygen).

Many of the investigated reactions provide an insight into a new area of research, *e.g.* the employment of the ruthenium-based catalysts for the oxidation of HMF in water or ionic liquids. It is now up to researchers to find the optimal ways to improve the presented processes and ultimately transfer them to large scale applications, in order to comply with the growing demand for the new, bio-based chemical industry.

8. *References*

[1] R. A. Sheldon, *Green Chem.* **2008**, *10*, 359.

[2] U.S. Environmental Protection Agency, *Introduction to the Concept of Green Chemistry*, **2010**; available online at: http://www.epa.gov/greenchemistry/pubs/about_gc.html.

[3] M. Narodoslawsky, A. Niederl-Schmidinger, L. Halasz, *J. Cleaner Prod.* **2008**, *16*, 164.

[4] J. H. Gary, G. E. Handwerk, *Petroleum Refining Technology and Economics (2nd ed.)*, Marcel Dekker Ltd., **1984**, ISBN: 0-8247-7150-8.

[5] B. Kamm, M. Kamm, *Adv. Biochem. Engin./Biotechnol.* **2007**, *105*, 175.

[6] M. Crocker, C. Crofcheck, *Energeia* **2006**, *17*, 1.

[7] Y. Xu, M. A. Hanna, L. Isom, *The Open Agriculture Journal* **2008**, *2*, 54.

[8] T. Werpy, G. Petersen, U.S. DoE, **2004**, No. DOE/GO-102004-1992; available online at: http://www.nrel.gov/docs/fy04osti/35523.pdf.

[9] J. J. Bozell, G. R. Petersen, *Green Chem.* **2010**, *12*, 539.

[10] R. Hammerschlag, *Environ. Sci. Technol.* **2006**, *40*, 1744.

[11] P. S. Nigam, A. Singh, *Prog. Energy Combust. Sci.* **2011**, *37*, 52.

[12] G. Knothe, *Top. Catal.* **2010**, *53*, 714.

[13] C. Moreau, M. N. Beglacem, A. Gandini, *Top. Catal.* **2004**, *27*, 11.

[14] P. Gallezot, *Green Chem.* **2007**, *9*, 295.

[15] A. Corma, S. Iborra, A. Velty, *Chem. Rev.* **2007**, *107*, 2411.

[16] X. Tong, Y. Ma, Y. Li, *Appl. Catal., A* **2010**, *385*, 1.

[17] K. Egeblad, J. Rass-Hansen, C. C. Marsden, E. Taarning, C. H. Christensen, "Heterogeneous Catalysis for Production of Value-Added Chemicals from Biomass", in *Catalysis, Volume 21* (Ed. J. J. Spivey), RSC Publishing, **2009**, ISBN: 978-0-85404-249-4.

[18] C. H. Christensen, J. Rass-Hansen, C. C. Marsden, E. Taarning, K. Egeblad, *ChemSusChem* **2008**, *1*, 283.

[19] C. B. Field, M. J. Behrenfeld, J. T. Randerson, P. Falkowski, *Science* **1998**, *281*, 237.

[20] L. A. Lucia, D. S. Argyropoulos, L. Adamopoulos, A. R. Gaspar, *Can. J. Chem.* **2006**, *84*, 960.

[21] R. A. Sheldon, *Pure Appl. Chem.* **2000**, *72*, 1233.

[22] M. J. Climent, A. Corma, S. Iborra, *Chem. Rev.* **2011**, *111*, 1072.

[23] G. Rothenberg, *Catalysis: Concepts and Green Applications*, Wiley-VCH, **2008**, ISBN: 978-3-527-31824-7.

[24] Z. Ma, F. Zaera, "Heterogeneous Catalysis by Metals", in *Encyclopedia of Inorganic Chemistry* (Ed. R. A. Scott), Wiley, **2011**, ISBN: 978-1-1199-9428-2.

[25] P. N. R. Vennestrøm, C. H. Christensen, S. Pedersen, J.-D. Grunwaldt, J. M. Woodley, *ChemCatChem* **2010**, *2*, 249.

[26] T. Ståhlberg, W. Fu, J. M. Woodley, A. Riisager, *ChemSusChem* **2011**, *4*, 451.

[27] T. S. Hansen, J. M. Woodley, A. Riisager, *Carbohydr. Res.* **2009**, *344*, 2568.

[28] T. Ståhlberg, M. G. Sørensen, A. Riisager, *Green Chem.* **2010**, *12*, 321.

[29] K. D. O. Vigier, F. Jerome, *Top. Curr. Chem.* **2010**, *295*, 63

[30] T. S. Hansen, J. Mielby, A. Riisager, *Green Chem.* **2011**, *13*, 109.

[31] M. Tan, L. Zhao, Y. Zhang, *Biomass Bioenergy* **2011**, *35*, 1367.

[32] F. Yang, Q. Liu, X. Bai, Y. Du, *Bioresour. Technol.* **2011**, *102*, 3424.

[33] F. K. Kazi, A. D. Patel, J. C. Serrano-Ruiz, J. A. Dumesic, R. P. Anex, *Chem. Eng. J.* **2011**, *169*, 329.

[34] M. E. Zakrzewska, E. Bogel-Łukasik, R. Bogel-Łukasik, *Chem. Rev.* **2011**, *111*, 397.

[35] R. J. Sheehan, "Terephthalic Acid, Dimethyl Terephthalate, and Isophthalic Acid", in *Ullmann's Encyclopedia of Industrial Chemistry*, Wiley-VCH, **2002**; DOI: 10.1002/14356007.a26_19.

[36] J. Lewkowski, *ARKIVOC*, **2001**, *(i)*, 17.

[37] W. Partenheimer, V. V. Grushin, *Adv. Synth. Catal.* **2000**, *343*, 102.

[38] M. L. Ribeiro, U. Schuchardt, *Catal. Commun.* **2003**, *4*, 83.

[39] M. Kröger, U. Prüße, K.-D. Vorlop, *Top. Catal.* **2000**, *13*, 237.

[40] P. Vinke, W. van der Poel, H. van Bekkum, *Stud. Surf. Sci. Catal.* **1991**, *59*, 385.

[41] F. Koopman, N. Wierckx, J. H. de Winde, H. J. Ruijssenaars, *Bioresour. Technol.* **2010**, *101*, 6291.

[42] M. A. Lilga, R. T. Hallen, J. Hu, J. F. White, M. J. Gray, U.S. Patent 20080103318, **2008**.

[43] M. A. Lilga, R. T. Hallen, M. Gray, *Top. Catal.* **2010**, *53*, 1264.

[44] O. Casanova, S. Iborra, A. Corma, *ChemSusChem* **2009**, *2*, 1138.

[45] S. E. Davis, L. R. Houk, E. C. Tamargo, A. K. Datye, R. J. Davis, *Catal. Today* **2011**, *160*, 55.

[46] N. K. Gupta, S. Nishimura, A. Takagaki, K. Ebitani, *Green Chem.* **2011**, *13*, 824.

[47] E. Taarning, I. S. Nielsen, K. Egeblad, R. Madsen, C. H. Christensen, *ChemSusChem* **2008**, *1*, 1.

[48] O. Casanova, S. Iborra, A. Corma, *J. Cat.* **2009**, *265*, 109.

[49] G. C. Bond, P. A. Sermon, G. Webb, D. A. Buchanan, P. B. Wells, *J. Chem. Soc., Chem. Commun.* **1973**, 444.

[50] A. S. K. Hashmi, G. Hutchings, *Angew. Chem. Int. Ed.* **2006**, *45*, 7896.

[51] A. Corma, H. Garcia, *Chem. Soc. Rev.* **2008**, *37*, 2096.

[52] G.-J. ten Brink, I. W. C. E. Arends, R. A. Sheldon, *Science* 2000, *287*, 1636.

[53] T. Mallat, A. Baiker, *Chem. Rev.* **2004**, *104*, 3037.

[54] M. Haruta, N. Yamada, T. Kobayashi, S. Iijima, *J. Catal.* **1989**, *115*, 301.

[55] M. Haruta, *Catal. Today* **1997**, *36*, 153.

[56] G. H. Du, Q. Chen, R. C. Che, Z. Y. Yuan, L.-M. Peng, *Appl. Phys. Lett.* **2001**, *79*. 3702.

[57] M. Haruta, M. Daté, *Appl. Catal., A* **2001**, *222*, 427.

[58] G. H. Du, Q. Chen, P. D. Han, Y. Yu, L.-M. Peng, *Phys. Rev. B* **2003**, *67*, 035323.

[59] A. Abad, P. Concepción, A. Corma, H. Garcia, *Angew. Chem. Int. Ed.* **2005**, *44*, 4066.

[60] S. Zhang, Q. Chen, L.-M. Peng, *Phys. Rev. B* **2005**, *71*, 014104.

[61] D. I. Enache, J. K. Edwards, P. Landon, B. Solsona-Espriu, A. F. Carley, A. A. Herzing, M. Watanabe, C. J. Kiely, D. W. Knight, G. J. Hutchings, *Science* **2006**, *311*, 362.

[62] C. H. Christensen, B. Jørgensen, J. Rass-Hansen, K. Egeblad, R. Madsen, S. K. Klitgaard, S. M. Hansen, M. R. Hansen, H. C. Andersen, A. Riisager, *Angew. Chem. Int. Ed.* **2006**, *45*, 4648.

[63] I. S. Nielsen, E. Taarning, K. Egeblad, R. Madsen, C. H. Christensen, *Catal. Lett.* **2007**, *116*, 35.

[64] N. Zheng, G. D. Stucky, *Chem. Commun.* **2007**, 3862.

[65] L. Miao, Y. Ina, S. Tanemura, T. Jiang, M. Tanemura, K. Kaneko, S. Toh, Y. Mori, *Surf. Sci.* **2007**, *601*, 2792.

[66] H. Miyamura, R. Matsubata, Y. Miyazaki, S. Kobayashi, *Angew. Chem. Int. Ed.* **2007**, *46*, 4151.

[67] S. K. Klitgaard, K. Egeblad, U. V. Mentzel, A. G. Popov, T. Jensen, E. Taarning, I. S. Nielsen, *Green Chem.* **2008**, *10*, 419.

[68] J. Jiang, Q. Gao, Z. Chen, *J. Mol. Catal. A: Chem.* **2008**, *280*, 233.

[69] P. Fristrup, L. B. Johansen, C. H. Christensen, *Catal. Lett.* **2008**, *120*, 184.

[70] S. Kegnæs, J. Mielby, U. V. Mentzel, C. H. Christensen, A. Riisager, *Green Chem.* **2010**, *12*, 1437.

[71] W. C. Ketchie, M. Murayama, R. J. Davis, *J. Catal.* **2007**, *250*, 264.

[72] W. C. Ketchie, M. Murayama, R. J. Davis, *Top. Catal.* **2007**, *44*, 307.

[73] W. C. Ketchie, Y.-L. Fang, M. S. Wong, M. Murayama, R. J. Davis, *J. Catal.* **2007**, *250*, 94.

[74] B. Jørgensen, S. E. Christiansen, M. L. D. Thomsen, C. H. Christensen, *J. Catal.* **2007**, *251*, 332.

[75] C. Marsden, E. Taarning, D. Hansen, L. Johansen, S. K. Klitgaard, K. Egeblad, C. H. Christensen, *Green Chem.* **2008**, *10*, 168.

[76] E. Taarning, A. T. Madsen, J. M. Marchetti, K. Egeblad, C. H. Christensen, *Green Chem.* **2008**, *10*, 408.

[77] E. Taarning, I. S. Nielsen, K. Egeblad, R. Madsen, C. H. Christensen, *ChemSusChem* **2008**, *1*, 75.

[78] S. K. Klitgaard, A. T. DeLa Riva, S. Helveg, R. M. Werchmeister, C. H. Christensen, *Catal. Lett.* **2008**, *126*, 213.

[79] T. J. Donohoe, *'Oxidation and Reduction in Organic Synthesis'*, Oxford University Press, Oxford, **1994**.

[80] T. W. Hansen, J. B. Wagner, P. L. Hansen, S. Dahl, H. Topsøe, C. J. H. Jacobsen, *Science* **2001**, *294*, 1508.

[81] I. W. C. E. Arends, T. Kodama, R. A. Sheldon, *Top. Organomet. Chem.* **2004**, *11*, 277.

[82] A. Klerke, S. K. Klitgaard, R. Fehrmann, *Catal. Lett.* **2009**, *541*, 541.

[83] K. Rovik, S. K. Klitgaard, S. Dahl, C. H. Christensen, I. Chorkendorff, *Appl. Catal., A* **2009**, *358*, 269.

[84] M. Pagliaro, S. Campestrini, R. Ciriminna, *Chem. Soc. Rev.* **2005**, *34*, 837.

[85] A. Dijksman, I. W. C. E. Arends, R. A. Sheldon, *Platinum Metals Rev.* **2001**, *45*, 15.

[86] S. Chang, M. Lee, S. Ko, P. H. Lee, *Synth. Commun.* **2002**, *32*, 1279.

[87] A. Köckritz, M. Sebek, A. Dittmar, J. Radnik, A. Brückner, U. Bentrup, M.-M. Pohl, H. Hugl, W. Mägerlein, *J. Mol. Catal. A: Chem.* **2006**, *246*, 85.

[88] M. P. Chęciński, A. Brückner, J. Radnik, A. Köckritz, *Appl. Catal., A* **2009**, *366*, 212.

[89] E. Vanover, Y. Huang, L. Xu, M. Newcomb, R. Zhang, *Org. Lett.* **2010**, *12*, 2246.

[90] Y. Zhai, H. Liu, B. Liu, Y. Liu, J. Xiao, W. Bai, *Trans. Met. Chem.* **2007**, *32*, 570.

[91] Z. Q. Lei, Q. X. Kang, X. Z. Bai, Z. W. Yang, Q. H. Zhang, *Chin. Chem. Lett.* **2005**, *16*, 846.

[92] V. Farmer, T. Welton, *Green Chem.* **2002**, *4*, 97.

[93] F. Vocanson, Y. P. Guo, I. L. Namy, H. B. Kagan, *Synth. Commun.* **1998**, *28*, 2577.

[94] H. Ji, T. Mizugaki, K. Ebitani, K. Kaneda, *Tetrahedron Lett.* **2002**, *43*, 7179.

[95] M. Musawir, P. N. Davey, G. Kelly, I. V. Kozhevnikov, *Chem. Commun.* **2003**, 1414.

[96] S. Venkatesan, A. S. Kumar, J.-F. Lee, T.-S. Chan, J.-M. Zen, *Chem. Commun.* **2009**, 1912.

[97] K. Yamaguchi, K. Mori, T. Mizugaki, K. Ebitani, K. Kaneda, *J. Am. Chem. Soc.* **2000**, *122*, 7144.

[98] K. Mori, K. Yamaguchi, T. Mizugaki, K. Ebitani, K. Kaneda, *Chem. Commun.* **2001**, 461.

[99] K. Yamaguchi, N. Mizuno, *Chem. Eur. J.* **2003**, *9*, 4353.

[100] M. Kotani, T, Koike, K. Yamaguchi, N. Mizuno, *Green Chem.* **2006**, *8*, 735.

[101] J. W. Kim, K. Yamaguchi, N. Mizuno, *Angew. Chem. Int. Ed.* **2008**, *47*, 9249.

[102] N. Mizuno, K. Yamaguchi, *Catal. Today* **2008**, *132*, 18.

[103] K. Yamaguchi, N. Mizuno, *Synlett* **2010**, *16*, 2365.

[104] D. V. Bavykin, A. A. Lapkin, S. T. Kolaczkowski, P. K. Plucinski, *Appl. Catal., A* **2005**, *288*, 175.

[105] K. Kaneda, T. Yamashita, T. Matsushita, K. Ebitani, *J. Org. Chem.* **1998**, *63*, 1750.

[106] T. Matsushita, K. Ebitani, K. Kaneda, *Chem. Commun.* **1999**, 265.

[107] Z. Opre, J.-D. Grunwaldt, M. Maciejewski, D. Ferri, T. Mallat, A. Baiker, *J. Catal.* **2005**, *230*, 406.

[108] Z. Opre, J.-D. Grunwaldt, T. Mallat, A. Baiker, *J. Mol. Catal. A* **2005**, *242*, 224.

[109] B. Veldurthy, J. M. Clacens, F. Figueras, *Adv. Synth. Catal.* **2005**, *347*, 767.

[110] J. Kiwi, R. Prins, *Chem. Phys. Lett.* **1986**, *126*, 579.

[111] M. Lakshmi Kantam, U. Pal, B. M. Choudary, S. Bhargava, *Adv. Synth. Catal.* **2008**, *350*, 1225.

[112] J. Preiss, M. L. Biggs, E. Greenberg, *J. Biol. Chem.* **1967**, *242*, 2292.

[113] B. Gontero, J. C. Meunier, J. Ricard, *Plant Sci. Lett.* **1984**, *36*, 195.

[114] K. K. Shieh, B. J. Donnelly, H. A. Lee, U.S. Patent 3834988, **1974**.

[115] J. I. Di Cosimo, V. K. Diez, M. Xu, E. Iglesia, C. R. Apesteguia, *J. Catal.* **1998**, *178*, 499.

[116] P. Wasserscheid, T. Welton, *Ionic Liquids in Synthesis*, Wiley-VCH, **2008**, ISBN: 978-3-527-31239-9.

[117] J. Yadav, B. Reddy, K. Reddy, K. Gayathri, A. Prasad, *Tetrahedron Lett.* **2003**, *44*, 6493.

[118] J. Peng, F. Shi, Y. Gu, Y. Deng, *Green Chem.* **2003**, *5*, 224.

[119] A. J. Walker, N. C. Bruce, *Tetrahedron* **2004**, *60*, 561.

[120] X.-E. Wu, L. Ma, M.-X. Ding, L.-X. Gao, *Synlett* **2005**, 607.

[121] G. S. Owens, A. Durazo, M. M. Abu-Omar, *Chem. Eur. J.* **2002**, *8*, 3053.

[122] W.-H. Lo, H.-Y. Yang, G.-T.Wei, *Green Chem.* **2003**, *5*, 639.

[123] B. Martiz, R. Keyrouz, S. Gmouh, M. Vaultier, V. Jouikov, *Chem. Commun.* **2004**, 674.

[124] G. Bianchini, M. Crucianelli, F. D. Angelis, V. Neri, R. Saladino, *Tetrahedron Lett.* **2005**, *46*, 24272.

[125] A. Wolfson, S. Wuyts, D. E. De, Vos, I. F. J. Vankelecom, P. A. Jacobs, *Tetrahedron Lett.* **2002**, *43*, 8107.

[126] H. Sun, X. Li, J. Sundermeyer, *J. Mol. Catal. A: Chem.* **2005**, *240*, 119.

[127] N. Jiang, A. J. Ragauskas, *J. Org. Chem.* **2007**, *72*, 7030.

[128] H.-Y. Shen, H.-L. Mao, L.-Y. Ying, Q.-H. Xia, *J. Mol. Catal. A: Chem.* **2007**, *276*, 73.

[129] E. Farhangi, A. Rahmati, *Appl. Catal., A* **2008**, *338*, 14.

[130] M. Dabiri, P. Salehi, M. Bahramnejad, *Synth. Commun.* **2010**, *40*, 3214.

[131] O. Basle, N. Borduas, P. Dubois, J. M. Chapuzet, T.-H. Chan, J. Lessard, C.-J. Li, *Chem. Eur. J.* **2010**, *16*, 8162.

[132] C.-X. Miao, J.-Q. Wang, B. Yu, W.-G. Cheng, J. Sun, S. Chanfreau, L.-N. He, S.-J. Zhang, *Chem. Commun.* **2011**, *47*, 2697.

[133] S. M. Payne, F. M. Kerton, *Green Chem.* **2010**, *12*, 1648.

[134] R. P. Swatloski, J. D. Holbrey, R. D. Rogers, *Green Chem.* **2003**, *5*, 361.

[135] J. L. Anthony, J. L. Anderson, E. J. Maginn, J. F. Brennecke, *J. Phys. Chem. B* **2005**, *109*, 6366.

[136] L. Ferguson, P. Scovazzo, *Ind. Eng. Chem. Res.* **2007**, *46*, 1369.

[137] J. Kumelan, l. Pérez-Salado Kamps, D. Tuma, G. Maurer, *J. Chem. Eng. Data* **2009**, *54*, 966.

[138] Z. Du, J. Ma, F. Wang, J. Liu, J. Xu, *Green Chem.* **2011**, *13*, 554.

[139] P. Verdeguer, N. Merat, A. Gaset, *J. Mol. Cat.* **1993**, *85*, 327.

[140] A. Gandini, M. N. Beglacem, *Prog. Polym. Sci.* **1997**, *22*, 1203.

[141] A. Gandini, *Green Chem.* **2011**, *13*, 1061.

[142] K.T. Hopkins, W. D. Wilson, B. C. Bender, D. R. McCurdy, J. E. Hall, R. R. Tidwell, A. Kumar, M. Bajic, D. W. Boykin, *J. Med. Chem.* **1998**, *41*, 3872.

[143] J. Ma, Z. Du, J. Xu, Q. Chu, Y. Pang, *ChemSusChem* **2011**, *4*, 51.

[144] X. Tong, Y. Ma, Y. Li, *Appl. Catal., A* **2010,** *385*, 1.

[145] H. J. Yoon, J. W. Choi, H. S. Jang, J. K. Cho, J. W. Byun, W. J. Chung, S. M. Lee, Y. S. Lee, *Synlett* **2011**, 165.

[146] G. A. Halliday, R. J. Young Jr., V. V. Grushin, *Org. Lett.* **2003**, *5*, 2003.

[147] C. Carlini, P. Patrono, A. M. R. Galetti, G. Sbrana, V. Zima, *Appl. Catal., A* **2005**, *289*, 197.

[148] O. C. Navarro, A. C. Canós, S. I. Chornet, *Top. Catal.* **2009**, *52*, 304.

[149] X. Xiang, L. He, Y. Yang, B. Guo, D. Tong, C. Hu, *Catal. Lett.* **2011**, *141*, 735.

[150] F. K. Kazi, A. D. Patel, J. C. Serrano-Ruiz, J. A. Dumesic, R. P. Annex, *Chem. Eng. J.* **2011**, *169*, 329.

[151] M. Lakshmi Kantam, S. Reddy, B. Sreedhar, C. Venkat Reddy, F. Figueras, "A Novel Efficient Ru Catalyst for Oxidation of Alcohols by Molecular Oxygen", in *Proceedings from the 6th World Congress on Oxidation Catalysis*, **2009**.

[152] A. Desmartin-Chomel, B. Hamad, J. Palomeque, N. Essayem, G. Bergeret, F. Figueras, *Catal. Today* **2010**, *152*, 110.

[153] K. Fischer, M. Wilken, *J. Chem. Thermodyn.* **2001**, *33*, 1285.

[154] S. S. S. R. Putluru, A. Riisager, R. Fehrmann, *Appl. Catal., B* **2010**, *97*, 333.

[155] C. Moreau, R. Durand, C. Pocheron, D. Tichit, *Stud. Surf. Sci. Catal.* **1997**, *108*, 399.

[156] K. Shimizu, R. Uozumi, A. Satsuma, *Catal. Commun.* **2009**, *10*, 1849.

[157] M. S. Holm, K. Egeblad, P. N. R. Vennestrøm, C. G. Hartmann, M. Kustova, C. H. Christensen, *Eur. J. Inorg. Chem.* **2008**, 5185.

[158] A. Corma, *Chem. Rev.* **1997**, *97*, 2373.

[159] D. Mravec, J. Hudec, I. Janotka, *Chem. Pap.* **2005**, *59*, 62.

[160] D. Coster, A. L. Blumenfeld, J. J. Fripiat, *J. Phys. Chem.* **1994**, *98*, 6201.

[161] B. M. Weckhuysen, D. E. Keller, *Catal. Today* **2003**, *78*, 25.

[162] *Solvents Polarity Indexes*, Burdick & Jackson; available online at: http://macro.lsu.edu/howto/solvents/Polarity%20index.htm.

[163] C. P. Vinod, K. Wilson, A. F. Lee, *J. Chem. Technol. Biotechnol.* **2011**, *86*, 161.

[164] J. Rass-Hansen, H. Falsig, B. Jørgensen, C. H. Christensen, *J. Chem. Technol. Biotechnol.* **2007**, *82*, 329.

[165] J.-E. Bäckvall, *Modern Oxidation Methods*, Wiley-VCH, **2004**, ISBN: 3-527-30642-0.

[166] K. Weissermel, H.-J. Arpe, *Industrial Organic Chemistry (4th edn.)*, Wiley-VCH, **2003**, ISBN: 3-527-30578-5.

[167] H. Ebner, H. Follmann, S. Sellmer, "Vinegar", in *Ullmann's Encyclopedia of Industrial Chemistry*, Wiley-VCH, **2002**; DOI: 10.1002/14356007.a27_403.

[168] T. W. Simpson, A. N. Sharpley, R. W. Howarth, H. W. Paerl, K. R. Mankin, *J. Environ. Qual.* **2008**, *37*, 318.

[169] N. Zotova, K. Hellgardt, G. H. Kelsall, A. S. Jessiman, K. K. Hii, *Green Chem.* **2010**, *12*, 2157.

[170] H. Cheung, R. S. Tanke, G. P. Torrence, "Acetic Acid", in *Ullmann's Encyclopedia of Industrial Chemistry*, Wiley-VCH, **2002**; DOI: 10.1002/14356007.a01_045.

[171] C. Thomas, *Coord. Chem. Rev.* **2003**, *243*, 125.

[172] D. L. Kamble, S. T. Nandibewoor, *J. Phys. Org. Chem.* **1998**, *11*, 171.

[173] J. Han, Y. Liu, R. Guo, *Adv. Funct. Mater.* **2009**, *19*, 1112.

[174] H. Rajesh, U. S. Ozkan, *Ind. Eng. Chem. Res.* **1993**, *32*, 1622-1630.

[175] X. Li, E. Iglesia, *Chem. Eur. J.* **2007**, *13*, 9324.

[176] T. Nishimura, N. Kakiuchi, M. Inoue, S. Uemura, *Chem. Commun.* **2000**, 1245.

[177] K. Mori, T. Hara, T. Mizugaki, K. Ebitani, K. Kaneda, *J. Am. Chem. Soc.* **2004**, *126*, 10657.

[178] M. Nagai, R. D. Gonzalez, *Ind. Eng. Chem. Prod. Res. Dev.* **1985**, *24*, 525.

[179] T. Takei, N. Iguchi, M. Haruta, *Catal. Surv. Asia* **2011**, *15*, 80.

[180] A. Kleiman-Shwarsctein, A. B. Laursen, F. Cavalco, W. Tang, S. Dahl, I. Chorkendorff, **2011,** *submitted for publication*.

[181] S. Imamura, I. Fukuda, S. Ishida, *Ind. Eng. Chem. Res.* **1988**, *27*, 718.

[182] H. Liu, E. Iglesia, *J. Phys. Chem. B* **2005**, *109*, 2155.

[183] S. Pavasupree, Y. Suzuki, S. Pivsa-Art, S. Yoshikawa, *J. Solid State Chem.* **2005**, *178*, 128.

[184] G. Magesh, B. Viswanathan, R. P. Viswanath, T. K. Varadarajan, *Indian J. Chem., Sect A* **2009**, *48A*, 480.

[185] G. N. Vayssilov, Y. Lykhach, A. Migani, T. Staudt, G. P. Petrova, N. Tsud, T. Skála, A. Bruix, F. Illas, K. C. Prince, V. Matolin, K. M. Neyman, J. Libuda, *Nat. Mater.* **2011**, *10*, 310.

[186] D. R. Larkin, *J. Org. Chem.* **1990**, *55*, 1563.

[187] H. Yu, K. Zeng, Y. Zhang, F. Peng, H. Wang, J. Yang, *J. Phys. Chem. C* **2008**, *112*, 11875.

[188] P. Haider, B. Kimmerle, F. Krumeich, W. Kleist, J.-D. Grunwaldt, A. Baiker, *Catal. Lett.* **2008**, *125*, 169.

[189] M. Haruta, *Chem. Rec.* **2003**, *3*, 75.

[190] R. D. Monte, J. J. Kašpar, *Mater. Chem.* **2005**, *15*, 633.

[191] M. Sugiura, M. Ozawa, A. Suda, T. Suzuki, T. Kanazawa, *Bull. Chem. Soc. Jpn.* **2005**, *78*, 752.

[192] W. Li, H. Liu, E. Iglesia, *J. Phys. Chem. B* **2006**, *110*, 23337.

[193] M. T. Holtzapple, R. R. Davison, M. K. Ross, S. Aldrett-Lee, M. Nagwani, C.-M. Lee, C. Lee, S. Adelson, W. Kaar, D. Gaskin*, Appl. Biochem. Bitotechnol.* **1999**, *77*, 609.

[194] P. G. Blake, K. G. Hole, *J. Chem. Soc*. *B* **1966**, 577-579.

[195] J. M. Vohs, M. A. Barteau, *Surf. Sci.* **1988**, *201*, 481.

[196] K. S. Kim, M. A. Barteau, *Langmuir* **1988**, *4*, 945.

[197] T. R. Felthouse, *J. Am. Chem. Soc.* **1987**, *109*, 7566.

[198] E. Takezawa, S. Sakaguchi, Y. Ishii, *Org. Lett.* **1999**, *1*, 713.

[199] J. L. Courtney, K. F. Swansbor, *Rev. Pure Appl. Chem.* **1972**, *22*, 47.

[200] V. S. Martín, J. M. Palazón, C. M. Rodríguez, C. R. Nevill Jr., "Ruthenium(VIII) Oxide", in *Encyclopedia of Reagents for Organic Synthesis*, John Wiley & Sons, **2006**; DOI: 10.1002/047084289X.rr009.pub2.

[201] H. H. Horowitz, H. S. Horowitz, J. M. Longo, U.S. Patent 4434031, **1984**.

[202] T. R. Felthouse, P. B. Fraundorf, R.M. Friedman, C. L. Schosser, *J. Catal.* **1991**, *127*, 393.

[203] F. Nikaidou, H. Ushiyama, K. Yamaguchi, K. Yamashita, N. Mizuno, *J. Phys. Chem. C* **2010**, *114*, 10873.

[204] W. Reutemann, H. Kieczka, "Formic Acid", in *Ullmann's Encyclopedia of Industrial Chemistry*, Wiley-VCH, **2002**; DOI: 10.1002/14356007.a12_013.

[205] S. D. Senanayake, D. R. Mullins, *J. Phys. Chem. C* **2008**, *112*, 9744.

CHEMSUSCHEM

DOI: 10.1002/cssc.200900059

Gold-Catalyzed Aerobic Oxidation of 5-Hydroxymethylfurfural in Water at Ambient Temperature

Yury Y. Gorbanev,[a] Søren K. Klitgaard,[a] John M. Woodley,[b] Claus H. Christensen,[c] and Anders Riisager*[a]

The aerobic oxidation of 5-hydroxymethylfurfural, a versatile biomass-derived chemical, is examined in water with a titania-supported gold-nanoparticle catalyst at ambient temperature (30 °C). The selectivity of the reaction towards 2,5-furandicarboxylic acid and the intermediate oxidation product 5-hydroxymethyl-2-furancarboxylic acid is found to depend on the amount of added base and the oxygen pressure, suggesting that the reaction proceeds via initial oxidation of the aldehyde moiety followed by oxidation of the hydroxymethyl group of 5-hydroxymethylfurfural. Under optimized reaction conditions, a 71% yield of 2,5-furandicarboxylic acid is obtained at full 5-hydroxymethylfurfural conversion in the presence of excess base.

Introduction

The focus on technologies that facilitate conversion of biorenewables into transportation fuels and chemicals has increased markedly in recent years.[1,2] Today's economic growth requires industrial processes to be sustainable, thus making biomass a fundamental feedstock for chemical production,[3] and a shift from conventional petrochemical feedstocks towards biomass-based feedstocks is of both environmental and economical importance for the future production of commodity chemicals.[4]

Sugars, in the form of mono- and disaccharides, are readily available from various biomass sources by, for example, enzymatic hydrolysis[5] and form a useful feedstock for the production of versatile chemicals. For example, hexose monosaccharides such as glucose and fructose can be catalytically dehydrated into 5-hydroxymethylfurfural (HMF). HMF is a chemical precursor for the production of 2,5-furandicarboxylic acid (FDA) by oxidation (Scheme 1) using various oxygen sources, process designs, and catalyst types.[6–8] The US Department of Energy biomass program has identified FDA as one of the twelve chemicals obtained from biomass in biorefineries that can be used as chemical building blocks in the future.[9] In particular the presence of two carboxylic groups in FDA makes it a valuable polymer building block and, thus, a possible alternative to presently used terephthalic, isophthalic, and adipic acids produced from fossil-based resources.

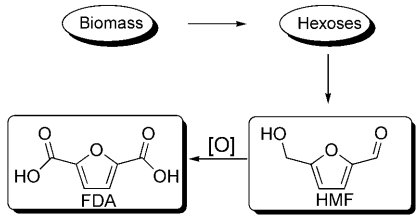

Scheme 1. Biomass-based feedstocks can be converted to versatile molecules such as, for example, 5-hydroxymethylfurfural (HMF), which can be oxidized to the polymer building block 2,5-furandicarboxylic acid (FDA).

In order to comply with the need for the clean production of value-added chemicals such as FDA from HMF, there is a demand for aerobic catalytic systems that use dioxygen as oxidant and produce only water as a byproduct. Heterogeneous metal catalysts are of particular interest in this context because HMF, being both an aromatic aldehyde and an alcohol, may be oxidized using such catalysts, although there are limited reports on this reaction. However, Vinke et al. have demonstrated the oxidation of aqueous HMF to FDA in near-quantitative yield under basic reaction conditions with a Pt/Al_2O_3 catalyst at 60 °C.[10]

Instead of the fully oxidized product FDA the partially oxidized intermediate 2,5-diformylfuran (DFF) is in fact more frequently obtained. For example, Halliday et al. have reported the oxidation of HMF to DFF with oxygen by using ion-exchange resins and vanadyl phosphate (VPO) catalysts as part of a direct in situ transformation of fructose to DFF (with yields up to 45%) without isolation of the intermediate.[11] Similarly, Carlini et al. have oxidized HMF, both as a starting reagent and after producing it in a one-pot conversion from fructose, to the corresponding dialdehyde in a biphasic water/methyliso-

[a] *Y. Y. Gorbanev, S. K. Klitgaard, Prof. A. Riisager*
Department of Chemistry and
Centre for Catalysis and Sustainable Chemistry
Technical University of Denmark
Building 207, 2800 Kgs. Lyngby (Denmark)
Fax: (+45) 4588-3136
E-mail: ar@kemi.dtu.dk

[b] *Prof. J. M. Woodley*
Department of Chemical and Biochemical Engineering
Technical University of Denmark
Building 229, 2800 Kgs. Lyngby (Denmark)

[c] *C. H. Christensen*
Haldor Topsøe A/S
Nymøllevej 55, 2800 Kgs. Lyngby (Denmark)

butylketone (MIBK) medium as well as in pure organic solvent with metal-doped unsupported/TiO_2-supported VPO catalysts under an oxygen pressure of 1 MPa.[12] For the mixed solvent system the yield remained lower than 10% (3–10% HMF conversion; 60–100% selectivity) whereas better conversion rates and selectivities were obtained in MIBK alone (98% conversion; 50% selectivity) or in other low-polarity organic solvents (e.g., benzene, toluene). Yields of up to 81% (conversion 84%; selectivity 97%) were obtained in the polar solvent dimethylformamide.

The above-described compound DFF is often used as an intermediate for the production of FDA. However, catalytic routes that lead to the formation of FDA without isolating DFF as an intermediate have also been reported.[13] Ribeiro and Schuchardt obtained FDA from fructose in 71% yield via HMF formation (72% conversion from fructose; 99% selectivity) using silica-encapsulated cobalt acetylacetonate as a bifunctional acid-redox catalyst at 160 °C and an air pressure of 2 MPa.[14] Furthermore, Lilga et al. have recently patented an industrially promising method to oxidize HMF to FDA in up to 98% yield (100% conversion; up to 98% selectivity) at 100 °C and 1 MPa oxygen pressure using a Pt/ZrO_2 catalyst.[15]

In addition to the catalyst systems described above, gold has also been found to be an excellent catalyst for the oxidation of both aromatic and aliphatic alcohols to their corresponding acids or esters with oxygen as the oxidant under benign conditions.[16–25] Recently, aerobic oxidation of HMF in methanol with titanium dioxide-supported gold nanoparticles was reported by Taarning et al. to give 2,5-furandimethylcarboxylate in 98% selectivity and 60% isolated yield at 130 °C using an oxygen pressure of 4 bar (1 bar = 10^5 Pa) and added base (sodium methoxide) as the promoter.[23] In contrast, while the promoting effect of base on the aqueous-phase oxidation of glycerol and CO has been described,[17] no report to date has described the base-promoted oxidation of aqueous HMF by gold catalysts.

Accordingly, we have in this work examined the aerobic oxidation of HMF in basic aqueous solution at ambient temperature using a commercial heterogeneous Au/TiO_2 catalyst. More specifically, the influences of the oxidant (dioxygen) pressure and the amount of hydroxide base on the selectivity and yield of the reaction are reported, along with a hypothesis on the oxidation pathway.

Results and Discussion

Initially, the oxidation of HMF was performed with 20 equivalents of sodium hydroxide at 20 bar oxygen pressure (ca. 8 mmol) at 30 °C (Scheme 2a). The oxidation reaction was followed by using HPLC to measure the concentration of the reaction products (with acidic eluent to obtain the FDA).

The measured yields of all observed reaction products are plotted against the reaction time (HMF was fully converted) in Figure 1. HMF initially underwent relatively fast oxidation to 5-hydroxymethyl-2-furancarboxylic acid (HMFCA) before being further oxidized to FDA (Scheme 2b), as also previously found in methanol solution.[23] Thus, no indication supporting a reaction route involving initial oxidation of the HMF alcohol group due to stabilizing electron effects of the furan ring and formyl group, as claimed by Vinke et al.,[10] was found under these reaction conditions.

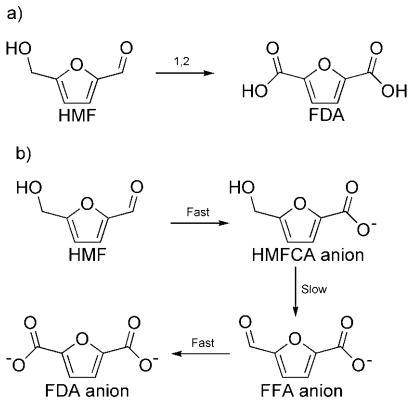

Scheme 2. a) Oxidation of HMF to FDA. 1) Au/TiO_2, OH^-/H_2O, $P(O_2) = 20$ bar, 30 °C; 2) H^+. b) Possible route for the HMF oxidation reaction via initial oxidation of the formyl group.

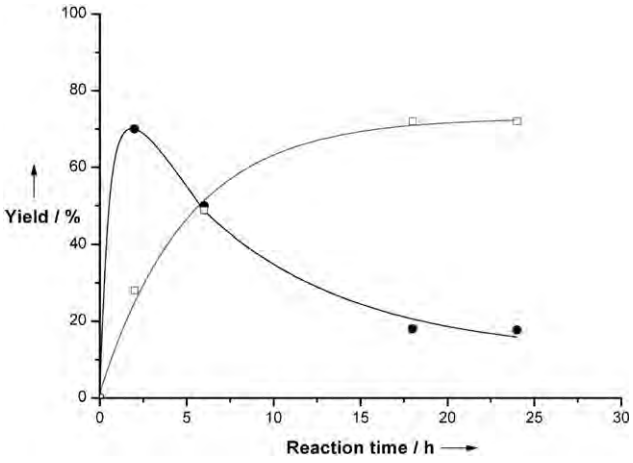

Figure 1. Product formation as a function of reaction time in the oxidation of HMF by dioxygen in aqueous solution using 1 wt% Au/TiO_2 catalyst (20 equiv NaOH, 20 bar O_2, 30 °C; FDA: □, HMFCA: ●). Lines were added to guide the eye.

An 18 h control reaction conducted under an inert nitrogen atmosphere in the absence of dioxygen (but with all other reaction conditions unchanged) also resulted in full HMF conversion, but with product yields of 51% HMFCA, 38% 2,5-dihydroxymethylfuran (DHMF), and 11% levulinic acid (LA). This result suggests that under the generally applied reaction conditions byproducts form partly by the Cannizzaro reaction (disproportionation of HMF into HMFCA and DHMF[15]) and partly by HMF degradation, thereby limiting the available FDA yield. Hence, under optimized conditions a maximum FDA yield of 71% was obtained after 18 h of reaction. Interestingly, HMF degradation apparently resulted in LA formation in the ab-

sence of oxidant while traces of formic acid (FA) were exclusively formed in the presence of dioxygen (vide infra).

HMF was also oxidized in the presence of various amounts of NaOH in the reaction mixture, as shown in Figure 2. The use of aqueous KOH gave identical results.

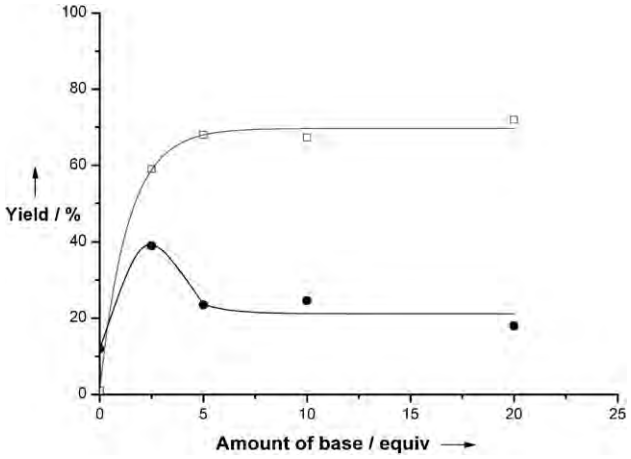

Figure 2. Product formation as a function of the introduced amount of base (NaOH) in the oxidation HMF by dioxygen in aqueous solution using 1 wt% Au/TiO_2 catalyst (20 bar O_2, 30 °C, 18 h; FDA: □, HMFCA: ●). Lines were added to guide the eye.

In reactions with low amounts of added NaOH base (2.5 equiv.) the yield of the intermediate oxidation product (HMFCA) was high relative to FDA, resulting only in a moderate yield of FDA at full HMF conversion. In contrast, the conversion of HMF was only 13% without added base (12% and 1% yields of HMFCA and FDA, respectively), suggesting deactivation of the gold catalyst by the initially formed acids as also previously reported for alcohol oxidation in a methanol solution.[25] Additionally, precipitation of the formed FDA onto the catalyst surface may also have hampered the reaction significantly in the absence of base, where the solubility of FDA is quite low.[15]

The formation of byproducts was largely avoided at all examined base concentrations (for both NaOH and KOH), with only traces of up to 3% FA being observed at the higher base concentrations examined along with FDA and HMFCA yields of about 70% and 25%, respectively. Unexpectedly, LA was not observed, in contrast to what is usually found when HMF is degraded by rehydration in aqueous acidic medium.[2,6] Moreover, no conversion was observed under the applied reaction conditions when LA was introduced as a substrate in place of HMF. This suggests that the trace of FA generated from HMF degradation was formed by a route that does not involve LA formation. A possible route could involve peroxides generated in situ from oxygen, which have also been found to induce byproduct formation by C–C bond cleavage in the gold-catalyzed aerobic oxidation of aqueous glycerol.[16,17] This would also explain why FA was not formed in the absence of dioxygen (vide supra).

In addition to the reactions described at 20 bar oxygen pressure (vide supra), reactions with added NaOH were also examined at both lower and higher oxygen pressures (10 and 30 bar, respectively; Figure 3).

As shown in Figure 3, an initial increase in the oxygen pressure from 10 to 20 bar (or 30 bar) markedly increased the formation of FDA relative to HMFCA (from 43% to 71%), whereas

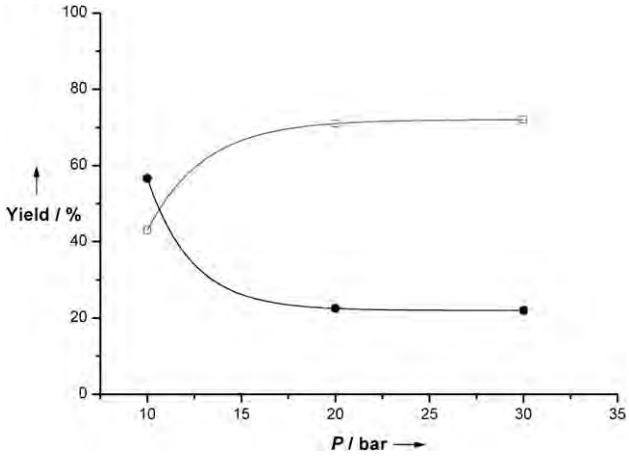

Figure 3. Product formation in as a function of the oxidant pressure in the aerobic oxidation of HMF in aqueous solution using 1 wt% Au/TiO_2 catalyst (20 equiv NaOH, 30 °C, 18 h; FDA: □, HMFCA: ●). Lines were added to guide the eye.

full HMF conversion was achieved at all pressures. This indicates that an insufficient amount of oxygen was dissolved to facilitate the full reaction at 10 bar. Furthermore, it confirms that the aldehyde moiety of HMF is more easily oxidized than the hydroxymethyl group (thereby leading to initial formation of HMFCA), in accordance with previous findings for analogous oxidations performed in methanol.[24] As no intermediate DFF product was observed during the reaction, it further implies that the final aldehyde oxidation step from DFF to FDA is faster than the initial aldehyde oxidation, as shown in Scheme 2b.

Upon reuse (after filtration and drying) the catalyst used in the reaction at 20 bar with 20 equiv. of added base yielded a lower activity towards the oxidation, resulting in a 5–10% lower HMFCA conversion at comparable reaction times. Analysis of the post-reaction mixture by inductively coupled plasma (ICP) spectrometry confirmed that this correlated well with gold leaching (corresponding to <4% of the original metal inventory).

Conclusions

In the present work the oxidation of aqueous HMF to FDA by a heterogeneous supported gold catalyst and oxygen has been investigated. Under optimized basic reaction conditions, a 1 wt% Au/TiO_2 catalyst was found to oxidize HMF into FDA in 71% yield at 30 °C in 18 h with 20 bar oxygen. Lower pressures or low concentrations of base (i.e., corresponding to less than five equivalents) afforded relatively more of the intermediate oxidation product HMFCA compared to FDA. Ob-

served traces of FA were proposed to originate, in part, from peroxide degradation of the initially formed LA produced by HMF rehydration, while base prevented deactivation of the gold catalyst and possibly also stabilized the FDA product in its anionic form.

The reaction procedure introduced in this work involves HMF oxidation at ambient temperature using an abundant and environmentally friendly oxidant and solvent. When combined, these features make the protocol an interesting alternative to oxidation reactions based on stoichiometric amounts of heavy metal oxidants (e.g., chromium and manganese oxygenates) that have traditionally been applied to the oxidation of substrates with similar functionalities.[26] Further development of the catalyst system to circumvent the significant metal leaching and thus improve catalyst durability is in progress.

Experimental Section

Materials: 5-hydroxymethylfurfural (>99%), levulinic acid (98%), formic acid (98%), sodium hydroxide (>98%), and potassium hydroxide (>98%) were acquired from Sigma–Aldrich. 2,5-furandicarboxylic acid (>99%) and 5-hydroxymethyl-2-furancarboxylic acid (>99%) were purchased from Toronto Research Chemicals Inc. and dioxygen (99,5%) was obtained from Air Liquide Denmark. All chemicals were used as received. For the oxidation reactions a commercial 1 wt% Au/TiO_2 catalyst was used (Mintek, Brunauer–Emmett–Teller (BET) surface area 49 $m^2 g^{-1}$), which by high-resolution transmission electron microscopy analysis (JEM 2000FX microscope, 300 kV; sample mounted on a 300 mesh copper grid coated with holey carbon film) was found to contain gold particles with an average size of 4–8 nm.

Oxidation reactions: Oxidations were carried out in a stirred Parr minireactor autoclave equipped with internal thermocontrol (T316 steel, Teflon beaker insert, 25 mL). In each reaction the autoclave was charged with 126 mg of HMF (1 mmol) and a solution of alkali hydroxide (0.1–0.8 g, 2.5–20 mmol) in 10 mL water. Subsequently, 1 wt% Au/TiO_2 catalyst was added (0.197 g, 0.01 mmol Au) and the autoclave was flushed and then pressurized with dioxygen (10–30 bar, ca. 4–12 mmol) and maintained at 30 °C for a given period under stirring (800 rpm). After the reaction, the autoclave was cooled to room temperature (i.e., 20 °C) and after filtering off the catalyst a sample was taken out for HPLC analysis (Agilent Technologies 1200 series, Aminex HPX-87H column from Bio-Rad, 300 mm × 7.8 mm × 9 μm, flow 0.6 mL min^{-1}, solvent 5 mM H_2SO_4, temperature 60 °C). Reference samples were used to quantify the products. Reported results are averaged data (<7% absolute error) obtained from 2–3 separate reactions with an apparent carbon mass balance of >90% (no CO_2 product observed by TCD GC analysis). ICP analysis (Perkin–Elmer ELAN 6000 with cross-flow nebulizer and argon plasma) was performed on the diluted post-reaction mixture and quantified with an ICP standard solution (1.000 g L^{-1}, Fluka).

Acknowledgements

The authors thank Prof. J. E. T. Andersen (Department of Chemistry, Technical University of Denmark) for ICP measurements. This work was supported by The Danish National Advanced Technology Foundation and Novozymes A/S.

Keywords: biomass · gold · oxygen · supported catalysts · titania

[1] P. Gallezot, *Green Chem.* **2007**, *9*, 295–302.
[2] A. Corma, S. Iborra, A. Velty, *Chem. Rev.* **2007**, *107*, 2411–2502.
[3] B. Kamm, M. Kamm, *Adv. Biochem. Eng./Biotechnol.* **2007**, *105*, 175–204.
[4] C. H. Christensen, J. Rass-Hansen, C. C. Marsden, E. Taarning, K. Egeblad, *ChemSusChem* **2008**, *1*, 283–289.
[5] T. Schäfer, T. W. Borchert, V. S. Nielsen, P. Skagerlind, K. Gibson, K. Wenger, F. Hatzack, L. B. Nilsson, S. Salmon, S. Pedersen, H. P. Heldt-Hansen, P. B. Poulsen, H. Lund, K. M. Oxenbøll, G. F. Wu, H. H. Pedersen, H. Xu, *Adv. Biochem. Eng./Biotechnol.* **2007**, *105*, 59–131.
[6] J. Lewkowski, ARKIVOC **2001**, *I*, 17–54.
[7] E. Taarning, C. H. Christensen, *Chim. Oggi* **2007**, *25*, 70–73.
[8] C. Moreau, M. N. Belgacemb, A. Gandinib, *Top. Catal.* **2004**, *27*, 11–30.
[9] T. Werpy, G. Petersen, *Top Value Added Chemicals from Biomass Vol.1* **2004**, 26–28; available at: http://www.osti.gov/bridge (accessed May 2009).
[10] P. Vinke, W. van der Poel, H. van Bekkum, *Stud. Surf. Sci. Catal.* **1991**, *59*, 385–394.
[11] G. A. Halliday, R. J. Young, Jr., V. V. Grushin, *Org. Lett.* **2003**, *5*, 2003–2005.
[12] C. Carlini, P. Patrono, A. M. R. Galletti, G. Sbrana, V. Zima, *Appl. Catal. A* **2005**, *289*, 197–204.
[13] W. Partenheimer, V. V. Grushin, *Adv. Synth. Catal.* **2001**, *343*, 102–111.
[14] M. L. Ribeiro, U. Schuchardt, *Catal. Commun.* **2003**, *4*, 83–86.
[15] M. A. Lilga, R. T. Hallen, J. Hu, J. F. White, M. J. Gray, US Patent 20080103318, **2008**.
[16] W. C. Ketchie, M. Murayama, R. J. Davis, *J. Catal.* **2007**, *250*, 264–273.
[17] W. C. Ketchie, M. Murayama, R. J. Davis, *Top. Catal.* **2007**, *44*, 307–317.
[18] W. C. Ketchie, Y.-L. Fang, M. S. Wong, M. Murayama, R. J. Davis, *J. Catal.* **2007**, *250*, 94–101.
[19] C. H. Christensen, B. Jørgensen, J. Rass-Hansen, K. Egeblad, R. Madsen, S. K. Klitgaard, S. M. Hansen, M. R. Hansen, H. C. Andersen, A. Riisager, *Angew. Chem.* **2006**, *118*, 4764–4767; *Angew. Chem. Int. Ed.* **2006**, *45*, 4648–4651.
[20] S. K. Klitgaard, K. Egeblad, U. V. Mentzel, A. G. Popov, T. Jensen, E. Taarning, I. S. Nielsen, C. H. Christensen, *Green Chem.* **2008**, *10*, 419–423.
[21] C. Marsden, E. Taarning, D. Hansen, L. Johansen, S. K. Klitgaard, K. Egeblad, C. H. Christensen, *Green Chem.* **2008**, *10*, 168–170.
[22] E. Taarning, A. T. Madsen, J. M. Marchetti, K. Egeblad, C. H. Christensen, *Green Chem.* **2008**, *10*, 408–414.
[23] E. Taarning, I. S. Nielsen, K. Egeblad, R. Madsen, C. H. Christensen, *ChemSusChem* **2008**, *1*, 75–78.
[24] B. Jørgensen, S. E. Christiansen, M. L. D. Thomsen, C. H. Christensen, *J. Catal.* **2007**, *251*, 332–337.
[25] S. K. Klitggard, A. T. DeLa Riva, S. Helveg, R. M. Werchmeister, C. H. Christensen, *Catal. Lett.* **2008**, *126*, 213–217.
[26] T. J. Donohoe, *Oxidation and Reduction in Organic Synthesis*, Oxford University Press, Oxford, **1994**.

Received: February 22, 2009

Contents lists available at ScienceDirect

Chemical Engineering Research and Design

journal homepage: www.elsevier.com/locate/cherd

Process integration for the conversion of glucose to 2,5-furandicarboxylic acid

A. Boisen[a], T.B. Christensen[a], W. Fu[b], Y.Y. Gorbanev[c], T.S. Hansen[c], J.S. Jensen[b], S.K. Klitgaard[c], S. Pedersen[a], A. Riisager[c], T. Ståhlberg[c], J.M. Woodley[b,*]

[a] Novozymes A/S, 2880 Bagsværd, Denmark

[b] Center for BioProcess Engineering, Department of Chemical and Biochemical Engineering, Technical University of Denmark, 2800 Lyngby, Denmark

[c] Center for Sustainable and Green Chemistry, Department of Chemistry, Technical University of Denmark, 2800 Lyngby, Denmark

ABSTRACT

The development of biorefineries means that a key feedstock for many new processes will be sugars in various forms, such as glucose or fructose. From these feedstocks a range of chemicals can be synthesized using heterogeneous catalysis, immobilized enzymes, homogeneous catalysts, soluble enzymes, fermentations or combinations thereof. This presents a particularly interesting process integration challenge since the optimal conditions for each conversion step will be considerably different from each other. Furthermore, compared to oil-based refineries the feedstock represents a relatively high proportion of the final product value and therefore yield and selectivity in these steps are of crucial importance. In this paper using the conversion of glucose to 2,5-furandicarboxylic acid and associated products as an example, alternative routes will be compared with respect to achievable selectivity, and achievable yield.

Keywords: Biorefineries; Glucose isomerase; 5-Hydroxymethylfurfural; 2,5-Furandicarboxylic acid

1. Introduction

While the increasing cost of oil is driving particular interest in the production of new fuels from biomass there is little doubt that today of equal importance is the production of chemicals from biomass. Indeed for the supply of fuels in the future there are many potential sources aside from biomass. In a world with limited (or very expensive) oil it is less clear where the chemicals of the future will originate. There is currently an existing infrastructure based on the use of the seven established platform chemicals (toluene; benzene; xylene; 1,3-butadiene; propylene; ethene; methane). In the short term one could consider if we can use the same infrastructure and just create the seven chemicals from alternative sources. However in the longer term it will be necessary to devise new processes based on a different set of platform chemicals. One group will be based around glucose (the hydrolytic product of starch and therefore readily available from biomass). In a biorefinery it will be necessary to develop a structure which can manage a range of feedstocks, a range of technologies and a range of products. This presents a considerable challenge for design and optimization as well as process integration. In order to illustrate the complexity and the challenge that lies ahead we have studied one specific example with a defined starting and endpoint: the production of 5-hydroxymethylfurfural (HMF) or 2,5-furandicarboxylic acid (FDA) from glucose or fructose. Greatest value is obtained by going the whole way from glucose to FDA. However even in this small reaction pathway there are many alternative technologies. Some can be integrated together, some give the required yield and selectivity, some are difficult to implement and others are untested at scale. This illustrates very well the challenge that design engineers face. To date glucose finds its major use in food applications (as a feedstock for sorbitol and high fructose corn syrup). The possibility of non-food products like HMF or FDA implies the use of other technologies not governed by the strict

* Corresponding author.
E-mail address: jw@kt.dtu.dk (J.M. Woodley).
Received 7 October 2008; Received in revised form 28 May 2009; Accepted 14 June 2009
0263-8762/$ – see front matter
doi:10.1016/j.cherd.2009.06.010

food regulations. Nevertheless all the potential technologies (whether approved for food or non-food production) need to be able to overcome the pH and temperature instability and limited solubility in organic solvents. It is because of the nature of glucose therefore that one obvious starting point is to use enzymatic catalysis (water based and under mild conditions). In this paper we will review the alternative technologies and routes from glucose to FDA, and discuss some of the limitations and challenges.

2. Biomass as a raw material for biorefineries

Nature is producing vast amounts of biomass driven by sunlight via photosynthesis:

$$nCO_2 + nH_2O \rightarrow (CH_2O)_n + nO_2$$

However, utilization of biomass for producing chemicals and fuels is still in its infancy with only 3.5% being used for food or non-food purposes. Plant biomass consists mainly of carbohydrates, lignin, protein and fats. Out of an estimated 170 billion metric tons of biomass produced every year roughly 75% are in the form of carbohydrates which makes biomass carbohydrates the most abundant renewable resource (Röper, 2002). Together with their amenability towards enzymatic processes this makes carbohydrates the center of attention when looking for new and greener feedstocks to replace petroleum for producing commodity chemicals as well as fuels. In plant biomass most of the carbohydrates are stored as sugar polymers such as starch, cellulose or hemicellulose.

Starch is the second largest biomass produced on earth and commonly found in vegetables, such as corn, wheat, rice, potatoes and beans. The total world production in 2004 was 60 million tons of which more than 70% came from corn. Starch consists of chains of glucose molecules, which are linked together by α-1,4 and α-1,6 glycosidic bonds. The two major parts of starch are amylose (20–30%), essentially linear α-1,4 glucan chains and amylopectin (70–80%), a branched molecule containing 4–5% α-1,6 linkages.

Starch is industrially hydrolyzed to glucose by the three enzymes: α-amylase, glucoamylase, and pullulanase (Schäfer et al., 2007). Bacterial α-amylases (EC 3.2.1.1) catalyze the hydrolysis of internal α-1,4 glycosidic bonds. This reduces the viscosity, which is necessary for further processing. Glucoamylase (EC 3.2.1.3) is an exo-amylase that is added to the partly hydrolyzed starch after liquefaction. Glucose units are removed in a stepwise manner from the non-reducing end of the molecule. The third enzyme is pullulanase (EC 3.2.1.41). Industrially used pullulanases are heat stable enzymes, which act simultaneously with glucoamaylase during saccharification. Pullulanases catalyze the hydrolysis of the α-1,6 linkages in amylopectin, and especially in partially hydrolysed amylopectin. Typical process conditions for production of glucose from starch are given in Table 1.

Cellulose is a glucose polymer consisting of linear chains of glucopyranose units linked together via β-1,4 glucosidic bonds. Unlike starch, cellulose is a crystalline material where inter- and intra-molecular hydrogen bonding gives rise to the very stable cellulose fiber. Hemicellulose is a polysaccharide consisting of short highly branched chains of different carbohydrate units, including five- as well as six-carbon units (e.g. xyloses, galactose, glucose, mannose and arabinose). Hemicelluloses are much easier to hydrolyze than cellulose. The structured portion of biomass, such as straw, corn stover, grasses and wood, is made of lignocellulose composed mainly of cellulose (30–60%), hemicellulose (20–40%) and lignin (10–30%). Both cellulose and hemicellulose consist of carbohydrate components whereas lignin is a highly branched aromatic polymer.

Currently, there is intensive research on the use of lignocellulosic raw material as a biomass source for producing chemicals and fuels (as exemplified by many of the other articles in this special edition). However this research still faces considerable challenges due to lignocellulose being remarkably resistant towards hydrolysis and enzymatic attack (Peters, 2007). Energy demanding thermal pre-treatment of lignocellulose is necessary in order to break up the extremely stable cellulose–hemicellulose–lignin composites prior to adding cellulose-hydrolyzing enzymes and the current situation does not allow the efficient use of lignocellulosic materials. Nevertheless, there is little doubt given the great abundance of lignocellulose that in the future this will become an attractive option. It is therefore important to continue to develop processes that can economically convert lignocellulose into chemicals. Moreover, glucose is one of the most abundant monosaccharides in biomass, accessible by enzymatic or chemical hydrolysis from starch, sugar or cellulose. Furthermore, a range of chemical products can be obtained from glucose which gives it a key position as a basic raw material/building block.

3. Glucose – a biorefinery building block

Fermentation of polymer building blocks is already under commercial introduction. For example, Cargill produces lactic acid by fermentation and products based on polylactic acid are being introduced to the market. Several companies focus on succinic acid as a polymer building block, but also as a potential raw material for chemicals (e.g. butanediol). 1,3-propandiol is marketed by DuPont Tate & Lyle BioProducts for Sorona™ polytrimethylene terephthalate (PTT) polyester. Likewise Cargill is working on developing 3-hydroxypropionic acid (3-HP). 3-HP is a potential raw material for existing chemicals such as propanediol and acrylic acid. Polyhydroxyalkanoate (PHA) is marketed by Telles, a J/V between ADM and Metabolix. Roquette, the French starch producer, has commercialized isosorbide, a derivative of sorbitol. Isosorbide is used as a co-monomer for high temperature polyethylene terephthalate. However, even if commercialization of polymer building blocks made by fermentation is commercially underway, the technology has certain drawbacks such as loss of carbon as CO_2, low yields and difficult recovery of the products

Table 1 – Process conditions for production of glucose from starch.

Process	Temperature (°C)	Dry substance content (%)	pH	Process time (h)
Jet cooking/dextrinization	105/95	30–35	5.2–5.6	0.1/1–2
Saccharification	60	30–35	4.3–4.5	25–50

from the fermentation broth. The technology presented here (combined chemical and enzymatic catalysis from glucose) has the potential to overcome these problems and represents a promising next generation technology.

One chemical transformation (besides fermentations) of carbohydrate monomers for the degradation of functionality is the dehydration reaction. This facilitates the removal of some of the functional groups in carbohydrates and allows the formation of defined building blocks. Triple dehydration of glucose yields HMF—a building block molecule that subsequently can be transformed into a multitude of bio-based chemicals. By a subsequent hydration reaction or an oxidation, HMF can be converted into levulininc acid or FDA, respectively. Both of these molecules are on the list of the 12 bio-based platform chemicals identified as being of highest potential to be converted into new families of useful molecules (Werpy and Petersen, 2004). In the following we will focus on the dehydration of glucose to HMF as an example of the need to efficiently combine enzymatic aqueous processes with inorganic heterogeneous catalytic processes that have so far mainly been developed for running reactions within the petrochemical industry.

HMF is in itself a rather unstable molecule. It can be found in natural products such as honey and a variety of heat processed food products formed in the thermal decomposition of carbohydrates. Interestingly, HMF can be chemically converted into a range of other valuable chemicals. The oxidation of HMF is of particular interest. Here, the ultimate objective is to obtain FDA as suggested by Schiwek et al. (1991). The diacid can be used as a replacement for terephthalic acid in the production of polyethylene terephthalate and polybutylene terephthalate (Gandini and Belgacem, 1997; Kunz, 1993) which was recently reviewed by Moreau et al. (2004). The partially oxidized compounds can also be used as polymer building blocks although these are more difficult to produce selectively. FDA is a chemically very stable compound. Its only current uses are in small amounts in fire foams and in medicine where it can be used to remove kidney stones.

Several extensive reviews describing the chemistry of HMF and its derivatives have been reported (see Fig. 1). The most recent review focuses on chemical transformation of biomass to a variety of chemicals with particular emphasis on the dehydration of monosaccharides giving either furfural (from pentoses) or HMF from hexoses, respectively (Corma et al., 2007). Moreau et al. (2004) described the recent catalytic advances in substituted furans from biomass and focused especially on the ensuing polymers and their properties. A review by Lewkowski (2001) on the chemistry of HMF and its derivatives also appeared recently. Two other relevant reviews are from Cottier and Descotes (1991) and Kuster (1990).

The mechanism for the dehydration of fructose to HMF has been interpreted to proceed via two different routes; either via acyclic compounds or cyclic compounds (Haworth and Jones, 1944; Kuster, 1990; Van Dam et al., 1986; Antal et al., 1990). Besides HMF, the acid-catalyzed dehydration can lead to several other by-products such as insoluble polymers, called humins or humic acids. In an industrial process it is very important to find the right process conditions that avoid the formation of humins as these, besides lowering the selectivity of the reaction, potentially can clog up your reactor or deactivate the heterogeneous catalysts.

In spite of all the research carried out within this area an efficient way of producing HMF or its corresponding dicarboxylic acid, FDA, still remains to be found. Traditionally, chemists have been struggling with finding an inexpensive way of producing pure HMF. Given the immense field of its application, it is interesting that relatively few of the listed reviews have described the challenges that might be faced in

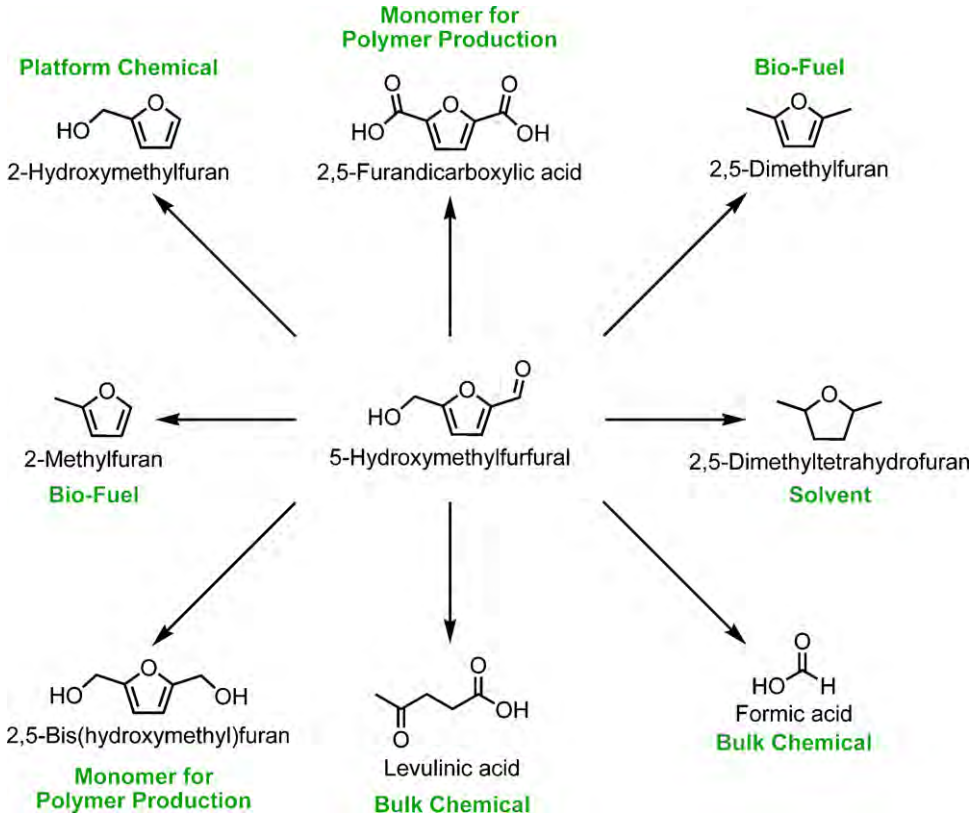

Fig. 1 – HMF as a precursor for a range of commercial chemicals.

Table 2 – Typical reaction conditions for immobilized glucose isomerase.

Process	Temperature (°C)	Dry substance content (%)	pH	Process time (h)
Isomerization	50–60	40–50	7–8	0.3–3

a biorefinery manufacturing HMF or its derivatives. The most likely biorefinery scenario will not be restricted to one product but make a series of high and low value products (including fuel). This allows the biorefinery to shift focus from one product to another if the market changes. In the case of HMF or FDA production this means that producing purely HMF or FDA is not the ultimate target and side-streams producing other valuable products besides HMF or FDA can actually be of benefit. One potential by-product of value is levulinic acid. This is formed via a rehydration of HMF to give levulininc acid along with formic acid. Both of these molecules are valuable products that are potentially worth isolating as side streams. In this respect the goal of completely selective dehydration may in the future be misplaced.

The synthesis of HMF is based on the acid-catalyzed triple dehydration of C6-sugar monomers, mainly glucose and fructose. However, various polysaccharides have also been reported as HMF sources (Rapp, 1987). The most convenient method for the preparation of HMF is by dehydration of fructose. When starting from ketohexoses (such as fructose) the dehydration reaction proceeds more efficiently and selectively. This can be explained by aldohexoses (such as glucose) only being able to enolyze to a low degree which is considered the limiting step in the production of HMF from glucose. However, glucose is the favored source of HMF due to the lower cost of glucose compared to fructose. Fructose may be obtained by enzyme or acid-catalyzed hydrolysis of sucrose and inulin or by the isomerization of glucose to fructose. Inulin is a linear β-2,1 linked fructose polymer which is terminated by a single glucose unit. It is found as a food reserve in a number of plants including Jerusalem artichoke and chicory. Industrially fructose is produced from glucose by the enzyme glucose isomerase (EC 5.3.1.5). The equilibrium conversion under industrial conditions is 50% making chromatographic separation necessary in order to obtain the industrial product of 55% fructose, which has sweetness similar to sucrose. Glucose isomerase is used industrially as an immobilized enzyme with typical reaction conditions as shown in Table 2.

Commercial immobilized glucose isomerase preparations used in a packed column have half-lives between 100 and 200 days. Most columns therefore last for more than 1 year and productivities are typically around 15 tons of syrup dry substance/kg immobilized enzyme.

4. Case studies

4.1. *Case 1: conversion of glucose/fructose to HMF*

To date most of the work regarding the acid-catalyzed conversion of fructose, and to a less extent glucose, into HMF has been carried out in aqueous reaction media. Obviously water being very abundant and non-hazardous is the preferred solvent of choice when exploring green and sustainable chemistry. Furthermore water is a good solvent for dissolving the monosaccharide substrates (fructose and glucose) as well as the product, HMF. However the dehydration of fructose to yield HMF in aqueous media is hampered by a competitive rehydration process resulting in the by-products levulinic acid and formic acid. In addition soluble and insoluble polymerization products (humins), that are thought to arise from the self- and cross-polymerization of HMF, fructose and other by-products seem to be more pronounced in an aqueous reaction medium than an organic one (Van Dam et al., 1986). Nevertheless, several interesting papers have been published on the dehydration of fructose into HMF. The conversion of glucose into HMF is more difficult and as a result there are only a few publications on this process.

4.1.1. *Aqueous media*

Several mineral acids such as HCl, H_2SO_4 and H_3PO_4 have been employed in the homogeneous catalyzed dehydration of fructose to yield HMF (Newth, 1951; Mednick, 1962; Román-Leshkov et al., 2006). So far, however, the yield and selectivity of reactions carried out in aqueous reaction media are not comparable to those observed in aprotic high-boiling organic solvents such as DMSO where the solvent also serves as the catalyst (Musau and Munavu, 1987). Despite high yields and selectivity, the cost of removing high-boiling solvents makes these solvents unsuitable for industrial and large-scale processes. Heterogeneous catalysts have, due to separation and recycling considerations, drawn more attention than homogenous catalysts. The use of various acidic heterogeneous catalysts such as niobic acid ($Nb_2O_5{\cdot}nH_2O$) and niobium phosphate ($NbOPO_4$) have been reported to have an intermediate selectivity of about 30% for the production of HMF at about 80% conversion of fructose (Carniti et al., 2006). Zirconium and titanium phosphates/pyrophosphates have been shown to have a very high selectivity of up to 100% at 100 °C in a period of 18 min for the formation of HMF in water. However as the reaction time increases, the selectivity drops fast which is thought to be due to the formation of polymeric by-products. Additionally, titanium oxides (TiO_2), zirconium oxides (ZrO_2) and H-form zeolites catalyze the dehydration reaction (Moreau et al., 1996). Especially interesting is the direct conversion of glucose to HMF which can be enhanced up to 5-fold compared to the hydrothermal dehydration, by employing an α-TiO_2 at 200 °C (Watanabe et al., 2005a,b). The main disadvantage with these catalysts seems to be the high temperature needed in order for the reaction to proceed without limited selectivity and conversion rates. Highly acidic cation-exchange resins such as those derivatized with sulfonic acid groups are also effective catalysts, providing the acidity of mineral acids together with the advantages of the heterogeneous catalysts (Rigal et al., 1981). These, often polystyrene based resins, can only tolerate temperatures up to around 130 °C, which reduces the range of their application. However this temperature range seems to be sufficient to overcome the activation energy barrier, when simultaneously applying the effect of microwave heating (Qi et al., 2008).

4.1.2. *Modified aqueous media and two-phase systems*

Phase modifiers have within the last couple of years proved very effective in promoting the conversion of fructose to HMF. Polar organic solvents that are miscible with water are added in order to increase the rate of the reaction to HMF and reduce the rate of the rehydration process forming by-products (Van

Dam et al., 1986). Commonly employed aqueous phase modifiers are acetone, DMSO and polyethylene glycol (PEG) (Qi et al., 2008; Chheda et al., 2007; Van Dam et al., 1986). A further modification of the aqueous phase system is the introduction of a second immiscible phase to create a two-phase reaction system. An organic phase extracts the HMF from the aqueous phase as it is produced and consequently reduces the formation of rehydration and polymeric by-products. Even with an initial concentration of fructose as high as 50 wt%, remarkable results with selectivity of 77% and a conversion of 90% at 180 °C with HCl as the catalyst have been reported. In comparison similar conditions in water resulted only in a selectivity of 28% and a conversion of 51% (Román-Leshkov et al., 2006).

4.1.3. *Non-aqueous organic solvents*

Until now, the best results for the dehydration of fructose to HMF have been made in high-boiling organic solvents. The low concentration of water prevents the rehydration of HMF to levulinic acid and formic acid. Iodine catalyzes the dehydration of the fructose part of sucrose in anhydrous DMF at 100 °C. Glucose is unaffected under the same conditions (Bonner et al., 1960). High selectivity has also been obtained when using PEG-600 as a solvent together with catalytic HCl. With the acid present a 1:1 solution of fructose and PEG-600 can be obtained at 85 °C (Kuster and Laurens, 1977). The first really high yields were reported by Nakamura and Morikawa (1980) using a strongly acidic ion-exchange resin as the catalyst in DMSO at 80 °C. These conditions gave a yield of 90% after 8 h. The rate of the reaction was strongly affected by the type of resin used (Nakamura and Morikawa, 1980). Quantitative yields, without the use of a catalyst, were reported soon after in DMSO at 100 °C for 16 h (Brown et al., 1982). Good results were also obtained during an investigation of the optimum fructose concentration in DMSO. With 8.5 molar equivalents of DMSO with respect to fructose, a yield of 92% was obtained at 150 °C without any catalyst after 2 h (Musau and Munavu, 1987).

None of the above examples are suitable for production on a large-scale. High-boiling aprotic solvents such as DMSO, DMF and NMP are all miscible with water as well as many other common organic solvents. This makes separation of the desired products very difficult. Furthermore, both DMF and NMP are considered to be teratogenic.

4.1.4. *Supercritical/subcritical solvents*

Since the best results for the dehydration of hexoses to HMF have been in high-boiling organic solvents, the use of low-boiling solvents in their sub- or supercritical state would be an interesting alternative. Subcritical water has emerged in recent years as a feasible alternative to organic solvents at larger scale. Its unique intrinsic acidic and basic properties, makes it particularly interesting as a reaction medium for the dehydration of carbohydrates. When glucose is dehydrated in pure subcritical water, HMF is formed with greater selectivity than when using sulfuric acid or sodium hydroxide as catalysts under the same pressures and temperatures (Simkovic et al., 1987). Watanabe et al. (2005a) explored the use of different TiO_2 and ZrO_2 catalysts in highly compressed water. The anatase-TiO_2 catalyst showed both basic and acidic properties and catalyzed the conversion of glucose to HMF. Yields were only about 20%, but the selectivity was more than 90%. The basic properties of the catalyst were thought to catalyze the isomerization of glucose to fructose, whereas the acidic properties were thought to catalyze the dehydration (Watanabe et al., 2005b). Yields of up to 50% were obtained when using fructose as the starting sugar and different zirconium phosphates as catalysts in subcritical water. No rehydration products were observed, yet the highest selectivity was not more than 61%. By-products were humins and furaldehyde (Asghari and Yoshida, 2006). Interesting results have recently been reported on the catalytic effect of H_3PO_4, H_2SO_4 and HCl in the direct conversion of glucose to HMF in water at 523 K. It was concluded that the weakest acid, H_3PO_4, was the best catalyst for the conversion of glucose into HMF and the strongest acid, HCl, was the best catalyst for the conversion of HMF to levulinic acid. The best yield for HMF was 40% (Takeuchi et al., 2008). More extensive studies on the kinetics of the dehydration of D-glucose and D-fructose in sub- and supercritical water have been made as well as the behavior of HMF under similar conditions (Kabyemela et al., 1999; Asghari and Yoshida, 2007; Chuntanapum et al., 2008).

Nevertheless, the overall results from sub- and supercritical water have so far been unsatisfactory in terms of yields. Bicker et al. (2003) explored other low-boiling solvents such as acetone, methanol and acetic acid. An acetone/water mixture at 180 °C and 20 MPa gave 99% conversion of fructose and a selectivity of 77% to HMF. This excellent result was explained by the structural similarities between acetone and DMSO, which would promote the furanoid form of fructose and hence favor the formation of HMF. The authors also propose a continuous process for the reaction (Bicker et al., 2003, 2005).

4.1.5. *Ionic liquids*

Another attractive alternative to high-boiling organic solvents is the use of ionic liquids. Their unique physical properties such as negligible vapor pressure and non-flammability make them particularly suitable as solvents for large-scale production. There is a possibility to design and functionalize the ions of the ionic liquid, giving them ability to work both as solvent and reagent for certain reactions. There are several examples of ionic liquids that have the ability to solubilize natural polymers such as cellulose, starch and chitin. This opens an excellent opportunity to convert crude biomass into fine chemicals (Liu et al., 2005; El Seoud et al., 2007).

The first dehydrations of fructose and glucose with the help of ionic liquids date back 25 years. Fructose was dehydrated in the presence of pyridinium chloride to HMF in high purity with 70% yield. The corresponding result for glucose was only 5% (Fayet and Gelas, 1983). In 1-butyl-3-methylimidazolium tetrafluoroborate and 1-butyl-3-methylimidazolium hexafluorophosphate, yields up to 80% from fructose were obtained using DMSO as a co-solvent and Amberlyst-15 resin as the catalyst. The DMSO helped to solubilize the starting fructose and the reaction was faster than in DMSO alone. Performing the reaction in 1-butyl-3-methylimidazolium tetrafluoroborate alone gave a yield of 50% within 3 h (Lansalot-Matras and Moreau, 2003). The best results so far from fructose were made by using the acidic 1-H-3-methylimidazolium chloride as reaction medium. This acted both as solvent and catalyst giving a yield of 92% after 15–45 min at 90 °C. There was no sign of HMF decomposition and glucose remained completely unreacted (Moreau et al., 2006). Recently remarkably good results were found using the ionic liquid 1-ethyl-3-methylimidazolium chloride together with $CrCl_2$, giving a total yield of 70% HMF directly from glucose and virtually no levulinic acid. The authors propose that the actual catalytic specie is the $CrCl_3^-$ ion formed together with the solvent

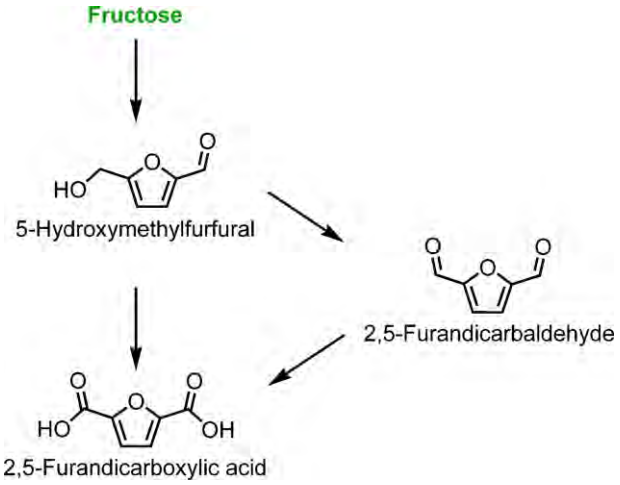

Fig. 2 – Oxidation of HMF to DFF and FDA.

and that it catalyzes the isomerization of β-glucopyranose to fructofuranose, which is subsequently dehydrated to HMF (Zhao et al., 2007). Bao et al. (2008) concluded that ionic liquids with a Lewis acid moiety were more efficient than those with a Brønsted acid counterpart when dehydrating fructose. These ionic liquids were also successfully immobilized on silica, giving a yield of up to 70% from fructose to HMF and completely retained their catalytic activity after five reaction cycles (Bao et al., 2008).

4.2. *Case 2: HMF oxidation to 2,5-diformylfuran and FDA*

FDA has been identified by the U.S. Department of Energy (DOE) biomass program as one of the 12 chemicals that in the future can be used as a feedstock from biomass in biorefineries (Werpy and Petersen, 2004). Due to the presence of the two carboxylic acid groups, FDA is considered to be a biorenewable building block to form polymers from biomass and therefore become an alternative to terephthalic, isophthalic and adipic acids, which are all produced from fossil fuels. Sugars in the form of mono- and disaccharides are easily available from biomass. The hexose type monosaccharides such as glucose and fructose can be catalytically dehydrated into HMF (Corma et al., 2007; Gallezot, 2007; Moreau et al., 2004). HMF can then be oxidized into FDA using a variety of routes and reaction types with stochiometric amount of oxidants. Most of them are described in a review by Lewkowski (2001), including electrochemical oxidation, use of barium and potassium permanganates, nitric acid and chromium trioxide. In this section we will focus on the recently reported catalytic routes for the oxidation of HMF into FDA.

4.2.1. *Oxidation of HMF to DFF*

Though production of FDA from HMF has been of great interest recently, there are few papers on catalytic aerobic oxidation of HMF. In the catalytic route to form FDA the partially oxidized intermediate 2,5-diformylfuran (DFF) is often observed (Fig. 2).

The dialdehyde is a useful product to form other derivatives, and a number of studies have reported on the selective formation of DFF. Thus, Halliday et al. (2003) reported oxidation of HMF to DFF using an in situ reaction protocol where HMF was directly generated from fructose and not isolated. Hence, using ion-exchange resins and, then, VOP-type catalysts the authors obtained DFF with a maximum yield of 45% based on fructose (Halliday et al., 2003). Carlini et al. (2005) reported that HMF, as a starting reagent or produced one pot from fructose, was oxidized to the corresponding dialdehyde in water with methylisobutylketone (MIBK), as well as pure organic solvents, with vanadyl phosphate (VPO) based catalysts (Zr, Nb, Cr, Fe modified) as such or using a TiO_2 support at 75–200 °C and 1 MPa. However, the reported yields were low ($H_2$0:MIBK = 0:30–5:30, HMF conversion 3–10%, selectivity to DFF 100–60%, respectively). Considering the oxidation as a stand-alone reaction and changing the solvents to less polar ones (benzene, toluene) better conversion rates and selectivity were obtained, and using MIBK as a solvent lead to 98% conversion with 50% selectivity. However, in DMF the results are even better (at 150 °C) giving 84% conversion and 97% selectivity.

4.2.2. *Oxidation of HMF to FDA*

The above-described DFF may either be used as a valuable by-product or as an intermediate for obtaining FDA. On the other hand, catalytic reactions leading to the formation of FDA are also reported.

Partenheimer and Grushin (2000) obtained DFF from HMF using metal bromide catalysts (Co/Mn/Zr/Br). The reactions were carried out in acetic acid at atmospheric pressure and also at 70 bar; the yields were 57% and 63% with the conversion of HMF 98% and 92%, respectively. Cobalt as a catalyst was also used by Ribeiro and Schuchardt (2003). Using cobalt acetylacetonate as a bi-functional acidic and redox catalyst encapsulated in silica in an autoclave at 160 °C, they obtained FDA, from fructose via HMF formation, with 99% selectivity to FDA at 72% conversion of fructose. By in situ oxidation of HMF to FDA starting from fructose, Kröger et al. (2000) described a way of producing FDA via acid-catalyzed formation and subsequent oxidation of HMF in a MIBK/water mixture using solid acids for fructose transformation and PtBi-catalyst encapsulated in silicone and swollen in MIBK. The reaction was carried out in a reactor divided with a PTFE-membrane in order to prevent the oxidation of fructose. However, though in principle the integration process has been described, the yields remain quite low. The resulting yield of FDA was 25% based on fructose. In the oxidation of HMF to FDA the use of noble metals was first studied by Vinke et al. (1991). Here, mainly Pd, Pt, Ru supported on different carriers were used as the aerobic oxidation catalysts. Although all the noble metals revealed catalytic activities, only Pt supported on Al_2O_3 remained stable and active and gave quantitative yields of FDA. The reactions were carried out in water at pH 9 using a reaction temperature of 60 °C and a partial oxygen pressure of 0.2.

4.2.3. *Oxidation of HMF to FDA derivatives*

A new approach to the oxidation of HMF has been reported recently by Taarning et al. (2008) using methanol as both solvent and reagent. They performed a reaction with a gold nanoparticle catalyst in an autoclave at 130 °C and 4 bars of dioxygen, and obtaining FDA with 98% yield (according to GC analysis) and 60% isolated yield after sublimation.

5. Process technology

Table 3 indicates some of the key features of possible routes for the conversion of fructose to HMF. A number of observations can be made:

Table 3 – Key features of possible routes for the conversion of fructose to HMF.

Mode of operation[a]	Catalyst[b]	Temp.	Fructose concentration	Solvent media[c]	Highest yield	Reference
B	Hetero.	80 °C	3–4% (w/w)	Water, MIBK	41%	Carlini et al. (2005)
B	Homo.	170 °C	10% (w/w)	Water, DMSO, MIBK, 2-butanol, DCM	87%	Chheda et al. (2007)
B	Homo.	90 °C	3–50% (w/w)	$HMIM^+Cl^-$	92%	Moreau et al. (2006)
B	Hetero.	165 °C	10% (w/w)	Water, MIBK	69%	Moreau et al. (1996)
B	Hetero.	80 °C	6% (w/w)	Water	42%	Carlini et al. (2004)
			3% (w/w)		59%	
B	Homo.	180 °C	30% (w/w)	Water, DMSO, PVP, MIBK, 2-butanol	76%	Román-Leshkov et al. (2006)
			50% (w/w)		71%	
B	Hetero.	90 °C	10% (w/w)	Water, DMSO, PVP, MIBK, 2-butanol	59%	Román-Leshkov et al. (2006)
			30% (w/w)		54%	
B	Hetero.	110 °C	6–10% (w/w)	Water	31%	Carlini et al. (1999)
B		100 °C	6–10% (w/w)	Water, MIBK	74%	
C		85 °C	10–20% (w/w)	Water	26%	
B	Hetero.	100 °C	6% (w/w)	Water	85%	Benvenuti et al. (2000)
C	Hetero.	165 °C	0.5–3.5% (w/w)	Water, MIBK	–	Rivalier et al. (1995)

[a] Process is continuous (C) or batch (B).
[b] Catalyst is homogenous (homo.) or heterogenous (hetero.).
[c] Solent media are: methylisobutylketone (MIBK), dimethyl sulfoxide (DMSO), poly(1-vinyl-2-pyrrolidinone) (PVP), dicholormethane (DCM), and 1-H-3-methyl imidazolium chloride ($HMIM^+Cl^-$).

- Catalyst type
  A variety of catalysts like mineral and organic acids, salts, and solid acid catalysts such as ion-exchange resins and zeolites have been used in the dehydration reaction. The homogeneous acid-catalyzed processes are frequently associated with low selectivity (30–50%) for HMF at a relatively high conversion (50–70%) (Carlini et al., 1999). Moreover, problems related to separation and recycling of the mineral acid as well as of plant corrosion are expected. Thus, recent research has been based on heterogeneous acid catalysts which have considerable potential for industrial application (Carlini et al., 1999).
- Mode of operation
  The dehydration process has mostly been studied in batch operated reactors. Few researchers have examined a continuous process. One exception is the work reported by Kuster and Laurens (1977), who developed a continuous homogeneous catalyzed process for dehydration of fructose to HMF by using a tube reactor with polyethyleneglycol-600 as the solvent. Dehydration of fructose in a continuous stirred tank reactor with phosphoric acid and MIBK as a solvent was also reported by Kuster and van der Steen (1977).
- Media
  The dehydration of hexoses and pentoses has been studied in water, organic solvents, biphasic systems, ionic liquids, and near- and supercritical water. The most convenient solvent for dehydration of fructose to HMF is water. However, water is the reactant in the reverse reaction. Moreover, with the presence of water, HMF decomposes to levulinic acid, formic acid and humins. Organic solvents are thus introduced to improve the dehydration reaction by shifting the equilibrium and suppressing HMF hydrolysis. Relatively high yields were reported for the use of DMSO with ion-exchange catalysts (Nakamura and Morikawa, 1980; Rigal and Gaset, 1985) and quantitative yields of HMF were also reported by heating fructose in the absence of catalyst (Brown et al., 1982; Musau and Munavu, 1987). In spite of the advantages of using DMSO, the difficulties of separation limit its application. Moreover, possible toxic sulfur containing by-products from decomposition of DMSO may cause a risk to health and the environment (Moreau et al., 2004). A biphasic reactor system has been developed to suppress HMF degradation by using organic solvent to separate HMF immediately from the reaction medium as it forms. Consequently some work has been carried out to find the proper extraction solvent. Amongst the solvents reported, MIBK is the most commonly used solvent for extraction of HMF. Due to its relatively low-boiling point, it is relatively easy to separate HMF from MIBK. In general, poor HMF partitioning in the organic solvents leads to the use of large amounts of solvent. Purification of the diluted HMF product thus causes large energy expenditure in the subsequent process (Chheda et al., 2007).

5.1. *New technology*

Román-Leshkov et al. (2006) developed a cost-effective method to produce HMF using a biphasic batch reactor system with phase modifiers. They obtained D-fructose to HMF in high yields (>80%) at high fructose concentrations (10–50 wt%) and delivered the product in a separation-friendly solvent. In the biphasic reactor system, DMSO and/or poly(1-vinyl-2-pyrrolidinone) (PVP) were added as modifiers to suppress the formation of dehydration by-products in the aqueous phase with HCl as the acid catalyst. The product was continuously extracted into an organic phase MIBK modified with 2-butanol to enhance partitioning from the reactive aqueous solution. In this study, they reported an improvement in selectivity from 60 to 75% by adding small amounts of aqueous phase modifiers (such as DMSO and PVP) in the biphasic reactor system. Additionally, by optimizing the partitioning of HMF product into the organic phase, the process not only minimized the degradation of HMF in the aqueous phase, but also achieved efficient product recovery.

Zhao et al. (2007) used a metal chloride catalyst in an ionic liquid for the dehydration of HMF. In this reaction, the only water present in the system was from the dehydration of fructose to HMF reaction, which indicated that the conditions for HMF degradation to levulinic and formic acids were not met. By using this metal chloride in ionic liquid, the reaction could take place at reduced temperature, 80 °C for fructose dehy-

dration, and 100 °C for glucose. 90% yield was achieved from fructose and 70% yield from glucose.

Bicker et al. (2003) reported the use of benign solvents such as acetone, methanol or acetic acid in a sustainable process outline. They reported the dehydration of D-fructose to HMF in sub- and supercritical acetone/water mixtures. The use of this reaction media resulted in higher yields of HMF (77% selectivity, 99% conversion). No solid impurities (humins) were formed. The authors also claimed the potential for a technical process based on this low-boiling point solvent, whereby a price for HMF of about 2 Euro/kg could be achieved if fructose was available at a price of around 0.5 Euro/kg.

However all these new technology approaches for making HMF from fructose have been carried out at a small scale. On a larger scale Rapp has reported yields of ~2.5 kg HMF from aqueous dehydration of fructose (Rapp, 1987). The production of HMF, close to a kg scale, has also been reported using DMSO as the reaction media (M'Bazoa et al., 1990). Nevertheless since high selectivity is crucial for implementing this reaction on an industrial scale, the recent research has been highly focused on alternative routes for improving the selectivity of the dehydration reaction.

5.2. *Process implementation, integration and scale-up*

In order to comply with the demands of efficient and specific conversions of the chemical reactants in a biorefinery with a minimum of economic cost, a special focus on process implementation, integration and scale-up must be paid. The development of combined biological and chemical catalytic reactions without intermediate recovery steps has the potential to become an important future direction for carrying out sustainable organic syntheses (Hailes et al., 2007).

The synthesis of a variety of important chemical building blocks involves multistep reactions often catalyzed by a chemical or biological catalyst. In many cases, the optimal operating conditions are rather different for the individual steps of such synthesis reactions. However, it could prove favorable if such reaction steps are combined or integrated, allowing them to occur concurrently, in proximity to one another, and at or close to their respective optimal operating conditions. Also from an engineering point of view, integration of unit operations could contribute to among other things simpler design, less equipment and less piping (Koolen, 1998). Furthermore, integration could reduce operating time and costs as well as consumption of chemicals and use of energy (Bruggink et al., 2003). An important aspect of process integration is the different working condition for the individual reactions. When the aim is to match different reactions involving enzymes, important factors such as enzyme stabilities, reaction rates, reaction media (e.g. pH, temperature, pressure) and reactor design must be considered. Tools to aid integration of different processes include reactor compartmentalization (Fournier et al., 1996; Byers et al., 1993; de Jong et al., 2008; Chen et al., 1997), medium engineering (Bao et al., 2008; Zhao et al., 2007), ISPR (Freeman et al., 1993; Woodley et al., 2008), optimized reactor designs (Stankiewicz and Moulijn, 2003) and multifunctional catalysts (Bruggink et al., 2003).

The conversion of glucose to FDA involves three steps, each with different optimal physical and chemical parameters like pH, temperature and pressure. Furthermore, the catalysts are of different nature with a bio-catalyst (enzyme) in the isomerization of glucose to fructose and a number of potential chemical catalysts of both heterogeneous and homogeneous nature in the following dehydration and oxidation reactions. While the potential for integration exists, it is only via an economic evaluation that such options can be further considered. A valuable process implementation tool to achieve both qualitative and quantitative understanding of the reaction processes and their potential for improvement is mathematical modeling. A good model should facilitate knowledge and understanding of the chemical reactions and include in a quantitative manner the most important physical and chemical governing parameters. As more is understood about the alternative synthetic routes to FDA, the appropriate modeling tools will also need to be developed.

6. Future outlook

With the implementation of biorefineries and increased interest in biofuel it is clear that the associated sugar-based chemistry will provide a rich variety of chemical products as building blocks for higher value molecules. The extent to which this happens depends on two factors. First the economics of the biorefinery will act as a driver in many cases to provide a means to develop higher value products alongside fuel. Ultimately the value of each product tree will need to be evaluated alongside the associated cost of implementing additional technology. Secondly it is clear that new technology and improved catalytic methods are required to produce high value building blocks such as FDA. Some of the more promising routes lie in new media such as ionic liquids but it is also clear that far higher selectivities are required. In this respect enzyme based catalysis will have a particular and likely expanding role in the future development of biorefinery technology. Finally, the implementation of new technology for biorefineries must be evaluated within the context of green chemistry and the necessary environmental requirements. For example the selection of organic solvents and catalysts must adhere to the criteria for sustainable processing. This is essential in order to ensure that new processes use sustainable processing methods as well as making use of sustainable resources.

Acknowledgements

The authors wish to thank Novozymes A/S, the Technical University of Denmark and the Advanced Technology Programme (Denmark) for financial support. The Center for Sustainable and Green Chemistry is sponsored by The Danish National Research Foundation.

References

Antal, M.J., Mok, W.S.L. and Richards, G.N., 1990, Mechanism of formation of 5-(hydroxymethyl)-2-furaldehyde from D-fructose and sucrose. Carbohydrate Research, 199: 91–109.

Asghari, F.S. and Yoshida, H., 2006, Dehydration of fructose to 5-hydroxymethylfurfural in sub-critical water over heterogeneous zirconium phosphate catalysts. Carbohydrate Research, 341: 2379–2387.

Asghari, F.S. and Yoshida, H., 2007, Kinetics of the decomposition of fructose catalyzed by hydrochloric acid in subcritical water: formation of 5-hydroxymethylfurfural, levulinic, and formic acids. Industrial & Engineering Chemistry Research, 46: 7703–7710.

Bao, Q., Qiao, K., Tomida, D. and Yokoyama, C., 2008, Preparation of 5-hydroxymethylfurfural by dehydration of fructose in the presence of acidic ionic liquid. Catalysis Communications, 9: 1383–1388.

M'Bazoa, C., Raymond, F. Rigal, L., Gaset, A., 1990, Procede de fabrication d'hydroxymethylfurfural (HMF) de purete elevee, FR patent 2669635 A1.

Benvenuti, F., Carlini, C., Patrono, P., Galetti, A.M.R., Sbrana, G., Massucci, M.A. and Galli, P., 2000, Heterogeneous zirconium and titanium catalysts for the selective synthesis of 5-hydroxymethyl-2-furaldehyde from carbohydrates. Applied Catalysis A: General, 193: 147–153.

Bicker, M., Hirth, J. and Vogel, H., 2003, Dehydration of fructose to 5-hydroxymethylfurfural in sub- and supercritical acetone. Green Chemistry, 5: 280–284.

Bicker, M., Kaiser, D., Ott, L. and Vogel, H., 2005, Dehydration of D-fructose to hydroxymethylfurfural in sub- and supercritical fluids. The Journal of Supercritical Fluids, 36: 118–126.

Bonner, T.G., Bourne, E.J. and Ruszkiewicz, M., 1960, The iodine-catalyzed conversion of sucrose into 5-(hydroxymethyl)furfuraldehyde. Journal of the Chemical Society, 787–791.

Brown, D.W., Floyd, A.J., Kinsman, R.G. and Roshan-Ali, Y., 1982, Dehydration reactions of fructose in nonaqueous media. Journal of Chemical Technology and Biotechnology, 2: 920–924.

Bruggink, A., Schoevaart, R. and Kieboom, T., 2003, Concepts of nature in organic synthesis: cascade catalysis and multistep conversions in concert. Organic Process Research & Development, 7(5): 622–640.

Byers, J.P., Shah, M.B., Fournier, R.L. and Varanasi, S., 1993, Generation of a pH gradient in an immobilized enzyme-system. Biotechnology and Bioengineering, 42: 410–420.

Carlini, C., Giuttari, M., Galletti, A.M.R., Sbrana, G., Armaroli, T. and Busca, G., 1999, Selective saccharides dehydration to 5-hydroxymethyl-2-furaldehyde by heterogeneous niobium catalysts. Applied Catalysis A: General, 183: 295–302.

Carlini, C., Patrono, P., Galletti, A.M.R. and Sbrana, G., 2004, Heterogeneous catalysts based on vanadyl phosphate for fructose dehydration to 5-hydroxymethyl-2-furaldehyde. Applied Catalysis A: General, 275: 111–118.

Carlini, C., Patrono, P., Galletti, A.M.R., Sbrana, G. and Zima, V., 2005, Selective oxidation of 5-hydroxymethyl-2-furaldehyde to furan-2,5-dicarboxaldehyde by catalytic systems based on vanadyl phosphate. Applied Catalysis A: General, 289: 197–204.

Carniti, P., Gervasini, A., Biella, S. and Auroux, A., 2006, Niobic acid and niobium phosphate as highly acidic viable catalysts in aqueous medium: fructose dehydration reaction. Catalysis Today, 118: 373–378.

Chen, G.D., Fournier, R.L. and Varanasi, S., 1997, Experimental demonstration of pH control for a sequential two-step enzymatic reaction. Enzyme and Microbial Technology, 21(7): 491–495.

Chheda, J.N., Román-Leshkov, Y. and Dumesic, J.A., 2007, Production of 5-hydroxymethylfurfural and furfural by dehydration of biomass-derived mono- and poly-saccharides. Green Chemistry, 9: 342–350.

Chuntanapum, A., Yong, T.L.-K., Miyake, S. and Matsumura, Y., 2008, Behavior of 5-HMF in subcritical and supercritical water. Industrial & Engineering Chemistry Research, 47: 2956–2962.

Corma, A., Iborra, S. and Velty, A., 2007, Chemical routes for the transformation of biomass into chemicals. Chemical Reviews, 107(6): 2411–2502.

Cottier, L. and Descotes, G., 1991, 5-Hydroxymethylfurfural synthesis and chemical transformations. Trends in Heterocyclic Chemistry, 2: 233–248.

de Jong, J., Verheijden, P.W., Lammertink, R.G.H. and Wessling, M., 2008, Generation of local concentration gradients by gas–liquid contacting. Analytical Chemistry, 80(9): 3190–3197.

El Seoud, O.M., Koschella, A., Fidale, L.C., Dorn, S. and Heinze, T., 2007, Applications of ionic liquids in carbohydrate chemistry: a window of opportunities. Biomass, 9: 2629–2647.

Fayet, C. and Gelas, J., 1983, Nouvelle méthode de préparation du 5-hydroxyméthyl-2-furaldéhyde par action de sels d'ammonium ou d'immonium sur les mono-, oligo- et poly-saccharides. Accès direct aux 5-halogénométhyl-2-furaldéhydes. Carbohydrate Research, 122: 59–68.

Fournier, R.L., et al., 1996, Demonstration of pH control in a commercial immobilized glucose isomerase. Biotechnology and Bioengineering, 52(6): 718–722.

Freeman, A., Woodley, J.M. and Lilly, M.D., 1993, In-situ product removal as a tool for bioprocessing. Bio/Technology, 11: 1007–1012.

Gallezot, P., 2007, Process options for converting renewable feedstocks to bioproducts. Green Chemistry, 9: 295–302.

Gandini, A. and Belgacem, M.N., 1997, Furans in polymer chemistry. Progress in Polymer Science, 22: 1203–1379.

Hailes, H.C., Dalby, P.A. and Woodley, J.M., 2007, Integration of biocatalytic conversions into chemical syntheses. Journal of Chemical Technology and Biotechnology, 82(12): 1063–1066.

Halliday, G.A., Young, R.J., Jr. and Grushin, V.V., 2003, One-pot, two-step, practical catalytic synthesis of 2,5-diformylfuran from fructose. Organic Letters, 5(11): 2003–2005.

Haworth, W.N. and Jones, W.G.M., 1944, The conversion of sucrose into furan compounds. Part I. 5-Hydroxymethylfurfuraldehyde and some derivatives. Journal of the Chemical Society, 2: 667–670.

Kabyemela, B.M., Adschiri, T., Malaluan, R.M. and Arai, K., 1999, Glucose and fructose decomposition in subcritical and supercritical water: detailed reaction pathway, mechanisms, and kinetics. Industrial & Engineering Chemistry Research, 38: 2888–2895.

Koolen, J.L.A., 1998, Simple and robust design of chemical plants. Computers & Chemical Engineering, 22: S255–S262.

Kröger, M., Prüße, U. and Vorlop, K.-D., 2000, A new approach for the production of 2,5-furandicarboxylic acid by in situ oxidation of 5-hydroxymethylfurfural starting from fructose. Topics in Catalysis, 13: 237–242.

Kuster, B.F.M., 1990, 5-Hydroxymethylfurfural (HMF). A review focusing on its manufacture. Starch, 42(8): 314–321.

Kuster, B.F.M. and Laurens, J., 1977, Preparation of 5-hydroxymethylfurfural. Part II. Dehydration of fructose in a tube reactor using polyethyleneglycol as solvent. Stärke, 29: 172–176.

Kuster, B.F.M. and van der Steen, H.J.C., 1977, Preparation of 5-hydroxymethylfurfural. Part I. Dehydration of fructose in a continuous stirred tank reactor. Stärke, 29: 99–103.

Kunz, M., 1993, Inulin and inulin-containing crops, Fuchs, A. (ed) (Elsevier Publishing Company, Amsterdam), p. 149.

Lansalot-Matras, C. and Moreau, C., 2003, Dehydration of fructose into 5-hydroxymethylfurfural in the presence of ionic liquids. Catalysis Communications, 4: 517–520.

Lewkowski, J., 2001, Synthesis, chemistry and applications of 5-hydroxymethylfurfural and its derivatives. Arkivoc, (i): 17–54.

Liu, Q., Janssen, M.H.A., van Rantwijk, F. and Sheldon, R.A., 2005, Room-temperature ionic liquids that dissolve carbohydrates in high concentrations. Green Chemistry, 7: 39–43.

Mednick, M.L., 1962, Acid-base-catalyzed conversion of aldohexose into 5-(hydroxymethyl)-2-furfural. Journal of Organic Chemistry, 27: 398–403.

Moreau, C., Finiels, A. and Vanoye, L., 2006, Dehydration of fructose and sucrose into 5-hydroxymethylfurfural in the presence of 1-H-3-methylimidazolium chloride acting both as solvent and catalyst. Journal of Molecular Catalysis A: Chemical, 253: 165–169.

Moreau, C., Belgacem, M.N. and Gandini, A., 2004, Recent catalytic advances in the chemistry of substituted furans from carbohydrates and in the ensuing polymers. Topics in Catalysis, 27(1–4): 11–30.

Moreau, C., Durand, R., Razigade, S., Duhamet, J., Faugeras, P., Rivalier, P., Ros, P. and Avignon, G., 1996, Dehydration of fructose to 5-hydroxymethylfurfural over H-mordenites. Applied Catalysis A: General, 145: 211–224.

Musau, R.M. and Munavu, R.M., 1987, The preparation of 5-hydroxymethyi-2-furaldehyde (HMF) from D-fructose in the presence of DMSO. Biomass, 13: 67–74.

Nakamura, Y. and Morikawa, S., 1980, The dehydration of D-fructose to 5-hydroxymethyl-2-furaldehyde. Bulletin of the Chemical Society of Japan, 53: 3705–3706.

Newth, F.H., 1951, The formation of furan compounds from hexoses. Advances in Carbohydrate Chemistry, 6: 83–106.

Partenheimer, W. and Grushin, V.V., 2000, Synthesis of 2,5-diformylfuran and furan-2,5-dicarboxylic acid by catalytic air-oxidation of 5-hydroxymethylfurfural. Unexpectedly selective aerobic oxidation of benzyl alcohol to benzaldehyde with metal/bromide catalysts. Advanced Synthesis & Catalysis, 343(1): 102–111.

Peters, D., 2007, Raw materials. Advanced Biochemical Engineering/Biotechnology, 105: 1–30.

Qi, X., Watanabe, M., Aida, T.M. and Smith, R.L., Jr., 2008, Catalytic dehydration of fructose into 5-hydroxymethylfurfural by ion-exchange resin in mixed-aqueous system by microwave heating. Green Chemistry, 10: 799–805.

Rapp, M.K., 1987, Process for the preparation of 5-hydroxymethylfurfural, including a crystalline product, using exclusively water as solvent, DE Patent 3601281 A1.

Ribeiro, M.L. and Schuchardt, U., 2003, Cooperative effect of cobalt acetylacetonate and silica in the catalytic cyclization and oxidation of fructose to 2,5-furandicarboxylic acid. Catalysis Communications, 4: 83–86.

Rigal, L. and Gaset, A., 1985, Optimization of the conversion of D-fructose to 5-hydroxymethyl-2-furancarboxaldehyde in a water-solvent-ion exchanger triphasic system. Biomass, 8: 267–276.

Rigal, L., Gaset, A. and Gorrichon, J.-P., 1981, Selective conversion of fructose to 5-hydroxymethyl-2-furancarboxaldehyde using a water-solvent-ion-exchange resin triphasic system. Industrial & Engineering Chemistry Product Research and Development, 20: 719–721.

Rivalier, P., Duhamet, J., Moreau, C. and Durand, R., 1995, Development of a continuous catalytic heterogeneous column reactor with simultaneous extraction of an intermediate product by an organic-solvent circulating in countercurrent manner with the aqueous-phase. Catalysis Today, 24: 165–171.

Román-Leshkov, Y., Chheda, J.N. and Dumesic, J.A., 2006, Phase modifiers promote efficient production of hydroxymethylfurfural from fructose. Science, 312: 1933–1937.

Röper, H., 2002, Renewable raw materials in Europe—industrial utilisation of starch and sugar. Starch, 54(3–4): 89–99.

Schiwek, H., Munir, M., Rapp, K.M., Schneider, B. and Vogel, M., 1991, New developments in the use of sucrose as an industrial bulk chemical, in Carbohydrates as Organic Raw Materials, Lichtenthaler, F.W. (ed) (VCH, Weinheim), pp. 57–94.

Schäfer, T., Borchert, T.W., Nielsen, V.S., Skagerlind, P., Gibson, K., Wenger, K., Hatzack, F., Nilsson, L.D., Salmon, S., Pedersen, S., Heldt-Hansen, H.P., Poulsne, P.B., Lund, H., Oxenbøll, K.M., Wu, G.F., Pedersen, H.H. and Xu, H., 2007, Industrial enzymes. Advances in Biochemical Engineering/Biotechnology, 105: 59–131.

Simkovic, I., Leesonboon, T., Mok, W. and Antal, M.J., Jr., 1987, Dehydration of carbohydrates in supercritical water. Preprints of Papers: American Chemical Society, Division of Fuel Chemistry, 32(2): 129–132.

Stankiewicz, A. and Moulijn, J.A., (2003). *Re-Engineering the Chemical Processing Plant: Process Intensification*. (Marcel Dekker, Inc, New York, USA).

Takeuchi, Y., Jin, F., Tohji, K. and Enomoto, H., 2008, Acid catalytic hydrothermal conversion of carbohydrate biomass into useful substances. Journal of Materials Science, 43: 2472–2475.

Taarning, E., Nielsen, I.S., Egeblad, K., Madsen, R. and Christensen, C.H., 2008, Chemicals from renewables: aerobic oxidation of furfural and hydroxymethylfurfural over gold catalysts. ChemSusChem, 1: 75–78.

Van Dam, H.E., Kieboom, A.P.G. and Van Bekkum, H., 1986, The conversion of fructose and glucose in acidic media: formation of hydroxymethylfurfural. Starch/Stärke, 38: 95–101.

Vinke, P., van der Poel, W. and van Bekkum, H., 1991, On the oxygen tolerance of noble metal catalysts in liquid phase alcohol oxidations. Studies in Surface Science and Catalysis, 59: 385–394.

Watanabe, M., Aizawa, Y., Iida, T., Nishimura, R. and Inomata, H., 2005a, Catalytic glucose and fructose conversions with TiO_2 and ZrO_2 in water at 473 K: relationship between reactivity and acid–base property determined by TPD measurement. Applied Catalysis A: General, 295: 150–156.

Watanabe, M., Aizawa, Y., Iida, T., Aida, T.M., Levy, C., Sue, K. and Inomata, H., 2005b, Glucose reactions with acid and base catalysts in hot compressed water at 473 K. Carbohydrate Research, 340: 1925–1930.

Werpy, T. and Petersen, G. (eds), 2004, Top value added chemicals from biomass, US Department of Energy, Office of Scientific and Technical Information, No. DOE/GO-102004-1992, http://www.nrel.gov/docs/fy04osti/35523.pdf.

Woodley, J.M., Bisschops, M., Straathof, A.J.J. and Ottens, M., 2008, Future directions for in-situ product removal (ISPR). Journal of Chemical Technology and Biotechnology, 83: 121–123.

Zhao, H., Holladay, J.E., Brown, H. and Zhang, Z.C., 2007, Metal chlorides in ionic liquid solvents convert sugars to 5-hydroxymethylfurfural. Science, 316: 1597–1600.

Top Catal
DOI 10.1007/s11244-011-9754-2

ORIGINAL PAPER

Effect of Support in Heterogeneous Ruthenium Catalysts Used for the Selective Aerobic Oxidation of HMF in Water

Yury Y. Gorbanev · Søren Kegnæs · Anders Riisager

Abstract Heterogeneous ruthenium-based catalysts were applied in the selective, aerobic oxidation of 5-hydroxymethylfurfural, a versatile biomass-derived chemical, to form 2,5-furandicarboxylic acid. The oxidation reactions were performed in water with dioxygen as the oxidant at different pressures without added base. Catalysts were prepared by depositing catalytically active $Ru(OH)_x$ species on a number of different supports, such as titanium-, aluminum-, cerium-, zirconium-, magnesium- and lanthanum oxides, magnetite, spinel, hydrotalcite and hydroxyapatite. All the catalysts were found to be active in the oxidation reactions, and the choice of support was demonstrated to be important for the catalytic performance.

Keywords 5-hydroxymethylfurfural · 2,5-furandicarboxylic acid · Oxidation · Ruthenium · Supported catalysts

1 Introduction

In recent years, the interest for production of fine and bulk chemicals from biomass-based resources has increased significantly [1]. An example of such a bio-based chemical is 2,5-furandicarboxylic acid (FDA) [2]. FDA can be prepared by selective oxidation of 5-hydroxymethylfurfural (HMF) which is available from hexose monosaccharides, e.g. glucose and fructose, by acid-catalyzed dehydration [3, 4]. This makes FDA a bio-renewable feedstock directly available from biomass. FDA has in particular been promoted as an important renewable building block for production of plastic, due to its similarity to the fossil feedstock terephthalic acid [1].

Selective oxidation of organic molecules has attracted increasing attention over the past decade, especially with molecular oxygen [5–9]. In aerobic oxidations, air or molecular oxygen are used as the oxidants instead of classical metal oxides, containing, e.g. chromium or manganese. Oxygen is considered a "green" oxidant because it produces water as the only by-product unlike the aforementioned metal oxides, which generate stoichiometric amounts of metal waste. From an economic point of view, aerobic oxidation is also very attractive due to the low cost of oxygen and its unlimited accessibility.

A number of different heterogeneous catalyst systems have previously been reported for the selective oxidation of HMF to FDA. One of the first successful studies was made by Vinke et al. [10] using supported Pd or Pt catalysts under alkaline conditions. Here, ruthenium supported on carbon was also shown to be an active catalyst for the reaction, though not giving quantitative yield and possessing low catalyst stability. A Pt/C catalyst promoted with bismuth was further applied for HMF oxidation by Kröger et al. [11]. Recently, Corma and coworkers further showed that also gold nanoparticles supported on different metal oxides can catalyze the selective oxidation of HMF to FDA in good yields, although only in presence of base [12].

Several reactions are known in the literature to be catalyzed by ruthenium-based catalysts [13–16], including oxidation reactions [17]. However, the number of reports on heterogeneous ruthenium-based oxidation catalysts is limited and (beside Vinke et al. [10]) primarily reported by the groups of Kaneda [18, 19] and Mizuno [20, 21] for oxidations of alcohols to oxo compounds in organic solvents.

Y. Y. Gorbanev · S. Kegnæs · A. Riisager (✉)
Centre for Catalysis and Sustainable Chemistry,
Department of Chemistry, Technical University of Denmark,
Kemitorvet 207, 2800 Kgs Lyngby, Denmark
e-mail: ar@kemi.dtu.dk

Published online: 07 September 2011

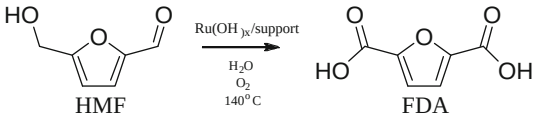

Scheme 1 Aerobic oxidation of HMF to FDA with supported $Ru(OH)_x$ catalyst in water without added base

Very recently we have shown that it is possible to oxidize HMF aerobically to FDA using a heterogeneous, ruthenium oxide-hydroxide catalyst [22]. In this study, $Ru(OH)_x$ was supported on three different magnesium-containing supports: MgO (magnesium oxide), $MgAl_2O_4$ (spinel) and $Mg_6Al_2(CO_3)(OH)_{16}{\cdot}4H_2O$ (hydrotalcite), and a clear support dependence on the catalyst activity and FDA yield was found.

Here we present the usage of other heterogeneous $Ru(OH)_x$-based catalysts in the selective aerobic oxidation of HMF to FDA. Several catalysts were prepared with different supports, characterized by electron paramagnetic resonance (EPR), x-ray powder diffraction (XRPD), nitrogen sorption (BET area), transmission electron microscopy (TEM) and energy dispersive spectroscopy (EDS) and their catalytic activity compared. Notably, the oxidations were conducted in water and without the addition of base (Scheme 1). The effect of oxygen pressure and reaction time on the yield of FDA was examined.

2 Experimental

2.1 Materials

HMF (>99%), 2-furoic acid (98%), levulinic acid (LA) (98%), formic acid (FA) (98%), ruthenium(III) chloride (purum), hydrotalcite (HT), magnetite (>98%), hydroxyapatite (HAp) (>97%), aluminium oxide (>99.9%), zirconium oxide (99%), lanthanum(III) nitrate hexahydrate (99.99%) and sodium hydroxide (>98%) were acquired from Sigma-Aldrich. Ruthenium(III) nitrate hexahydrate (99.9%) and magnesium nitrate hexahydrate (p.a.) were obtained from Merck. Cerium oxide (99.5%) and lanthanum(III) oxide (99.9%) were purchased from Alfa Aesar. Magnesium oxide (p.a.) was purchased from Riedel-de Haën AG. 2,5-Diformylfuran (DFF) (98%) was obtained from ABCR GmbH & Co. 2,5-Furandicarboxylic acid (FDA) (>99%) and 5-hydroxymethyl-2-furan-carboxylic acid (HMFCA) (> 99%) were purchased from Toronto Research Chemicals Inc. and dioxygen (99,5%) from Air Liquide Denmark. All chemicals were used as received.

2.2 Catalyst Preparation

Magnesium-lanthanum oxide was prepared by co-precipitation and supported $Ru(OH)_x$ catalysts by deposition–precipitation procedures described elsewhere [20, 21, 23].

21.7 g (0.05 mol) $La(NO_3)_3{\cdot}6H_2O$ and 38.4 g (0.15 mol) $Mg(NO_3)_2{\cdot}6H_2O$ were dissolved in 250 mL water. Then 1 M solution of KOH was added in small portions to maintain pH around 12 over a time period of 8 h. Hereafter, the formed precipitate was filtered, washed with water and calcined at 650 °C for 6 h.

4.88 g of support (i.e. TiO_2, Al_2O_3, Fe_3O_4, CeO_2, ZrO_2, MgO, $MgAl_2O_4$, HT, La_2O_3 or HAp) was added to 143 mL of 8.3 mM aqueous $RuCl_3$ solution (1.19 mmol Ru). After stirring for 15 min, 28 mL of 1 M NaOH solution was added and the mixtures were stirred for 18 h. Then the catalysts were filtered off, washed thoroughly with water (colourless filtrates suggested absence of ruthenium ions) and dried at 140 °C for 40 h. A similar preparation procedure was applied for $MgO{\cdot}La_2O_3$ supported catalyst, except that no base was added to the mixture. Approximately 4.9 g of each catalyst was obtained containing 2.4 wt% Ru.

2.3 Oxidation Reactions

HMF oxidation reactions were carried out in stirred Parr autoclaves equipped with internal thermocontrol (T316 steel, Teflon™ beaker insert, 100 mL). In each reaction the autoclave was charged with 63 mg of HMF (0.5 mmol) and 10 mL of water. This initial HMF concentration (0.05 M) was chosen to ensure complete dissolution by extrapolation of the experimental data on FDA solubility in water to 140 °C. Subsequently, the supported $Ru(OH)_x$ catalyst was added (0.025–0.105 g, 0.006–0.025 mmol Ru) and the autoclave was flushed and then pressurized with dioxygen (1–40 bar, ca. 1.6–64 mmol) and maintained at 140 °C for a given period of time under stirring (700 rpm).

After the reaction, the autoclave was rapidly cooled on ice bath to room temperature (i.e. 20 °C) and a sample taken out for HPLC analysis (Agilent Technologies 1200 series, Aminex HPX-87H column from Bio-Rad, 300 mm × 7.8 mm × 9 µm, flow 0.6 mL/min, solvent 5 mM H_2SO_4, temperature 60 °C) after filtering off the catalyst and measuring of the pH value. FDA concentration was measured in a similar way, after addition of 1 mL of 1 M NaOH solution to the post-reaction mixture. Reference samples were used to quantify the products. In recycling studies the catalyst was filtered off from the post-reaction mixture, washed with 0.1 M NaOH and water, and dried at 140 °C for 12 h before reuse.

2.4 Catalyst Characterization

XRPD patterns were recorded using a Huber G670 powder diffractometer (Cu-K_α radiation, $\lambda = 1.54056$ Å) in the 2θ interval 5–100°.

EPR spectra (X band) were measured with a Bruker EMX-EPR spectrometer at room temperature with a rectangular 4102 ST cavity operating in the TE102 mode. The microwave source was a Bruker ER 041 XG Microwave bridge with frequencies around 9.22 GHz.

TEM images were recorded on a FEI Tecnai Transmission Electron Microscope at 200 kV with samples deposited on a carbon support. EDS analysis was performed with an Oxford INCA system.

Surface areas were determined by nitrogen sorption measurements at liquid nitrogen temperature on a Micromeritics ASAP 2020. The samples were outgassed in vacuum at 150 °C for 4 h prior to the measurements. The total surface areas were calculated according to the BET method.

Inductively coupled plasma spectrometry (ICP) analysis was performed on diluted post-reaction mixture and quantified with ICP standard solutions (Fluka) on a Perkin Elmer ELAN 6000 with cross-flow nebulizer and argon plasma.

3 Results and Discussion

XRPD analysis of the prepared $Ru(OH)_x$ catalysts with TiO_2, CeO_2 or $MgO{\cdot}La_2O_3$ support (2.4 wt% Ru) did not reveal crystalline ruthenium oxide phases. However, at higher metal loading, corresponding to 40 wt% Ru, ruthenium dioxide was clearly found (diffractograms of $Ru(OH)_x/TiO_2$ materials are shown in Fig. 1). This observation could indicate that amorphous ruthenium oxide might also be present in the 2.4 wt% Ru catalysts.

In the recorded EPR spectra of the catalysts (not shown) trace amounts of Ru(III) could only be identified in the hydrotalcite-supported 2.4 wt% catalyst. However, in the $Ru(OH)_x/TiO_2$ material with 40 wt% Ru, ruthenium(III) was also identified, thus suggesting that both oxidation states were present in the ruthenium oxide, i.e. $RuO_2{\cdot}Ru_2O_3$, with RuO_2 as the major component and Ru(III) oxide in trace amount [24].

TEM images of the prepared $Ru(OH)_x/TiO_2$ and $Ru(OH)_x/CeO_2$ catalysts are presented in Fig. 2. Ruthenium species were not observed on the surface of titania, possibly due to their small size and the microscope resolution.

EDS analysis was performed on both whole catalyst samples and on random areas on the catalysts (see Fig. 2). Atomic ratios of Ru:Ti and Ru:Ce were determined to be 1.8:98.2 and 3.7:96.3, respectively, on both the whole catalyst and random area measurements. Thus, the weight percentage of Ru on titania and ceria was found to be 2.32 and 2.26 wt%, respectively, which is in good accordance with the expected content calculated from the preparation procedure.

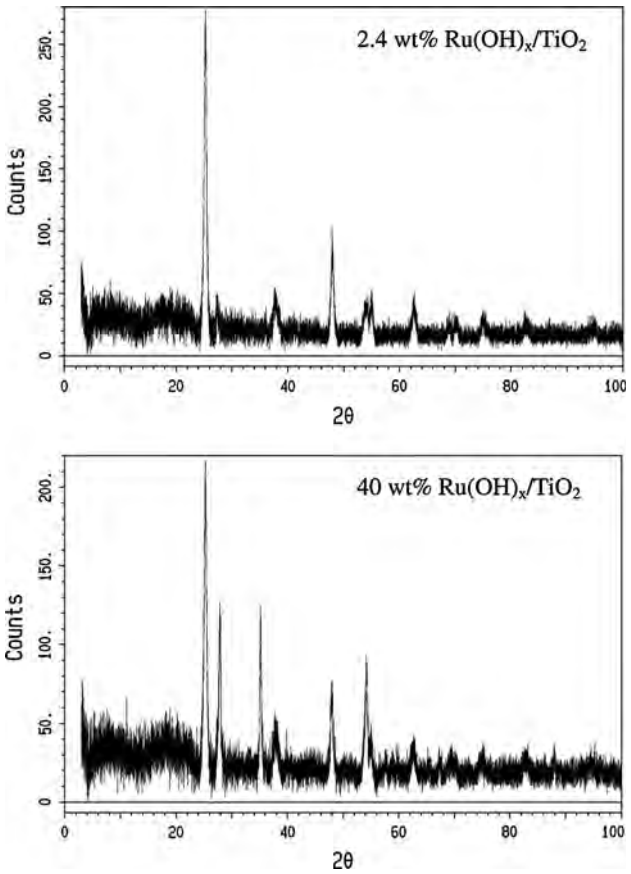

Fig. 1 XRPD diffractograms of 2.4 and 40 wt% $Ru(OH)_x/TiO_2$ catalysts

In previous work, we explored the oxidation reaction of HMF to FDA in water solutions with added base using titania-supported gold nanoparticle catalyst [4]. Here, we initially investigated $Ru(OH)_x/TiO_2$ as catalyst in the HMF oxidation reaction in aqueous media without added base.

Firstly, experiments were carried out at 1 bar dioxygen pressure at 140 °C. After 2 h of reaction most of the HMF remained unconverted under these reaction conditions with less than 1% of FDA being formed. However, already at this reaction time decomposition to formic acid (FA) occurred resulting in a yield of 13.8% which increased to 55.4% after 20 h of reaction. FDA yield amounted after this reaction time to only 2.3%.

Further, we investigated the reaction at increased oxygen pressures. The products formed in oxidation reactions at 2.5 and 20 bars of dioxygen as a function of reaction time are presented in Fig. 3a and b, respectively.

The observed intermediate products were identified as HMFCA and DFF, as also previously found [4, 22].

At both examined oxygen pressures a significant formation of formic acid occurred, which was not the case in the

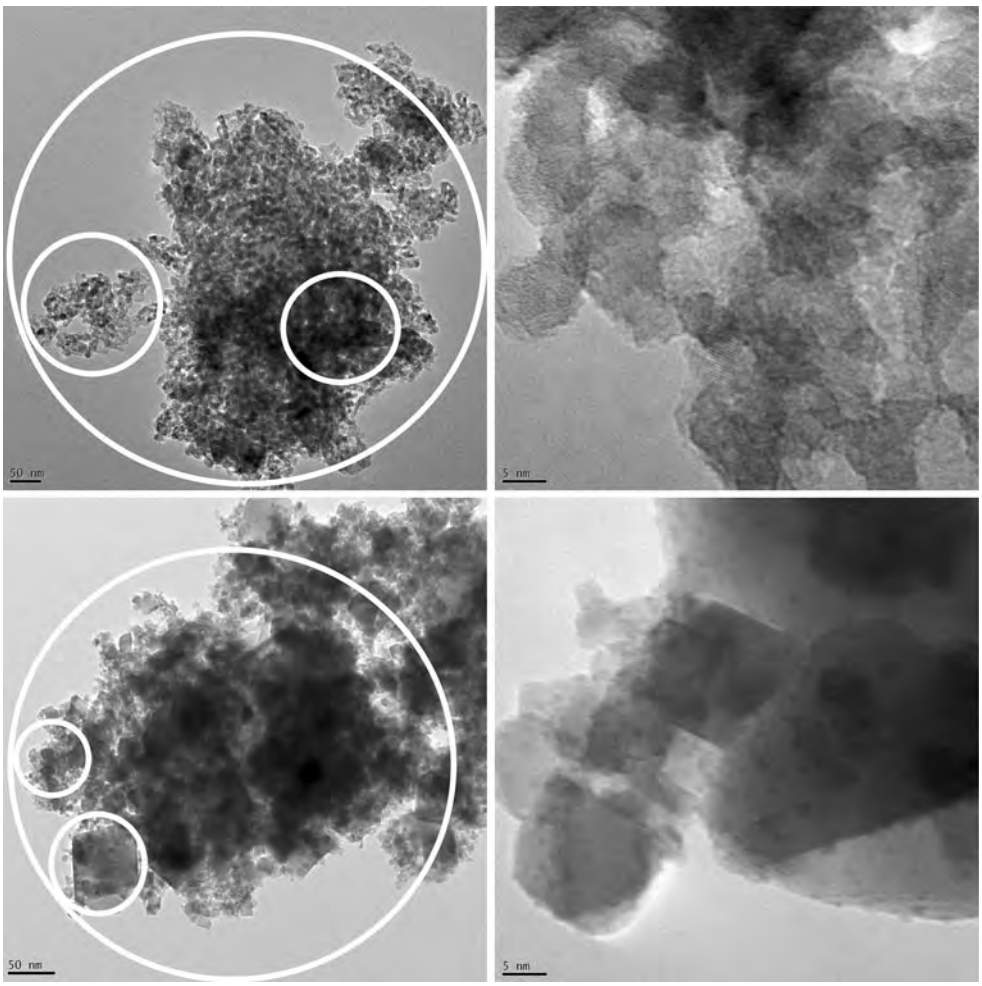

Fig. 2 High-resolution TEM images of the 2.4 wt% $Ru(OH)_x/TiO_2$ catalyst (*top*) and 2.4 wt% $Ru(OH)_x/CeO_2$ catalyst (*bottom*). *White circles* represent the areas analyzed by EDS

analogous Au/TiO_2-catalyzed aqueous oxidation [4]. Here, presence of sodium hydroxide facilitated FDA formation and prevented the formation of the acid-catalyzed degradation products [1, 4, 25]. Nevertheless, at 20 bars of dioxygen the formation of FDA occurred significantly faster than at 2.5 bar with the $Ru(OH)_x/TiO_2$ catalyst, whereas the reaction rate for degradation did not seem to increase. Thus, by performing oxidation of HMF in water solutions with $Ru(OH)_x/TiO_2$ catalyst at elevated pressure, it proved possible to obtain high selectivity towards 2,5-furandicarboxylic acid and high substrate conversion, while avoiding the formation of degradation by-products, such as FA and LA.

Different metal oxide supports, spinel ($MgAl_2O_4$), hydrotalcite [HT; $Mg_6Al_2(CO_3)(OH)_{16}{\cdot}4(H_2O)$] and hydroxyapatite [HAp; $Ca_{10}(PO_4)_6(OH)_2$] were screened in order to find a system with supported $Ru(OH)_x$ species that could provide high selectivity towards desirable oxidation products.

Characteristics of the screened supports and corresponding catalysts are compiled in Table 1. The results obtained in HMF oxidation with the catalysts are shown in Fig. 4.

As seen in Fig. 4, catalysts with basic magnesium-containing support generally showed high efficiency in HMF to FDA oxidation, whereas the usage of other oxides (e.g. ZrO_2 and Al_2O_3) induced the formation of formic acid. Fe_3O_4 and hydroxyapatite supported $Ru(OH)_x$ catalyst revealed good selectivities towards FDA formation, however, in both cases formation of solid humins was observed constituting approximately 30% of the mass balance.

The supported catalysts with basic carrier materials, i.e. MgO, $MgO{\cdot}La_2O_3$ and HT gave excellent selectivities and substrate conversions resulting in FDA yields above 95%. However, ICP analysis of the post-reaction solutions showed presence of magnesium ions, indicating that the support dissolved to a certain extent during reaction [23, 26]. This was confirmed by the relative high pH values measured in post-reaction mixtures with these supports, which was obtained from basic hydroxides formed upon

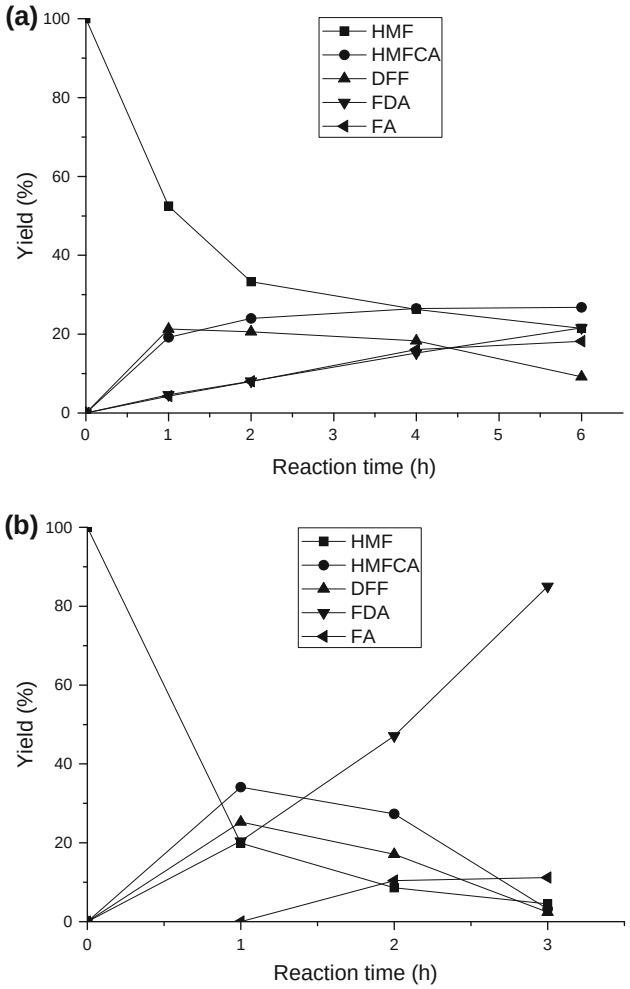

Fig. 3 HMF oxidation with $Ru(OH)_x/TiO_2$ catalyst in water at 2.5 bars O_2 (**a**) and 20 bars O_2 (**b**) (0.05 M HMF, 140 °C, 5 mol% Ru to HMF)

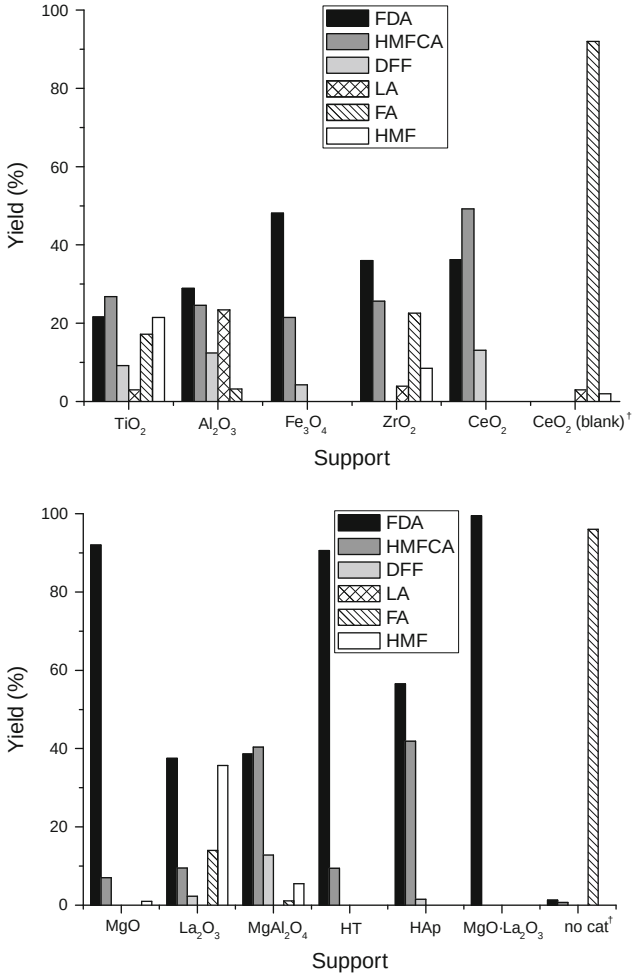

Fig. 4 Product yields in HMF oxidation reaction with $Ru(OH)_x$/support catalysts (0.05 M HMF, 2.5 bars O_2, 140 °C, 6 h, 5 mol% Ru). †The reaction time was 18 h

Table 1 Supports applied for oxidation of aqueous HMF to FDA with heterogeneous $Ru(OH)_x$ catalysts

Support	Support surface area (m^2/g)	Catalyst surface area (m^2/g)	Reaction time (h)	pH after reaction
TiO_2	123	128	6	2
Al_2O_3	149	145	6	2
Fe_3O_4	44	45	6	2
ZrO_2	53	97	6	2
CeO_2	62	8	6	2
CeO_2 (blank)	62	–	18	3
MgO	30	27	6	10
La_2O_3	59	5	6	8
$MgAl_2O_4$	63	54	6	2
HT	8	6	6	7
HAp	17	25	6	3
$MgO{\cdot}La_2O_3$	30	68	6	8
No cat	–	–	18	1

dissolution of the support accompanied by formation of salts of the acid products.

In order to elucidate the effect of the magnesium-containing supports, a control experiment was conducted in which $Ru(OH)_x/TiO_2$ catalyst was used together with two mole equivalents of $MgCl_2$. The reaction was carried out at reaction conditions identical to the support screening experiments (0.05 M HMF, 140 °C, 6 h). Although HMF was fully converted in the control experiment, only 3 and 2% of FDA and HMFCA were formed, respectively, while the rest constituted formic acid. This strongly suggested that the support played an important role with respect to the catalyst performance, rather than simply providing magnesium ions.

A similar pattern was also observed in a blank experiment when no catalyst was introduced into the reaction mixture. Here, formic acid was formed in 92% yield, while yield of FDA and other oxidation products was less than 1%.

Apart from magnesium-containing supports, good oxidation performance was also observed for ceria-supported catalyst, as seen in Fig. 4. Although selectivity towards FDA was only moderate in the time frame of 6 h, no degradation products were here observed. Hence, $Ru(OH)_x/CeO_2$ was further tested in the catalyzed HMF oxidation at different pressures (Fig. 5).

The obtained data clearly suggested that it was possible to avoid formation of undesirable degradation products by use of elevated pressures, whereas ambient pressure (i.e. 1 bar of O_2) led to formation of 3% formic acid after 1 h of reaction. Therefore, with a desire to perform the reaction at lowest possible pressure, we investigated the product formation over time at 2.5 bars pressure (Fig. 6).

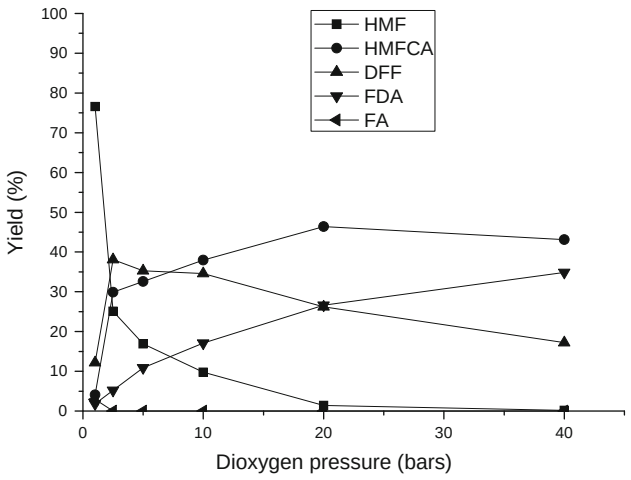

Fig. 5 HMF oxidation with $Ru(OH)_x/CeO_2$ catalyst in water at different oxygen pressures (0.05 M HMF, 140 °C, 1 h, 5 mol% Ru to HMF)

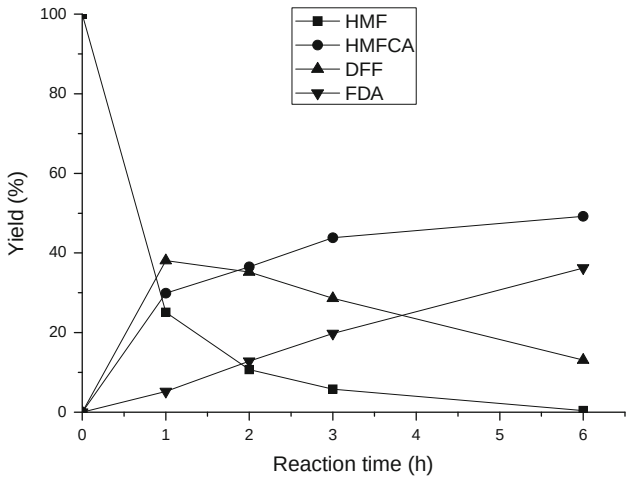

Fig. 6 HMF oxidation with $Ru(OH)_x/CeO_2$ catalyst in water (0.05 M HMF, 140 °C, 2.5 bar O_2, 5 mol% Ru to HMF)

As observed from Fig. 6, the FDA yield constituted 38% under applied conditions after 6 h, which is higher than the FDA yield observed when $Ru(OH)_x/TiO_2$ was used as the catalyst under the same reaction conditions (see Fig. 3a). The yield of FDA increased to 60% after 18 h of reaction. However, HMFCA contributed 10% to the mass balance while no formic acid or levulinic acid were detected in the post-reaction mixture, possibly due to degradation of the formed FA and LA at extended reaction times.

Importantly, upon re-use the $Ru(OH)_x/CeO_2$ catalyst revealed no loss of activity, providing 38 and 36% yield of FDA after 6 h of reaction in second and third runs, respectively. This clearly demonstrated the applicability of the ceria catalyst system in line with the study performed by Corma and coworkers [12], in which gold nanoparticles deposited on ceria showed superior performance in aerobic oxidations compared to Au/TiO_2 in the absence of base.

4 Conclusions

A number of $Ru(OH)_x$/support catalysts were prepared and identified as highly efficient catalysts for aerobic oxidation of HMF to FDA under base-free and low to moderate oxygen pressures. Especially, ceria-supported catalysts showed higher activities and selectivities compared to those based on TiO_2 as a support.

Further development of the catalytic systems, screening of different substrates and additional catalyst characterization are in progress.

Acknowledgments We thank Bodil Holten and Ass. Prof. Susanne L. Mossin (Centre for Catalysis and Sustainable Chemistry, Department of Chemistry, Technical University of Denmark) for BET and EPR measurements, Jacob S. Jensen (Department of Chemical and Biochemical Engineering, Technical University of Denmark) for

FDA solubility data and Andras Kovacs (Center for Electron Nanoscopy, Technical University of Denmark) for TEM and EDS measurements. The work was supported by The Danish National Advanced Technology Foundation and Novozymes A/S.

References

1. Bozell JJ, Petersen GR (2010) Green Chem 12:539
2. Boisen A, Christensen TB, Fu W, Gorbanev YY, Hansen TS, Jensen JS, Klitgaard SK, Pedersen S, Riisager A, Ståhlberg T, Woodley JM (2009) Chem Eng Res Des 87:1318
3. Moreau C, Belgacem MN, Gandini A (2004) Top Catal 27:11
4. Gorbanev YY, Klitgaard SK, Woodley JM, Christensen CH, Riisager A (2009) ChemSusChem 2:672
5. Mallat T, Baiker A (2004) Chem Rev 104:3037
6. ten Brink G-J, Arends IWCE, Sheldon RA (2000) Science 287:1636
7. Christensen CH, Jørgensen B, Rass-Hansen J, Egeblad K, Madsen R, Klitgaard SK, Hansen SM, Hansen MR, Andersen HC, Riisager A (2006) Angew Chem Int Ed 45:4648
8. Marsden C, Taarning E, Hansen D, Johansen L, Klitgaard SK, Egeblad K, Christensen CH (2008) Green Chem 10:168
9. Kegnæs S, Mielby J, Mentzel UV, Christensen CH, Riisager A (2010) Green Chem 12:1437
10. Vinke P, van der Poel W, van Bekkum H (1991) Stud Surf Sci Catal 59:385
11. Kröger M, Prüße U, Vorlop K-D (2000) Top Catal 13:237
12. Casanova O, Iborra S, Corma A (2009) ChemSusChem 2:1138
13. Hansen TW, Wagner JB, Hansen PL, Dahl S, Topsøe H, Jacobsen CJH (2001) Science 294:1508
14. Klerke, Klitgaard SK, Fehrmann R (2009) Catal Lett 541:541
15. Schwab P, Grubbs RH, Ziller JW (1996) J Am Chem Soc 118:100
16. Rovik K, Klitgaard SK, Dahl S, Christensen CH, Chorkendorff I (2009) Appl Catal A 358:269
17. Pagliaro M, Campestrini S, Ciriminna R (2005) Chem Soc Rev 34:837
18. Ji H-B, Ebitani K, Mizugaki T, Kaneda K (2002) Catal Commun 3:511
19. Mori K, Kanai S, Hara T, Mizugaki T, Ebitani K, Jitsukawa K, Kaneda K (2007) Chem Mater 19:1249
20. Nikaidou F, Ushiyama H, Yamaguchi K, Yamashita K, Mizuno N (2010) J Phys Chem C 114:10873
21. Mizuno N, Yamaguchi K (2008) Catal Today 132:18
22. Gorbanev YY, Kegnæs S, Riisager A (2011) Catal Lett (accepted)
23. Veldurthy B, Clacens JM, Figueras F (2005) Adv Synth Catal 347:767
24. Kiwi J, Prins R (1986) Chem Phys Lett 126:579
25. Ståhlberg T, Grau Sørensen M, Riisager A (2010) Green Chem 12:321
26. Lakshmi Kantam M, Pal U, Choudary BM, Bhargava S (2008) Adv Synth Catal 350:1225

Selective aerobic oxidation of 5-hydroxymethylfurfural in water over solid ruthenium hydroxide catalysts with magnesium-based supports

Yury Y. Gorbanev · Søren Kegnæs · Anders Riisager

Abstract Solid catalyst systems comprised of ruthenium hydroxide supported on magnesium-based carrier materials (spinel, magnesium oxide and hydrotalcite) were investigated for the selective, aqueous aerobic oxidation of the biomass-derived chemical 5-hydroxymethylfurfural (HMF) into 2,5-furandicarboxylic acid (FDA), a possible plastics precursor. The novel catalyst systems were characterized by nitrogen physisorption, XRPD, TEM and EDS analysis, and applied for the oxidation with no added base at moderate to high pressures of dioxygen and elevated temperatures. The effects of support, temperature and oxidant pressure were studied and optimized to allow a quantitative yield of FDA to be obtained.

Keywords 5-hydroxymethylfurfural · 2,5-furandicarboxylic acid · aerobic oxidation · ruthenium hydroxide catalysts

1 Introduction

Biomass is a viable feedstock for production of both chemicals and novel fuels, which eventually can replace crude oil and gas (fossil feedstocks) as major raw materials [1]. 5-Hydroxymethylfurfural (HMF) is a product of the dehydration of hexose carbohydrates obtained from lignocellulosic biomass by, e.g. enzymatic hydrolysis [2, 3].

HMF can be readily oxidized to different potentially important products, such as maleic anhydride [4], 2,5diformylfuran (DFF) [5, 6], 2,5-durandicarboxylic acid (FDA) (Scheme 1) or its dimethyl ester [7-11]. FDA has been established by the U.S. Department of Energy (DOE) biomass program as one of the twelve chemicals that in the future can be used as chemical building block from biomass in biorefineries [12, 13]. In particular, the two carboxylic groups present in FDA make it a valuable polymer building block and hence a possible renewable alternative to terephthalic, isophthalic, adipic and other currently used acids, produced from fossil-based resources [14].

Ruthenium-based catalysts are generally known for their aptitude in aerobic oxidation reactions [15-17] including applications for oxidation of alcohols to produce aldehydes or ketones. Hence, homogeneous Ru-complex catalysts have been found to generate aldehydes or ketones in almost quantitative yields when employed in organic solvents [18, 19] or ionic liquids [20]. A more preferred way to oxidize HMF involve heterogeneous catalysis, due to ease of catalyst separation in possible industrial processes [1]. Accordingly, supported ruthenium hydroxide catalysts have recently been reported to be efficient catalysts for aerobic

Y. Y. Gorbanev · S. Kegnæs · A. Riisager (✉)
Centre for Catalysis and Sustainable Chemistry, Department of Chemistry,
Technical University of Denmark, DK-2800 Kgs. Lyngby, Denmark
E-mail: ar@kemi.dtu.dk

oxidation reactions. $Ru(OH)_x$ supported on ceria has been shown to oxidize alcohols to corresponding ketones, aldehydes and acids, and also aldehydes to acids with high yields at 80-140°C at ambient air pressure [21], whereas a $Co(OH)_2$ co-promoted catalyst afforded high activity even at room temperature [22]. Kozhevnikov et al. [23] performed oxidation of primary alcohols to aldehydes using mixed Ru-Co oxide with 95 % yield in toluene at 110°C under oxygen atmosphere. Similarly, a ruthenium-functionalized nickel hydroxide composite catalyst ($Ru/Ni(OH)_2$) has been used to oxidize alcohols quantitatively to aldehydes or ketones in organic solvents at 90°C in the presence of molecular oxygen [24].

Additionally, Kaneda et al. [25, 26] and Mizuno et al. [27-31] have reported selective aerobic oxidations of aromatic and aliphatic alcohols to aldehydes and ketones and amines to amides with $Ru(OH)_x$ supported by alumina, magnetite and hydroxyapatite. Alcohols and amines were oxidized to produce aldehydes/ketones and amides/nitriles, respectively, at 80-150°C under ambient pressure of O_2 in toluene or $PhCF_3$ with yields above 99 %. Furthermore, alumina-supported ruthenium hydroxide have been used for oxidation of alcohols in a continuous multifunctional reactor [32].

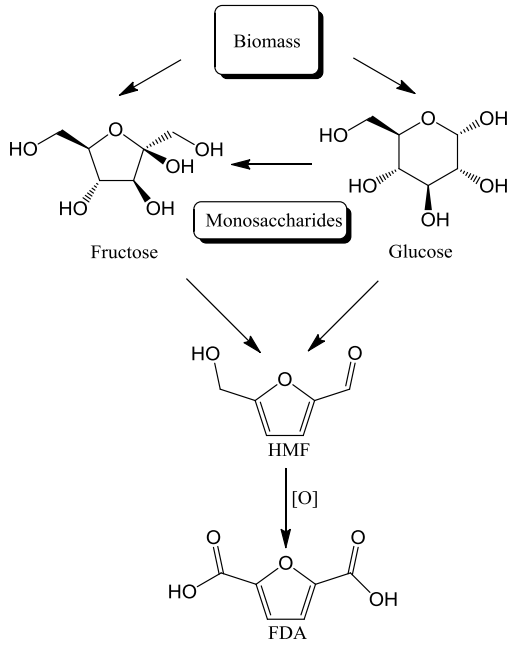

Scheme 1 The schematic route for biomass conversion to 2,5-furandicarboxylic acid (FDA)

Catalyst supports with basic functionality like e.g. hydrotalcite and hydroxyapatite have also been investigated [29, 30]. Synthetic Ru-Co-Al and Ru-Al-Mg hydrotalcites have been reported to catalyze aerobic oxidation of aliphatic and aromatic alcohols in toluene at 60°C under ambient dioxygen pressure, producing aldehydes and ketones in above 90 % yield. Ruthenium- and ruthenium-cobalt-promoted hydroxyapatite gave yields higher than 99 % [35, 36].

Recently, we have screened and obtained promising results for the oxidation of HMF with ruthenium hydroxide catalysts on various common supports such as, e.g. MgO, $MgAl_2O_4$, CeO_2 [37]. In this work we have elaborated the study and investigated the selective oxidation of HMF to FDA with solid catalysts containing $Ru(OH)_x$ species supported on the porous magnesium-containing supports: magnesium oxide, spinel and hydrotalcite (HT) (Scheme 2). The reactions were conducted in water with molecular oxygen as

the oxidizing agent as a cheap and abundant resource. The catalysts were characterized and the effect of reaction time, pressure and temperature on the catalytic performance were studied and optimized to obtain near quantitative yield of FDA.

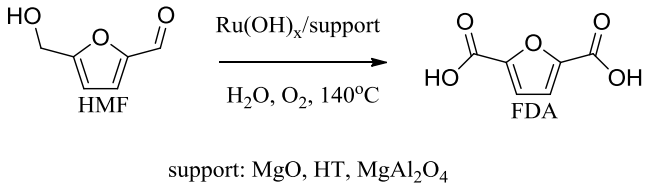

Scheme 2 Aerobic oxidation of HMF to FDA with supported $Ru(OH)_x$ catalyst in water

2 Experimental

2.1 Materials

5-Hydroxymethylfurfural (HMF) (>99 %, Sigma-Aldrich), 2-furoic acid (98 %, Sigma-Aldrich), levulinic acid (98 %, Sigma-Aldrich), formic acid (FA) (98 %, Sigma-Aldrich), ruthenium(III) chloride (purum, Sigma-Aldrich), hydrotalcite $Mg_6Al_2(CO_3)(OH)_{16}\cdot 4H_2O$ (HT) and spinel $MgAl_2O_4$ (purum, Sigma-Aldrich), sodium hydroxide (>98 %, Sigma-Aldrich), magnesium oxide (p.a., Riedel-de Haën AG), 2,5-diformylfuran (98 %, ABCR GmbH & Co.KG), 2,5-furandicarboxylic acid (FDA) (>99 %, Toronto Research Chemicals Inc.), 5-hydroxymethyl-2-furancarboxylic acid (HMFCA) (>99 %, Toronto Research Chemicals Inc.) and dioxygen (99.5 %, Air Liquide Denmark) were all used as received.

2.2 Catalyst preparation and characterization

4.876 g of support (i.e. MgO, $MgAl_2O_4$ or HT) were added to 143 ml of 8.3 mM aqueous $RuCl_3$ solution (1.19 mmol Ru). After stirring for 15 min, 28 ml of 1 M NaOH solution was added and the mixtures were stirred for 18 h. Then the catalysts were filtered off, washed thoroughly with water until the filtrates were neutral (colourless filtrates suggested absence of ruthenium ions) and dried at 140°C for 40 h. Approximately 4.9 g of each catalyst was obtained containing 2.4 wt% Ru.

XRPD patterns were recorded using a Huber G670 powder diffractometer (Cu-K_α radiation, λ = 1.54056 Å) in the 2θ interval 5-100°.

Surface areas were determined by nitrogen adsorption and desorption measurements at liquid nitrogen temperature on a Micrometrics ASAP 2020. The samples were outgased in vacuum at 100°C for 4 h prior to measurements. The total surface areas were calculated according to the BET method.

TEM images were recorded on a FEI Tecnai Transition Electron Microscope at 200 kV with samples deposited on a carbon support. EDS analysis was performed with an Oxford INCA system.

2.3 Oxidation reactions

Oxidations were carried out in stirred Parr mini-reactor autoclaves equipped with internal thermocontrol (T316 steel, Teflon™ beaker insert, 100 ml). In each reaction the autoclave was charged with 63 mg of HMF (0.5 mmol) and 10 ml of water. Initial HMF concentration (0.05 M) solution was chosen based on experimental data on FDA solubility in water and extrapolation of this data to 140°C values area. Subsequently, the supported 2.4 wt% $Ru(OH)_x$ catalyst was added (0.105 g, 0.025 mmol Ru). The autoclave was flushed and pressurized with dioxygen (1-40 bar, ca. 1.6-64 mmol) and maintained at 140°C for a given period of time under stirring (700 rpm). After the reaction, the autoclave was rapidly cooled with ice to room temperature. The reaction mixture was made basic with 1 ml of 1 M NaOH solution before filtering off the catalyst, or filtered directly without base, followed by analysis using HPLC (Agilent Technologies 1200 series, Aminex HPX-87H column from Bio-Rad, 300 mm x 7.8 mm x 9 µm, flow 0.6 mL/min, solvent 5 mM H_2SO_4, temperature 60°C). In all figures where the product distribution is shown as a function of time each data point corresponds to an individual reaction run.

ICP analysis (Perkin Elmer ELAN 6000 with cross-flow nebulizer and argon plasma) was performed on diluted post-reaction mixtures and quantified with ICP standard solutions.

3 Results and discussion

3.1 Catalyst characterization

The BET surface areas of the applied support materials and the prepared catalysts are listed in Table 1. The surface areas of the catalysts were very much dependent on the choice of the metal oxide and, as expected, a small decrease in the surface areas was observed between the pure supports and the final catalysts. Moreover, X-ray powder diffraction (XRPD) patterns of the supported catalysts (not shown) revealed exclusively peaks originating from the respective supports, since the ruthenium content on the catalysts was too low to allow detection.

Representative transmission electron microscopy (TEM) images of the prepared catalysts are presented in Fig. 1. Notably, only agglomerated crystallites of the respective supports were observed on the TEM images with no noticeable ruthenium particles even at higher resolution. EDS analysis of the catalyst samples (performed on the parts shown in white circles) revealed an uneven distribution of ruthenium species on the surfaces of the catalysts with highest basicity, i.e. magnesium oxide and HT. The measured Ru contents are compiled in Table 1.

Table 1 Characteristics of supports and supported $Ru(OH)_x$ catalysts

Material	BET surface area (m^2/g)	Ru content (wt%)[a]
MgO	30	-
$Ru(OH)_x/MgO$	27	0.75 (1), 2.48 (2)
$MgAl_2O_4$	63	-
$Ru(OH)_x/MgAl_2O_4$	53	2.41 (1), 2.42 (2)
HT	8	-
$Ru(OH)_x$/HT	6	0.25 (1), 7.55 (2)

[a]The Ru contents are based on Ru:Al atomic ratios provided by EDS. The values of (1) and (2) are related to the areas numbered 1 and 2 on Fig. 1 for the respective support.

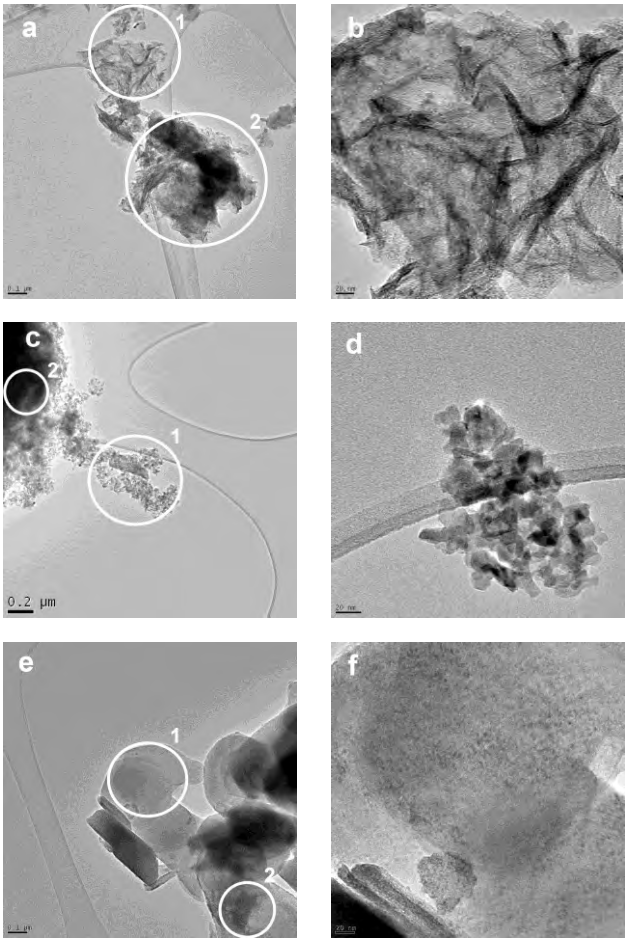

Fig. 1 TEM images of $Ru(OH)_x/MgO$ (a,b), $Ru(OH)_x/MgAl_2O_4$ (c,d) and $Ru(OH)_x$/HT (e,f) catalysts. White circles represent the areas analyzed by EDS

3.2 Aerobic oxidation of HMF

Initially, the catalyzed oxidation of HMF to FDA was investigated with $Ru(OH)_x$/HT catalyst in water in the absence of added base at 1 bar dioxygen pressure and a reaction temperature of 140°C. In Fig. 2 the formation of products is shown as a function of reaction time.

As seen in the figure, HMF was fully converted after 26 h of reaction and a quantitative yield of FDA was obtained after a reaction time of 38 h. Importantly, no product degradation was observed during the examined time period. Two intermediate oxidation products were observed; 2,5-diformylfuran (DFF) and 2-hydroxymethyl-5-furancarboxylic acid (HMFCA), thus suggesting a competitive reaction pathway for HMF oxidation with intermediate products formation, DFF and HMFCA, followed by oxidation to FDA (Scheme 3). This pathway is similar to the route previously established for the gold-catalyzed conversion of HMF [10, 11], however both rates of the formation and subsequent oxidation of HMFCA and DFF appeared to be similar under applied reaction conditions (i.e., 140°C and 1 bar of O_2 pressure).

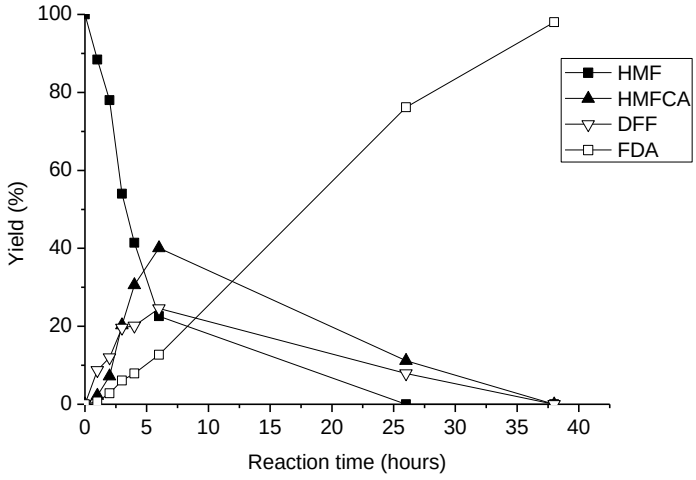

Fig. 2 Product yields in HMF oxidation with $Ru(OH)_x$/HT catalyst in water (0.05 M HMF, 1 bar O_2, 140°C, 5 mol% Ru to HMF)

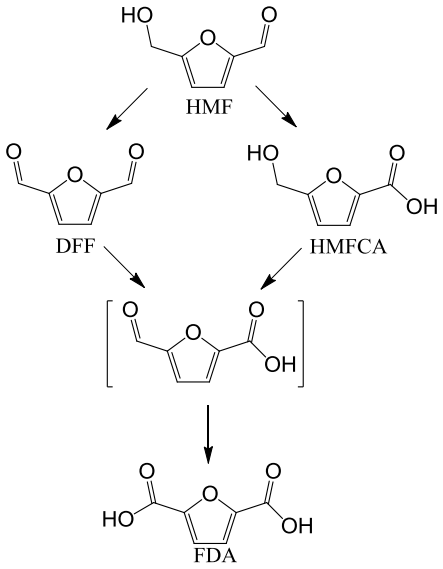

Scheme 3 Reaction pathway from HMF to FDA by aerobic oxidation via the competitive formation of the two intermediate products DFF and HMFCA

Fig. 3 shows the distribution of oxidation products obtained after oxidation of HMF for 1 h with $Ru(OH)_x$/HT catalyst at oxygen pressures of 1-40 bar and constant reaction temperature of 140°C. As shown in the figure, it proved possible to get full conversion of HMF within one hour by increasing the pressure of oxygen. Moreover, it is evident from the low pressure results that the oxygen pressure dependence was larger on DFF formation than on HMFCA formation (i.e. higher reaction order of oxygen in the rate expression for DFF formation), resulting in a higher rate of oxidation of the alcohol moiety on HMF compared to the aldehyde group. When performing the reaction at 10 bar for 1 h it proved therefore possible to form DFF with a relatively high selectivity of about 75 %.

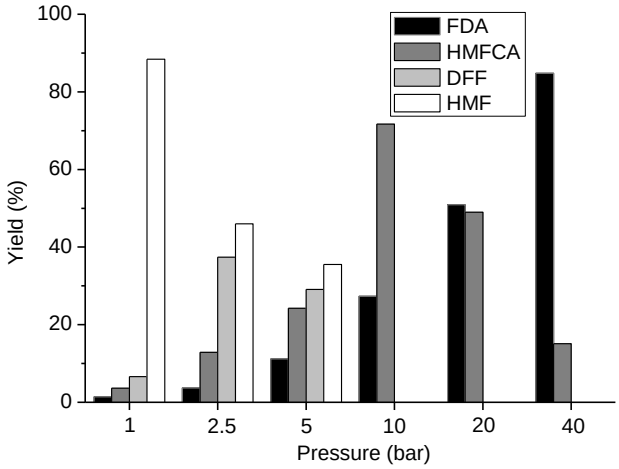

Fig. 3 Product yields in HMF oxidation with $Ru(OH)_x$/HT catalyst in water (0.05 M HMF, 1 h, 140°C, 5 mol% Ru to HMF)

In order to elucidate the temperature effect on product formation, a series of experiments were performed with $Ru(OH)_x$/HT catalyst with a reaction of 6 h with 2.5 bar of oxygen at different reaction temperatures (Fig. 4). The reaction temperature drastically affected the performance of the catalyst which converted essentially all the HMF within 6 h at 100°C and above. The major product formed at 100°C was HMFCA (about 80 %, with a selectivity of approximately 85 %) while only low amounts of FDA and DFF were formed (5-8 %). However, at higher temperatures only FDA was observed giving almost quantitative yield at 140°C. The absence of DFF after 6 h of reaction time is most likely a result of easier oxidation of the aldehyde functionality [38].

The stability of HMF under the applied reaction conditions was confirmed by conducting an experiment with pure HT support. Here HMF remained essentially unconverted with only ca. 2 % of HMF been oxidized and converted to HMFCA (1.3 %) and FDA (0.7 %), respectively.

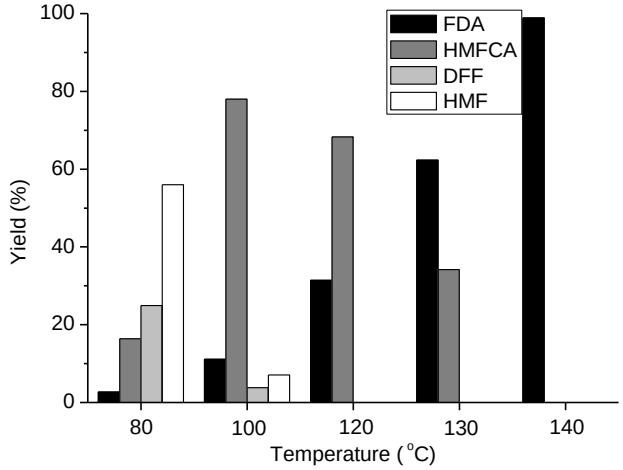

Fig. 4 Product yields in HMF oxidation with $Ru(OH)_x$/HT catalyst in water (0.05 M HMF, 6 h, 2.5 bar O_2, 5 mol% Ru to HMF)

To examine the effect of the support on the catalytic activity for the ruthenium-catalyzed conversion of HMF to FDA, catalysts with the alternative magnesium supports, MgO and $MgAl_2O_4$, were also prepared and tested in the oxidation reaction (characteristics of the supports and catalysts are shown in Table 1). The performance of the catalysts were tested under 2.5 bar of oxygen and 140°C, which was shown to be optimal reactions conditions for the HT supported catalyst (see Fig. 4). The obtained product yields as a function of reaction time are presented in Fig. 5a-c.

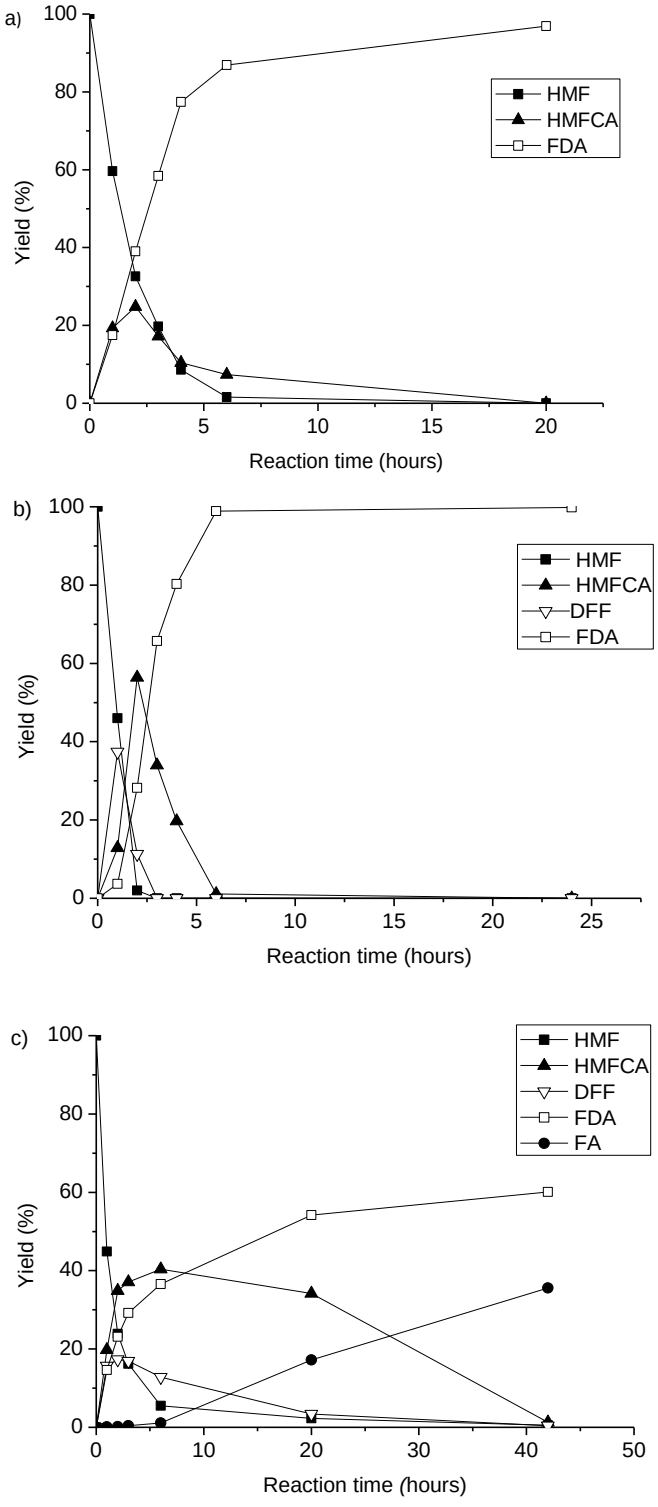

Fig. 5 Product yields in HMF oxidation with $Ru(OH)_x$ catalysts in water supported on (a) MgO, (b) HT or (c) $MgAl_2O_4$ (0.05 M HMF, 2.5 bar O_2, 140°C, 5 mol% Ru to HMF)

The results in Fig. 5 demonstrate that $Ru(OH)_x$ supported on MgO or HT under the applied reaction conditions was able to convert almost all of HMF to FDA, as expected. However, for the $Ru(OH)_x/MgAl_2O_4$ catalyst (Fig. 5c) the activity was lower, resulting in a yield of 60 % of FDA after 42 h. Furthermore, a substantial amount (35 %) of formic acid was formed after 42 h with this catalyst. Formic acid, in accordance with literature, may originate from degradation of HMF and FDA [39]. Interestingly, no degradation products were observed when the more basic supports magnesium oxide and hydrotalcite were used. Recently, Corma and co-workers reported that usage of ceria-supported gold catalyst in HMF oxidation in basic aqueous media led to formation of both ring-opening degradation products and 2-furoic acid [40].

To increase the yield of FDA and limit the formation of formic acid when using $Ru(OH)_x/MgAl_2O_4$, the effect of oxygen pressure on the HMF oxidation was further investigated. Reactions were performed at 140°C with a reaction time of 1 h (Fig. 6).

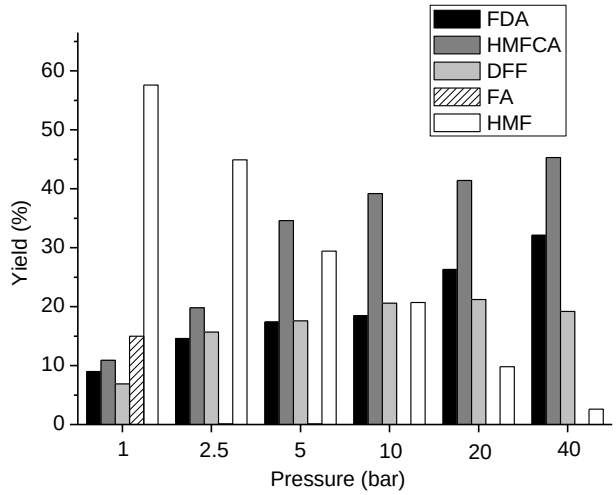

Fig. 6 Product yields in HMF oxidation with $Ru(OH)_x/MgAl_2O_4$ catalyst in water (0.05 M HMF, 1 h, 140°C, 5 mol% Ru to HMF)

Using the $Ru(OH)_x/MgAl_2O_4$ catalyst the yield of HMFCA and FDA increased when the oxygen pressure was increased, especially up to 5 bar as also found for the $Ru(OH)_x$/HT catalyst (see Fig. 3). Notably, however, an increase in dioxygen pressure from 1 to 2.5 bars resulted in significantly lower formation of formic acid – from 15 to 0.1 %. Based on this observation, the time dependence experiment with the spinel-based catalyst was redone at 5 bar (Fig. 7) instead of 2.5 bar (see Fig. 5c) in order to minimize the byproduct.

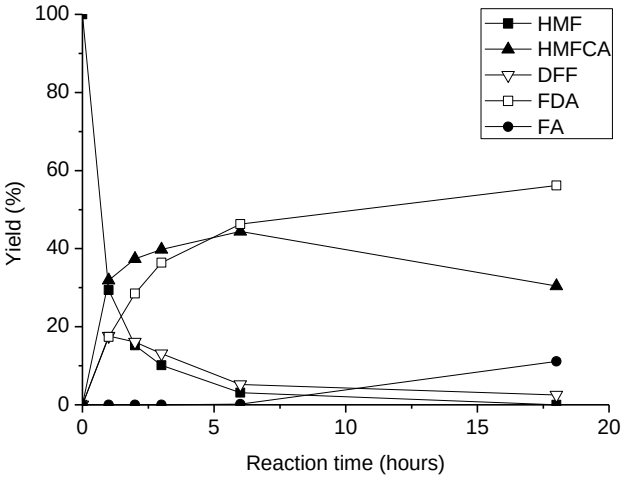

Fig. 7 Product yields in HMF oxidation with $Ru(OH)_x/MgAl_2O_4$ catalyst in water (0.05 M HMF, 5 bar O_2, 140°C, 5 mol% Ru to HMF)

From Fig. 5c and 7 it is clear that at both 2.5 and 5 bar of dioxygen pressure formic acid formation initiated as the reaction progressed and high relative concentration of the products (i.e. HMFCA, DFF and FDA) accumulated. This indicated that a gradual increase in acidity of the media due to FDA formation could induce furan cycle decomposition. To understand these results in more detail, a control experiment with only $Ru(OH)_x/MgAl_2O_4$ catalyst and FDA (10 ml H_2O, 0.078 g (0.5 mmol) FDA, 2.5 bar O_2, 140^{o}C, 16 h) was performed to test the stability of FDA in the presence of the catalyst. The experiment revealed that 78 % of the initial amount of FDA remained unconverted after the 16 h of reaction whereas partial degradation led to formation of 18 % formic acid. This clearly established the formic acid - at least partially – to originate from FDA, and possibly also from HMF or the intermediate products HMFCA and DFF. Accordingly, it is possible to limit the formation of formic acid in the reaction when using $Ru(OH)_x/MgAl_2O_4$ catalyst by applying short reaction time and high relative oxygen pressure.

Application of different magnesium-containing supports resulted in different amounts and distributions of products (see Fig. 5a-c). To understand this difference post-reaction solutions from experiments with each of the catalysts were analyzed by ICP for magnesium and ruthenium content (Table 2).

Table 2 ICP analysis of the post-reaction solutions from the aerobic HMF oxidation using supported $Ru(OH)_x$ catalysts (0.05 M HMF, 2.5 bar O_2, 140°C, 5 mol% Ru to HMF)

Entry	Support	$[Mg^{2+}]$ (g/L)	Mg dissolved (%)[c]	$[Ru^{n+}]$ (mg/L)	Ru dissolved (%)[c]	pH[d]
1[a]	HT	0.980	26	0.030	0.013	7
2[a]	MgO	1.590	38	0.035	0.015	10
3[b]	$MgAl_2O_4$	0.157	0.9	0.046	0.020	2

[a]Measured after 6 h of reaction. [b]Measured after 42 h of reaction. [c]Based on the overall element loading. [d]Measured pH values of the post-reaction solutions.

The ICP analysis confirmed presence of magnesium ions in all post-reaction solutions. Especially, for the HT- and MgO-supported catalysts (Table 2, entries 1 and 2) the amount of leached magnesium was high (26-38 %). Notably, the concentration of Mg^{2+}-ions leached from the HT-supported catalyst corresponded to about the amount (i.e. concentration) of FDA formed, thus indicating that the HT support acted as a solid base in the reaction and ionized the FDA to form a Mg-salt which most likely proved more stable towards degradation. Interestingly, hydrotalcite-supported gold nanoparticle catalyst was, in contrast, recently reported to be reusable and apparently stable in the oxidation of HMF in water under ambient oxygen pressure and elevated temperature [41].

For the MgO support a similar tendency was also observed. The fact that HT dissolved during reaction and neutralized some of the formed FDA also explains the otherwise unexpected neutral pH value measured of the post-reaction solution. Similarly, the high pH value of 10 in the post-reaction solution with magnesium oxide support can be associated to its enhanced dissolution under the reaction conditions (Table 2, entry 2).

As the basicity of the respective support decreases in the order MgO>HT>$MgAl_2O_4$ [42], the absence of the DFF product in the HMF oxidation reaction with magnesium oxide support (Fig. 5a) might be further explained by the highly basic media (Table 2), possibly facilitating Cannizzaro reaction of the dialdehyde. Single crystal XRD analysis of the isolated Mg-FDA salt will be reported in due course.

In contrast to the HT and MgO supports, the spinel support remained significantly more stable under the reaction conditions permitting only a small amount (0.9 %) of the magnesium to dissolve in the acidic post-reaction solution. Accordingly, the formation of formic acid when using $MgAl_2O_4$ support can be rationalized to be related to lower stability and higher degradation of FDA and HMF in acidic media. In line with this, no degradation of substrate were observed in reactions with catalysts based on the HT and MgO supports, since the solutions here were maintained at high pH throughout the reactions due to partial dissolution of the supports. Additionally, the results of the XRPD analysis did not reveal any change in the spinel structure before and after its employment in the reaction (see Supplementary information, Fig. S1).

In Table 2 the measured amounts of ruthenium in the post-reaction solutions are also reported. Importantly, only an extremely small amount (0.01-0.02 %) of the ruthenium metal on the catalysts was dissolved in the examined post-reaction solutions, thus making especially the $Ru(OH)_x/MgAl_2O_4$ catalyst

prone for re-use. Hence, an experiment was performed where this catalyst was recovered by filtration, washed with base and water (to remove any FDA precipitated on the surface of the catalyst after cooling down the reaction mixture) and re-used (Fig. 8). As seen from the results, the spinel-supported ruthenium catalyst preserved its initial activity clearly making this stable heterogeneous $Ru(OH)_x$ oxidation catalysts interesting for further investigations.

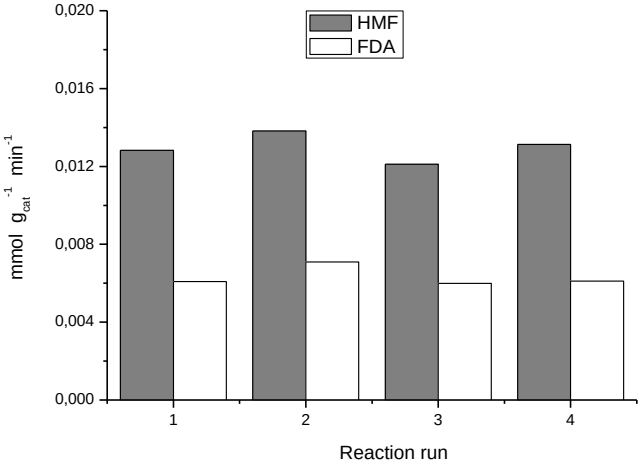

Fig. 8 Rates of HMF conversion and FDA formation per gram of the catalyst in the recycling of $Ru(OH)_x/MgAl_2O_4$ catalyst in water (0.05 M HMF, 5 bar O_2, 140°C, 5 mol% Ru to HMF, 6 hours of reaction time).

4 Conclusions

Supported catalysts with catalytically active $Ru(OH)_x$ species deposited on the three magnesium-based supports hydrotalcite (HT), magnesium oxide (MgO) and spinel ($MgAl_2O_4$), have been applied for aerobic oxidation of HMF to FDA in water without added base. All three catalysts were found to effectively catalyze the oxidation of HMF. However, both HT and MgO supports dissolved partly under the reaction conditions liberating significantly amounts of Mg^{2+} ions, thus making the mixtures basic. This resulted in formation of Mg-FDA salts stabilized against further degradation. The spinel support, on the other hand, remained stable under the reaction conditions which allowed performing the oxidation reaction under base free conditions.

The reported data suggests that the reaction pathway for aerobic oxidation of HMF to FDA with the $Ru(OH)_x$ supported catalysts proceed via relatively slow initial competitive oxidation to DFF and HMFCA (Scheme 3). The subsequent oxidations to form the product are fast since no other intermediates (e.g. 5-formylfuran-2-carboxylic acid) were observed.

Importantly, only very low amounts (<0.02 %) of the ruthenium metal inventory was found to dissolve from the catalysts (irrespectively of the support dissolution) under the applied reaction conditions. Combined with the observation that $Ru(OH)_x/MgAl_2O_4$ preserved its activity upon reuse, makes this and analogous catalyst systems based on stable supports attractive alternatives to present aerobic HMF

oxidation catalysts based on metal nanoparticles (e.g. gold catalysts), which often is less active upon reuse due to particle sintering [10, 43].

Acknowledgements

The authors thank Bodil Holten (Centre for Catalysis and Sustainable Chemistry, DTU Chemistry) for experimental assistance. The work was supported by The Danish National Advanced Technology Foundation and Novozymes A/S.

References

1. Rinaldi R, Schüth F (2009) Energy Environ Sci 2:610
2. Park J, Seyama T, Shiroma R, Ike M, Srichuwong S, Nagata K, Arai Sanoh Y, Kondo M, Tokuyasu K (2009) Biosci Biotechnol Biochem 73:1072
3. Schäfer T, Borchert TW, Nielsen VS, Skagerlind P, Gibson K, Wenger K, Hatzack F, Nilsson LB, Salmon S, Pedersen S, Heldt-Hansen HP, Poulsen PB, Lund H, Oxenbøll KM, Wu GF, Pedersen HH, Xu H (2007) Adv Biochem Eng Biotechnol 105:59
4. Du Z, Ma J, Wang F, Liu J, Xu J (2011) Green Chem 13:554
5. Navarro OC, Canós AC, Chornet SI (2009) Top Catal 52:34
6. Ma J, Du Z, Xu J, Chu Q, Pang Y (2011) ChemSusChem 4:51
7. Grabowski G, Lewkowski J, Skowroński R (1991) Electrochim Acta 36:1995
8. Lilga MA, Hallen RT, Hu J, White JF, Gray MJ (2008) US 20080103318
9. Casanova O, Iborra S, Corma A (2009) J Catal 265:109
10. Gorbanev YY, Klitgaard SK, Woodley JM, Christensen CH, Riisager A (2009) ChemSusChem 2:672
11. Taarning E, Nielsen IS, Egeblad K, Madsen R, Christensen CH (2008) ChemSusChem 1:75
12. Werpy T, Petersen G (2004) Top Value Added Chemicals from Biomass, 1: 26; available at: http://www.osti.gov/bridge
13. Bozell JJ, Petersen GR (2010) Green Chem 12:539
14. Boisen A, Christiansen TB, Fu W, Gorbanev YY, Hansen TS, Jensen JS, Klitgaard SK, Pedersen S, Riisager A, Ståhlberg T, Woodley JM (2009) Chem Eng Res Des 87:1318
15. Dijksman A, Arends IWCE, Sheldon RA (2001) Platinum Metals Rev 45:15
16. Chang S, Lee M, Ko S, Lee PH (2002) Synth Commun 32:1279
17. Vanover E, Huang Y, Xu L, Newcomb M, Zhang R (2010) Org Lett 12:2246
18. Zhai Y, Liu H, Liu B, Liu Y, Xiao J, Bai W (2007) Trans Met Chem 32:570
19. Lei ZQ, Kang QX, Bai XZ, Yang ZW, Zhang QH (2005) Chin Chem Lett 16:846
20. Farmer V, Welton T (2002) Green Chem 4:97
21. Vocanson F, Guo YP, Namy IL, Kagan HB (1998) Synth Commun 28:2577
22. Ji H, Mizugaki T, Ebitani K, Kaneda K (2002) Tetrahedron Lett 43:7179
23. Musawir M, Davey PN, Kelly G, Kozhevnikov IV (2003) Chem Commun 1414
24. Venkatesan S, Kumar AS, Lee J-F, Chan T-S, Zen J-M (2009) Chem Commun 1912
25. Yamaguchi K, Mori K, Mizugaki T, Ebitani K, Kaneda K (2000) J Am Chem Soc 122:7144
26. Mori K, Yamaguchi K, Mizugaki T, Ebitani K, Kaneda K (2001) Chem Commun 461
27. Yamaguchi K, Mizuno N (2003) Chem Eur J 9:4353
28. Kotani M, Koike T, Yamaguchi K, Mizuno N (2006) Green Chem 8:735
29. Kim JW, Yamaguchi K, Mizuno N (2008) Angew Chem Int Ed 47: 9249
30. Mizuno N, Yamaguchi K (2008) Catal Today 132:18
31. Yamaguchi K, Mizuno N (2010) Synlett 16:2365
32. Bavykin DV, Lapkin AA, Kolaczkowski ST, Plucinski PK (2005) Appl Catal A 288:175
33. Kaneda K, Yamashita T, Matsushita T, Ebitani K (1998) J Org Chem 63:1750
34. Matsushita T, Ebitani K, Kaneda K (1999) Chem Commun 265
35. Opre Z, Grunwaldt J-D, Maciejewski M, Ferri D, Mallat T, Baiker A (2005) J Catal 230:406
36. Opre Z, Grunwaldt J-D, Mallat T, Baiker A (2005) J Mol Catal A 242:224
37. Gorbanev YY, Kegnæs S, Riisager A (2011) Top Catal (accepted for publication)
38. Marsden C, Taarning E, Hansen D, Johansen L, Klitgaard SK, Egeblad K, Christensen CH (2008) Green Chem 10:168
39. Lewkowski J (2001) AKRIVOC (i) 17-54.

40. Casanova O, Iborra S, Corma A (2009) ChemSusChem 2:1138
41. Gupta NK, Nishimura S, Takagaki A, Ebitani K (2011) Green Chem 11:824
42. Di Cosimo JI, Diez VK, Xu M, Iglesia E, Apesteguia CR (1998) J Catal 178:499
43. Hashmi ASK, Hutchings G (2006) Angew Chem Int Ed 45:7896

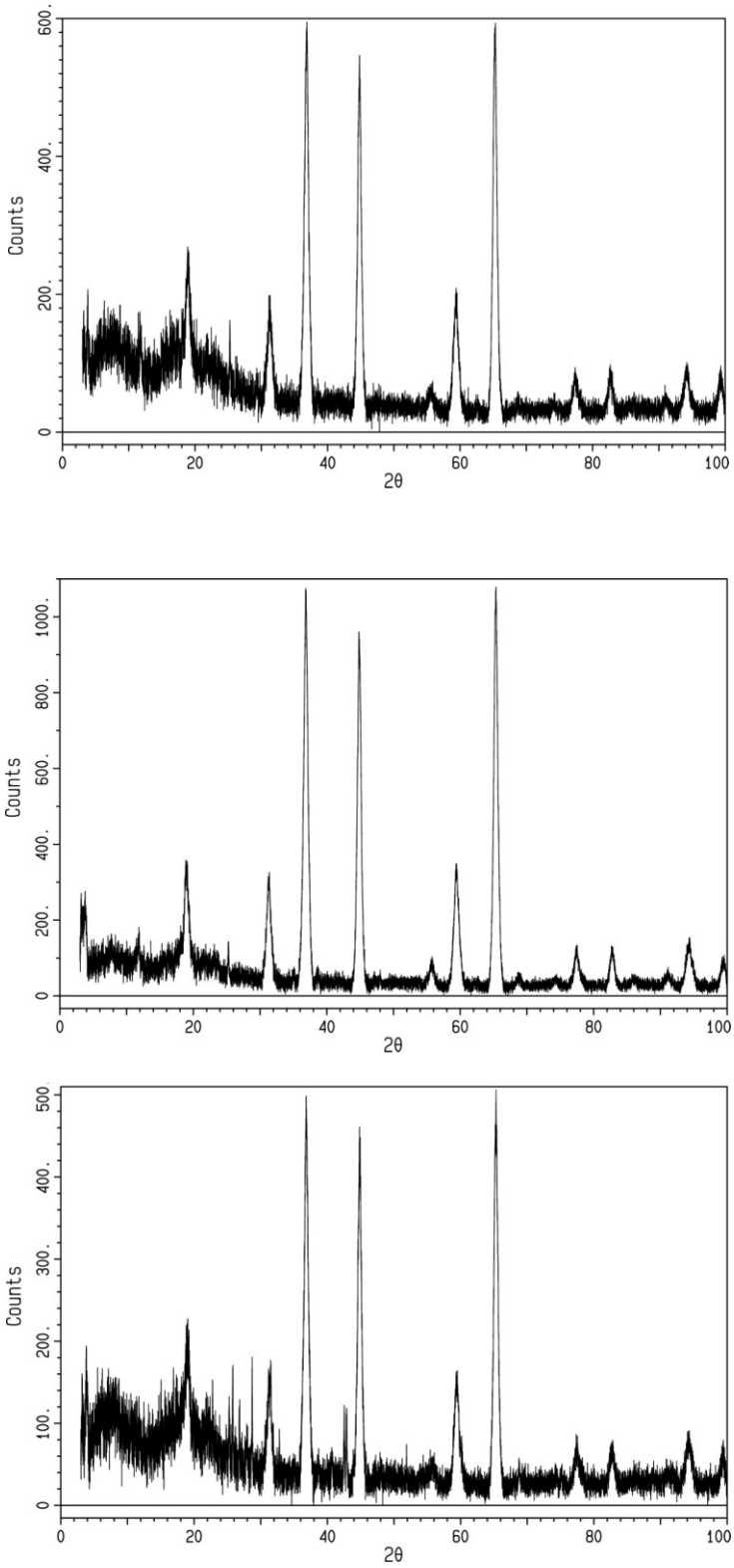

Figure S1. XRPD diffractograms of pure spinel $MgAl_2O_4$ (top), 2.4 wt% $Ru(OH)_x/MgAl_2O_4$ before (center) and after the reaction (bottom). Reaction conditions: 10 mL of 0.05 M HMF, 140°C, 5 mol% Ru, 5 bar O_2, 18 hours of reaction time.

Aerobic Oxidation of 5-(Hydroxymethyl)furfural in Ionic Liquids with Heterogeneous Ruthenium Catalysts

Tim Ståhlberg, Ester Eyjólfsdóttir, Yury Y. Gorbanev and Anders Riisager*

May 9, 2011

Abstract

The aerobic oxidation of 5-(hydroxymethyl)furfural was investigated over heterogeneous ruthenium hydroxide catalyst in ionic liquids. Several different catalyst supports together with several different ionic liquids were tested. The best result was obtained in [EMIm][OAc] at 30 bar of oxygen over $Ru(OH)_x/La_2O_3$ which afforded 48 % of FDA. Catalytic activity was detected in the ionic liquid after the catalyst was filtered off revealing that the oxidation was partially homogeneous.

1 Introduction

In all segments of the chemical industry oxidations of various functional groups play a vital role in the derivatization of chemical compounds. This has traditionally been made with stoichiometric reagents such as chromium(VI) compounds, permanganate, iodate compounds and peroxy acids [1] which have toxicity issues and produce a large amount of waste per kilo formed product. [2] In order to relinquish the use of these reagents the chemical industry and the scientific community are pursuing oxidations

*Centre for Catalysis and Sustainable Chemistry, Department of Chemistry, Technical University of Denmark, DK-2800 Kgs. Lyngby, Denmark, E-mail: ar@kemi.dtu.dk

with environmentally benign oxidants such as hydrogen peroxide and molecular oxygen together with efficient and selective catalysts.[3,4]

Recently the group of Yamaguchi[5] developed a heterogeneous ruthenium hydroxide catalyst that has proven to be a versatile and highly active catalyst for aerobic oxidations. The catalyst works exceedingly well connection with common functional group transformations such as oxidations of alcohols[6] and the oxygenation of primary amines to amides.[7]

Ionic liquids (ILs) are interesting alternatives to conventional molecular solvents due to their negligible vapor pressure, non-flammability and unique dissolving abilities for polar compounds.[8] Oxidations in ILs have been widely studied for several applications such as the oxidative Glaser coupling,[9] functional group oxidations such as alcohols to aldehydes or ketones[10] and the oxidation of alkanes.[11] Several examples of epoxidations of alkenes[12] and other miscellaneous functional group transformations[13] in ILs are also found in the literature. In most cases the oxidant is H_2O_2, but also stoichiometric reagents such as NaOCl, Dess-Martin periodate, MnO_2 and *meta*-chloroperoxybenzoic acid (mCPBA) have been reported. The most commonly employed ILs are 1-butyl-3-methylimidazolium tetrafluoroborate ([BMIm][BF_4]) and 1-butyl-3-methylimidazolium hexafluorophosphate ([BMIm][PF_6]). The ideal oxidant in a green chemical process is molecular oxygen and aerobic oxidations over homogeneous catalysts in ILs have been reported by various groups.[14–16]

Deriving chemicals from biomass has received significant attention among chemists in later years. In particular 5-(hydroxymethyl)furfural (HMF), formed from the dehydration of hexose sugars, has been in the spotlight since it is believed to be an essential platform chemical in the future biopetrochemical industry.[17,18] An important derivative is 2,5-furandicarboxylic acid (FDA) formed from the oxidation of HMF and which is intended to replace terephtalic acid as a monomer in plastics.[19] The catalytic oxidation of HMF was initially studied by the group of van Bekkum using heterogeneous platinum and palladium catalysts.[20,21] This has been followed up in later years with studies on $Co(acac)_3$,[22] gold nanoparticles[23–25] and a more detailed study of platinum catalysts on different supports made by Lilga et al.[26] The oxidation of HMF goes via diformyl

furfural (DFF) or 5-hydroxymethyl-2-furancarboxylic acid (HMFCA) to 5-formyl-2-furancarboxylic acid (FFCA) which is rapidly converted to FDA.[20] HMF can also be oxidized to DFF selectively,[27,28] and to maleic anhydride using vanadium catalysts.[29] The different oxidation products of HMF are depicted in Scheme 1.

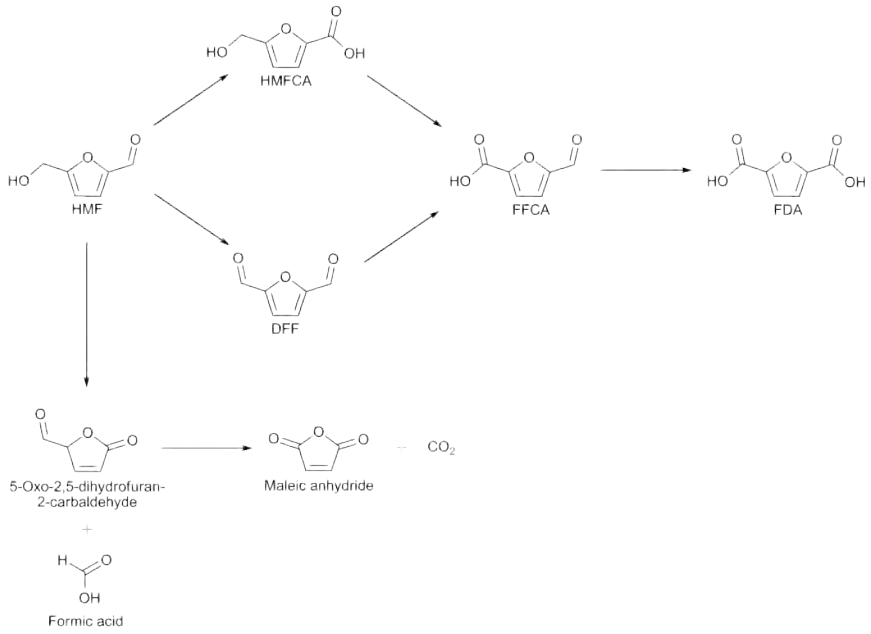

scheme 1: Different oxidation products of HMF.[20,29]

The synthesis of HMF from sugars benefits particularly from using certain ILs as solvents and an overall process from HMF to FDA in ILs would thus be advantageous.[30] In addition to this, the exceedingly low solubility of FDA in water and other conventional solvents makes an oxidation process of HMF in ILs by the use of heterogeneous catalysts a palpable option. In such a process the reaction mixture would be filtered from catalyst and water added to the resulting IL/FDA mixture making FDA precipitate. The aqueous IL would then be stripped of water and recycled.

To the best of our knowledge no investigation of heterogeneous catalysts for aerobic oxidations in ILs has been reported. Our objective in this study was to investigate the stability and performance of heterogeneous $Ru(OH)_x$ catalysts on different supports in ILs for the aerobic oxidation of HMF to FDA. The reaction was studied at different reaction conditions and leakage tests of ruthenium were made to investigate the stability

of the catalyst in ILs.

2 Experimental

2.1 Materials

5-Hydroxymethylfurfural (HMF) (>99%), 2-furoic acid (98%), levulinic acid (LA) (98%), formic acid (FA) (98%), ruthenium(III) chloride (purum), hydrotalcite (HT), magnetite (>98%), hydroxyapatite (HAp) (>97%), aluminium oxide (>99.9%), zirconium oxide (99%), lantanum(III) nitrate hexahydrate (99.99%) and sodium hydroxide (>98%) were acquired from Sigma-Aldrich. Ruthenium(III) nitrate hexahydrate (99.9%) and magnesium nitrate hexahydrate (p.a.) were obtained from Merck. Cerium oxide (99.5%) and lanthanum(III) oxide (99.9%) were purchased from Alfa Aesar. Magnesium oxide (p.a.) was purchased from Riedel-de Haën AG. 2,5-Diformylfuran (DFF) (98%) was obtained from ABCR GmbH & Co. 2,5-Furandicarboxylic acid (FDA) (>99%) and 5-hydroxymethyl-2-furan-carboxylic acid (HMFCA) (>99%) were purchased from Toronto Research Chemicals Inc. and dioxygen (99,5%) from Air Liquide Denmark. 1-ethyl-3-methylimidazolium dicynamide ([EMIm][$(CN)_2$]) and 1,3-dimethylimidazolium dimethyl phosphate ([MMIm][Me_2PO_4]) were purchased from Solvent Innovation while all other ionic liquids were obtained from BASF (>95 %). All chemicals were used as received.

All catalysts were synthesized according to literature.[Ref Yury] The screening experiments were performed using a Radley Carousel 12 Plus Basic System. High pressure oxidation reactions were carried out in stirred Parr autoclaves equipped with internal thermocontrol (T316 steel, Teflon^{TM} beaker insert, 100 ml). All samples were analyzed by HPLC (Agilent 1200 series, Bio-Rad Aminex HPX-87H, 300 mm x 7.8 mm pre-packed column, 0.005 M H_2SO_4 mobile phase, 60 ^oC, 0.6 mL/min).

2.2 Definitions of Yield and Selectivity

The yields and selectivities were based on conversion of HMF and confirmed by calibration of standard solutions of the products and reactants involved.

$$\texttt{HMF conversion} = \frac{1 - (\texttt{HMF concentration in product})}{\texttt{Starting amount of HMF}} \tag{1}$$

$$\texttt{Yield FDA/HMFCA/DFF} = \frac{\texttt{Amount of FDA/HMFCA/DFF}}{\texttt{Starting amount of HMF}} \tag{2}$$

2.3 Reaction procedure for screening experiments at ambient pressure

Catalyst (100 mg, 0.025 mmol Ru) and IL (1.0 g) were mixed in a 40 mL tube and stirred at 140 ^{o}C for 10 minutes. HMF (70 mg, 0.56 mmol) was added and the mixture was stirred in an open flask for 24 hours. The reaction was cooled down to ambient temperature and diluted to 10 mL with 0.1 M NaOH. The catalyst was filtered off and the resultant solution analyzed by HPLC.

2.4 Reaction procedure for high pressure experiments

Catalyst (0.5 g, 0.125 mmol Ru), HMF (350 mg, 2.78 mmol) and IL (12.0 g) were mixed in a Parr autoclave, pressurized with dioxygen (10 bar) and stirred at 140 ^{o}C for 5 hours. The reaction was cooled down to ambient temperature and diluted to 100 mL with 0.1 M NaOH. The catalyst was filtered off and the resultant solution analyzed by HPLC.

2.5 Reaction procedure for leakage test

Catalyst (100 mg, 0.025 mmol Ru) and [EMIm][OAc] (1.0 g) were mixed in 40 mL tube and stirred at 100 ^{o}C for 3 hours. The catalyst was filtered off affording a black colored liquid. HMF (70 mg, 0.56 mmol) was added to the liquid and the mixture was stirred in an open flask at 100 ^{o}C for 24 hours. The reaction was cooled down

to ambient temperature, diluted to 10 mL with 0.1 M NaOH, filtered and analyzed by HPLC.

3 Results and discussion

The ILs best suited for the synthesis of HMF from fructose or glucose has proven to be 1-ethyl-3-methylimidazolium chloride ([EMIm]Cl) and 1-butyl-3-methylimidazolium chloride ([BMIm]Cl).[30] An initial screening of $Ru(OH)_x$ on various supports in [EMIm]Cl was thus made. A high temperature was chosen in order to reduce the impact of viscosity of the mixture formed between the catalyst and IL. The screening was meant to be a comparison between the different types of supports and the lower solubility of oxygen at elevated temperature was at this stage disregarded. The experiments were made in open tubes with magnetic stirring. The results are shown in Table 1.

Table 1: HMF oxidation in [EMIm]Cl with $Ru(OH)_x$ on various supports as catalyst.[a]

		Conversion (%)	Molar Yield (%)		
Entry	Catalyst	HMF	DFF	HMFCA	FDA
1	$Ru(OH)_x/TiO_2$	92	0	1	3
2	$Ru(OH)_x$/spinel	89	0	7	3
3	$Ru(OH)_x/Fe_2O_3$	99	0	14	5
4	$Ru(OH)_x/ZrO_2$	84	0	3	5
5	$Ru(OH)_x/CeO_2$	86	0	7	4
6	$Ru(OH)_x$/HAp	81	0	4	4
7	$Ru(OH)_x$/HT	100	0	20	5
8	$Ru(OH)_x$/MgO	100	0	20	2
9	$Ru(OH)_x/La_2O_3$	100	0	25	1

[a] Reaction conditions: 1.0 g [EMIm]Cl, 68 mg (0.54 mmol) HMF, 100 mg catalyst (2.5 wt% Ru), 140 °C, 24 hours, ambient pressure.

All catalysts exhibited activity in the IL. The yield of FDA was nevertheless low, but an indication of which catalysts were the most promising candidates for further study could be derived from the yields of HMFCA. The best catalysts were $Ru(OH)_x/Fe_2O_3$, $Ru(OH)_x$/HT, $Ru(OH)_x$/MgO and $Ru(OH)_x/La_2O_3$, which gave yields of HMFCA in the range of 14-25 %. Notably, no DFF was observed in any of these experiments.

After activity had been proven, albeit with low yields, the study was expanded to include more ILs. Our study did not include [BMIm][BF_4] and [BMIm][PF_6] which were commonly employed in the early publications on oxidation in ILs. These tend to form HF upon contact with moisture which could be detrimental to reaction in-

termediates as well as catalyst. The ions of the ILs chosen are depicted in Scheme 1. The most promising catalysts from the first screening together with the catalyst that had proven to be best in water, $Ru(OH)_x/CeO_2$[Ref: Yury] were tested. Additionally, the catalyst precursor $RuCl_3$ was included for comparison. Most of the reactions afforded very low yields for the different oxidation products and only a few exceptions gave interesting results for further studies. For 1-ethyl-3-methylimidazolium acetate ([EMIm][OAc]) formation of FDA was observed with $Ru(OH)_x/La_2O_3$ and $Ru(OH)_x$/spinel. Surprisingly 6 % of FDA was also formed when using the $RuCl_3$ proving that the oxidation also worked under homogeneous conditions. Formation of HMFCA was also observed for all other catalysts in [EMIm][OAc] indicating that the oxygen solubility was higher compared to other ILs. Another IL that showed promise was 1-ethyl-3-methylimidazolium hydrogen sulfate ([EMIm][HSO_4]) that afforded 19 % FDA using $Ru(OH)_x$/HT. When employing $Ru(OH)_x/CeO_2$ in the same IL 9 % of DFF was formed while no other oxidation products were observed along with a slightly lower conversion for HMF compared to $Ru(OH)_x$/HT. The catalyst precursor $RuCl_3$ had no activity in [EMIm][HSO_4]. Two more ILs had noteworthy results, tributylmethylammonium methylsulfate ([Bu_3MeN][$MeOSO_3$]) and 1,2,4-trimethylpyrazolioum methylsulfate ([Me_3Pyraz][$MeOSO_3$]) both showed DFF formation when using $Ru(OH)_x$/spinel. The HMF conversion was much higher in [Me_3Pyraz][$MeOSO_3$] for $Ru(OH)_x$/spinel compared to $Ru(OH)_x/La_2O_3$ suggesting that some interaction with the IL and spinel resulted in species that had a detrimental effect on HMF stability. The results for the most interesting ILs are summarized in Table 2 while the complete screening of all ILs can be found in supporting information.

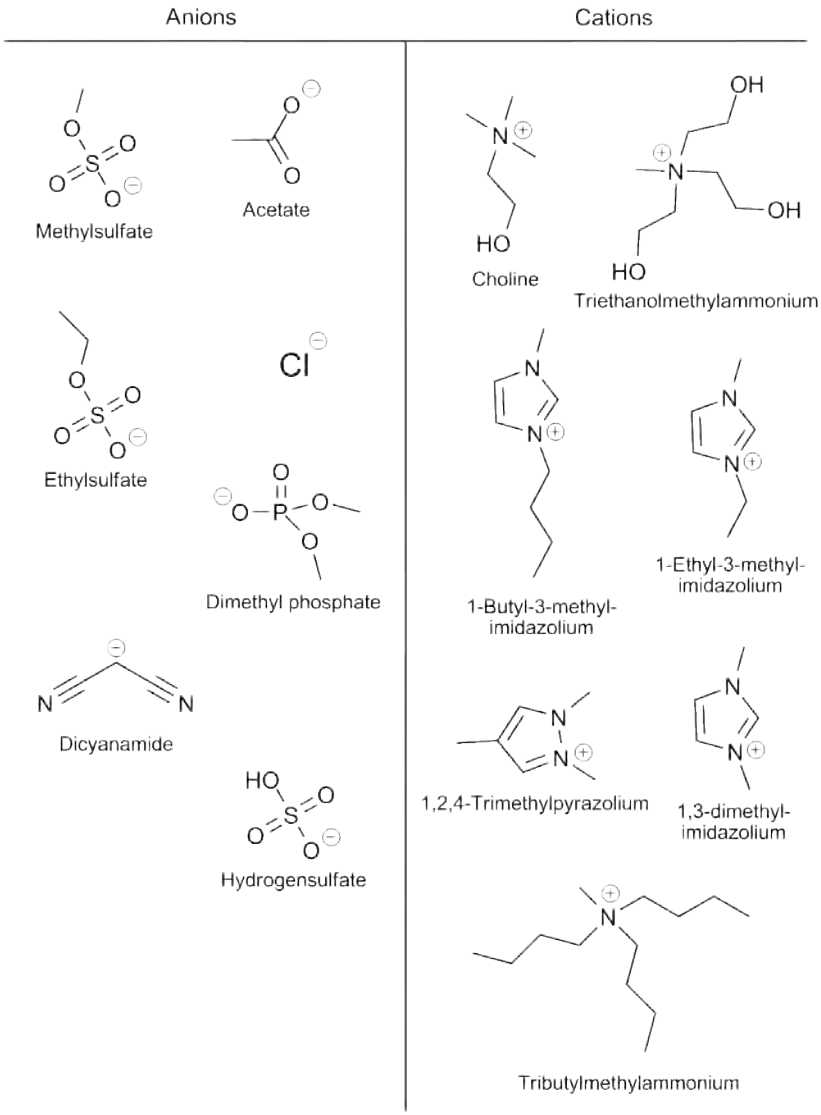

scheme 2: The cations and anions of the ILs used in the oxidation screening.

Table 2: HMF oxidation in different ILs with $Ru(OH)_x$ on various supports as catalyst.[a]

			Conversion (%)	Molar Yield (%)		
Entry	IL	Catalyst	HMF	DFF	HMFCA	FDA
1	[EMIm][HSO_4]	$Ru(OH)_x$/HT	99	1	0	19
2	[EMIm][HSO_4]	$Ru(OH)_x$/spinel	55	3	0	0
3	[EMIm][HSO_4]	$Ru(OH)_x/CeO_2$	77	9	1	0
4	[EMIm][HSO_4]	$RuCl_3$	84	0	0	0
5	[EMIm][HSO_4]	$Ru(OH)_x/La_2O_3$	71	3	0	0
6	[EMIm][OAc]	$Ru(OH)_x$/HT	93	0	13	0
7	[EMIm][OAc]	$Ru(OH)_x$/spinel	99	0	27	13
8	[EMIm][OAc]	$Ru(OH)_x/CeO_2$	55	1	2	0
9	[EMIm][OAc]	$RuCl_3$	100	0	27	6
10	[EMIm][OAc]	$Ru(OH)_x/La_2O_3$	100	0	30	10
11	[Bu_3MeN][$MeOSO_3$]	$Ru(OH)_x$/spinel	64	12	0	0
12	[Me_3Pyraz][$MeOSO_3$]	$Ru(OH)_x$/spinel	95	6	0	0
13	[Me_3Pyraz][$MeOSO_3$]	$Ru(OH)_x/La_2O_3$	46	10	0	0

[a] Reaction conditions: 1.0 g IL, 68 mg (0.54 mmol) HMF, 100 mg catalyst (2.5 wt% Ru), 140 °C, 24 hours, ambient pressure.

From our previous work[31] we knew that [EMIm][OAc] has a detrimental effect on HMF stability and decided therefore to investigate the effect of lowering the temperature. Both [EMIm][HSO_4] and [Bu_3MeN][$MeOSO_3$] proved to be very viscous in combination with the catalyst at 100 °C why experiments with these liquids were only performed at lower temperature in autoclave with mechanical stirring in the later high-pressure experiments. In Figure 1 the oxidation of HMF in [EMIm][OAc] with Ru(OH)x/spinel at 100 °C over time is shown. The final yield of FDA was lower than in the high-temperature experiments and no DFF was detected, whereas the yield of HMFCA was higher and almost amounted to 50 %. The conversion of HMF remained high accentuating the need of faster oxidation kinetics to avoid degradation.

The best result at 100 °C was obtained with La_2O_3 as support. The HMF conversion had reached maximum already after 6 hours which coincided with an HMFCA yield of 58 %. The amount of HMFCA then declined slowly to form FDA which reached a yield of around 10 % after 30 hours.

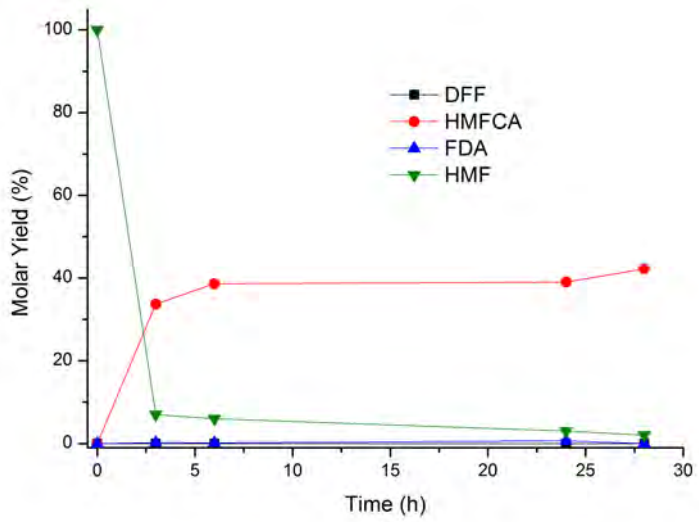

Figure 1: Oxidation of HMF with Ru(OH)x/spinel in [EMIm][OAc] at 100 °C.

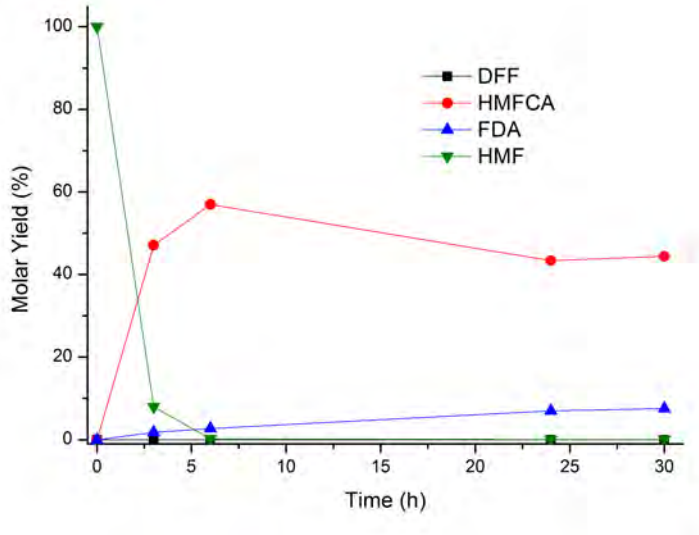

Figure 2: Oxidation of HMF with Ru(OH)x/La_2O_3 in [EMIm][OAc] at 100 °C.

3.1 High Pressure Oxidations

The open-flask experiments from above showed potential for oxidations at higher pressure. The generally low solubility of molecular oxygen in ILs leads to the assumption that pressures significantly higher than ambient are required to reach full conversion of HMFCA to FDA. In addition to the oxidation products in previous attempts at atmospheric pressure, formic acid (FA) was formed to various extent at higher pressure. A summary of the autoclave experiments is shown in Table 3.

Table 3: HMF oxidation in different ILs with $Ru(OH)_x$ on various supports as catalyst.[a]

					Conversion (%)	Molar Yield (%)			
Entry	IL	Catalyst	$P\,O_2$ (bar)	T (^oC)	HMF	FA	DFF	HMFCA	FDA
1	$[EMIm][HSO_4]$	$Ru(OH)_x$/spinel	10	140	58	0	3	1	0
2	[EMIm][OAc]	$Ru(OH)_x$/spinel	10	140	100	0	0	4	14
3	$[EMIm][HSO_4]$	$Ru(OH)_x$/HT	10	100	32	0	18	3	0
4	[EMIm][OAc]	$Ru(OH)_x/La_2O_3$	10	100	97	31	0	34	23
5	$[Bu_3MeN][MeOSO_3]$	$Ru(OH)_x$/HT	30	100	60	0	26	16	1
6	$[Bu_3MeN][MeOSO_3]$	$Ru(OH)_x$/spinel	30	100	62	0	18	26	3
7	$[EMIm][HSO_4]$	$Ru(OH)_x$/HT	30	100	52	0	25	8	0
8	[EMIm][OAc]	$Ru(OH)_x/La_2O_3$	30	100	98	30	0	12	48

[a] Reaction conditions: 12 g IL, 350 mg (2.78 mmol) HMF, 0.5 g catalyst (2.5 wt% Ru, 0.125 mmol), 5 hours.

The first autoclave experiments at 10 bar of dioxygen and 140 ^oC gave very different results depending on the IL and the catalyst. Using $Ru(OH)_x$/HT in $[EMIm][HSO_4]$ an identical FDA yield as in the open flask experiment was obtained, whereas $Ru(OH)_x/La_2O_3$ in [EMIm][OAc] actually resulted in a decrease in yield from 13 % to 10 %. The only improvement at 10 bar of dioxygen and 140 ^oC was obtained from $Ru(OH)_x$/HT in $[Bu_3MeN][MeOSO_3]$ which afforded an HMFCA yield of 30 % and an FDA yield of 10 %. The corresponding results for the open flask experiments were 12 % of DFF while no HMFCA or FDA was observed. All reactions showed an additional 10 % of FA, something which was not detected in the open flask experiments.

In the light of the results from lowering the temperature for the open flask experiments, high pressure attempts at 100 ^oC were conducted. For $Ru(OH)_x$/HT in $[EMIm][HSO_4]$ this resulted in a significant reduction in HMF conversion from 99 % to 32 % and no formation of FDA whereas HMFCA and DFF were afforded with 3 % and 18 % of yield respectively. This was most likely a consequence of higher viscosity making mixing more difficult, resulting in slower mass transfer. The same issue appeared in the case of $Ru(OH)_x$/spinel in $[Bu_3MeN][MeOSO_3]$ where the FDA yield was lowered from 10 % to 1 %. Improvement was observed at 100 ^oC for $Ru(OH)_x/La_2O_3$ in

[EMIm][OAc] where as much as 23 % of FDA was formed along with 34 % of HMFCA. Clearly the detrimental effect of [EMIm][OAc] for HMF stability was reduced and conversion to the desired product was favored when decreasing the temperature.

The final adjustment made was to increase the pressure even further to 30 bar. This gave a slight increase in HMF conversion from 32 to 52 % for $Ru(OH)_x$/HT in [EMIm][HSO_4], but still with no FDA formed. The best result was obtained for $Ru(OH)_x/La_2O_3$ in [EMIm][OAc] which afforded an FDA yield of as much as 48 % and an HMFCA yield of 12 %. In addition to this 30 % of FA was formed suggesting that some oxidative degradation was favored at elevated pressure [EMIm][OAc].

3.2 Leakage of Ruthenium

Heterogeneous catalysts can be sensitive to leakage of the active catalytic specie on the support, something which can be deceptive when interpreting experimental results. If there is leakage the catalysis is not necessarily heterogeneous but homogeneous which might make product recovery problematic. The conditions for the experiments above were such that leakage was not unlikely and the experiments using the catalyst precursor $RuCl_3$ at ambient pressure had already showed that the oxidation could also work homogeneously. High temperatures in combination with different ILs were harsh conditions why we decided to test the stability for our two most successful catalysts in [EMIm][OAc]. The catalysts were stirred in [EMIm][OAc] at 100 ^oC for three hours after which the catalysts were removed by hot filtration. The resultant liquid received a black color indicating that leakage ruthenium had occurred. To investigate if the black substance had a catalytical effect the IL was stirred in an open flask together with HMF for 24 hours. This afforded a substantial amount of HMFCA proving that the heterogeneous catalyst had leaked active catalytic specie into the IL and that the catalytic oxidation was at least partially homogeneous. The results are presented in Table 4.

Table 4: HMF oxidation in [EMIm][OAc] filtered off from $Ru(OH)_x/La_2O_3$ and $Ru(OH)_x$/spinel.[a]

	Conversion (%)	Molar Yield (%)		
Catalyst	HMF	DFF	HMFCA	FDA
$Ru(OH)_x/La_2O_3$	100	0	44	4
$Ru(OH)_x$/spinel	100	0	44	4

[a] Reaction conditions: 1.0 g [EMIm][OAc], 68 mg (0.54 mmol) HMF, 100 °C, 24 hours, ambient pressure.

4 Conclusions

The oxidation of HMF was investigated in various ILs and different types of heterogeneous ruthenium hydroxide catalysts. The IL best suited for the oxidation was [EMIm][OAc] which afforded an FDA yield of 48 % using $Ru(OH)_x$ on La_2O_3 support. The oxidation proved nevertheless to be homogeneous since experiments using an IL from which the catalyst was filtered off showed catalytic effect in the IL. The lower performance of some catalysts might in fact be the consequence of a higher stability which prevents leakage. A hetereogeneous mechanism in the ILs cannot be ruled out, even though the yields of the leakage tests were comparable to the ones using the normal procedure with the heterogeneous catalyst.

An apparent improvement of the yield was found when lowering the temperature and increasing the pressure. Even though [EMIm][OAc] is notorious in degrading HMF and naturally not ideal as solvent for HMF oxidation, its higher solubility for oxygen made it the best solvent in our experiments. In several ILs the stirring was limited because of high viscosity which most likely had an impact on mass transfer and consequently on conversion and yield.

In order to find a successful and suitable catalyst for large scale purposes for FDA production it would most likely benefit from being a homogeneous water soluble catalyst. This would enable an easy recovery of FDA after complete reaction by crystallization from water. The catalyst and IL would end up in the mother liquid and after removal of water the IL/catalyst system could be recycled for the next batch. A heterogeneous catalyst could still be an option if one with high resistance to the ILs in question could be obtained. Evidently, the catalysts presented herein prepared by the deposition-precipitation method make out catalysts that cannot withstand the combina-

tion of ILs even at moderate temperatures. Alternative heterogeneous aerobic catalysts would be of interest in a further study of this reaction as well as the study of other aerobic oxidations in ILs. The advantage of using an IL as solvent for aerobic oxidations with heterogeneous catalysts is obvious when your product or any of the reactants have low solubility in conventional solvents.

We believe that this work provides valuable insights about the scope and limitations of aerobic oxidations in ILs using heterogeneous ruthenium hydroxide catalysts. The study also shows that the IL [EMIm][OAc] worked well as a solvent for aerobic oxidations making it an attractive alternative as reaction media considering its unique dissolving properties. Our work will continue with the study of aerobic oxidations in ILs using heterogeneous catalysts prepared by different methods.

5 Acknowledgment

The reported work was supported by the Danish National Advanced Technology Foundation in cooperation with Novozymes A/S. Special gratitude to BASF for providing the ionic liquids.

References

[1] M. B. Smith and J. March, *March's Advanced Organic Chemistry: Reactions, Mechanisms, and Structure, 5th Edition.*, John Wiley & Sons, Ltd., 2000.

[2] R. A. Sheldon, *J. Mol. Catal. A: Chem.*, 1996, **107**, 75–83.

[3] B.-Z. Zhan and A. Thompson, *Tetrahedron*, 2004, **60**, 2917–2935.

[4] R. A. Sheldon, M. Wallau, I. W. C. E. Arends and U. Schuchardt, *Acc. Chem. Res.*, 1998, **31**, 485–493.

[5] K. Yamaguchi and N. Mizuno, *Synlett*, 2010, **2010**, 2365,2382–.

[6] M. Kotani, T. Koike, K. Yamaguchi and N. Mizuno, *Green Chem.*, 2006, **8**, 735–741.

[7] J. Kim, K. Yamaguchi and N. Mizuno, *Angew. Chem., Int. Ed.*, 2008, **47**, 9249–9251.

[8] P. Wasserscheid and T. Welton, *Ionic Liquids in Synthesis*, Wiley-VCH Verlag GmbH & Co. KGaA, 2008.

[9] J. Yadav, B. Reddy, K. Reddy, K. Gayathri and A. Prasad, *Tetrahedron Lett.*, 2003, **44**, 6493–6496.

[10] (*a*) J. Yadav, B. Reddy, A. Basak and A. Venkat Narsaiah, *Tetrahedron*, 2004, **60**, 2131–2135; (*b*) A. J. Walker and N. C. Bruce, *Tetrahedron*, 2004, **60**, 561–568; (*c*) X.-E. Wu, L. Ma, M.-X. Ding and L.-X. Gao, *Synlett*, 2005, **2005**, 607–610.

[11] (*a*) J. Peng, F. Shi, Y. Gu and Y. Deng, *Green Chem.*, 2003, **5**, 224–226; (*b*) Z. Li and C.-G. Xia, *J. Mol. Catal. A: Chem.*, 2004, **214**, 95–101.

[12] (*a*) G. S. Owens and M. M. Abu-Omar, *Chem. Commun.*, 2000, 1165–1166; (*b*) G. S. Owens, A. Durazo and M. M. Abu-Omar, *Chem.–Eur. J.*, 2002, **8**, 3053–3059; (*c*) K.-H. Tong, K.-Y. Wong and T. H. Chan, *Org. Lett.*, 2003, **5**, 3423–3425; (*d*) Z. Li and C.-G. Xia, *Tetrahedron Lett.*, 2003, **44**, 2069–2071; (*e*) R. Bernini, E. Mincione, A. Coratti, G. Fabrizi and G. Battistuzzi, *Tetrahedron*, 2004, **60**, 967–971.

[13] (*a*) R. D. Singer and P. J. Scammells, *Tetrahedron Lett.*, 2001, **42**, 6831–6833; (*b*) W.-H. Lo, H.-Y. Yang and G.-T. Wei, *Green Chem.*, 2003, **5**, 639–642; (*c*) J. S. Yadav, B. V. S. Reddy, A. K. Basak and A. V. Narsaiah, *Chem. Lett.*, 2004, **33**, 248–249; (*d*) B. Martiz, R. Keyrouz, S. Gmouh, M. Vaultier and V. Jouikov, *Chem. Commun.*, 2004, 674–675; (*e*) G. Bianchini, M. Crucianelli, F. D. Angelis, V. Neri and R. Saladino, *Tetrahedron Lett.*, 2005, **46**, 2427–2432.

[14] A. Wolfson, S. Wuyts, D. E. De, Vos, I. F. J. Vankelecom and P. A. Jacobs, *Tetrahedron Lett.*, 2002, **43**, 8107–8110.

[15] V. Farmer and T. Welton, *Green Chem.*, 2002, **4**, 97–102.

[16] (*a*) I. A. Ansari and R. Gree, *Org. Lett.*, 2002, **4**, 1507–1509; (*b*) J.-R. Wang, L. Liu, Y.-F. Wang, Y. Zhang, W. Deng and Q.-X. Guo, *Tetrahedron Lett.*, 2005, **46**, 4647–4651; (*c*) H. Sun, X. Li and J. Sundermeyer, *J. Mol. Catal. A: Chem.*, 2005, **240**, 119–122; (*d*) N. Jiang and A. J. Ragauskas, *Org. Lett.*, 2005, **7**, 3689–3692; (*e*) N. Jiang and A. J. Ragauskas, *Tetrahedron Lett.*, 2006, **48**, 273–276; (*f*) N. Jiang and A. J. Ragauskas, *J. Org. Chem.*, 2007, **72**, 7030–7033; (*g*) H.-Y. Shen, H.-L. Mao, L.-Y. Ying and Q.-H. Xia, *J. Mol. Catal. A: Chem.*, 2007, **276**, 73–79; (*h*) A. Shaabani, A. H. Rezayan, M. Heidary and A. Sarvary, *Catal. Commun.*, 2008, **10**, 129–131; (*i*) A. Shaabani, E. Farhangi and A. Rahmati, *Appl. Catal., A*, 2008, **338**, 14–19; (*j*) L. Lin, L. Ji and Y. Wei, *Catal. Commun.*, 2008, **9**, 1379–1382; (*k*) M. Dabiri, P. Salehi and M. Bahramnejad, *Synth. Commun.*, 2010, **40**, 3214–3225; (*l*) O. Basle, N. Borduas, P. Dubois, J. M. Chapuzet, T.-H. Chan, J. Lessard and C.-J. Li, *Chem.–Eur. J.*, 2010, **16**, 8162–8166; (*m*) C.-X. Miao, J.-Q. Wang, B. Yu, W.-G. Cheng, J. Sun, S. Chanfreau, L.-N. He and S.-J. Zhang, *Chem. Commun.*, 2011, **47**, 2697–2699.

[17] T. Werpy and G. Petersen, *US DOE*, 2004, **No. DOE/GO-102004-1992**, http://www.nrel.gov/docs/fy04osti/35523.pdf.

[18] J. J. Bozell and G. R. Petersen, *Green Chem.*, 2010, **12**, 539–554.

[19] A. Boisen, T. Christensen, W. Fu, Y. Gorbanev, T. Hansen, J. Jensen, S. Klitgaard, S. Pedersen, A. Riisager, T. Ståhlberg and J. Woodley, *Chem. Eng. Res. Des.*, 2009, **87**, 1318–1327.

[20] P. Vinke, H. van Dam and H. van Bekkum, *Stud. Surf. Sci. Catal.*, 1990, **55**, 147–158.

[21] P. Vinke, W. van der Poel and H. van Bekkum, *Stud. Surf. Sci. Catal.*, 1991, **59**, 385–394.

[22] M. L. Ribeiro and U. Schuchardt, *Catal. Commun.*, 2003, **4**, 83–86.

[23] E. Taarning, I. Nielsen, K. Egeblad, R. Madsen and C. Christensen, *ChemSusChem*, 2008, **1**, 75–78.

[24] Y. Gorbanev, S. Klitgaard, J. Woodley, C. H. Christensen and A. Riisager, *ChemSusChem*, 2009, **2**, 672–675.

[25] N. K. Gupta, S. Nishimura, A. Takagaki and K. Ebitani, *Green Chem.*, 2011, **13**, 824–827.

[26] M. A. Lilga, R. T. Hallen and M. Gray, *Top. Catal.*, 2010, **53**, 1264–1269.

[27] C. Carlini, P. Patrono, A. M. R. Galletti, G. Sbrana and V. Zima, *Appl. Catal., A*, 2005, **289**, 197–204.

[28] J. Ma, Z. Du, J. Xu, Q. Chu and Y. Pang, *ChemSusChem*, 2011, **4**, 51–54.

[29] Z. Du, J. Ma, F. Wang, J. Liu and J. Xu, *Green Chem.*, 2011, **13**, 554–557.

[30] T. Ståhlberg, W. Fu, J. M. Woodley and A. Riisager, *ChemSusChem*, 2011, n/a. doi: 10.1002/cssc.201000374.

[31] T. Ståhlberg, M. G. Sørensen and A. Riisager, *Green Chem.*, 2010, **12**, 321–325.

Aerobic Oxidation of 5-(Hydroxymethyl)furfural in Ionic Liquids with Solid Ruthenium Hydroxide Catalysts

Supporting info

Table S1. HMF oxidation in different ILs with various $Ru(OH_x$/support catalysts.

IL	Catalyst	DFF Yield	HMFCA yield	FDA Yield
[EMIm]Cl	$Ru(OH)_x$/HT	0,070804028	16,00630689	0,13295612
[BMIm]Cl	$Ru(OH)_x$/HT	0,10354173	17,51571666	0,16777805
[EMIm][HSO_4]	$Ru(OH)_x$/HT	0	0	0
[EMIm][$EtOSO_3$]	$Ru(OH)_x$/HT	0	3,816720246	0
[MMMPz][$MeOSO_3$]	$Ru(OH)_x$/HT	3,977328011	1,074896635	0,93905869
[EMIm][HSO_4]	$Ru(OH)_x$/HT	1,269877684	0,216654119	19,6389768
[EMIm][OAc]	$Ru(OH)_x$/HT	0	12,72391225	0
[$(EtOH)_3MeN$][$MeOSO_3$]	$Ru(OH)_x$/HT	0,43355294	0,089318233	0,01689616
[Bu_3MeN][$MeOSO_3$]	$Ru(OH)_x$/HT	2,081368893	2,38285229	1,06079244
[EMIm][$MeSO_3$]	$Ru(OH)_x$/HT	0	2,900268341	0,08257826
[EMIm][$(CN)_2$]	$Ru(OH)_x$/HT	0	4,162584992	0,40966956
[MMIm][dmp]	$Ru(OH)_x$/HT	0,11660439	3,766251617	1,2622931
[EMIm]Cl	$Ru(OH)_x$/spinel	0,026594644	6,666910062	2,37483207
[BMIm]Cl	$Ru(OH)_x$/spinel	0,02690033	8,270338732	1,9435581
[EMIm][HSO_4]	$Ru(OH)_x$/spinel	0	0	0
[EMIm][$EtOSO_3$]	$Ru(OH)_x$/spinel	0,432942168	1,757758785	2,24227279
[MMMPz][$MeOSO_3$]	$Ru(OH)_x$/spinel	6,385199575	0,054161206	0,01151869
[EMIm][HSO_4]	$Ru(OH)_x$/spinel	2,845183965	0,073801407	0,04317615
[EMIm][OAc]	$Ru(OH)_x$/spinel	0	26,99308961	13,2128887
[$(EtOH)_3MeN$][$MeOSO_3$]	$Ru(OH)_x$/spinel	0,953457889	0,032871346	0
[Bu_3MeN][$MeOSO_3$]	$Ru(OH)_x$/spinel	11,59681704	0,131071672	0,03921468
[EMIm][$MeSO_3$]	$Ru(OH)_x$/spinel	0,066793124	5,937930788	6,29130763
[EMIm][$(CN)_2$]	$Ru(OH)_x$/spinel	0	2,752721823	1,78676806
[MMIm][dmp]	$Ru(OH)_x$/spinel	0	4,800300555	3,45223524
[EMIm]Cl	$RuMnCe/CeO_2$	0,058546942	15,33721594	1,71921828
[BMIm]Cl	$RuMnCe/CeO_2$	0,072123117	18,06811352	1,88884855
[EMIm][HSO_4]	$RuMnCe/CeO_2$	5,589411028	0,403053449	0,02082786
[EMIm][$EtOSO_3$]	$RuMnCe/CeO_2$	0,399786039	0,276468717	1,79164542
[MMMPz][$MeOSO_3$]	$RuMnCe/CeO_2$	7,074472762	0,040708141	0,01724991
[EMIm][HSO_4]	$RuMnCe/CeO_2$	8,623083411	1,146372689	0,08420152
[EMIm][OAc]	$RuMnCe/CeO_2$	0	32,17892141	5,28716364
[$(EtOH)_3MeN$][$MeOSO_3$]	$RuMnCe/CeO_2$	1,106073965	0,02468869	0,01913795
[Bu_3MeN][$MeOSO_3$]	$RuMnCe/CeO_2$	4,982372876	0,069709599	0,09168695
[EMIm][$MeSO_3$]	$RuMnCe/CeO_2$	0,147045329	13,16018631	2,71089902
[EMIm][$(CN)_2$]	$RuMnCe/CeO_2$	0,914002119	1,249130562	2,21823921
[MMIm][dmp]	$RuMnCe/CeO_2$	0	5,860661978	0,67085913
[EMIm]Cl	$Ru(OH)_x/CeO_2$	0,064272978	1,174442238	4,06841574
[BMIm]Cl	$Ru(OH)_x/CeO_2$	0,067102594	2,389944131	2,22744141
[EMIm][HSO_4]	$Ru(OH)_x/CeO_2$	9,342746955	0,505718975	0,03140339

[EMIm][$EtOSO_3$]	$Ru(OH)_x/CeO_2$	0,869094509	0,704563573	0,65953931
[MMMPz][$MeOSO_3$]	$Ru(OH)_x/CeO_2$	2,864341637	0,47281649	0,24155566
[EMIm][HSO_4]	$Ru(OH)_x/CeO_2$	9,27996498	1,278926953	0,16175103
[EMIm][OAc]	$Ru(OH)_x/CeO_2$	1,008500243	1,745930103	0
[$(EtOH)_3MeN$][$MeOSO_3$]	$Ru(OH)_x/CeO_2$	0	30,09567456	7,28492069
[Bu_3MeN][$MeOSO_3$]	$Ru(OH)_x/CeO_2$	2,155178163	0,688323575	0,11817002
[EMIm][$MeSO_3$]	$Ru(OH)_x/CeO_2$	0,164582271	5,294319534	3,67200076
[EMIm][$(CN)_2$]	$Ru(OH)_x/CeO_2$	0,102409925	1,82046808	1,71042821
[MMIm][dmp]	$Ru(OH)_x/CeO_2$	0	4,314256671	1,11002854
[EMIm]Cl	$RuCl_3$	0,14310671	0,191459034	1,13665317
[BMIm]Cl	$RuCl_3$	0,079162156	0,306013093	2,06091135
[EMIm][HSO_4]	$RuCl_3$	0,036423904	0	0
[EMIm][$EtOSO_3$]	$RuCl_3$	0,471940036	0,425915764	0,01240707
[MMMPz][$MeOSO_3$]	$RuCl_3$	0,19665606	0,866128668	0,04030946
[EMIm][HSO_4]	$RuCl_3$	0,266778126	0,309619266	0,01240687
[EMIm][OAc]	$RuCl_3$	0,010402806	27,43259885	5,77204508
[$(EtOH)_3MeN$][$MeOSO_3$]	$RuCl_3$	0,810016718	5,84819074	0
[Bu_3MeN][$MeOSO_3$]	$RuCl_3$	0,673715719	0,423466196	0,45570047
[EMIm][$MeSO_3$]	$RuCl_3$	0,187405879	3,212126035	0,71398912
[EMIm][$(CN)_2$]	$RuCl_3$	0	2,722222707	1,33974239
[MMIm][dmp]	$RuCl_3$	0	4,89587498	0,64857314
[EMIm]Cl	$Ru(OH)_x/La_2O_3$	0,063292501	15,47691771	4,1646279
[BMIm]Cl	$Ru(OH)_x/La_2O_3$	0,369143712	13,48579416	1,67004139
[EMIm][HSO_4]	$Ru(OH)_x/La_2O_3$	4,673761673	0,030935694	0,01358797
[EMIm][$EtOSO_3$]	$Ru(OH)_x/La_2O_3$	0,042753936	3,563086131	2,4808596
[MMMPz][$MeOSO_3$]	$Ru(OH)_x/La_2O_3$	10,16178723	0,175311633	0,17676204
[EMIm][HSO_4]	$Ru(OH)_x/La_2O_3$	2,563480162	0,307852349	0,5863205
[EMIm][OAc]	$Ru(OH)_x/La_2O_3$	0	30,1392822	9,1913886
[$(EtOH)_3MeN$][$MeOSO_3$]	$Ru(OH)_x/La_2O_3$	0,438441628	0,087412714	0
[Bu_3MeN][$MeOSO_3$]	$Ru(OH)_x/La_2O_3$	1,614752118	0,692251445	0,15246527
[EMIm][$MeSO_3$]	$Ru(OH)_x/La_2O_3$	0,0585291	6,333034403	2,72253238
[EMIm][$(CN)_2$]	$Ru(OH)_x/La_2O_3$	0	1,723834128	2,02854364
[MMIm][dmp]	$Ru(OH)_x/La_2O_3$	0	5,892046083	0,82151138

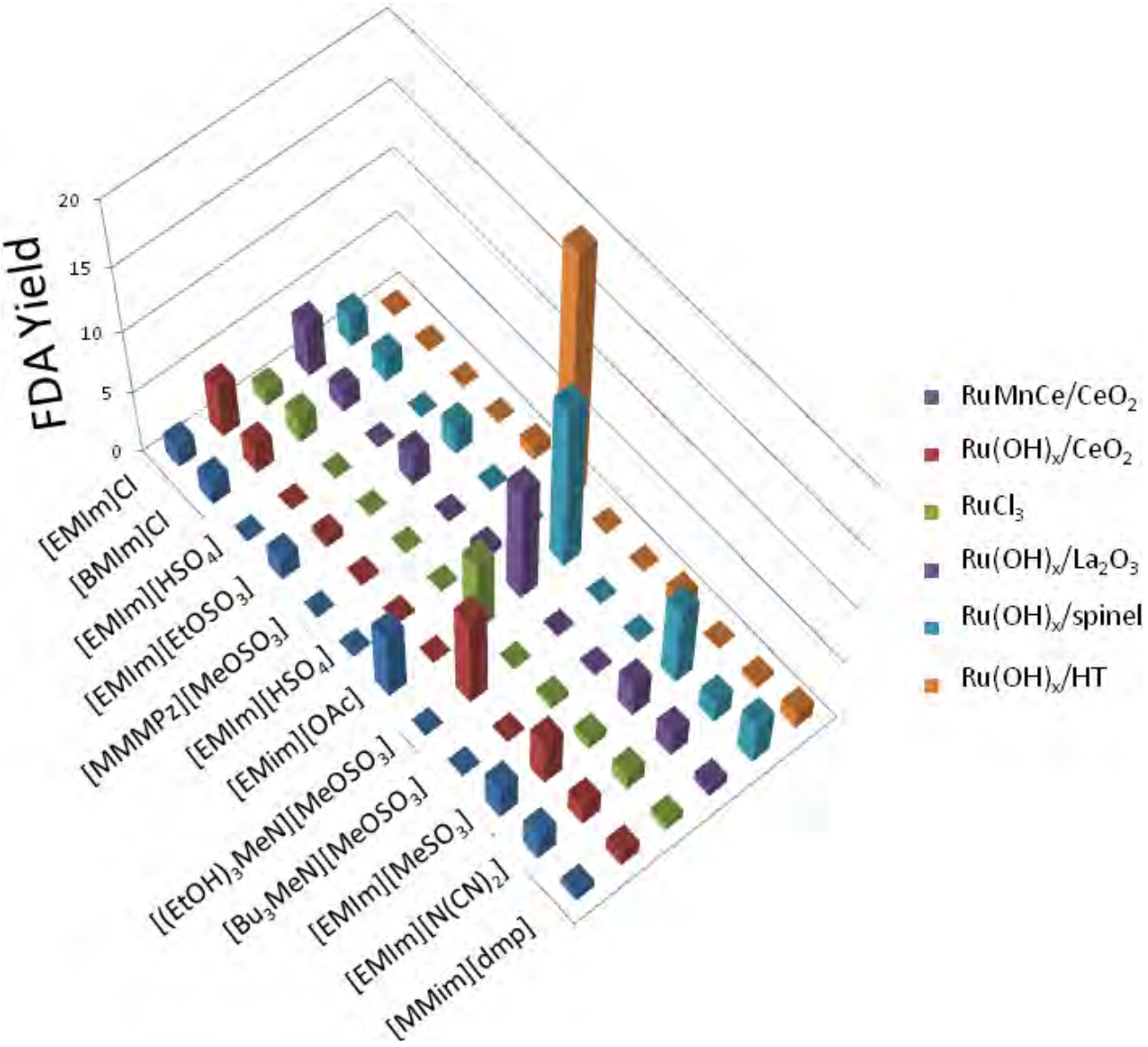
FDA Yield
20
15
10
5
0
[EMIm]Cl
[BMIm]Cl
[EMIm][HSO4]
[EMIm][EtOSO3]
[MMMPz][MeOSO3]
[EMIm][HSO4]
[EMim][OAc]
[(EtOH)3MeN][MeOSO3]
[Bu3MeN][MeOSO3]
[EMIm][MeSO3]
[EMIm][N(CN)2]
[MMim][dmp]
RuMnCe/CeO2
Ru(OH)x/CeO2
RuCl3
Ru(OH)x/La2O3
Ru(OH)x/spinel
Ru(OH)x/HT

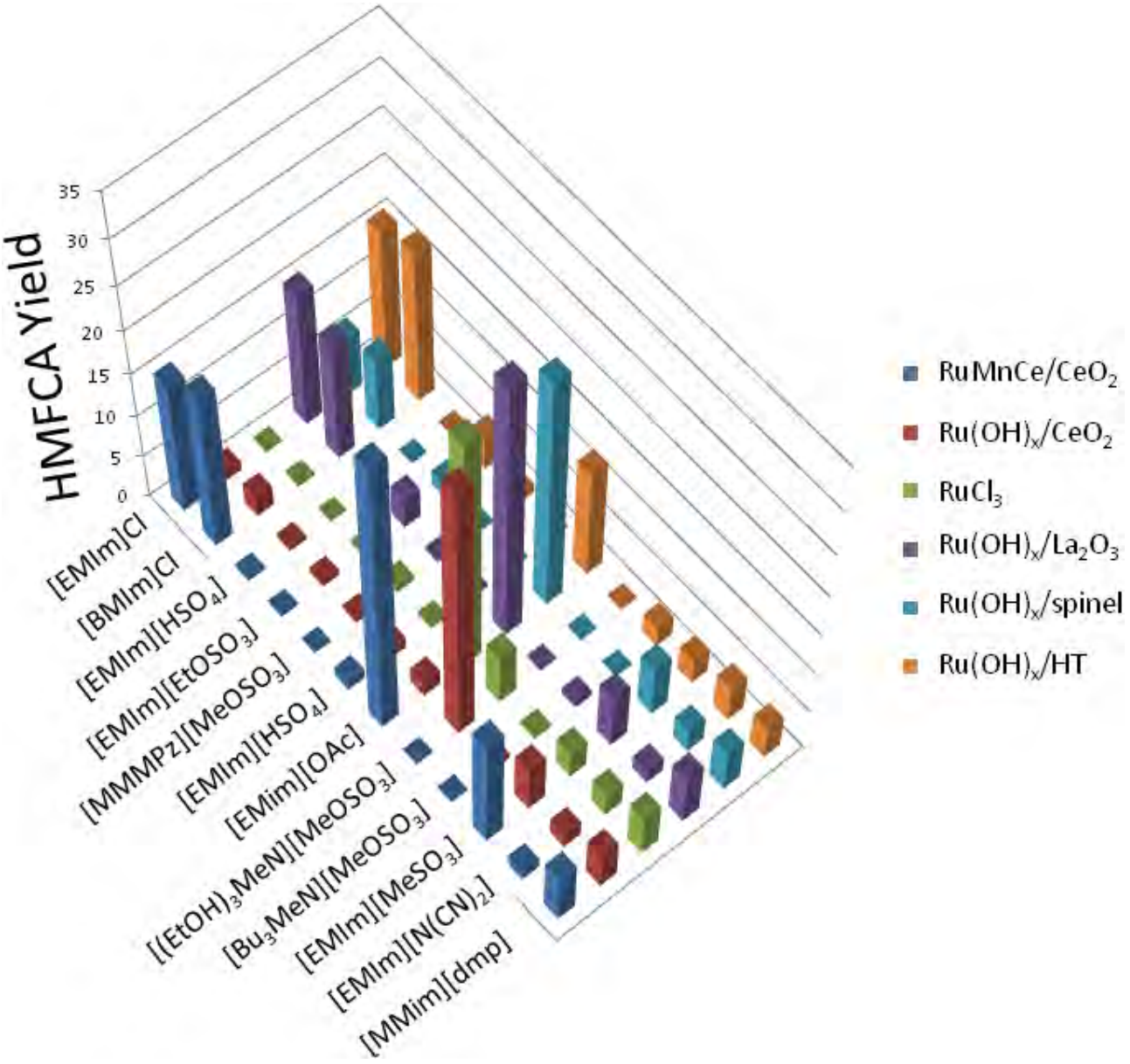
HMFCA Yield
35
30
25
20
15
10
5
0
[EMIm]Cl
[BMIm]Cl
[EMIm][HSO4]
[EMIm][EtOSO3]
[MMMPz][MeOSO3]
[EMIm][HSO4]
[EMim][OAc]
[(EtOH)3MeN][MeOSO3]
[Bu3MeN][MeOSO3]
[EMIm][MeSO3]
[EMIm][N(CN)2]
[MMim][dmp]
RuMnCe/CeO2
Ru(OH)x/CeO2
RuCl3
Ru(OH)x/La2O3
Ru(OH)x/spinel
Ru(OH)x/HT

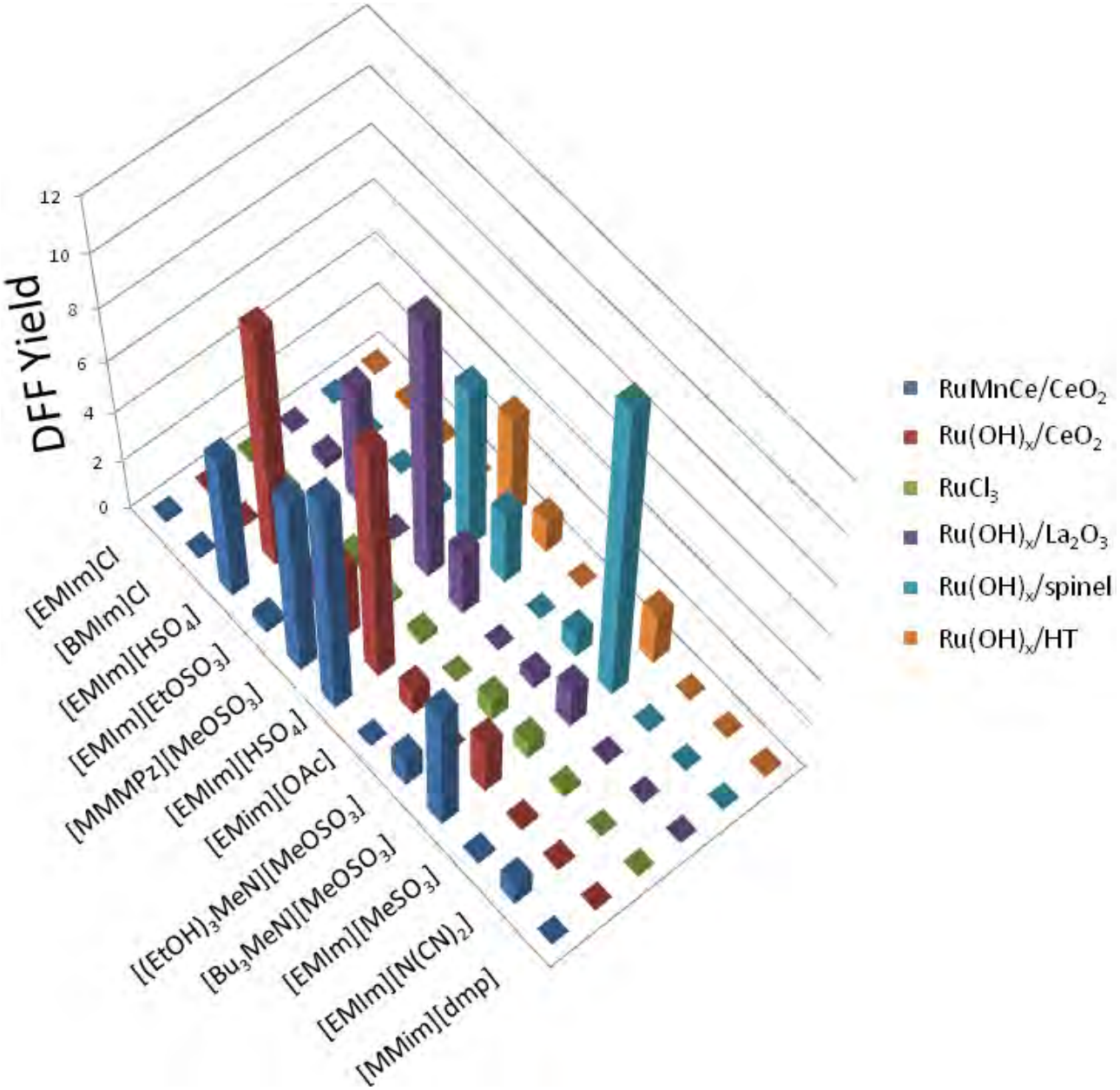
DFF Yield
12
10
8
6
4
2
0
[EMIm]Cl
[BMIm]Cl
[EMIm][HSO4]
[EMIm][EtOSO3]
[MMMPz][MeOSO3]
[EMIm][HSO4]
[EMim][OAc]
[(EtOH)3MeN][MeOSO3]
[Bu3MeN][MeOSO3]
[EMIm][MeSO3]
[EMIm][N(CN)2]
[MMim][dmp]
RuMnCe/CeO2
Ru(OH)x/CeO2
RuCl3
Ru(OH)x/La2O3
Ru(OH)x/spinel
Ru(OH)x/HT

DOI: 10.1002/cctc.200((will be filled in by the editorial staff))

Aerobic oxidation of 5-hydroxymethylfurfural to 2,5-diformylfuran with zeolites-supported vanadia catalysts: A lixiviation study

Irantzu Sádaba,[a] Yury Y. Gorbanev,[b] Søren Kegnæs,[b] Siva Sankar Reddy Putluru,[b] Anders Riisager*[b]

Aerobic oxidation of 5-hydroxymethylfurfural (HMF) to 2,5-diformylfuran (DFF) was investigated in organic solvents over vanadia-based catalysts supported on different zeolites. Four zeolitic supports (H-Beta, H-Y, H-Mordenite, H-ZSM5) were screened for the HMF oxidation in DMF with 10 wt% V_2O_5 catalysts. Catalysts were characterized by NH_3-TPD, nitrogen physisorption, SEM, EDS and XRPD. Special attention was paid to the homogeneous contribution arising from these solid catalysts. V_2O_5/H-Beta was found to provide the highest selectivity and lowest lixiviation. Several organic solvents were screened, such as *N*,*N*-dimethylformamide (DMF), methyl isobutyl ketone (MIBK), toluene, trifluorotoluene (TFT) and dimethylsulfoxide (DMSO). Catalysts with different vanadia loadings were explored, and zeolite H-Beta with 1 wt% of V_2O_5 was found to be a very stable, recyclable and non-leaching catalyst for the production of DFF under mild conditions in DMF. Additionally, in order to increase the DFF yield, oxidation of HMF at elevated pressures was investigated. Under optimized conditions, the reaction in DMSO afforded almost 100 % selectivity to DFF at 84 % HMF conversion, albeit with some extent of lixiviated species contribution to the total catalyst activity.

Introduction

Chemistry perpetually thrives on meeting the demands of the manufacturers, end users and, nowadays most importantly, the sustainability of chemical production processes. For the majority of the existence of chemical industry, abundant fossil feedstocks were available. However, their continuous exploitation together with an ever-increasing demand clearly indicates that the price of petroleum feedstock will greatly rise in the near future. This certainly affects the chemical industry, which shifts more and more towards renewable feedstocks.[1] Carbohydrates are one of the most important types of biomass feedstock. Sugars, in the form of mono- and disaccharides, are readily available from various biomass sources, including crop wastes, by, *e.g.* enzymatic hydrolysis, and constitute a useful feedstock for the production of versatile chemicals. For example, hexose monosaccharides such as glucose and fructose can be catalytically dehydrated into 5-hydroxymethylfurfural (HMF) in water, high-boiling organic solvents or ionic liquids.[2-4]

HMF is platform chemical that can be readily oxidized to form value-added chemicals, such as 2,5-furandicarboxylic acid (FDA), a possible polymer building block and therefore a replacement for terephtalic acid in plastics industry.[5] However, reported oxidation products of HMF are not limited by FDA.[5-7] Another potentially important product of HMF oxidation is 2,5-diformylfuran (DFF) [6] (Scheme 1).

DFF is a versatile compound, which can be obtained by *e.g.* glucose dehydration to HMF and its subsequent oxidation.[8,9] It possesses many different applications in industry; for instance, it can be used as a monomer building block for resins, and as a starting material for the synthesis of adhesives, composites, foams, binders, sealants, solvents, antifungal agents, organic conductors and macrocyclic ligands.[10-15]

Recently, a review by Li *et al.* [16] covered the various aspects of DFF production, including early works utilizing stoichiometric reagents as oxidants. Although reports on HMF oxidation to DFF by the means of aerobic heterogeneous catalysis are few, some of the available works describe utilization of different vanadium-based catalysts.[15,17-19] The aerobic oxidation of HMF with heterogeneous catalysts appears as a green process with a great perspective in biorefineries. A catalytic process of DFF production has recently been studied from a techno-economic point of view to estimate the minimum selling prices,[20] with the marked importance of the price and performance of the heterogeneous catalyst in the feasibility of the process.

[a] *Irantzu Sádaba*
Institute of Catalysis and Petrochemistry
CSIC
C/Marie Curie, 2, Cantoblanco, 28049 Madrid, Spain

[b] *Yury Y. Gorbanev, Søren Kegnæs, S. S. Reddy Putluru, Anders Riisager*
Centre for Catalysis and Sustainable Chemistry (CSC), Department of Chemistry
Technical University of Denmark (DTU)
Kemitorvet 207, DK-2800 Kgs. Lyngby, Denmark
E-mail: ar@kemi.dtu.dk

Supporting information for this article is available on the WWW under http://dx.doi.org/10.1002/cctc.200xxxxxx.

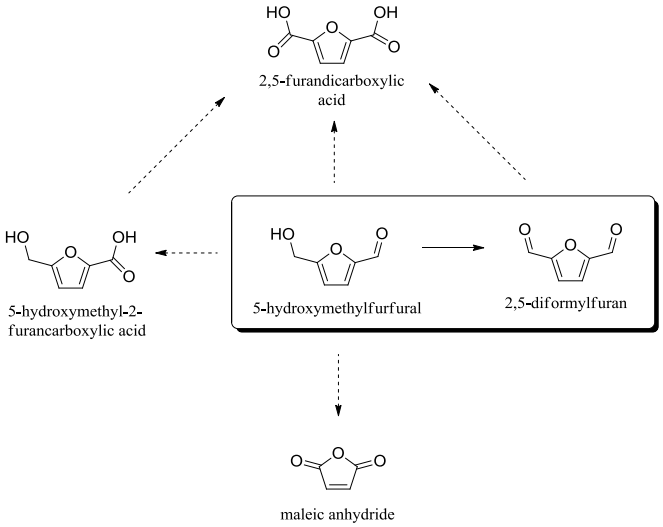

Scheme 1. Oxidation products of HMF.

In a research reported by Satsuma *et al.* [21] HMF was obtained from the dehydration of fructose using solid acids, such as zeolites H-Y and H-Beta. In general, zeolites – crystalline microporous aluminosilicates – have found a multitude of industrial applications as ion-exchangers, sorbents, etc. [22] High thermal stability and remarkably high surface areas make zeolites attractive for catalytic applications.[23-25] Hence, the exploration of a dual function heterogeneous catalytic system comprised of a zeolite support (for the fructose conversion to HMF) and aerobic catalytic species (for the oxidation of HMF) may potentially present a one-pot production route of DFF from biomass-derived monosaccharide. In fact, Chornet *et al.* utilized SBA-type mesoporous supports for vanadyl-based catalysts in the oxidation of HMF to DFF.[18]

Nevertheless, to date there are no reports in literature that would allow assessing the degree of lixiviation of catalytic species, and therefore the homogeneous contribution to the catalyst activity.

Here, we report the activity of different zeolite-supported vanadia catalysts (Scheme 2). Special attention was paid to the homogeneous contribution arising from the lixiviated species, in an attempt to avoid the leaching of the active phase and to improve the stability and recyclability of the catalyst.

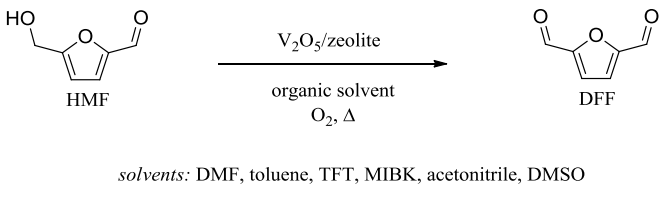

Scheme 2. Aerobic oxidation of HMF to DFF with supported vanadia catalysts in organic solvents.

Results and Discussion

Catalyst characterization

The results of the NH_3-TPD analysis of the four different zeolitic supports are presented in Table 1. As can bee seen from the results, H-Beta zeolite possessed the lowest acidity of the four examined supports (Table 1, entry 2).

Table 1. Characteristics of the prepared zeolitic supports.

Entry	Zeolite	Zeolite	Amount of absorbed ammonia,[b] μmol·g^{-1}
1	H-Y	H-Y	1138
2	H-Beta	H-Beta	1008
3	H-Mordenite	H-Mordenite	1418
4	H-ZSM5	H-ZSM5	1062

[a] Determined by nitrogen physisorption; calculated by BET method. [b] According to the results of NH_3-TPD analysis.

XRPD analysis of the prepared V_2O_5 catalysts with H-Beta zeolitic support (1, 3 and 10 wt% V_2O_5)[26] revealed only the peaks of the support, indicating an amorphous structure and high dispersion of the deposited vanadium species.

The results of the SEM-EDS and BET analysis of the prepared 1, 3 and 10 wt% V_2O_5/H-Beta catalysts are presented in Figure 1 and Table 2.

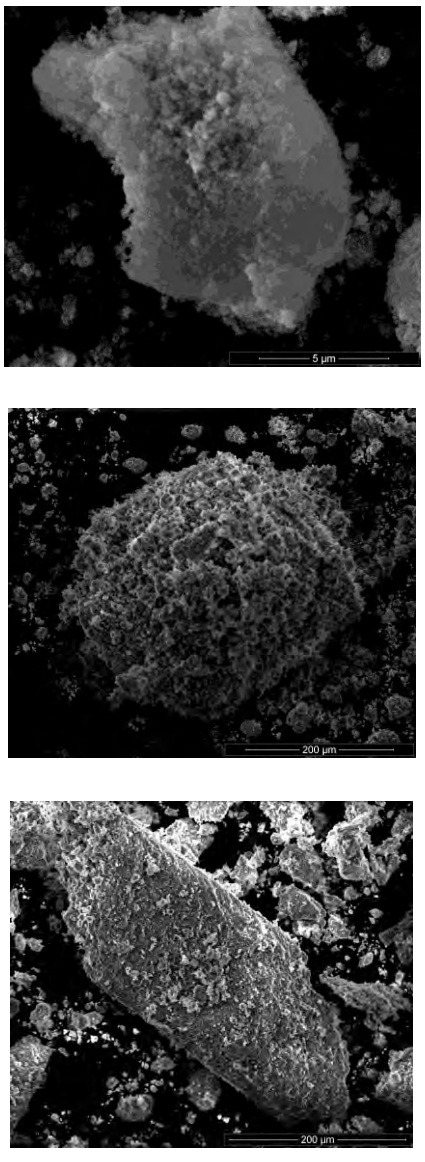

Figure 1. SEM images of the 1 (top), 3 (center) and 10 (bottom) wt% V_2O_5/H-Beta catalysts.

Table 2. Characteritics of the 1, 3 and 10 wt% V_2O_5/H-Beta catalysts.

Entry	Catalyst loading, wt%	Surface area,[a] m^2/g	Experimental V_2O_5 content,[b] wt%
1	0	680	-
2	1	532	0.97
3	3	430	3.08
4	10	437	10.16

[a] Determined by nitrogen physisorption; calculated by BET method. [b] Provided by EDS analysis; calculated on the basis of atomic V:Si and V:Al ratios.

As can be seen from the data in Table 2, the results of the EDS analysis were in good accordance with the desired weight loading of the prepared catalysts (Table 2, entries 2-4).

The surface area decreased in order 0 > 1 wt% > 3 wt% catalyst (entries 1-3), as expected. However, when the catalyst weight loading was increased from 3 to 10 wt%, no change in surface area was observed.

HMF oxidation at ambient pressure

Firstly, the prospects of using vanadia catalysts supported on different microporous zeolites (H-Beta, H-ZSM5, H-Y and H-Mordenite) were explored. 10 wt% V_2O_5 catalysts deposited on zeolites were prepared as described in the experimental section and employed in the aerobic oxidation of HMF in *N,N*-dimethylformamide. The substrate conversion and DFF yield plotted against the reaction time are presented in Figures 2a and 2b. DFF yield plotted against HMF conversion is presented in Figure 2c.

The reaction progress data showed that the HMF conversion increased within the examined timeframe (Figure 2a), whereas the yield of DFF decreased at the prolonged reaction time (1440 min) for at least three of the tested zeolites (Figure 2b). Here, when using V_2O_5/H-Mordenite catalyst, the yield of DFF decreased from ca. 17 to 14 % after 330 min and 1440 min of reaction, respectively. Similar tendency was observed when the vanadia catalysts supported on H-Beta and H-ZSM5 zeolites were employed. It was probably also the case in the reaction with the V_2O_5/H-Y catalyst, although at the compared data points the yield of DFF here appeared to increase. Nevertheless, the DFF selectivity plotted against HMF conversion in all the reactions showed a similar trend, irrespective of the zeolite used as the catalysts support (Figure 2c).

The highest selectivity to DFF at relatively high HMF conversion value was observed when V_2O_5/H-Beta catalyst was employed (Figure 2c). Notably, although all four tested zeolites were in H-form (*i.e.*, possessed Brønsted acidity detrimental for the stability of HMF[12]), zeolite H-Beta had lower aluminium content compared to other tested zeolites. It has been suggested by Zima *et al.* [17] that the Lewis type surface acidity, usually associated with the presence of coordinately unsaturated Al sites [27], can promote side reactions leading to undesired by-products. The employment of a catalyst comprised of V_2O_5 supported on Na-Beta zeolitic support (latter obtained *via* the ion-exchange) did not result in higher DFF selectivity. However, both HMF conversion and DFF yield decreased (31 % and 11 % after 330 min, respectively, compared to 51 % and 18 % of the H-form, as shown in Figure 2a,b). This unambiguously indicated the effect of the support acidity on the activity of the catalysts (*i.e.*, Brønsted acidity enhanced the overall catalytic activity), and a dominant role of the Lewis acidity on the side-reactions of HMF (*i.e.*, on the DFF selectivity). Thus, an above-discussed observed difference in catalytic behaviour of the V_2O_5 supported on four different zeolites could possibly be related to the observed, albeit not drastic, difference in the Lewis acidity of the supports (see Table 1).

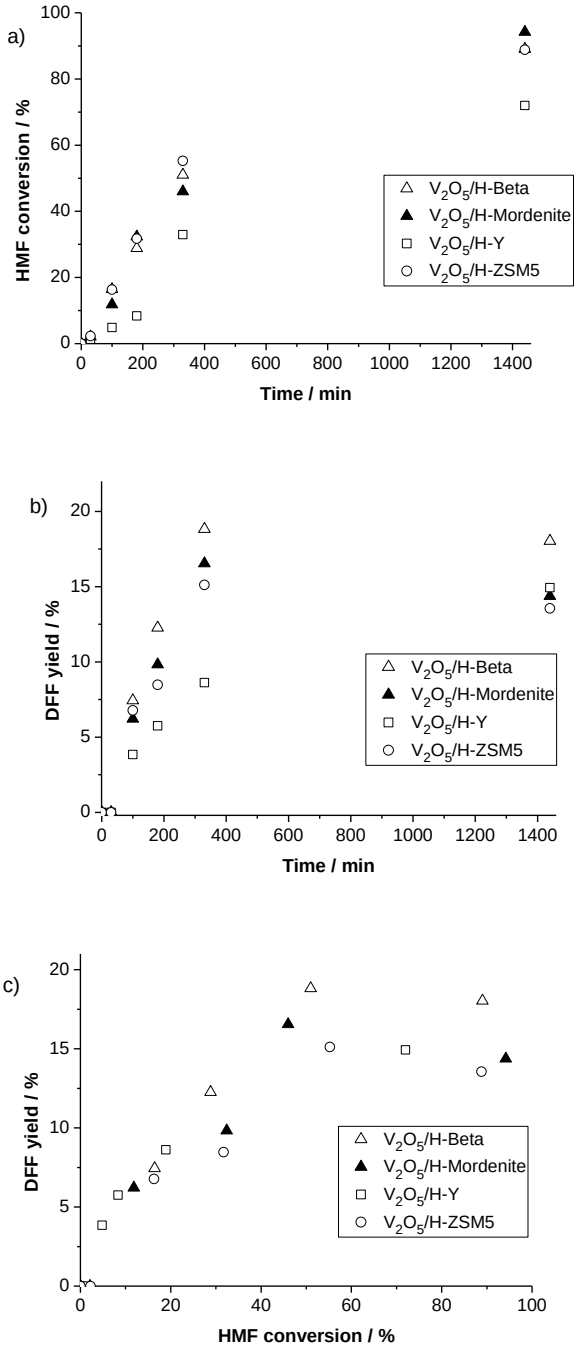

Figure 2. (a) HMF conversion, (b) DFF yield as a function of reaction time and (c) DFF yield as a function of HMF conversion in the aerobic oxidation of HMF in DMF with 10 wt% zeolite-supported V_2O_5 catalysts. Reaction conditions: 0.1 g HMF, 5 mL DMF, 0.01 g of 10 wt% V_2O_5/support catalyst (1.4 mol% V), O_2 flow (1 atm), 100ºC.

In preliminary studies, TiO_2-supported V_2O_5 catalyst exhibited high extent of catalytic species lixiviation.[28] Hence, the homogeneous contribution to the activity of the four 10 wt% zeolite-supported catalysts was investigated. Catalysts were kept under stirring in DMF for 330 min at 100ºC under the flow of oxygen. Then catalysts were filtered off and the filtrate was used as solvent for the aerobic oxidation of HMF. The conversion of HMF as found in these experiments is presented in Figure 3.

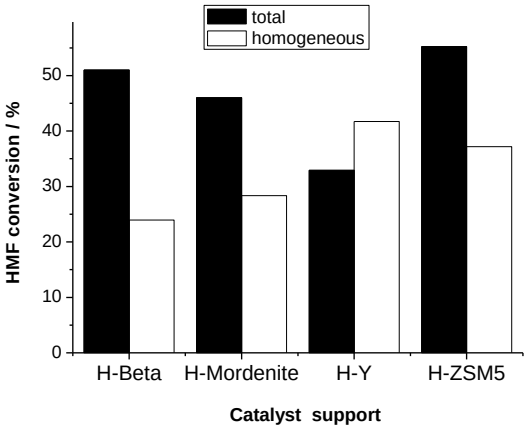

Figure 3. HMF conversion (total and contributed by lixiviated catalytic species) in the aerobic oxidation of HMF in DMF with 10 wt% V_2O_5/zeolite catalysts. Reaction conditions: 0.1 g HMF, 5 mL DMF, 0.01 g of 10 wt% V_2O_5/zeolite catalyst (1.4 mol% V), O_2 flow (1 atm), 100ºC, 330 min of the reaction time.

Importantly, when the reaction was performed without catalyst and with pure H-Beta zeolite, both the conversion of HMF and the yield of DFF remained under 1 % after 330 min. This clearly indicated that under the applied reaction conditions the conversion of HMF observed in the homogeneous test (Figure 3) can be fully related to the dissolved catalytic species. These obtained data showed that for V_2O_5/H-ZSM5 and V_2O_5/H-Mordenite catalysts over 60 % of the total catalyst activity was due to the catalytic species dissolved from the solid catalyst. Indeed, the use of *e.g.* V_2O_5/H-ZSM5 catalyst yielded in the total HMF conversion of 55 %, whilst HMF conversion of 37 % was contributed by the solubilised species.

The apparent higher HMF conversion arising from the homogeneous contribution with the V_2O_5/H-Y catalyst (Figures 2a, 3) might suggest that the dissolution of vanadia from the H-Y support takes longer than from the other examined catalysts. Therefore, in the lixiviation test, where the catalytically active vanadium species have already been dissolved, (Figure 3) the oxidation reaction proceeds faster than the reaction with the solid catalyst (Figure 2a).

In the scope of the superior DFF yield of V_2O_5/H-Beta catalyst in the HMF oxidation to DFF (see Figure 2b), and taking into consideration the lowest observed extent of the homogeneous contribution to the catalyst activity (ca. 45%; Figure 3), this catalyst was chosen for further investigation. The possible correlation between the leaching of the active phase and the vanadia content of the employed catalyst was explored. 1 and 3 wt% V_2O_5/H-Beta catalysts were prepared as described above and their catalytic activity was investigated. For that, 1, 3 and 10 wt% V_2O_5/H-Beta catalysts were utilized in the aerobic oxidation of HMF. Importantly, the vanadia/substrate ratio remained the same in all experiments. Total HMF conversion and homogeneous contribution are presented in Figure 4.

The observed substrate conversion was found to be 51 % and 54 % for the 10 and 3 wt% catalysts, respectively, whilst the 1 wt% catalyst exhibited a lower activity (21 % HMF conversion) (Figure 4a). This is likely due the presence of different vanadium species, corresponding to the different weight loading on a zeolitic support and hence the surface coverage.[29]

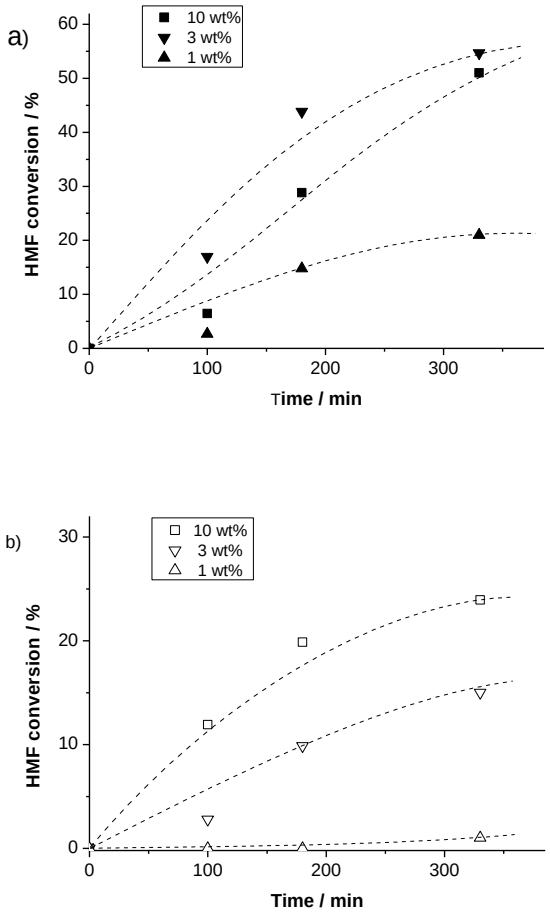

Figure 4. HMF conversion in the aerobic oxidation of HMF in DMF with 1-10 wt% V_2O_5/H-Beta catalysts as a function of reaction time: (a) total and (b) contributed by lixiviated species. Reaction conditions: 0.1 g HMF, 5 mL DMF, 1-10 wt% V_2O_5/H-Beta catalyst (1.4 mol% V), O_2 flow (1 atm), 100ºC.

Nonetheless, the homogeneous contribution to the total catalyst activity (related to the HMF conversion) decreased drastically with the decrease of the vanadium loading on the zeolite (Figure 4b). Indeed, in case of the 1 wt% catalyst, the leaching of the active phase (and thus the activity of the dissolved species) was essentially avoided. This indicated that the catalytic activity of this catalyst was provided entirely by the solid phase and there was no lixiviation of the V_2O_5 induced by the reaction medium. At the same time, the homogeneously catalysed HMF conversion with the 10 wt% V_2O_5/H-Beta catalysts constituted approximately half of the total, thus indicating that at 1 wt% loading the vanadium-containing species deposited on H-Beta zeolite are less prone to lixiviation from the surface of the support.[31]

Following the established negligible homogeneous contribution of the 1 wt% V_2O_5/H-Beta catalyst in DMF, the former catalyst was employed to study the effect of the solvent. Hence, the HMF aerobic oxidation was carried out in toluene, α,α,α-trifluorotoluene (TFT), methyl isobutyl ketone (MIBK), acetonitrile

and dimethylsulfoxide (DMSO). The results are shown in Figure 4. For comparison, the results of the HMF oxidation in DMF are also shown in Figure 5 (solid line).

Notably, HMF conversion of <2 % was observed when the reaction was performed in acetonitrile or DMSO at 100ºC under the flow of oxygen.

It can be seen from the data that although the conversion of HMF reached ca. 70 % when the reaction was performed in toluene or TFT already after 330 min of the reaction time, the yield of DFF remained around 5-10 %, thus clearly indicating the dominance of the side-reactions or reactions leading to the formation of humins, undetectable by HPLC or GC-MS. In the case of MIBK, HMF conversion proceeded to a much higher extent and constituted ca. 50 % after 330 min. At the same time, the yield of DFF was found to be almost as high (45 %). Thus, the reaction selectivity to DFF and DFF yield were found to be significantly higher after 330 min of the reaction time in MIBK compared to DMF. Also, it can be seen that the DFF yield increased with the reaction progress, in contrast to the reaction in DMF (Figure 5b).

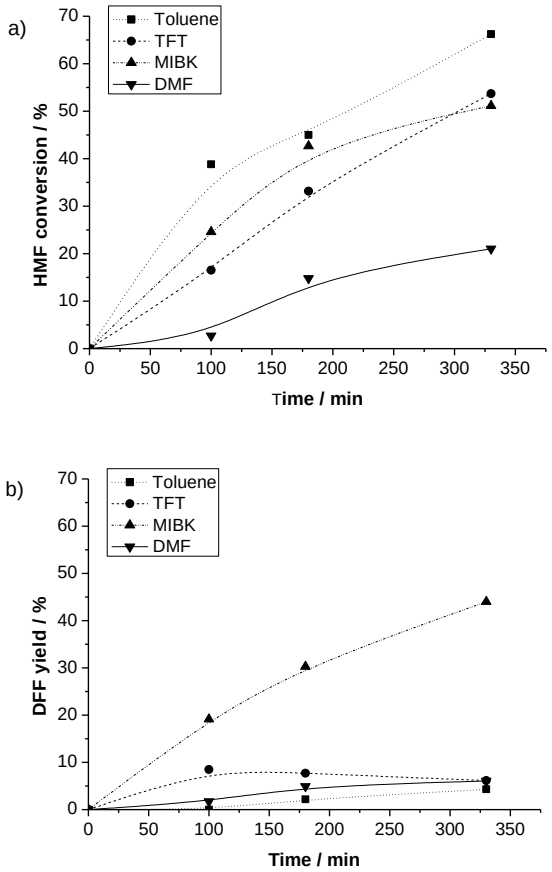

Figure 5. (a) HMF conversion and (b) DFF yield in the aerobic oxidation of HMF in organic solvents with 1 wt% V_2O_5/H-Beta catalyst as a function of reaction time. Reaction conditions: 0.1 g HMF, 5 mL solvent, 0.1 g catalyst (1.4 mol% V), O_2 flow (1 atm), 100ºC.

It is generally assumed that solvent polarity affects the activity of the catalyst, although there is no general agreement regarding the effect that this phenomenon has on the conversion and selectivity.[30] When vanadium-based catalysts were utilized, the conversion of HMF appeared to increase with the increased polarity.[17] In our case, different solvents with increasing polarity were used: MIBK, acetonitrile, DMF and DMSO (polarity indexes of 4.2, 5.8, 6.4 and 7.2, respectively[32]). Very low values of conversion (<5 %) were observed in acetonitrile and DMSO under applied conditions, while MIBK provided higher conversion and selectivity values compared to the previous runs in DMF. Besides, the selectivity to DFF was also improved by using MIBK as a solvent (Figure 5). According to these results, the polarity of the solvent did not appear to have a distinct effect on the catalyst activity, but it is noticeable that the medium plays an important role in the development of the reaction.

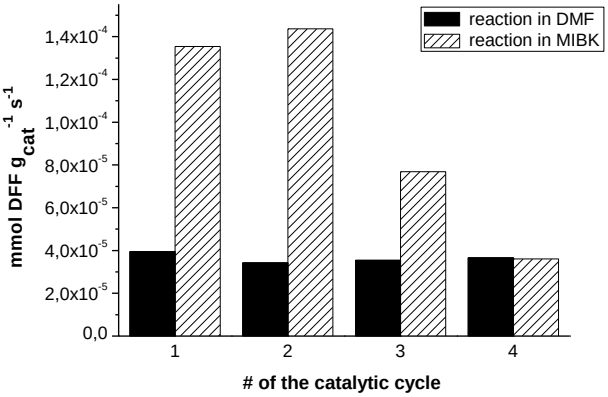

Figure 6. Rate of DFF formation per gram of the catalyst in the recycling of 1 wt% V_2O_5/H-Beta catalyst in DMF and MIBK. Reaction conditions: 0.1 g HMF, 5 mL solvent, 0.1 g catalyst (1.4 mol% V), O_2 flow (1 atm), 100ºC.

Further, the possibility of recycling the catalyst in two solvents, DMF and MIBK, was explored (Figure 6). It is seen from the results that the rate of DFF production per gram of catalyst remained constant in DMF even after four catalytic cycles. In the case of MIBK, the apparent deactivation of the catalyst took place after the second run. This can, among other reasons, be due to deposition of carbonaceous residues in the pores of the catalyst, blocking the access of the HMF to the active sites. Furthermore, when the homogeneous contribution test was performed in MIBK, high DFF yield (60 %) was observed immediately after adding the substrate (HMF) to the reaction medium containing lixiviated vanadium species. Since this yield did not increase in time, it might possibly be attributed to a presence of some very active oxidant species soluble in the medium, formed as a consequence of the interactions between the solvent and the catalyst.

HMF oxidation at elevated pressures

Although under the applied conditions the reaction in DMSO resulted in a very low HMF conversion (*vide supra*), a test experiment when the reaction was conducted in DMSO at 150ºC afforded a 30 % yield of DFF at 70 % HMF conversion after 24 hours (1440 min). Therefore, it proved possible to oxidize HMF in DMSO with the 1 wt% H-Beta-supported vanadia catalyst, albeit with a low DFF selectivity under applied conditions. This, together with the proven durability and recyclability of the 1 wt% V_2O_5/H-Beta catalyst in DMF, let us investigate the possibility of improving the DFF yield and selectivity by performing the reaction at elevated pressures. For this, the aerobic oxidation of HMF was performed in DMF under 2.5 bar of dioxygen pressure at 100ºC. DFF yield and HMF conversion are shown in Figure 7.

Evidently, both HMF conversion and DFF yield increased with the increase in the oxidant pressure. Approximately 90 % HMF

conversion and 25% DFF yield were obtained after 330 min at 2.5 bar of O_2, in contrast to 20 and 5 %, respectively, obtained under ambient pressure (see Figure 4). Interestingly, the DFF selectivity did not change with the pressure increase, and remained around 25 % in both cases. However, the only product observed by GC-MS and HPLC analysis was DFF, thus suggesting the formation of humins, possibly through polymerization or overoxidation.

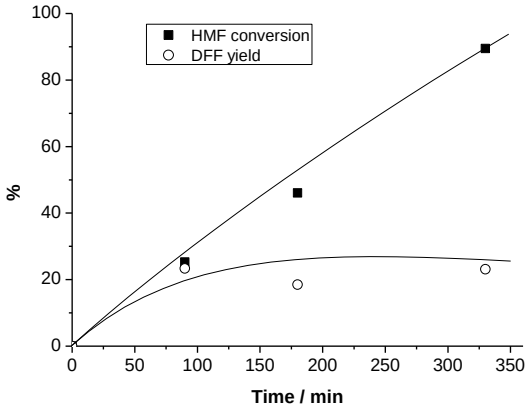

Figure 7. HMF conversion and DFF yield in the aerobic oxidation of HMF in DMF with 1 wt% V_2O_5/H-Beta catalyst as a function of reaction time. Reaction conditions: 0.1 g HMF, 5 mL solvent, 0.1 g catalyst (1.4 mol% V), 2.5 bar of O_2, 100ºC.

Table 3. HMF conversion and DFF yield and selectivity in the aerobic oxidation of HMF in organic solvents with 1 wt% V_2O_5/H-Beta catalyst under elevated pressure.[a]

Entry	*P*, bar	*T*, °C	Time, min	HMF conversion, %	DFF yield, %	DFF selectivity, %
1[b]	10	60	330	8	7	90
2[b]	10	80	330	55	23	41
3[c]	2.5	150	180	84	59	69
4[c]	2.5	150	330	>99	68	69
5[c]	10	150	180	91	67	74
6[c]	10	100	180	13	13	>99
7[c]	10	100	330	21	20	97
8[c]	10	100	1200	77	62	80
9[c]	10	125	180	84	82	98
10[c]	10	125	240	94	70	75
11[c]	10	125	330	>99	71	71
12[c]	40	100	330	44	41	95
13[c]	40	125	180	92	81	89

[a] Reaction conditions: 0.1 g HMF, 5 mL solvent, 0.1 g of 1 wt% V_2O_5/H-Beta catalyst (1.4 mol% V). [b] Reaction in DMF. [c] Reaction in DMSO.

Importantly, when a reaction under identical conditions was performed in MIBK (2.5 bar O_2, 100ºC), already after 90 min of the reaction the results of the HPLC analysis revealed large amounts of formic acid (ca. 20 % yield at 90 % HMF conversion). At the same time, substantial amounts of formed HMFCA and 5-formyl-2-furancarboxylci acid (FFCA) were observed using both GC-MS and HPLC, clearly indicating low selectivity of the reaction in MIBK under elevated pressures, with DFF yield constituting only 5 %.

The results of the further experiments of HMF oxidation in DMF and DMSO with 1 wt% V_2O_5/H-Beta catalyst are presented in Table 3.

The obtained data clearly indicates that the reaction in DMF resulted in much higher DFF selectivity at lower temperatures and higher oxidant pressure. Here, the selectivity of the reaction towards DFF formation was found to be 90 % and 41 %, when the reaction was carried out for 330 min at 60 and 80ºC, respectively (Table 3, entries 1 and 2). For comparison, the DFF selectivity after 330 min constituted only ca. 26 % when the reaction was performed under 2.5 bar of O_2 at 100ºC (see Figure 6). However, the DFF selectivity decreased drastically (from 90 to 41 %) when the temperature was increased from 60 to 80ºC.

Furthermore, the reaction in DMSO at 150ºC and 2.5 bar afforded high yields and selectivities of DFF at high values of the HMF conversion (Table 3, entries 3, 4). In fact, DFF yield and selectivity reached 68 and 69 %, respectively, at full HMF conversion already after 330 min of the reaction time under 2.5 bar of O_2 (entry 4). In contrast, in an experiment when the reaction was carried out in DMSO at 150ºC under ambient pressure, the respective values were found to be only 9 and19 %.

These results, together with the improved conversion and yield of the reaction in DMF under 10 bar pressure, suggested performing the aerobic oxidation of HMF in DMSO under 10 bar of O_2 pressure. Here, the reaction was carried out for 180 min at varying temperatures (Table 3, entries 5, 6, 9). It is seen from the data that the DFF selectivity decreased with the increase of temperature. Indeed, the selectivity was found to be ca. 99, 98 and 74 %, when the reaction was performed at 100, 125 and 150ºC, respectively. Notably, although providing high selectivity towards desired product, the reaction at 100ºC afforded only a very low HMF conversion (Table 3, entry 6). However, at prolonged reaction times, the increase in the HFM conversion and DFF yield were observed together with the decrease of the DFF selectivity (entries 6-8): from >99 % to 80 % after 180 and 1200 min, respectively (entries 6 and 8).

A similar tendency was observed when the progress of the reaction at 125ºC was explored. Here, DFF selectivity decreased with the reaction propagation from 98 after 180 min (84 % HMF conversion) to 71 % (>99 % HMF conversion) (Table 3, entries 9-11). In fact, the amount of DFF decreased in this case, suggesting a side-reaction leading to the gradual product degradation.

The increase of the oxidant pressure from 10 to 40 bar at 100ºC allowed to achieve higher, albeit less then 50 %, HMF conversion and DFF yield (entry 12) with approximately equal selectivity (ca. 95 %). At the same time, the reaction under 40 bar O_2 at 125ºC resulted in a lower DFF selectivity (89 %; entry 13) compared to that achieved under 10 bar (98 %; entry 9).

Further, a homogeneous test was conducted for the reaction with the highest achieved values of both substrate conversion and DFF selectivity (see Table 3, entry 9; 10 bar O_2, 125ºC, 180 min). The results are presented in Figure 8.

The obtained data showed that an equally high extent of the HMF conversion (approximately 84 %) was reached in the oxidation reaction with the lixiviated catalytic species, as well as when pure H-Beta zeolite was introduced in the reaction. The conversion in the absence of the catalyst (‘blank’ experiment) resulted in ca. 70 % conversion, indicating the instability of HMF

under the applied conditions. Interestingly, the yield of DFF was only 46 % when the lixiviated species were present in the medium, compared to the 82 % obtained with the supported catalyst. The use of pure zeolitic support afforded a 24 % DFF yield, and a low

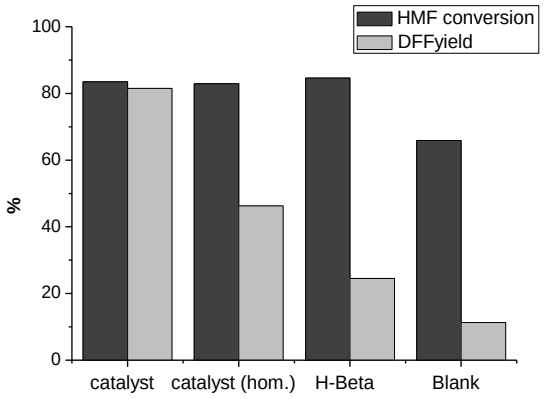

Figure 8. HMF conversion and DFF yield in the aerobic oxidation of HMF in DMSO with 1 wt% V_2O_5/H-Beta catalyst. Reaction conditions: 0.1 g HMF, 5 mL solvent, 0.1 g of 1 wt% V_2O_5/H-Beta catalyst (1.4 mol% V), 10 bar of O_2, 125ºC, 180 min reaction time.

but not negligible DFF yield (10 %) was observed when the reaction was performed in the absence of catalyst, thus making a direct evaluation of the homogeneous contribution difficult. However, it can be inferred that the solubilised species were not entirely responsible for the full catalyst activity. This fact implies that the active sites on the surface of the solid catalyst still had major a role in the catalytic reaction, although the extent of leaching cannot be neglected under these conditions.

Conclusions

Catalytically active V_2O_5 species supported on four different microporous zeolites were employed as the aerobic catalysts in the oxidation of HMF to DFF in organic solvents. For the first time, a detailed study on leaching and homogeneous contribution of supported vanadia catalysts has been performed. The relation between the loading of V_2O_5 on the surface of a zeolite and the homogeneous contribution to the catalyst activity was studied. For the catalysts with different amount (wt%) of deposited vanadium(V) oxide, the extent of the contribution provided by the lixiviated catalytic species decreased in order 10 wt% > 3 wt% > 1 wt%. Moreover, 1 wt% V_2O_5/H-Beta proved to be stable and recyclable in 4 catalytic cycles under atmospheric pressure.

Different reaction conditions were tested in order to increase the DFF yield. The effects of reaction temperature and oxidant pressure on the reaction progress were investigated. The yield of DFF was improved remarkably under elevated pressures. The choice of a solvent also had a very important effect on the reaction selectivity, although the exact mechanism remained unclear.

Under optimized conditions, the reaction in DMSO at 125ºC under 10 bar of O_2 afforded 84 % DFF yield (>99 % selectivity) after 180 min of reaction time. However, under these conditions the contribution of the lixiviated species to the total activity could not be disregarded.

The characterization of the catalyst indicated the presence of a well dispersed vanadia supported over the zeolites, and the influence of the surface acidity of the solid on the conversion and selectivity.

The obtained results emphasized the importance of conducting experiments directed to the evaluation of the homogeneous contribution of solid catalysts in liquid phase reactions, so as to utilize stable and non-leaching catalysts.

Experimental Section

Materials: 5-Hydroxymethylfurfural (HMF) (>99 %), acetonitrile (≥99.9 %), toluene (anhydrous, 99.8 %), α,α,α-trifluorotoluene (TFT) (≥99 %), *N,N*-dimethylformamide (DMF) (≥99.9 %), ammonium metavanadate (≥99 %), oxalic acid (≥99 %), sodium nitrate (≥99 %) and anisole (99 %) were acquired from Sigma-Aldrich. Methyl isobutyl ketone (MIBK) (≥98 %) and dimethylsulfoxide (DMSO) (≥99 %) were purchased from Fluka. 2,5-Diformylfuran (DFF) (98 %) was supplied by ABCR GmbH & Co. Dioxygen (99.5 %) was purchased from Air Liquide Denmark. All NH_4-zeolites were obtained from Zeolyst International, USA. All chemicals were used as received.

Catalyst preparation: Commercial NH_4-ZSM5 (Si/Al=15), NH_4-Beta (Si/Al=25), NH_4-Mordenite (Si/Al=10) and NH_4-Y (Si/Al=8) zeolites were initially calcined at 550ºC for 5 hours to obtain the H-ZSM5, H-Beta, H-Mordenite and H-Y supports, respectively.

Vanadia catalysts supported on zeolites with 1–10 wt% V_2O_5 were prepared by wet impregnation of the supports with vanadium oxalate solution, as adopted from the literature.[33] In a typical experiment of 3 wt% zeolite-supported vanadia catalyst preparation, 1.75 mL of NH_4VO_3/oxalic acid aqueous solution (0.378 M) (prepared from ammonium metavanadate and oxalic acid in the molar ratio 1:2 at 70ºC) was added to 1 g of the zeolite using incipient wetness impregnation technique. Once the incipient wetness impregnation was completed, the solids were dried at 120ºC for 8 hours and then calcined at 500ºC for 5 hours to afford 3 wt% V_2O_5/zeolite catalysts.

For the preparation of Na-Beta support, 10 g of NH_4-Beta were suspended in 300 mL of 1 M aqueous solution of $NaNO_3$. The mixture was heated to 80°C and stirred for 1 hour. Afterwards, the zeoli5e was filtered and washed with distilled water. This procedure was repeated twice. Finally, the recovered Na-Beta material was dried and then calcined at 500°C for 5 hours.

Surface areas were determined by nitrogen sorption measurements at liquid nitrogen temperature on a Micromeritics ASAP 2020 pore analyzer. The samples were outgassed in vacuum at 150ºC for 4 hours prior to the measurements. The total surface areas were calculated according to the BET method.

SEM-EDS analysis was done on a FEI Quanta 200 F SEM operated at 20 kV, using an Oxford Instruments X-max (51xmx0005) EDS running the INCA Suite v 4.15 software. Spectra were fitted using program standards and converted to atomic ratios. Samples were mounted on a carbon tape fitted to aluminium sample holders.

Oxidation at ambient pressure: Experiments were performed using a Radley Carousel 12 Plus Basic System. In a typical experiment, 0.1 g (ca. 0.8 mmol) of HMF, 0.01-0.1 g of the 1-10 wt% V_2O_5/support catalyst (1.4 mol% V) and 5 mL of the solvent were put into a 40 mL reaction vial. 11 µL of anisole were added as an internal standard and the vial was equipped with a magnetic stirrer (800 rpm). Reactions were carried out under a flow of oxygen (1 atm) at 100-150ºC. During and after the reaction, samples of the reaction mixture were taken and after filtering off the catalyst analyzed by GC (Agilent Technologies 6890N with a flame ionization detector (FID), HP-5 column (30 m x 0.320 mm x 0.25 µm, J&W Scientific) and/or GC-MS (GC Agilent Technologies 6850 coupled with MS Agilent

Technologies 5975C, column HP-5MS (J & W Scientific, 30 m × 0.25 mm × 0.25 μm).

In the homogeneous test experiments, the same procedure was applied. After 330 min the content of the reaction vial was filtered, the filtrate was recovered and used to conduct subsequent reaction.

In the recycling test, the catalyst was recovered after the reaction by filtration, washed with the solvent and ethanol and dried overnight at room temperature before being applied in another reaction run.

High pressure oxidation reactions: Experiments were carried out in stirred Parr autoclaves equipped with internal thermocontrol (T316 steel, TeflonTM beaker insert, 100 mL). In a typical experiment, reactor was charged with 0.1 g HMF, 5 mL of solvent, 0.1 g of 1 wt% V_2O_5/H-Beta and 11 μL of anisole. The autoclave was then pressurized with 10-40 bar of oxygen and were kept stirring (800 rpm) at 100-150ºC. After the reaction, the autoclave was cooled to room temperature (*i.e.*, 20ºC) and after filtering off the catalyst a sample was taken out for GC and/or GC-MS analysis.

In the homogeneous test experiments, the same procedure was applied. After 180 min under 10 bar of O_2 at 125ºC the catalyst was filtered off the solvent, the filtrate was recovered and used to conduct a subsequent reaction.

Acknowledgements

The authors thank Bodil F. Holten (CSC, DTU) and Anders B. Laursen (CINF, DTU) for the catalyst characterization assistance. I. Sádaba is grateful to the Spanish National Research Council (CSIC) for a JAE-Predoc and for the financial support for the research stay at CSC, Technical University of Denmark.

Keywords: 5-Hydroxymethylfurfutal • 2,5-diformylfuran • zeolites • vanadia catalysts• homogeneous contribution

[1] M. Narodoslawsky, A. Niederl-Schmidinger, L. Halasz, *J. Cleaner Prod.* **2008**, *16*, 164-170.

[2] K. D. O. Vigier, F. Jerome, *Top. Curr. Chem.* **2010**, *295*, 63-92.

[3] T. S. Hansen, J. Mielby, A. Riisager, *Green Chem.* **2011**, *13*, 109-114.

[4] T. Ståhlberg, W. Fu, J. M. Woodley, A. Riisager, *ChemSusChem* **2011**, *4*, 451-458.

[5] Y. Y. Gorbanev, S. K. Klitgaard, C. H. Christensen, J. M. Woodley, A. Riisager, C*hemSusChem* **2009**, *2*, 672-675.

[6] A. Boisen, T. B. Christensen, W. Fu, Y. Y. Gorbanev, T. S. Hansen, J. S. Jensen, S. K. Klitgaard, S. Pedersen, A. Riisager, T. Ståhlberg, J. Woodley, *Chem. Eng. Res. Des.* **2009**, *87*, 1318-1327.

[7] Z. Du, J. Ma, F. Wang, J. Liu, J. Xu, *Green Chem.* **2011**, *13*, 554-557.

[8] P. Verdeguer, N. Merat, A. Gaset, *J. Mol. Cat.* **1993**, *85*, 327-344.

[9] A. Corma, S. Iborra, A. Velty, *Chem. Rev.* **2007**, *107*, 2411-2502.

[10] A. Gandini, M. N. Beglacem, *Prog. Polym. Sci.* **1997**, *22*, 1203-1379.

[11] K. T. Hopkins, W. D. Wilson, B. C. Bender, D. R. McCurdy, J. E. Hall, R. R. Tidwell, A. Kumar, M. Bajic, D. W. Boykin, *J. Med. Chem*. **1998**, *41*, 3872-3878.

[12] J. Lewkowski, *ARKIVOC*, **2001**, *(i)*, 17-54.

[13] C. Moreau, M. N. Beglacem, A. Gandini, *Top. Catal.* **2004**, *27*, 11-30.

[14] A. Gandini, *Green Chem.* **2011**, *13*, 1061-1083.

[15] J. Ma, Z. Du, J. Xu, Q. Chu, Y. Pang, *ChemSusChem* **2011**, *4*, 51-54.

[16] X. Tong, Y. Ma, Y. Li, *Appl. Catal., A* **2010**, *385*, 1-13.

[17] C. Carlini, P. Patrono, A. M. R. Galetti, G. Sbrana, V. Zima, *Appl. Catal., A* **2005**, *289*, 197-204.

[18] O. C. Navarro, A. C. Canós, S. I. Chornet, *Top. Catal.* **2009**, *52*, 304-314.

[19] X. Xiang, L. He, Y. Yang, B. Guo, D. Tong, C. Hu, *Catal. Lett.* **2011**, *141*, 735-741.

[20] F. K. Kazi, A. D. Patel, J. C. Serrano-Ruiz, J. A. Dumesic, R. P. Annex, *Chem. Eng. J*. **2011**, *169*, 329-338.

[21] K. Shimizu, R. Uozumi, A. Satsuma, *Catal. Commun.* **2009**, *10*, 1849-1853.

[22] M. S. Holm, K. Egeblad, P. N. R. Vennestrøm, C. G. Hartmann, M. Kustova, C. H. Christensen, *Eur. J. Inorg. Chem*. **2008**, 5185-5189.

[23] A. Corma, *Chem. Rev*. **1997**, *97*, 2373-2420.

[24] D. Mravec, J. Hudec, I. Janotka, *Chem. Pap*. **2005**, *59*, 62-69.

[25] N. M. Xavier, S. D. Lucas, A. P. Rauter, *Appl. Catal., A* **2009**, *305*, 84-89.

[26] See Supporting information, Figure S1.

[27] D. Coster, A. L. Blumenfeld, J. J. Fripiat, *J. Phys. Chem.* **1994**, *98*, 6201-6211.

[28] Figure S2.

[29] B. M. Weckhuysen, D. E. Keller, *Catal. Today* **2003**, *78*, 25-46.

[30] C. Moreau, R. Durand, C. Pocheron, D. Tichit, *Stud. Surf. Sci. Catal.* **1997**, *108*, 399-406.

[31] Figure S3 in the Supporting information shows the results of the usage of 1 wt% V_2O_5/Na-Beta. Similar tendency (lower values of conversion and yield and, importantly, same selectivity) was observed compared to the results with 10 wt% V_2O_5/H-Beta and 10 wt% V_2O_5/Na-Beta.

[32] *Solvents Polarity Indexes*, Burdick & Jackson; available online at: http://macro.lsu.edu/howto/solvents/Polarity%20index.htm.

[33] S. S. R. Putluru, A. Riisager, R. Fehrmann, *Appl. Catal., B* **2010**, *97*, 333-339.

Received: ((will be filled in by the editorial staff))
Published online: ((will be filled in by the editorial staff))

Supporting information

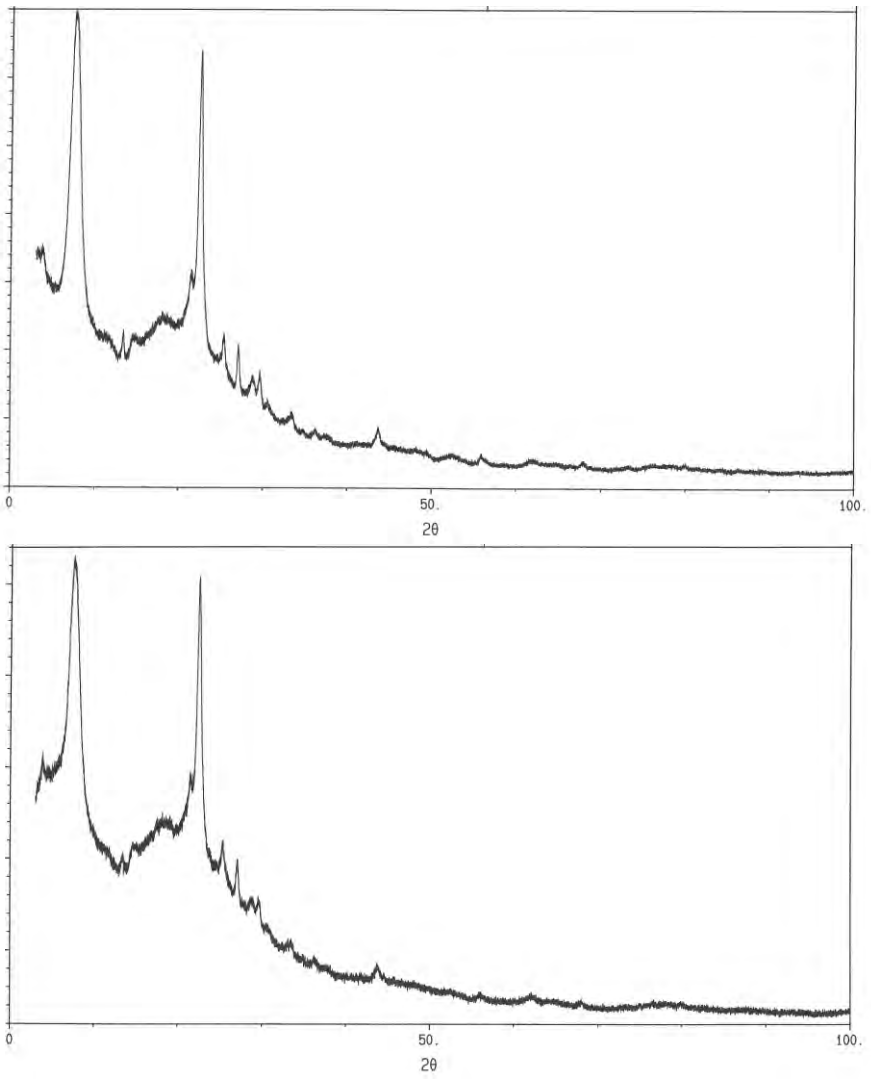

Figure S1. XRPD diffractograms of the 10 wt% V_2O_5/H-Beta (top) and pure H-Beta zeolite (bottom).

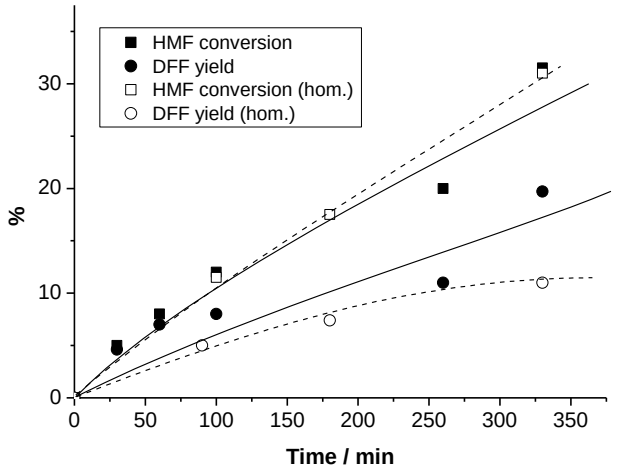

Figure S2. HMF conversion and DFF yield (full and contributed by lixiviated catalytic species) in the aerobic oxidation of HMF in DMF with 5 wt% V_2O_5/TiO_2 catalyst as a function of reaction time. Reaction conditions: 0.1 g HMF, 5 mL DMF, 11 µL anisole, 0.01 g of 5 wt% V_2O_5/TiO_2 (0.7 mol% V), O_2 flow (1 atm), 100°C.

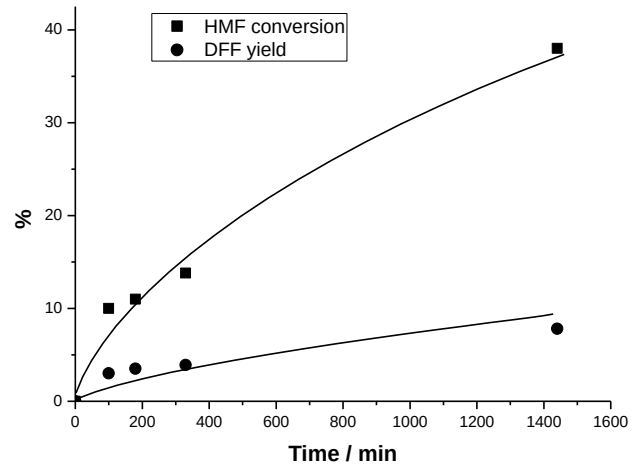

Figure S3. HMF conversion and DFF yield in the aerobic oxidation of HMF in DMF with 1 wt% V_2O_5/Na-Beta catalyst as a function of reaction time. Reaction conditions: 0.1 g HMF, 5 mL DMF, 11 µL anisole, 1 wt% V_2O_5/Na-Beta (1.4 mol% V), O_2 flow (1 atm), 100°C.

Chemicals from renewable alcohols: Selective aerobic oxidation of aqueous ethanol into acetic acid over heterogeneous ruthenium catalysts

Yury Y. Gorbanev,[a] Søren Kegnæs,[a] Christopher W. Hanning,[a] Thomas W. Hansen[b] and Anders Riisager[a]*

[a]*Centre for Catalysis and Sustainable Chemistry, Department of Chemistry, Technical University of Denmark, DK-2800 Kgs. Lyngby, Denmark*

[b]*Center for Electron Nanoscopy, Technical University of Denmark, DK-2800 Kgs. Lyngby, Denmark*

*Corresponding author
E-mail: ar@kemi.dtu.dk
Tel.: +4545252233
Fax: +4545883136

Abstract

Heterogeneous catalyst systems comprising ruthenium hydroxide supported on different carrier materials: titania, ceria and spinel ($MgAl_2O_4$), were applied in the selective aerobic oxidation reaction of aqueous solutions of ethanol to form acetic acid – an important bulk chemical and food product. The catalysts were characterized by TEM, EDS and nitrogen physisorption and utilized in the oxidation of 2.5-50 wt% aqueous ethanol solutions at elevated temperatures and pressures. The effects of carrier material, Ru metal loading, oxidant pressure, temperature, heat-treatment of catalysts and substrate concentration were studied and optimized to allow quantitative yields of acetic acid to be obtained.

Keywords: ethanol; acetic acid; oxidation; heterogeneous catalysis; ruthenium hydroxide catalysts

1. Introduction

Acetic acid is a highly important organic bulk chemical with the current annual production of approximately 8.5 million tonnes and annual growth rate of roughly 1 %.[1] Traditionally, acetic acid has been derived from ethanol via fermentation, a production route that is still used today to make vinegar (i.e. aqueous acetic acid).[2] Since the late 1990s, production of biomass-derived ethanol or 'bio-ethanol' has increased dramatically.[3] So far the main utilization of bio-ethanol has been as fuel additive, however, ethanol is a low value bulk chemical with potential to be a sustainable chemical feedstock when upgraded to other higher value products, e.g. bio-acetic acid.[4] Although such 'bio-acetic acid' only makes up a small volume of the total annual acetic acid production (i.e. 0.8 million tonnes per year),[2] this is still a significant volume positioning this production route in the lower end of the bulk chemical scale production.

As an alternative to fermentation of ethanol, various chemical pathways to aqueous acetic acid have already been shown in the literature. An obvious route is via the oxidation of an ethyl species using dioxygen,[5] which has been demonstrated with ethane,[6] ethanol and acetaldehyde[7] (Scheme 1). All of these methods have, however, only been shown on a lab scale and not successfully scaled up to industrial levels,[6] though the possibility of obtaining acetic acid from biomass via bio-ethanol would be an attractive route, that is not based on petrochemicals like the current large scale productions via methanol carbonylation[7] or the Wacker process of acetaldehyde oxidation.[6]

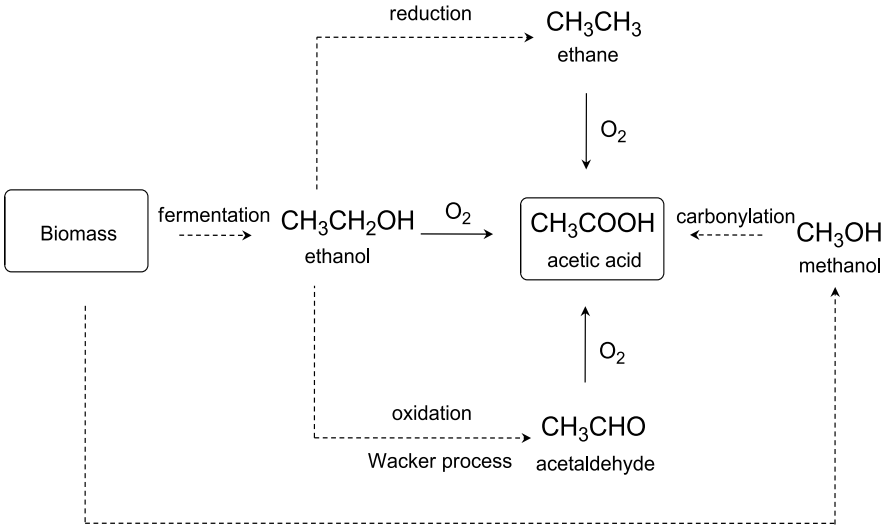

Scheme 1. Possible routes for the production of acetic acid from biomass.

For the oxidation of ethanol (not limited by aqueous conditions) studies have shown that supported gold,[4,8-10] copper/copper-chromium oxides,[11] molybdenum, vanadium, niobium mixed oxides,[12] palladium,[13-15] and platinum[16] catalysts can be used. Hence, Rajesh et al.[11] succeeded, by using either copper or copper-

chromium catalysts supported on γ-alumina, to achieve yields of acetaldehyde up to 27 % by the oxidation of ethanol. Li et al.[12] were able to show that supported mixed oxides containing molybdenum, vanadium and niobium provided 100 % ethanol conversion combined with a 95 % selectivity towards acetic acid. ten Brink and co-workers[13] demonstrated use of a homogeneous palladium catalyst in a biphasic system for the oxidation of both primary and secondary alcohols in an aqueous medium. Here conversions of over 90 % for a large variety of substrates were obtained with isolated yields of the corresponding ketone, aldehyde or carboxylic acid above 80 %. Nishimura et al.[14] made use of supported palladium catalyst to perform the oxidation of primary and secondary alcohols to aldehydes and ketones. Again, high conversions were combined with high isolated yields (>95 % and >85 %, respectively).

Gold catalysts supported on silica, titania, ceria, zinc and niobium oxides have been actively utilized by various research groups for the oxidation of ethanol in both liquid and gas phase, providing high conversion and selectivity towards acetic acid. Most of these results are summarized in the recent review by Haruta et al.[17] We have previously reported the possibility of selective oxidation of ethanol to acetic acid in aqueous solution utilizing $Au/MgAl_2O_4$ and Au/TiO_2 catalysts and dioxygen.[18,19] In this paper, we show the superior performance of supported $Ru(OH)_x$ as a catalyst for this process. Hence, $Ru(OH)_x$ catalysts supported on TiO_2, CeO_2 or $MgAl_2O_4$ were found to catalyze the aerobic oxidation of ethanol to acetic acid in aqueous solutions with moderate to excellent yields at relatively benign reaction conditions.

2. Experimental

2.1. Materials

Ethanol (99.9%, Kemetyl A/S), acetaldehyde (>99.5%, Sigma-Aldrich), acetic acid (99.8%, Riedel-de Haën AG), ruthenium(III) chloride (purum, 40-42% Ru, Sigma-Aldrich), titanium oxide (anatase, 99.7%, Sigma-Aldrich), spinel $MgAl_2O_4$ (Sigma-Aldrich), cerium oxide (99.5%, Alfa Aesar), sodium hydroxide (>98%, Sigma-Aldrich) and dioxygen (99.5%, Air Liquide Denmark) were all used as received.

2.2. Catalyst preparation and characterization

The catalysts were prepared by a method adapted from literature.[20-24] 2.44, 4.88, 9.76 g or 19.52 g of support (CeO_2, $MgAl_2O_4$ or TiO_2) were added to 143 ml of 8.3 mM aqueous $RuCl_3$ solution (1.19 mmol Ru). After stirring for 15 min, 28 ml of 1 M NaOH solution was added and the mixtures were stirred for 18 h. Then the catalysts were filtered off, washed thoroughly with water until neutral reaction (colourless filtrates suggested absence of ruthenium ions) and dried at 140°C for 40 h resulting in catalysts with optimally 4.7, 2.4, 1.2 and 0.6 wt% Ru, respectively.

Surface areas were determined by nitrogen physisorption measurements at liquid nitrogen temperature on Micrometrics ASAP 2020. The samples were outgassed in vacuum at 150°C for 6 hours prior

to measurements. The total surface areas were calculated according to the BET method. For transmission electron microscopy (TEM) characterization, samples were dispersed on a lacy amorphous carbon support film. Images were acquired using a FEI Tecnai Transmission Electron Microscope operated at 200 kV. EDS analysis was performed using an Oxford INCA system. XRPD patterns were recorded using a Huber G670 powder diffractometer (Cu-K_α radiation, λ = 1.54056 Å) in the 2θ interval 5-100^o.

For the study of heat treatment effects, catalysts were calcined at 170 and 450^{o}C in still air for 18 hours.

2.3. Oxidation reactions

Oxidations were carried out in stirred Parr autoclaves equipped with internal thermocontrol (T316 steel, Teflon™ beaker insert, 100 ml). In each reaction the autoclave was charged with 10 g of 2.5-50 wt% aqueous ethanol solutions.

The supported 0.6-4.7 wt% $Ru(OH)_x$ catalyst (weight percentage given on Ru metal basis) was added (0.05-0.42 g, 0.012-0.05 mmol Ru) to the solution and the autoclave was pressurized with dioxygen (10-30 bar, ca. 16-48 mmol) and maintained at 125-250^{o}C for a given period of time under stirring (500 rpm). After the reaction, the autoclave was rapidly cooled to room temperature (i.e. 20^{o}C). The reaction mixture was then filtered and analyzed using HPLC (Agilent Technologies 1200 series, Aminex HPX-87H column from Bio-Rad, 300 mm x 7.8 mm x 9 μm, flow 0.6 mL/min, solvent 5 mM H_2SO_4, temperature 60^{o}C) and/or GC-MS (GC Agilent Technologies 6850 coupled with MS Agilent Technologies 5975C, HP-5MS column from J & W Scientific, 30 m × 0.25 mm × 0.25 μm, 5 mol% phenylmethylpolysiloxane, flow gas He). In all figures where the product distribution is shown as a function of time each data point corresponds to an individual reaction run.

In a leaching test, the reaction was carried out at 150^{o}C under 10 bar of O_2 for 1 hour, then the catalyst was filtered off and the filtrate poured back into the autoclave. The autoclave was then re-pressurized with 10 bar O_2 and the reaction continued for 2 hours more.

3. Results and discussion

3.1. Catalyst characterization

The results of the XRPD and EPR analysis of the supported $Ru(OH)_x$ catalysts are described elsewhere.[25] The utilized catalysts were suggested to consist of hydrated amorphous mixed Ru^{4+} and Ru^{3+} species.

TEM images of the $Ru(OH)_x/CeO_2$ catalysts are presented in Figure 1 (TEM images of titania- and spinel-supported catalysts not shown). Ruthenium species were not observed on the surface of titania, possibly due to their small size. The EDS analysis data and BET surface areas of the applied support materials and the prepared catalyst samples are listed in Table 1.

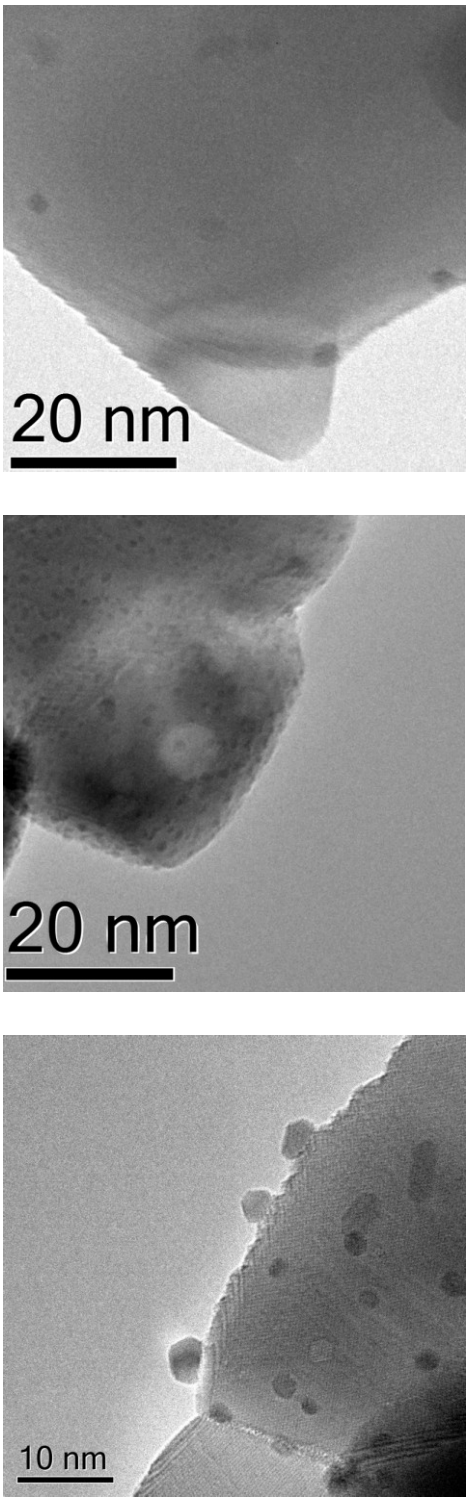

Figure 1. High-resolution TEM images of the 1.2 wt% (top), 2.4 wt% (center) and 4.7 wt% (bottom) $Ru(OH)_x/CeO_2$ catalysts.

Table 1. Characteristics of supports and supported $Ru(OH)_x$ catalysts.

Entry	Material	BET surface area (m^2/g)	Ru content[a] (wt%)	Particle size[b] (nm)
1	TiO_2	123	-	-
2	2.4 wt% $Ru(OH)_x/TiO_2$	128	2.32	n/a
3	$MgAl_2O_4$	63	-	-
4	1.2 wt% $Ru(OH)_x/MgAl_2O_4$	54	1.35	0.5 – 2
5	2.4 wt% $Ru(OH)_x/MgAl_2O_4$	53	2.41	n/a
6	CeO_2	62	-	-
7	1.2 wt% $Ru(OH)_x/ CeO_2$	8	1.31	0.6 – 2
8	2.4 wt% $Ru(OH)_x/ CeO_2$	8	2.26	0.8 – 3.5
9	4.7 wt% $Ru(OH)_x/ CeO_2$	8	4.56	1.5 – 6

[a]Based on Ru:Ti, Ru:Al, Ru:Ce atomic ratios provided by EDS (average for the analyzed sample).
[b]Determined from TEM imaging.

As seen from the data, the experimental ruthenium contents determined by EDS were in good accordance with the calculated amounts.

The nitrogen physisorption analysis revealed a moderate decrease in BET surface areas when the ruthenium species were deposited on $MgAl_2O_4$ support (Table 1, entries 3-5), as expected. Interestingly, the decrease in the BET surface area of $Ru(OH)_x$ catalysts supported on CeO_2 compared to pure CeO_2 was much more drastic (Table 1, entries 6-9), suggesting a change in morphology. Notably, however, in the cases of both spinel and ceria the decrease of the surface area did not apparently correlate with the weight loading of ruthenium (Table 1, entries 4-5 and 7-9).

The particle sizes of the deposit on 1.2, 2.4 and 4.7 wt% $Ru(OH)_x/CeO_2$ catalysts increased with increasing ruthenium loading (Table 1, entries 7-9). A few anomalously large agglomerates of ruthenium species were observed on the surface of cerium oxide. In contrast, the results from EDS analysis of the catalyst supported on spinel (Table 1, entry 4) revealed small variation in the amount of determined ruthenium, thus suggesting an improved dispersion of active species on the surface of spinel. With respect to catalytic performance, the contribution of the agglomerates is expected to be negligible, since the surface area

provided by these few large particles is insignificant compared to the collective surface area of the smaller particles.

3.2. Effect of the support

In our previous works[18,19] aerobic oxidation of bio-ethanol (5 wt% ethanol solution in water) to acetic acid with spinel- and titania-supported gold nanoparticle catalysts at elevated temperatures and high pressures was presented. Here, we investigated the aforementioned oxidation with $Ru(OH)_x$ supported on spinel, titania and ceria as catalysts (Figure 2). Titania, ceria and spinel are stable and attractive supports for various catalytic reactions, and they were also applied in our previous works on aerobic oxidation of bio-renewables.[26,27]

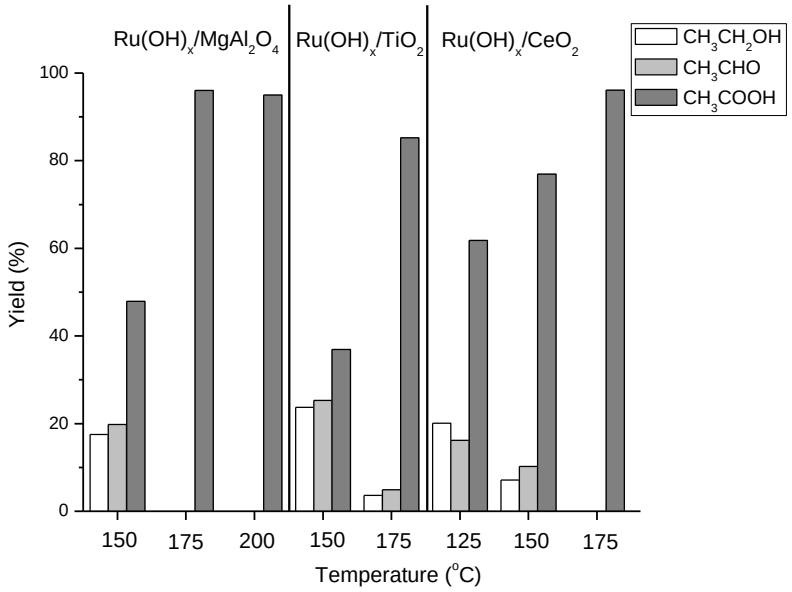

Figure 2. Product distribution in the aerobic oxidation of aqueous ethanol with supported 2.4 wt% $Ru(OH)_x$ catalysts at different temperatures (10 g of 5 wt% ethanol/H_2O, 0.23 mol% Ru, 30 bar O_2, 3 hours reaction time).

As seen in Figure 2, all three tested supported catalysts exhibited high activity in the aerobic oxidation of ethanol. At 175°C all three catalysts gave full conversion and yields above 90 % at 30 bar of oxygen after 3 hours of reaction. The efficiency of the spinel- and titania-supported catalysts proved to be comparable (vide supra), though the TiO_2-supported catalyst was slightly less effective under the applied reaction conditions. Interestingly, $Ru(OH)_x/CeO_2$ showed better catalytic performance in the oxidation reaction. In fact, even at the lower temperature (125°C) the product yields in the reaction when $Ru(OH)_x/CeO_2$ catalyst was applied were higher than the respective yields for TiO_2 and spinel at 150°C.

In order to investigate the effect of the support on the catalytic performance, a decrease in the reaction operating temperature was performed for two catalysts (ceria and spinel) while running reactions long enough to achieve high yields under these conditions (Figures 3a and 3b).

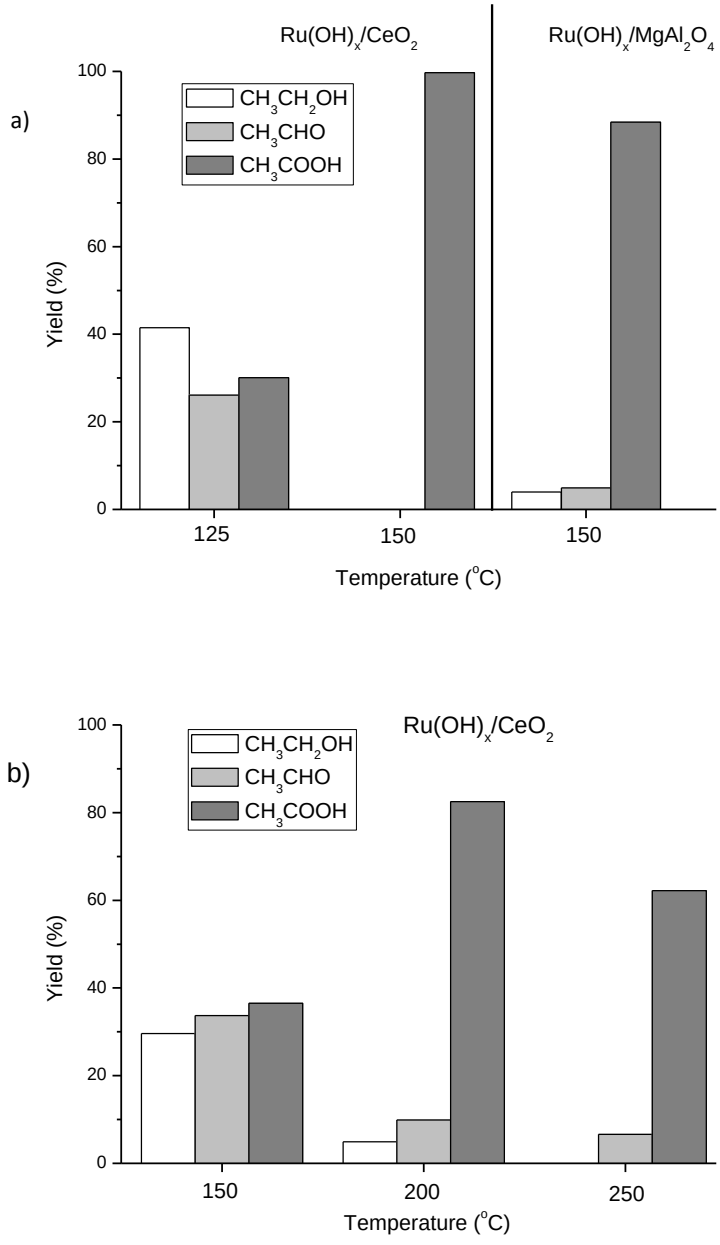

Figure 3. Product distribution in the aerobic oxidation of aqueous ethanol with the supported 2.4 wt% $Ru(OH)_x$ catalysts after (a) 20 hours and (b) 3 hours of reaction time (10 g of 5 wt% ethanol/H_2O, 0.23 mol% Ru, 10 bar O_2).

The results presented in Figure 3a indicated that ceria-supported ruthenium catalyst performed more efficiently than $Ru(OH)_x/MgAl_2O_4$ at the same reaction conditions, i.e. 10 bar of dioxygen and 150°C. The

results of the temperature variation (Figure 3b) showed that at 200°C an acetic acid yield above 80 % was already observed after only 3 hours of reaction time using the $Ru(OH)_x/CeO_2$ catalyst. However, an increased temperature of 250°C resulted in a lower yield of acetic acid (and lower overall carbon mass balance). This was likely due to the decomposition of aqueous acetic acid over ruthenium catalyst, similarly to reported by Imamura et al.,[28] who performed the oxidation of aqueous acetic acid over a catalyst comprised of RuO_2 supported on CeO_2 under 30 bar of O_2/N_2 mixture at 200°C. Notably, in our work no significant over-oxidation to CO_2 or other product degradation seemed to occur with $Ru(OH)_x/CeO_2$ catalyst even at 200°C, where the carbon mass balance still was intact (i.e., >95 %). Decreasing the temperature to 125°C affected the rate of the reaction, as expected, providing only ca. 40 % acetic acid yield at 70 % conversion of ethanol after 20 hours (Figure 3a).

Figure 4 presents product yields are plotted against reaction time in the oxidation reaction of 5 wt% aqueous ethanol solution with 2.4 wt% $Ru(OH)_x/CeO_2$ at 150 and 200°C under 10 bar O_2.

The data compiled in Figure 4 clearly demonstrated that the initially formed acetaldehyde was oxidized into acetic acid as the reaction progresses. Notably, acetaldehyde is thus an intermediate oxidation product under these conditions, rather than a final product as in the case reported by Iglesia et al.,[29] where ethanol was oxidized to acetaldehyde at low temperatures using RuO_2 supported on tin, titanium, aluminium, zirconium oxides and silica. At 200°C the aldehyde oxidation occurred relatively faster than at 150°C, making acetic acid the major product even already after 1 hour of reaction time.

In fact, a reaction pathway involving an initial formation of acetaldehyde is in good accordance with the mechanism of the alcohols oxidation to aldehydes and ketones over supported Ru(OH)x catalysts suggested by Mizuno an co-workers,[23,24,30] involving a formation of alkoxide species followed by β-hydride elimination.[30]

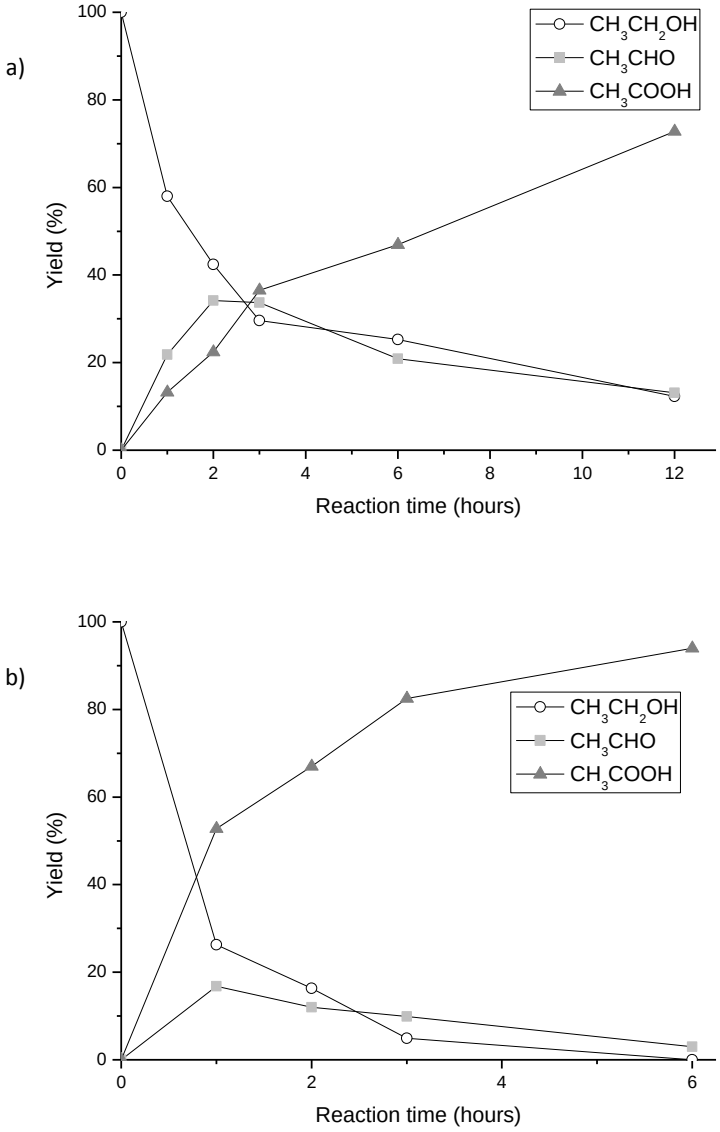

Figure 4. Product yields in the aerobic oxidation of aqueous ethanol with 2.4 wt% $Ru(OH)_x/CeO_2$ catalyst at (a) 150°C and (b) 200°C (10 g of 5 wt% ethanol/H_2O, 0.23 mol% Ru, 10 bar O_2).

3.3. Effect of the substrate concentration

In order to examine the influence of the ethanol concentration on the product formation, oxidation experiments with different initial concentrations (wt%) of ethanol in water were performed (Figures 5a and 5b).

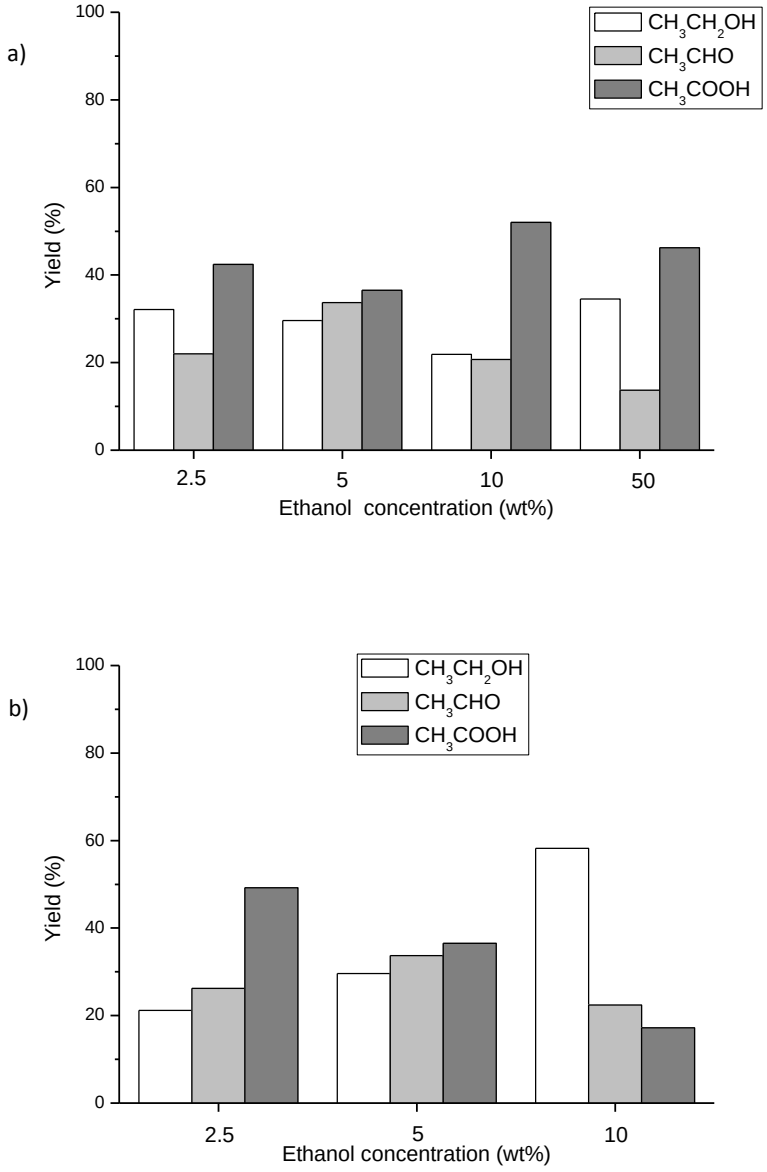

Figure 5. Product distribution in the aerobic oxidation of aqueous ethanol with 2.4 wt% $Ru(OH)_x/CeO_2$ catalyst (a) at constant catalyst to substrate ratio (0.23 mol%) and (b) with constant added amount (0.105 g) of the catalyst (10 g of ethanol/H_2O solution, 10 bar O_2, 150^oC, 3 hours reaction time).

Interestingly, no significant difference in catalyst performance was observed when the concentration of ethanol was changed from 2.5 wt% to 50 wt% in water (the catalyst to substrate ratio was kept constant) (Figure 5a). This clearly shows that the concentration does not affect the yield as much as the oxidant pressure or temperature, and indicates that the reaction is not kinetically controlled under the applied reaction conditions.

However, it is seen from Figure 5b that varying the concentration of the substrate effected the ethanol conversion and the product distribution within a certain period, i.e. after 3 hours of reaction time. In fact, a clear tendency of increased conversion and acetic acid yield in the order 2 wt% > 5 wt% > 10 wt% ethanol/water mixtures was observed. Obviously, this is correlated to the substrate:catalyst ratio, which decreased in the same order. Summarizing the results from Figures 5a and 5b, it is clear that the catalytic system is applicable for a wide range of alcohol concentrations, thus making it prone to be utilized for various applications, including fermented bio-ethanol oxidation.

3.4. Additional oxidation experiments with $Ru(OH)x/CeO_2$

As cerium oxide-supported ruthenium catalyst exhibited improved activity compared to TiO_2 and spinel supports, additional experiments to investigate its performance were conducted.

Table 2. Product yields in the aerobic oxidation of aqueous ethanol with 2.4 wt% ruthenium catalysts.[a]

Entry	Catalyst	Reaction time (hours)	Gas/pressure (bar)	Conversion (%)	Yield (%)	
				CH_3CH_2OH	CH_3CHO	CH_3COOH
1	-	3	O_2/10	11	2	3
2	CeO_2	3	O_2/10	17	7	9
3	$Ru(OH)_x/CeO_2$	3	O_2/10	72	34	37
4	$Ru(OH)_x/CeO_2$	90	O_2/10	>99	0	97
5	$Ru(OH)_x/CeO_2$	3	Ar/10	13	4	4

[a]Reaction conditions: 10 g of 5 wt% ethanol/H_2O, 0.23 mol% Ru (entries 3-5), 150°C.

The results in Table 2 suggest that the support itself, i.e. pure CeO_2, had low but not negligible catalytic activity. Here, the conversion of ethanol after 3 hours of reaction time increased from 11 %, when no catalyst or support was introduced to the reaction (Table 2, entry 1), to ca. 17 % in presence of CeO_2 (entry 2), while the product formation increased accordingly. This can possibly be due to the redox activity of cerium(IV) oxide usually ascribed to the Ce^{4+}/Ce^{3+} redox interactions on its surface.[31-33]

In contrast, the oxidation in argon atmosphere (Table 2, entry 5) appeared to be negligible, as anticipated. The small amount of the formed oxidation product could possibly originate from the oxygen dissolved in water and ethanol, due to insufficient removal when saturated with argon prior to the experiment.

Good catalytic activity was only observed with the catalyst containing ruthenium (Table 2, entry 3), thus suggesting that most of the catalytic activity originated from the metal inventory.

To obtain information on the product stability, an experiment was also carried out at prolonged reaction time (Table 2, entry 4). After 90 hours of continuous reaction, the product (acetic acid) was exclusively formed and remained stable; the ca. 2.5 % difference between conversion and yield could possibly be related to the almost negligible acetic acid degradation.

3.5. Effect of the $Ru(OH)_x$ loading on supports

In order to elucidate the effect of alteration of the loading of ruthenium on the surface of cerium oxide, 1.2 wt% and 4.7 wt% $Ru(OH)_x/CeO_2$ catalysts were also tested in the aerobic oxidation of ethanol (Table 3, Figure 6).

Table 3. Product yields in the aerobic oxidation of aqueous ethanol with supported $Ru(OH)_x$ catalysts.[a]

Entry	Catalyst[b]	Reaction time (hours)	Conversion (%)	Yield (%)	
			CH_3CH_2OH	CH_3CHO	CH_3COOH
1	1.2 wt% $Ru(OH)_x/CeO_2$	6	86	9	77
2	2.4 wt% $Ru(OH)_x/CeO_2$	6	75	21	47
3	4.7 wt% $Ru(OH)_x/CeO_2$	6	63	25	30
4	1.2 wt% $Ru(OH)_x/CeO_2$	3	71	27	43
5	1.2 wt% $Ru(OH)_x/CeO_2$ (re-use)	3	70	24	42
6	1.2 wt% $Ru(OH)_x/MgAl_2O_4$	3	45	15	27
7	2.4 wt% $Ru(OH)_x/MgAl_2O_4$	3	41	14	22
8	0.6 wt% $Ru(OH)_x/CeO_2$	6	99	1	98
9[c]	1.2 wt% $Ru(OH)_x/CeO_2$, CeO_2	6	99	2	97
10[d]	4.7 wt% $Ru(OH)_x/CeO_2$, CeO_2	6	76	24	49
11[e]	2.4 wt% $Ru(OH)_x/CeO_2$, CeO_2	6	83	16	65

[a]Reaction conditions: 10 g of 5 wt% ethanol/H_2O, 0.23 mol% Ru, 10 bar O_2, 150°C. [b]The mass of the introduced catalyst was altered in different experiments, while the Ru amount (relative to susbtrate) remained 0.23 mol% (entries 1-8). [c]0.21 g of 1.2 wt% $Ru(OH)_x/CeO_2$ with added 0.21 g of CeO_2. [d]0.053 g of 4.7 wt% $Ru(OH)_x/CeO_2$ with added 0.157 g of CeO_2. [e]0.105 g of 2.4 wt% $Ru(OH)_x/CeO_2$ with added 0.105 g of CeO_2.

It is seen that the change of the ruthenium loading from 1.2 to 4.7 wt% gradually decreased the activity of the catalyst (Table 3, entries 1-3). This may possibly be explained by the different particle sizes found in the ceria-supported catalysts (see Table 1). Higher ruthenium loading resulted in larger particles, and hence in a decrease of the number of active sites, which in turn decreased the activity of the catalyst. Also, the extraordinary properties of ceria as surface oxygen capacitor[33] and the catalytic properties of CeO_2 in the oxidation of aqueous ethanol (as was shown in Table 2) might facilitate the oxidation as more ceria is introduced in the reaction when the same substrate to catalyst ratio is used (e.g., 0.21 g of 1.2 wt% $Ru(OH)_x/CeO_2$ corresponds to 0.0525 g of 4.7 wt% $Ru(OH)_x/CeO_2$).

Interestingly, the decrease of the ruthenium loading on spinel did not significantly improve the results for the oxidation with spinel-supported $Ru(OH)_x$ catalysts (Table 3, entries 6 and 7). As was shown above, $MgAl_2O_4$, and especially with the deposited ruthenium, has higher surface area than CeO_2 (see Table 1, entries 3-9).

In order to further elucidate the effect of a ceria support, a 0.6 wt% $Ru(OH)_x/CeO_2$ catalyst was prepared and utilized in the oxidation of 5 wt% aqueous ethanol (Table 3, entry 8). Here, the results of a reaction with 0.42 g of 0.6 wt% $Ru(OH)_x/CeO_2$ were compared to the results of the usage of 0.21 g of 1.2 wt% $Ru(OH)_x/CeO_2$ with added 0.21 g of CeO_2 (i.e., both Ru mol% and support amount remained constant at two different ruthenium loadings) (entry 9). No difference in the products yields was observed, supporting the suggested hypothesis that both ceria and $Ru(OH)_x$ contributed to the overall catalyst activity. However, when a similar comparison between the performance of 1.2 and 4.7 wt% $Ru(OH)_x/CeO_2$ catalysts (0.23 mol% Ru, overall mass 0.21 g) was performed (Table 17, entries 1 and 10), it was shown that both substrate conversion and product yields were significantly lower in case of 4.7 wt% catalyst, even with added CeO_2. A similar result was obtained when reaction with 1.2 and 2.4 wt% catalysts were compared (Table 3, entries 1 and 11).

Thus, the obtained results suggest that: 1) a small variation in loading of the active species on spinel does not affect the particles size, which can explain similar performance for 1.2 and 2.4 wt% $Ru(OH)_x/MgAl_2O_4$; 2) at least some of the improved performance of the $Ru(OH)_x/CeO_2$ catalyst with lesser $Ru(OH)_x$ loading originates in the increase of the support amount (as spinel is a redox-inert support[18] in contrast to CeO_2); and 3) when the performance of the CeO_2-supported catalysts with decreasing $Ru(OH)_x$ loading is compared, after reaching some optimal size (possibly corresponding to about 1 wt% $Ru(OH)_x$) the particle size effect becomes insignificant compared to the catalytic activity of the increased amount of CeO_2.

A catalyst reuse experiment was also conducted. Here the reaction was first carried out with 1.2 wt% $Ru(OH)_x/CeO_2$ catalyst for 3 hours, then the catalyst was filtered off, washed with hot water, dried at 140^{o}C for 2 hours and another reaction was performed again (Table 3, entries 4 and 5). The obtained data shows that the catalyst was prone to reuse under the applied reaction conditions, as was previously found for the

$Ru(OH)_x$ supported on CeO_2 used for the catalytic aerobic oxidation of 5-hydroxymethylfurfural in water under elevated pressures and temperatures.[25]

As the preliminary test showed that 1.2 wt% ceria-supported ruthenium catalyst exhibited superior performance compared to 2.4 wt% ceria- as well as 1.2 and 2.4 wt% spinel-supported catalysts (Table 3), the time study of the reaction with the former catalyst was conducted (Figure 6). It is clearly seen that the 1.2 wt% catalyst exhibited higher activity than the 2.4 wt% catalyst under the same reaction conditions (see Figure 4a), allowing to obtain the yield of acetic acid above 90% after 12 hours of reaction time.

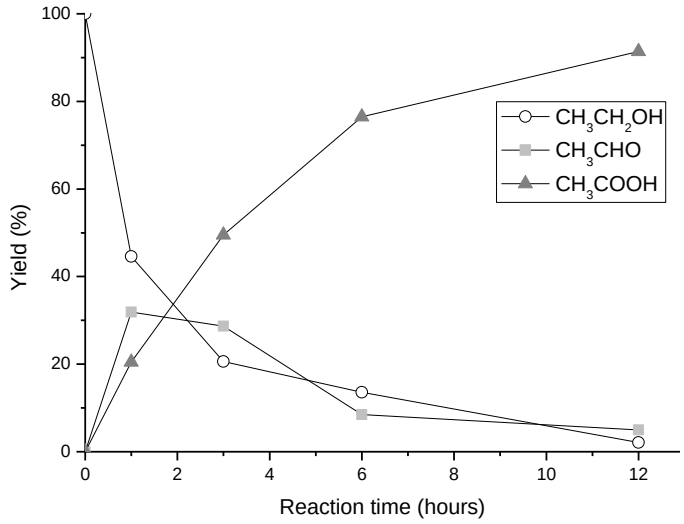

Figure 6. Product yields in the aerobic oxidation of aqueous ethanol with 1.2 wt% $Ru(OH)_x/CeO_2$ catalyst (10 g of 5 wt% ethanol/H_2O, 0.23 mol% Ru, 10 bar O_2, 150^oC).

3.6. Leaching test

Although the recovered catalyst proved to be reusable under the applied reaction conditions, an experiment was conducted in order to elucidate the homogeneous contribution in the catalyzed reaction, examining whether the catalytically active ruthenium species remained heterogeneous or were dissolved from the catalyst. The reaction was carried out at 150^oC under 10 bar of O_2 for 1 hour, then the catalyst was filtered off and the filtrate poured back into the autoclave. The autoclave was then re-pressurized with 10 bar O_2 and the reaction continued for 2 hours more (Figure 7).

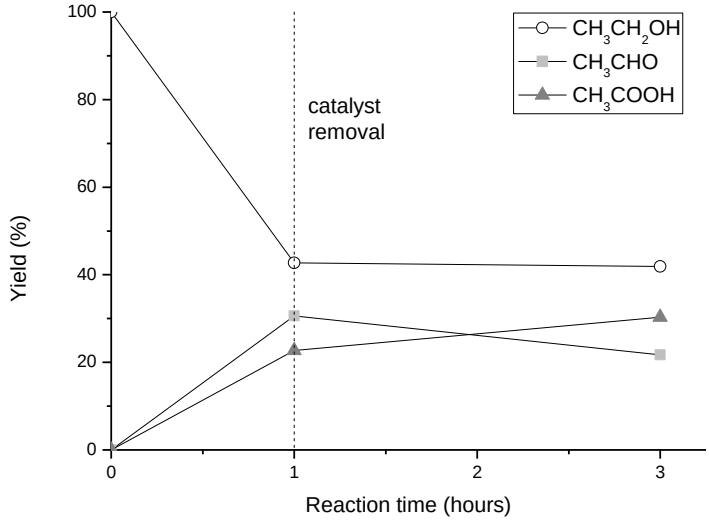

Figure 7. Product yields in the aerobic oxidation of aqueous ethanol with 1.2 wt% $Ru(OH)_x/CeO_2$ catalyst (10 g of 5 wt% ethanol/H_2O, 0.23 mol% Ru, 10 bar O_2, 150^oC).

Figure 7 shows that no substrate (ethanol) conversion occurred after the catalyst was removed (i.e. no catalytic species dissolved), while a certain amount of aldehyde was converted into acid. The latter reaction can however proceed without added catalyst,[34] and therefore it is expected to occur under the reaction conditions as well. As an additional experiment, the oxidation reaction was performed at the same conditions with acetaldehyde as the substrate. 1.2 wt% $Ru(OH)_x/CeO_2$ (0.23 mol% Ru) catalyst was introduced to the reaction with 10 g of 5 wt% acetaldehyde solution in water at 150^oC and 10 bar of O_2. After a reaction time of 3 hours, the yield of acetic acid constituted 86 % with 10 % of acetaldehyde remaining unconverted. This result, compared with the data from Table 3 and Figures 6 and 7, clearly indicates the initial oxidation of ethanol to acetaldehyde to be the performance determining step in the reaction process.

3.7. Effect of the catalyst calcination temperature

To elucidate the effect of the calcination on the activity of the catalyst, the results of the aqueous ethanol oxidation reaction with the non-treated catalyst was compared to the catalysts calcined at two different temperatures. The results are presented in Figure 8.

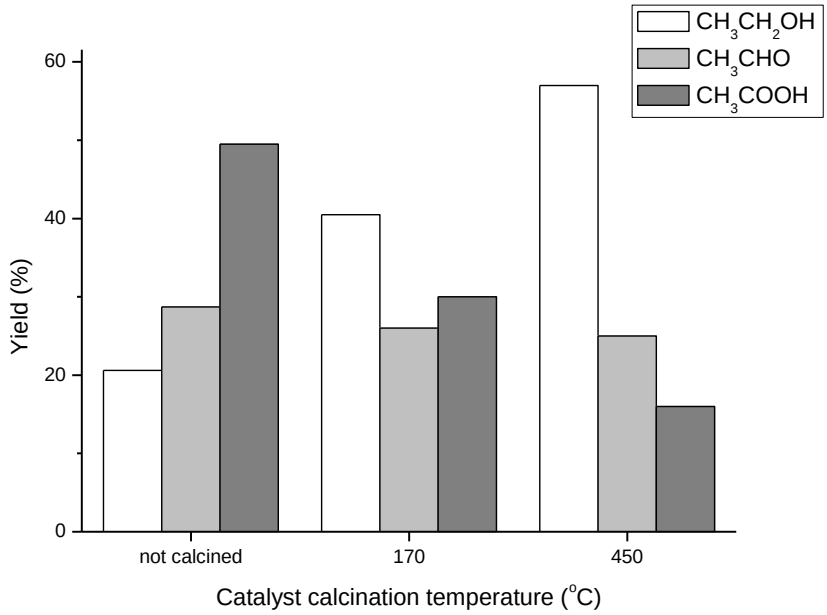

Figure 8. Product yields in the aerobic oxidation of aqueous ethanol with calcined 1.2 wt% $Ru(OH)_x/CeO_2$ catalysts. Reaction conditions: 10 g of 5 wt% ethanol/H_2O, 0.23 mol% Ru, 10 bar O_2, 150°C, 3 hours reaction time.

It is clearly seen from the presented results that the calcinations affected the activity of the catalyst. Indeed, within 3 hours of reaction time the usage of calcined catalysts resulted in decreased ethanol conversion and acetic yield, although the yield of acetaldehyde remained virtually the same (Figure 8). Moreover, both substrate conversion and acetic yield decreased with the increase of the catalyst calcination temperature. This was in good accordance with the results reported by Yang et al.,[35] where a decrease in the aerobic catalyst perfromance was observed when hydrated ruthenium oxide catalytic species were annealed in N_2 at high temperatures, ascribed to the dehydration of ruthenium species. Similarly, Laursen et al.[36] reported for the supported RuO_x catalysts a heat-induced particle sintering accompanied by the formation of crystalline RuO_2 from the initially amorphous[25] ruthenium species.

Interestingly, an increase in the catalyst heat-treatment temperature only to 170°C (compared to the catalyst drying temperature of 140°C) resulted in approximately 20 % decrease of ethanol conversion and acetic acid yield. This might also indicate that higher reaction temperatures (e.g. 200, 250°C) could eventually cause catalyst deactivation, though within the reaction timeframe (3-6 hours, see Figures 2, 3b, 4b) these effects were not clearly revealed. However, the above-discussed overoxidation of acetic acid at 250°C (Figure 3b) was possibly due to the presence of crystalline RuO_2, in accordance with the results reported by Imamura et al.[29] Nonetheless, it must be mentioned here that although the reaction conditions of e.g. 250°C

were discussed above (Figure 3b), the said reaction was carried out in aqueous solution, thus making an evaluation of the possible temperature effect on the catalyst deactivation difficult.

4. Conclusion

Highly selective and efficient aerobic oxidation of aqueous ethanol (2.5-50 wt%) to acetic acid with supported ruthenium hydroxide catalysts at elevated temperatures and oxygen pressures is reported. The performance of catalysts based on different supports increased in the order $Ru(OH)_x/TiO_2$ < $Ru(OH)_x/MgAl_2O_4$ < $Ru(OH)_x/CeO_2$. Furthermore, the activity of the CeO_2-supported $Ru(OH)_x$ catalysts was found to be dependant on the ruthenium species loading on the surface of the support and hence the particle size. The optimal performance was suggested to correspond to approximately 1 wt% $Ru(OH)_x$ loading with a particle size of 0.6 - 2 nm. Here, the increase of the loading resulted in a decrease of the catalytic activity contributed by ruthenium species, and a decrease in ruthenium loading did not improve $Ru(OH)_x$ catalytic activity. Importantly, the oxidation of aqueous ethanol solutions of high concentrations is shown to proceed with similar efficiency, thus providing opportunity for utilization of the catalyst systems in bio-ethanol upgrading.

Acknowledgments

The authors thank Bodil F. Holten at the Centre for Catalysis and Sustainable Chemistry for BET measurements. The A. P. Møller and Chastine Mc-Kinney Møller Foundation is gratefully acknowledged for its contribution towards the establishment of the Center for Electron Nanoscopy at the Technical University of Denmark.

References

(1) Weissermel, K.; Arpe, H.-J. *Industrial Organic Chemistry*, 4th edn.; Wiley-VCH: Weinheim, 2003; p 171.

(2) Ebner, H.; Follmann, H.; Sellmer, S. Vinegar. In *Ullmann's Encyclopedia of Industrial Chemistry*, 7th edn.; Wiley-VCH: Weinheim, 2005.

(3) Simpson, T. W.; Sharpley, A. N.; Howarth, R. W.; Paerl, H. W.; Mankin, K. R. *J. Environ. Qual.* **2008**, 37, 318-24.

(4) Rass-Hansen, J.; Falsig, H.; Jørgensen, B.; Christensen, C. H. *J. Chem. Technol. Biotechnol.* **2007**, 82, 329-333.

(5) Zotova, N.; Hellgardt, K.; Kelsall, G. H.; Jessiman, A. S.; Hii, K. K. *Green Chem.* **2010**, 12, 2157-2163.

(6) Cheung, H.; Tanke, R. S.; Torrence, G. P. Acetic acid. In *Ullmann's Encyclopedia of Industrial Chemistry*, 7th edn.; Wiley-VCH: Weinheim, 2005.

(7) Thomas, C. *Coord. Chem. Rev.* **2003**, 243, 125-142.

(8) Kamble, D. L.; Nandibewoor, S. T. *J. Phys. Org. Chem.* **1998**, 11, 171–176.

(9) Nielsen, I. S.; Taarning, E.; Egeblad, K.; Madsen, R.; Christensen, C. H. *Catal. Lett.* **2007**, 116, 35-40.

(10) Han, J.; Liu, Y.; Guo, R. *Adv. Funct. Mater.* **2009**, 19, 1112–1117.

(11) Rajesh, H.; Ozkan, U. S. *Ind. Eng. Chem. Res.* **1993**, 32, 1622-1630.

(12) Li, X.; Iglesia, E.; *Chem. Eur. J.* **2007**, 13, 9324-9330.

(13) ten Brink, G.-J.; Arends, I. W. C. E.; Sheldon, R. A. *Science* **2000**, 287, 1636-1639.

(14) Nishimura, T.; Kakiuchi, N.; Inoue, M.; Uemura, S. *Chem. Commun.* **2000**, 1245-1246.

(15) Mori, K.; Hara, T.; Mizugaki, T.; Ebitani, K.; Kaneda, K. *J. Am. Chem. Soc.* **2004**, 126, 10657-10666.

(16) Nagai, M.; Gonzalez, R. D.; *Ind. Eng. Chem. Prod. Res. Dev.* **1985**, 24, 525–531.

(17) Takei, T.; Iguchi, N.; Haruta, M. *Catal. Surv. Asia* **2011**, 15, 80-88.

(18) Christensen, C. H.; Jørgensen, B.; Rass-Hansen, J.; Egeblad, K.; Madsen, R.; Klitgaard, S. K.; Hansen, S. M.; Hansen, M. R.; Andersen, H. C.; Riisager, A. *Angew. Chem. Int. Ed.* **2006**, 45, 4648-4651.

(19) Jørgensen, B.; Christiansen, S. E.; Thomsen, M. L. D.; Christensen, C. H. *J. Catal.* **2007**, 251, 332-337.

(20) Yamaguchi, K.; Mizuno, N. *Chem. Eur. J.* **2003**, 9, 4353-4361.

(21) Kotani, M.; Koike, T.; Yamaguchi, K; Mizuno, N. *Green Chem.* **2006**, 8, 735-741.

(22) Kim, J. W.; Yamaguchi, K.; Mizuno, N; *Angew. Chem. Int. Ed.* **2008**, 47, 9249-9251.

(23) Mizuno, N.; Yamaguchi, K. *Catal. Today* **2008**, 132, 18-26.

(24) Yamaguchi, K.; Mizuno, N. *Synlett* **2010**, 16, 2365-2382.

(25) Gorbanev, Y. Y.; Kegnæs, S.; Riisager, A. *Top. Catal.* **2011**, DOI 10.1007/s11244-011-9754-2.

(26) Taarning, E.; Nielsen, I. S.; Egeblad, K.; Madsen, R.; Christensen, C. H. *ChemSusChem* **2008**, 1, 75-78.

(27) Gorbanev, Y. Y.; Klitgaard, S. K.; Woodley,J. M.; Christensen, C. H.; Riisager, A. *ChemSusChem* **2009**, 2, 672-675.

(28) Imamura, S; Fukuda, I.; Ishida, S. *Ind. Eng. Chem. Res.* **1988**, 27, 718-721.

(29) Liu, H.; Iglesia, E. *J. Phys. Chem. B* **2005**, 109, 2155-2163.

(30) Nikaidou, F.; Ushiyama, H.; Yamaguchi, K.; Yamashita, K.; Mizuno, N. *J. Phys. Chem. C* **2010**, 114, 10873-10880

(31) Pavasupree, S.; Suzuki, Y.; Pivsa-Art, S.; Yoshikawa, S. *J. Solid State Chem.* **2005**, 178, 128-134.

(32) Magesh, G.; Viswanathan, B.; Viswanath, R. P.; Varadarajan, T. K. *Indian J. Chem., Sect A* **2009**, 48A, 480-488.

(33) Vayssilov, G. N.; Lykhach, Y.; Migani, A.; Staudt, T.; Petrova, G. P.; Tsud, N.; Skála, T.; Bruix, A.; Illas, F.; Prince, K. C.; Matolin, V.; Neyman, K. M.; Libuda, J. *Nat. Mater.* **2011**, 10, 310-315.

(34) Larkin, D. R. *J. Org. Chem.* **1990**, 55, 1563-1568.

(35) Yu, H.; Zeng, K.; Zhang, Y.; Peng, F.; Wang, H.; Yang, J. *J. Phys. Chem. C* **2008**, 112, 11875-11880.

(36) Kleiman-Shwarsctein, A.; Laursen, A.; Cavalca, F.; Tang, W.; Dahl, S., Chorkendorff, I. **2011** *submitted*.

Highly dispersed ruthenium oxide as an aerobic catalyst for acetic acid synthesis

Anders B. Laursen,[*,†] Yury Y. Gorbanev,[‡] Filippo Cavalca,[¶] Alan Kleiman-Shwarsctein,[†] Anders Riisager,[‡] Søren Kegnæs,[‡] Ib Chorkendorff,[†] and Søren Dahl[*,†]

Center for individual nanoparticles, Technical University of Denmark, Centre for Catalysis and Sustainable Chemistry, Technical University of Denmark, and Center for Electron Nanoscopy, Technical University of Denmark

E-mail: a.b.laursen@fysik.dtu.dk; soren.dahl@fysik.dtu.dk

Abstract

The increasing need for shifting to renewable feedstocks in the chemical industry, have driven research towards using green aerobic and selective reactions to produce bulk chemicals. Here, we report the use of a ruthenium mixed oxide/hydroxide (RuO_x) on different support materials for the aerobic and selective oxidation of ethanol to acetic acid. The RuO_x was deposited using a new gas-phase reaction, which forms a nanoparticulate films of homogeneous size and dispersion on all the tested oxide supports. The particle size range from ca. 0.5-1.5nm. The catalytic activity was evaluated on TiO_2, hydrotalchite, spinel, $Na_2Ti_6O_{13}$-NTs,

[*]To whom correspondence should be addressed

[†]Center for individual nanoparticles - CINF, Department of Physics, Technical University of Denmark - DTU, Fysikvej build. 307, DK-2800 Kgs. Lyngby, Denmark

[‡]Centre for Catalysis and Sustainable Chemistry - CSC, Department of Chemistry, Technical University of Denmark - DTU, Kemitorvet build. 207, DK-2800 Kgs. Lyngby, Denmark

[¶]Center for Nanoscopy - CEN, Technical University of Denmark - DTU, Fysikvej build. 307, DK-2800 Kgs. Lyngby, Denmark

ZnO, γ-Al_2O_3, WO_3, CeO_2, and $Ce_{0.5}Zr_{0.5}O_2$ supports. All the catalyst showed a decent activity although it varied significantly as did selectivity towards acetic acid with respect to CO_2. The CeO_2 supported RuO_x had the highest activity of all the tested support materials, this was regardless of the surface area and loading of the support - when normalized to Ru-loading. This was attributed to the highly uniform size of the RuO_x deposits, demonstrating that the deposition is suitable for producing small nanoparticles at high loadings. This is to our knowledge the first time this deposition procedure has been utilized for making heterogeneous RuO_x catalysts. The effects of heat-treatment was investigated and high valence states and a high degree of hydration was found to promote the catalytic activity. Furthermore, the influence of the oxygen storage in $Ce_{0.5}Zr_{0.5}O_2$ was investigated to elucidate the promotional effect of the CeO_2, however, no increased activity was observed.

Introduction

The need for synthesizing bulk chemicals from alternative feedstock rather than fossil increases as the fossil resources becomes ever more scarce. This production of bulk chemicals should be as benign as possible for the environment or "green".[1] One such bulk chemical is acetic acid which is produced on the 2.8 million ton scale in 1999.[2] The production of biomass-derived ethanol or "bio-ethanol" has increased dramatically since the late 1990's.[3] This bio-ethanol could find use as a versatile, sustainable chemical feedstock for the green production of acetic acid by oxidation of the bio-ethanol to "bio-acetic acid".[4]

Selective partial oxidation of organic molecules has attracted increasing attention over the past decade, especially using molecular oxygen, *i.e.* aerobic oxidations.[5–14] Aerobic oxidations are considered a "green" process because the only by-product is water, unlike the classic metal oxide oxidants, which generate stoichiometric amounts of metal waste.[15,16] Furthermore, aerobic oxidation is also attractive due to the low cost of oxygen and its unlimited accessibility.

RuO_2 is perhaps most well known as the most active electrocatalyst for the oxygen evolution reaction (OER).[17] Several reactions are also known in literature to be catalyzed by ruthenium-based

catalysts, *e.g.* ammonia decomposition,[18] metathesis reactions,[19] dehydrogenation of ethane,[20] and oxidation reactions.[21] However, the number of reports on heterogeneous ruthenium-based oxidation catalysts is limited, and primarily focused on the oxidation of alcohols to oxo compounds in organic solvents by Kaneda et al.,[22,23] Mizuno et al.[24,25] Vinke et al.,[14] and in aqueous solution by Gorbanev et al.[26,27] In this work we focus on the green aerobic and selective oxidation of ethanol (CH_3CH_2OH) to acetic acid (CH_3COOH) in aqueous solution.

Recently, we reported a new procedure to conformal coat metal oxide supports with a high coverage of ruthenium oxide (RuO_x) nanoparticles.[28] The co-catalyst deposited according to this procedure on TiO_2 and WO_3, resulted in an improved water oxidation activity compared to the pristine semiconductor, mainly due to its catalytic OER activity. It was demonstrated that the nanoparticles covered the support in very thin and homogeneous layers, providing a high dispersion of the RuO_x nanoparticles.

In the present work the catalytic properties of this novel type of heterogeneous catalyst is investigated for the selective aerobic oxidation of ethanol. The active RuO_x were deposited on a variety of different supports, utilizing the same manufacturing procedure for all supports, to evaluate the support effect on the catalytic activity. The reaction was carried out at benign condition, *i.e.* in the absence of catalytic amounts of base, at only 10 bar O_2 pressure, and at 150°C, this gave close to quantitative yields of acetic acid, as reported by Gorbanev et al.[26] In this study it was demonstrated that $Ru(OH)_x$ supported on hydrotalchite, spinel, and cerium oxide was active for the selective aerobic oxidation of CH_3CH_2OH to CH_3COOH, and that cerium oxide gives the highest catalytic activity. In this study, the focus was on testing a variety of different supports for this selective oxidation. The support materials were chosen so as to have different acid/base, and redox properties. Using the gas phase RuO_x deposition method allowed the catalyst nanoparticles to be highly dispersed and relatively homogeneous in size across the variation in supports. This combination allowed for the straight forward comparison of the catalytic activity between the different supports. Furthermore, we attempted to elucidate the origin of the promotional effect of cerium oxide.

Experimental

Materials

The next reagents where use as recieved: Ethanol (CH_3CH_2OH) (99.9%, Kemetyl A/S), acetaldehyde (CH_3CHO) (99.5%, Sigma-Aldrich), acetic acid (CH_3COOH) (99.8%, Riedel-de Haën AG) and O_2 (99.5%, Air Liquide Denmark), $RuCl_3 \cdot xH_2O$ (99% ReagentPlus, (40-49 wt% Ru, Sigma-Aldrich), $KMnO_4$ (analysis pure, Merck), Dopamine Chloride (Sigma-Aldrich), Degussa P25 TiO_2 (Degussa), hydrotalcite (HT, $Mg_6Al_2(CO_3)(OH)_{16} \cdot 4\,(H_2O)$, courtesy of Haldor Topsøe), spinel ($MgAl_2O_4$, , courtesy of Haldor Topsøe), sodium titanate nanotubes ($Na_2Ti_6O_{13}$-NTs) were synthesized as described in literature,[29] ZnO (Sigma-Aldrich), γ-Al_2O_3 (Puralox TH100/150, Sasol), WO_3 (Sigma-Aldrich), and CeO_2 (nanopowder - Sigma-Aldrich), CeO_2, (AMR) and $Ce_{0.5}Zr_{0.5}O_2$ (AMR). Millipore water was obtained from a Milli-Q® water system with a water resistivity of 18.2 MΩ· cm.

Catalyst preparation

General details of the catalyst preparation have been reported previously[28] and are described below:

Step 1, functionalization of supports: 1 g support (TiO_2, hydrotalchite, spinel, $Na_2Ti_6O_{13}$-NTs, ZnO, γ-Al_2O_3, WO_3, CeO_2, and $Ce_{0.5}Zr_{0.5}O_2$) was suspended in a 20 mM dopamine chloride solution in 30 vol.% MeOH/millipore water by sonication for 30 min. The powder was recovered by centrifugation at 20,000 rpm for 60 min and decantation of the liquid. The powder was washed by resuspension in millipore water, centrifugation and decantation on the liquid; the washing procedure was repeated 4 times. The resulting powder was finally dried at 95°C overnight in air. The yield was around 90 % (by weight for a representative RuO_x/CeO_2 sample).

Step 2, RuO_x coating: 0.5 g of functionalized support was placed in a glass tube (4 mm diameter by 30 cm length) between two pyrex wool corks on the end of the tube. The tube was placed through a septum in a three necked flask. A fritted glass tube was also fitted, through a septum, in

the three necked flask and then connected to nitrogen gas with a needle valve to adjust the nitrogen flow (further setup details are given in[28]). 40 mg $RuCl_3 \cdot xH_2O$ was transferred to the flask with 10 ml millipore water, and the solution was then stirred for ca. 5 min. Then 80 mg $KMnO_4$ was transferred to the flask with another 10 ml millipore water and the flask sealed. A flow of N_2 was then introduced through the reaction mixture and the flow adjusted so that the powder was gently flowing. The flask was continuously stirred at 400 rpm throughout the deposition. Every hour the tube with the catalyst was rotated allowing for a homogeneous coating. After 4 h the deposition was considered finished and the powder collected and used without further preparation. The catalyst yield was around 84 % (by weight for a representative RuO_x/CeO_2 sample).

For samples with lower ruthenium loading the amount of $RuCl_3 \cdot xH_2O$ and $KMnO_4$ was halved and for high loading the amount was doubled compared to the procedure above. For the study of heat-treatment effects three samples, each of 0.3 g 1.8 wt% RuO_x/CeO_2 catalyst, was calcined at 170, 200 and 450°C, in air for 18 h. All other catalysts were tested without any heat-treatment.

The RuO_x deposited on TiO_2 was previously investigated by X-ray powder diffraction (XRPD) and X-ray photoelectron spectroscopy.[28] From the XRPD analysis it was determined that the RuO_x nanoparticles was amorphous. The valence state of the RuO_x was determined by XPS to be a mixture of Ru^{6+} and Ru^{3+} or $Ru(OH)_4$.[28] Whether the catalyst contained Ru^{3+} or $Ru(OH)_4$ could not be determined by XPS, hence, we use the notation RuO_x to describe the mixed oxide/hydroxide. The effect of heat-treatment on the RuO_x/TiO_2 catalyst was also investigated by XPS. Calcination at 250°C reduced and dehydrated the RuO_x into a mixed oxide/hydroxide consisting of RuO_2 and Ru^{3+} or hydrated RuO_2.[28] Furthermore, it was shown that the functionalization of the support with the dopamine chloride plays a key role in the deposition of RuO_x, as it did not occur on the pure supports.[28]

Catalyst characterization

Surface areas were determined by nitrogen physisorption measurements at liquid nitrogen temperature on a Micrometrics ASAP 2020. The samples were out-gassed in vacuum at 150°C for 6 h

prior to measurements. The total surface areas were calculated according to the BET method.

X-ray flourecent (XRF) measurements were used to determine the elemental composition using a PAN'alytical MiniPal 4. The MiniPal software (V. 0.6.B) using the built in "standardless" peak fit program. The measurements were calibrated to a series of samples of $RuCl_3 \cdot xH_2O$ impregnated onto CeO_2 powder in the concentration interval of interest.

Scaning Electrn Microscopy SEM (FEI Quanta 200 F) of the uncoated samples dropcast from CH_3CH_2OH suspension directly onto the sample holder. The microscope was a SEM, and images was obtained at 5 kV acceleration with the secondary electron emission detector.

Scanning transmission electron microscopy (STEM) images were obtained using a probe-corrected FEI Titan 80-300ST TEM and for the TEM images a FEI Tecnai T20 TEM microscopes. The Titan microscope was operated in STEM mode at 300kV accelerating voltage with 70.8 mrad inner detector angle. The powdered samples were dispersed on TEM copper grids with a holey carbon film. STEM HAADF and BF images were acquired simultaneously during every scan, thereby providing complementary data for efficient image analysis. STEM HAADF imaging is a technique sensitive to Z contrast, therefore particularly suitable for Ru deposition analysis on a variety of substrates. EDX spectra were recorded in STEM mode to study the spatial distribution of the catalyst material and compositional topography in order to provide additional information for the assessment of deposits composition and distribution.

Catalytic testing

Oxidations were carried out in stirred Parr autoclaves equipped with internal thermocontrol (T316 steel, Teflon® beaker insert, 100 ml). In each reaction the autoclave was filled with 10 g of 5 wt% of aqueous CH_3CH_2OH. Subsequently, the supported 0.9-3.4 wt% RuO_x catalyst (weight percentage given on Ru metal basis) was added (0.09-0.33 g for the different loadings, the amount was chosen to give ca. 0.03 mmol Ru in each run). The autoclave was then pressurized with O_2 (10 bar, ca. 16 mmol) and maintained at 150°C for a given period of time under stirring (500 rpm). After the reaction, the autoclave was rapidly cooled to room temperature, the reaction mixture

filtered immediately and analysed using HPLC (Agilent Technologies 1200 series, Aminex HPX-87H column from Bio-Rad, 300 mm x 7.8 mm x 9 μm, flow 0.6 mL/min, solvent 5 mM H_2SO_4, temperature 60°C). The time resolved measurements were preformed in batch mode, *i.e.* each data point corresponds to one experimental run. The HPLC was calibrated to CH_3CH_2OH, CH_3CHO, and CH_3COOH from which the carbon balance was calculated.

Results and discussion

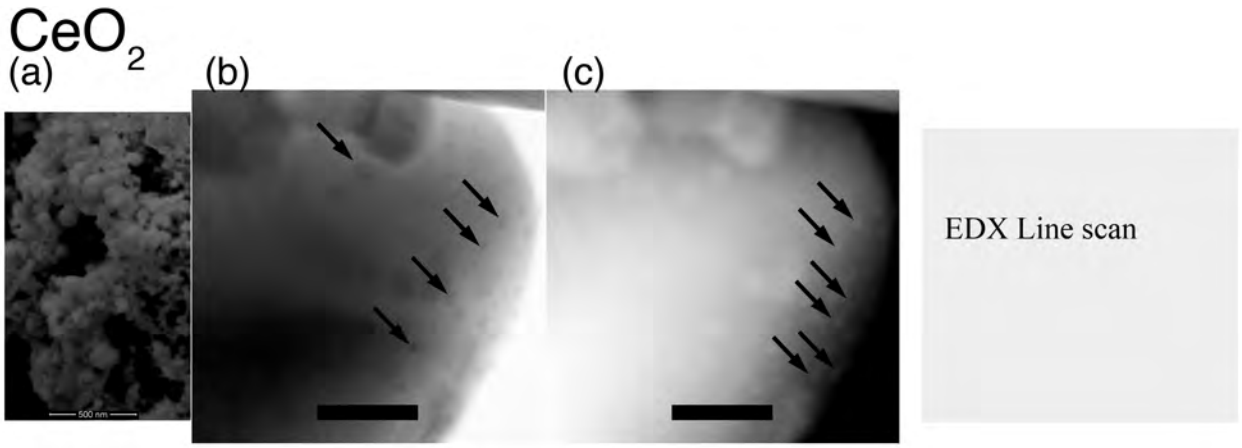

Figure 1: SEM images and STEM images, in BF and HAADF mode, of the 1.8 wt% RuO_x/CeO_2. All the materials are imaged in both STEM HAADF and BF simultaneously. The scale bar on the (a) image is 500 nm and for (b) and (c) 5 nm.

A recent study has shown that $Ru(OH)_x$ on CeO_2, prepared by impregnation, show almost quantitative yields for the aerobic oxidation of ethanol (CH_3CH_2OH) to acetic acid (CH_3COOH) at elevated temperatures and pressures.[26] In this study we accordingly use the experimental condition already reported,[26] *i.e.* 150°C, 10 bar O_2, and 3 h reaction time. Here, we present catalytic results for an array of catalyst supports tested in a batch reactor and prepared using our recently published gas-phase synthesis.[28] As this synthesis allows for the deposition of similar nanoparticles across different supports.

In literature it has been even suggested that 3 things may influence the activity towards selective oxidative dehydrogenation of CH_3OH: 1, the amount of high valence state Ru^{6+},[30] 2, the degree

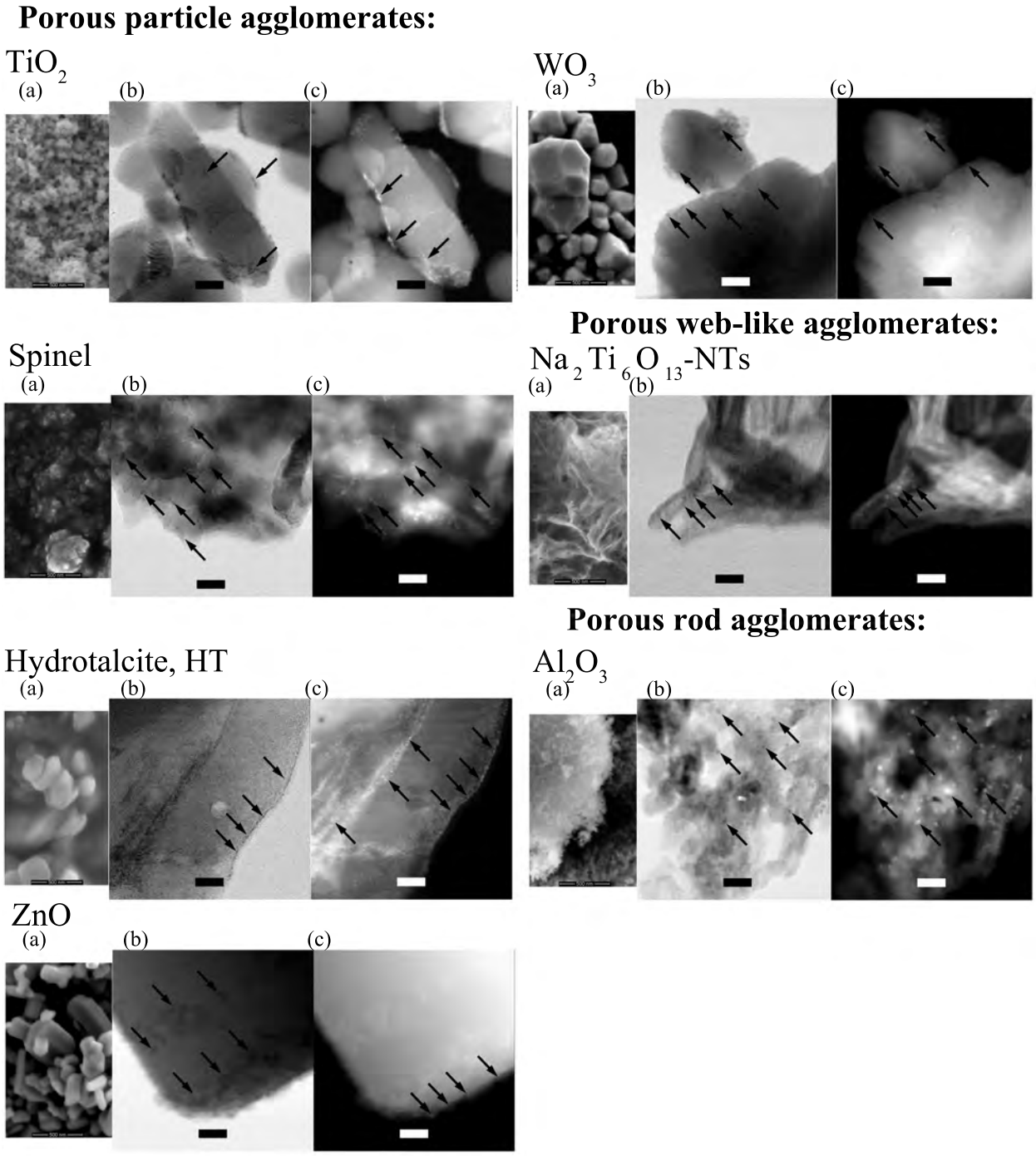

Figure 2: SEM images and STEM images, in BF and HAADF mode, of the TiO_2, HT, spinel, $Na_2Ti_6O_{13}$-NTs, ZnO, γ-Al_2O_3, and WO_3 sorted after morphology. All the materials are imaged in both STEM HAADF and BF simultaneously. The scale bar on the (a) images are 500 nm and for (b) and (c) they are 5 nm.

of hydration (the amount of $Ru(OH)_4$,[31] and 3, the particle size.[32] Li et al.[30] showed that activity could be correlated to the amount of Ru^{6+} in a ZrO_2 supported catalyst. The Ru^{6+} species were found to be dominant only at low loadings and was stabilized by the ZrO_2 support. Yu et al.[31] showed that the dehydration of $RuO_2 \cdot xH_2O$ on carbon nanotubes resulted in a decreased activity, but an increased selectivity towards formic acid and methyl formate, no CO_2 was observed. This is due to the reduced activity for the oxidative dehydrogenation, which is the rate determining step (determined by Liu et al.[32] from the kinetic isotope effect). Liu et al.[32] observed that for RuO_2 on SnO_2 the selectivity for the partial oxidation of CH_3OH to CH_2O decreased with decreasing particle size. The authors reason that small clusters will not easily lose lattice oxygen, which was shown to be a part of the rate determining step of the reaction. The optimal size was determined only based on the dispersion to be 3.5 Ru atoms/nm^2.[32] Liu et al.[32] also briefly investigated the activity of RuO_2 on SnO_2, and SiO_2 for the oxidative dehydrogenation of CH_3CHOH. In this work we will try to relate these observations to the behaviour of the gas-phase deposited RuO_x on the different supports.

We prepared catalysts supported on TiO_2 (Degussa P25), hydrotalcite (HT, $Mg_6Al_2(CO_3)(OH)_{16} \cdot 4\,H_2O$), spinel ($MgAl_2O_4$), sodium titanate nanotubes ($Na_2Ti_6O_{13}$-NTs), ZnO, γ-Al_2O_3 , WO_3, $Ce_{0.5}Zr_{0.5}O_2$ and two types of CeO_2 to determine the catalytic effect of the substrate on the yield and selectivity towards CH_3COOH.

To investigate the morphology of the support and the particles the catalysts were investigated by SEM and STEM. Figure 1 show the 1.8 wt% RuO_x/CeO_2 catalysts morphologies obtained from SEM and STEM. The support morphology was determined from the SEM image (Figure 1(a)) to be nanoparticulate with rounded particles stuck together in larger particle agglomerate. The individual support particles were approximately 100 nm with a large size distribution, and the agglomerates were on the micrometer length scale (see figure Figure 1(a)). In all the obtained SEM images (not shown) there was no observation of any particles with significantly different morphology this homogeneity was taken as an indication that the RuO_x deposits had not formed separated particles but was indeed supported on the CeO_2.

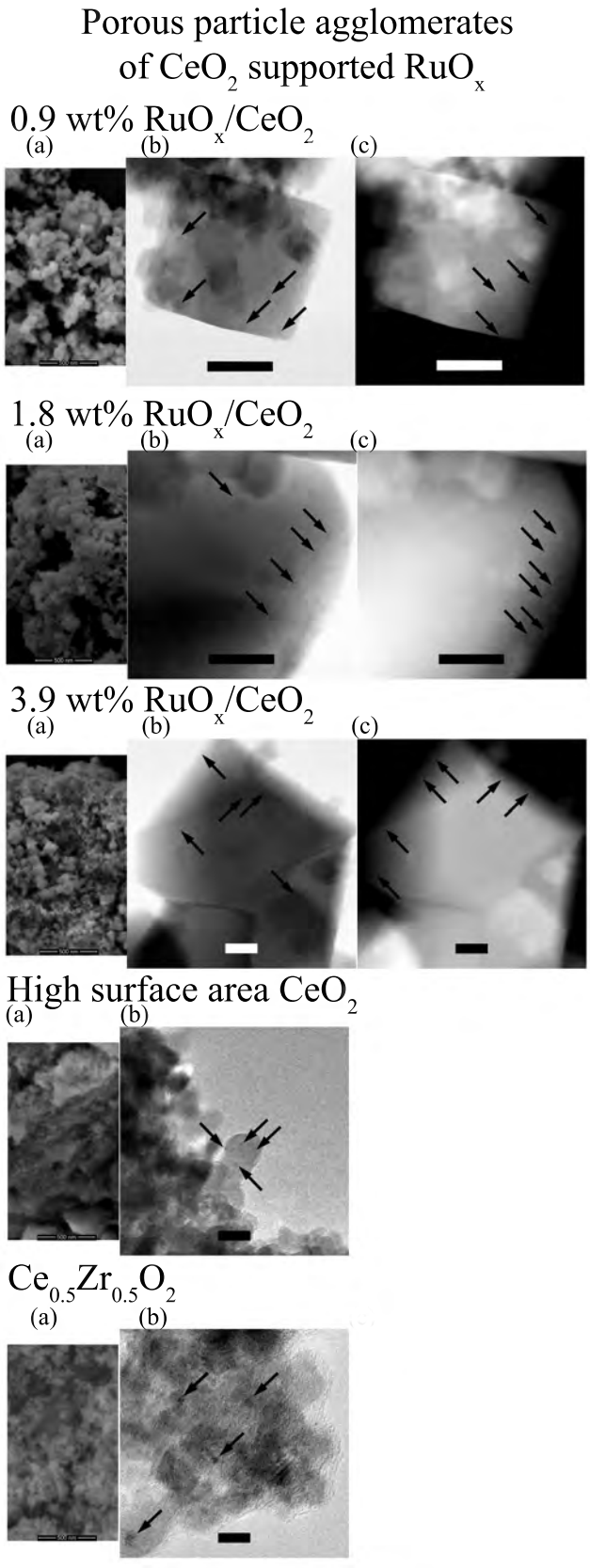

Figure 3: SEM images and STEM images, in BF and HAADF mode, of the different CeO_2 supported catalyst materials tested. All the materials are imaged in both STEM HAADF and BF simultaneously, except for high surface CeO_2 and $Ce_{0.5}Zr_{0.5}O_2$ which, due to strong charging effects in the microscope, could not be imaged in STEM mode. Instead, TEM images of the two latter substrates are shown. The scale bar on the (a) images are 500 nm and for (b) and (c) they are 5 nm.

From the BF and HAADF STEM images the deposited RuO_x could be identified. On supports like TiO_2, HT, γ-Al_2O_3, spinel, $Na_2Ti_6O_{13}$-NT, and ZnO RuO_x appears bright spot or patches in the HAADF images and dark in the corresponding BF due to its higher atomic number (Z) compared to the substrate (see Figure 2 and Figure 3(b) and (c)). The RuO_x deposits are indicated by the black arrows. This allowed for the easy determination of the size-distribution, morphology, and dispersion of the RuO_x deposits. However, for the CeO_2 and the Ce atom had a higher atomic weight than Ru, the latter could still be clearly distinguished from the support particles by comparing the BF and HAADF images as indicated by the arrows (see Figure 1(b) and (c)). That the deposits contained Ru was verified by an EDX line scan using a sub-nanometer sized electron probe (see Figure 1(d)). The deposited RuO_x particle film consists of individual particles which ranging from 0.5-1.2 nm in size, as estimated from representative STEM images.

Figure 2 and Figure 3 show representative SEM and STEM images of each of the supported RuO_x catalyst materials before the reaction. From the SEM images it is seen that the sample morphologies fall into one of three categories: (1) porous particle agglomerates, (2) porous web-like agglomerates, and (3) porous rod agglomerates. The most commonly observed support morphology was the particle-like, *i.e.* the TiO_2, spinel, HT, ZnO, WO_3(Figure 2), the four kinds of CeO_2(Figure 3) and the $Ce_{0.5}Zr_{0.5}O_2$(Figure 3) have this type of morphology. The $Na_2Ti_6O_{13}$-NTs form the web-like agglomerates(Figure 2), from the SEM images the individual tubes could not be clearly distinguished; but they could be resolved in STEM (see Figure 2). Although the γ-Al_2O_3(Figure 2) could not be imaged well due to heavy charging, the SEM images indicate that the agglomerates consisted of a rod-like morphology, which was also seen more clearly in STEM. The very small particle size of the TiO_2, spinel, CeO_2, and the $Ce_{0.5}Zr_{0.5}O_2$ made the individual particles almost indistinguishable at the resolution that could be obtained by SEM.

As each sample contained only one type of morphology in all the obtained images (only representative images are shown) it was tentatively concluded that the RuO_x had not formed large particles separated from the support in any of the catalysts; but had deposited as nanometer sized particles on the supports.

From the BF and HAADF STEM images in Figure 2 and Figure 3(b) and (c) the RuO_x morphology could be determined. TiO_2 showed a remarkably high deposition, as was also observed in the XRF and EDX analysis (Table 1), with the RuO_x particles distributed in large, homogeneous $\sim$1 nm thin amorphous particulate patches on the support particle surface (see Figure 2), which is consistent with our previous study.[28] The spinel support showed a homogeneous dispersions of evenly sized Ru nanoparticles in the 0.5-1 nm range (see Figure 2). The HT support was also coated by thin patches of Ru nanoparticles predominantly located at grain edges and forming nanoparticulate thin films (0.5-1.5 nm thick, see Figure 2). On the ZnO(Figure 2) , WO_3(Figure 2) and CeO_2(Figure 3) supports RuO_x patches of varying sizes up to 300 nm^2 was observed, these were also composed of particles in the 0.5-2 nm range (see Figure 2 and Figure 3). The high surface CeO_2 and $Ce_{0.5}Zr_{0.5}O_2$(Figure 3) were somewhat more difficult to analyze because of the small size of the support particles and the extensive charging effects in the electron beam. These exhibited a high coverage of uniformly distributed of evenly sized Ru nanoparticles. The vast majority of the tested substrates showed a homogeneous size distribution of the deposited RuO_x, the exception being the $Na_2Ti_6O_{13}$-NTs(Figure 2) which were only sparsely covered with RuO_x particles. Only in the smallest nanotube bundles could some RuO_x particles be distinguished. These seemingly coated both the inside and outside of the nanotubes with 0.5-1 nm RuO_x particles. We speculate that the low coverage was due to the high surface area of this support. Finally, RuO_x deposition on the Al_2O_3(Figure 2) was nearly identical, to that of the deposits on the spinel support, in terms of particle size and dispersion.

The above size distributions are tentatively determined from several representative STEM images and are listed in Table 1. Generally, the size distributions are seen to be quite narrow and of similar sizes, ensuring that the different supports could be directly compared. Table 1 also show a list of the catalysts prepared and some of the measured properties.

From Table 1 it is seen that the loading of each sample as measured locally by EDX and in the bulk by XRF differs significantly. Comparing these two results could serve to investigate the homogeneity of the sample at the nanoscale, *i.e.* if the two differ it was a sign that the sample was not

Table 1: Physical properties of the catalysts compared in this work. Catalysts marked with an $*$ in the table, showed a carbon mass balance of less than one, indicating complete oxidation to CO_2.

Name/Support	Ru loading [wt.%] XRF	Ru loading [wt.%] STEM-EDX[2]	BET surface area m^2/g	Ru particle size [1] nm
RuO_x/TiO_2 *	4.9	???	54	???
RuO_x/HT [3]	1.5	0.6	5	0.5-1.5
RuO_x/spinel *	1.5	3.2	89	0.5-1.0
$RuO_x/Na_2Ti_6O_{13}$-NTs *	1.5	1.9	214	0.8
RuO_x/ZnO *	1.3	1.1	9	???
RuO_x/γ-Al_2O_3	1.6	0.4	151	0.6-1.5
RuO_x/WO_3 *	1.3	5.8	2	0.8-1.0
RuO_x/CeO_2	0.9	3.3	62	0.5
RuO_x/CeO_2	1.8	1.9	58	0.5-1.2
RuO_x/CeO_2	3.4	3.8	60	0.6-0.8
RuO_x/hisuCeO_2	2.3	3.8	122	0.8-1.5
$RuO_x/Ce_{0.5}Zr_{0.5}O_2$	0.9	5.2	127	1.0-1.5

completely homogeneously coated. From the variations in concentration between EDX and XRF in Table 1 it was concluded that RuO_x supported on HT, spinel, WO_3, high surface area CeO_2, and $Ce_{0.5}Zr_{0.5}O_2$ were quite inhomogeneously coated with RuO_x. As stated above the STEM images showed that $Na_2Ti_6O_{13}$-NTs too was inhomogeneously coated with RuO_x. However, some variation between different areas of EDX is normally observed, indicating that such inhomogeneities is not uncommon. The inhomogeneity was speculated to be due to a difference in the coverage of dopamine - meaning that if a more complete dopamine coverage could be obtained for all samples the homogeneity would increase dramatically. The dopamine molecule was previously demonstrated to be a key participant in the RuO_x deposition mechanism.[28] It was also highly likely that the dispersion of the support powders by the gas stream affected the loading, so that if the powder was not flowing completely freely an inhomogeneous coating would result. In the present work it was chosen to adjust the Ru:CH_3CH_2OH ratio to 0.3 mol% for all catalysts in the subsequent experiments to eliminate this variation and allow for the direct comparison between the different supports.

In Figure 4 the various catalysts from Table 1 are compared on the basis of the CH_3CHO yield after 3 h of reaction. Most of the catalysts were stable under the employed conditions, with the exception being ZnO which formed an unidentifiable foam during the reaction. We expect that this by-product was likely the product of the amphoteric ZnO with the CH_3COOH; as indicated by the carbon balance being lower than one. The catalyst materials indicated by * in Table 1 showed a

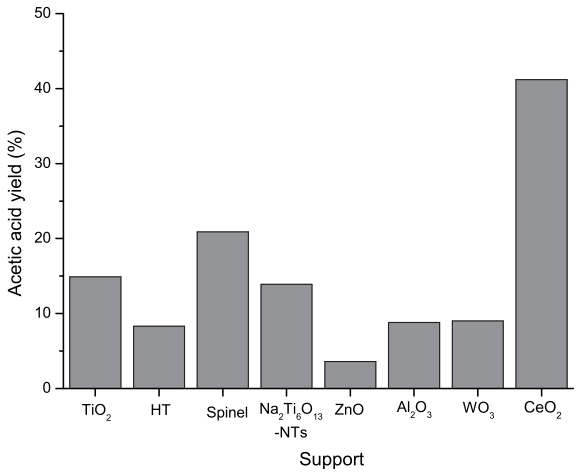

Figure 4: Yields of CH_3COOH in the aerobic oxidation reaction of CH_3CH_2OH with supported RuO_xcatalysts (5 wt% aqueous CH_3CH_2OH solution, 10 bar O_2, 150°C, ca. 0.3 mol% Ru to CH_3CH_2OH, and 3 h of reaction time).

mass balance of carbon less than one indicating the full oxidation of CH_3CH_2OH to CO_2. The mass balance varied between 30 and 40 % for the indicated samples. However, verification of the full oxidation to CO_2 could not be verified by the HPLC analysis. As the reaction mixtures were filtered before being analysed any coke formation (or other insoluble product) which could also have contribute to the deviation in the mass balance would not be detected either. Generally, it may be seen from Figure 4 that the TiO_2, Spinel, and CeO_2 catalysts gave the best performance. The optimal performance of CeO_2 was in line with what was observed in literature[26] for similar conditions; hence, the remainder of this work focused on the origin of the superior activity and selectivity towards CH_3COOH of RuO_x on CeO_2. It is speculated that the CeO_2 support showed a superior catalytic activity due the redox activity of Ce^{3+}/Ce^{4+}.

In Figure 5 the time-resolved plot is shown for the reaction with the RuO_x/CeO_2 catalyst. This figure shows that as the substrate was converted, the amount of CH_3CHO increased together with the CH_3COOH yield. This was expected, as it was previously demonstrated, *e.g.* for Au on TiO_2 that the oxidation of alcohols was much more difficult than the oxidation of aldehydes;[12,33,34] hence as the CH_3CHO is produced it is rapidly converted to CH_3COOH. After approximately 2.5 hours the yield of CH_3CHO remained almost constant in time, resembling a steady state-like situ-

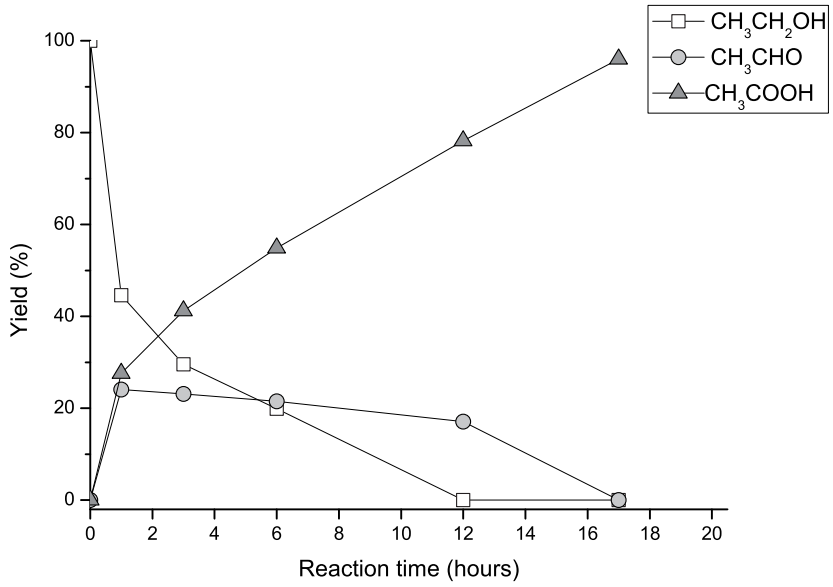

Figure 5: Yield of CH_3COOH in the aerobic oxidation reaction of CH_3CH_2OH with 1.8 wt% RuO_x/CeO_2 catalyst in water (5 wt% aqueous CH_3CH_2OH solution, 10 bar O_2, 150°C, ca. 0.3 mol% Ru to CH_3CH_2OH).

ation. After 12 hours, when all the CH_3CH_2OH was converted, the amount of CH_3CHO decreased gradually as the conversion from CH_3CH_2OH to CH_3COOH was completed after about 18 hours. This is in contrast to what was observed previously for RuO_2 on SiO_2 and SnO_2 supports,[32] where the conversion to CH_3COOH did not occur. Likely the difference in reaction conditions were at least partly responsible for this difference, *i.e.* 0.02-0.5 bar and 100°C versus 10 bar and 150°C. Other factors that could affect the selectivity include the particle size, RuO_x valence state, level of hydration, and crystallinity - these factors were investigated in the following. Liu et al.[32] find that an optimum in particle size must exist (which they determine as a dispersion of 3.5 Ru atoms/nm^2) just as is the case for the aerobic oxidation using Au, where an optimal performance was observed at particle sizes less than 10 nm.[35–37] To get an understanding of the effect of particle size in the RuO_x/CeO_2 system, the RuO_x loading was increased on the CeO_2 support which would normally lead to an increase in particle size. This was achieved by varying the amount of Ru-precursor reacted with the support, loadings of 0.9 wt%, 1.8 wt%, and 3.4 wt% Ru, respectively were obtained. In Figure 6 the effect on the conversion and yield of CH_3COOH is shown for the three different

loadings.

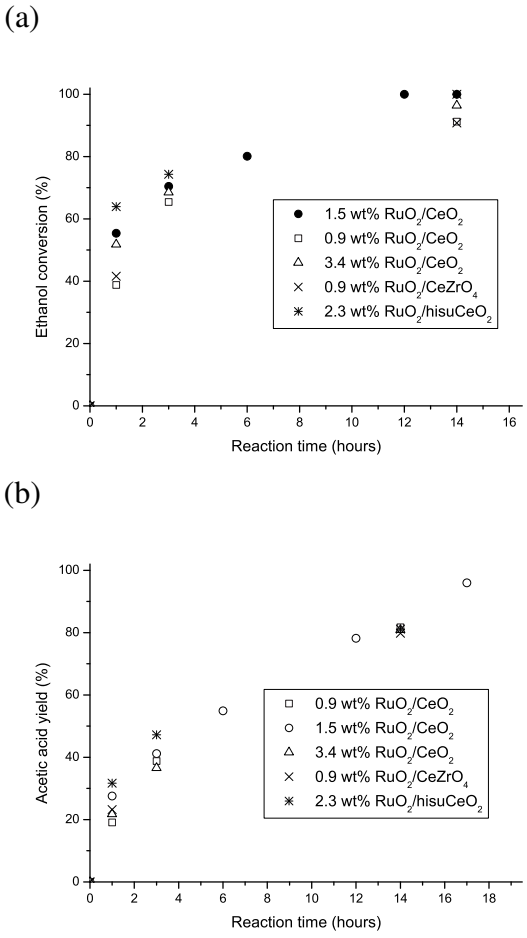

Figure 6: (a) The conversion of CH_3CH_2OH and (b) the yield of CH_3COOH in the aerobic oxidation reaction of CH_3CH_2OH with supported RuO_x catalysts (5 wt% aqueous CH_3CH_2OH solution, 10 bar O_2, 150°C, ca. 0.3 mol% Ru to CH_3CH_2OH). The missing points at intermediate times were ommitted due to time constraints.

From Figure 6 it is seen that, within the experimental uncertainty there was no difference in catalytic activity with the variation in loading. As the experiments are normalized to the Ru content (ca. 0.3 mol%Ru to CH_3CH_2OH), the similar efficiency was interpreted as an indication that the RuO_x particles were the same size and morphology. From the STEM images shown in Figure 2 and Figure 3, and summarized in Table 1, it was clearly seen that the particle size in fact did not vary significantly with the loading.

This was in contrast to what has usually been observed for catalysts prepared by impregnation, where particle size most often increases with loading. Thus, this deposition method lack the nor-

mal loading-size dependence which is a clear advantage. The usual way to get high loadings and small nanoparticles is to use a high surface area support, which is often difficult to make and thus expensive. In the synthesis strategy employed here, a regular surface area support could potentially reach just as high loadings while keeping the small nanoparticle size. If a high surface area support is economically feasible an even higher loading could then be achieved with the same small nanoparticle size. This property is a good feature for a potential industrial process where a higher loading means a more compact catalyst bed and correspondingly smaller equipment. To test this hypothesis further, a sample was made on a high surface area CeO_2 (RuO_x/hisuCeO_2). The surface area of the support was 122 m^2/g compared to 60 m^2/g for the regular CeO_2, and the obtained loading of the catalyst was 2.3 wt%. In Figure 6 the CH_3CH_2OH conversion and CH_3COOH yield obtained using the RuO_x/hisuCeO_2 are compared to those catalysts made with the regular CeO_2; but no significant difference in catalytic activity was seen. The experiments were conducted so that if the active particles are the same size and shape for both the regular and high surface area supports no difference would be observed as the amount of catalyst used was normalized to amount of RuO_x, which was exactly what was seen. This enforced the idea that this deposition method was indeed very suited for obtaining high loadings of small nanoparticles nanoparticles, independent of the surface area of the support. The slightly higher yield of CH_3COOH after 1 and 3 h of the high surface area compared to the regular CeO_2 catalyst may be ascribed to the difference in dispersion of the catalyst in the solution, *i.e.* differences in mass transport to the catalyst or simply measurement inaccuracies. This differrence disappears at longer reaction times, as would be expected if it was caused by diffusion limitations.

It should be noted that the time to reach full conversion for all catalysts described here was slightly longer than what was observed in literature for catalysts made by incipient wetness impregnation with 1.2 wt% loading; but slightly faster than that with 2.4 wt% loading(normalized to the amount of Ru).[26] This was likely due to either the difference in particle size, or valence state (which was not determined for the incipient wetness impregnated catalysts), the level of hydration, or the nanoparticle crystallinity.

The particle size observed for the incipient wetness impregnation was around 0.6-2 nm for the most active samples and 0.8-3.5 nm for the sample with comparable activity to that observed in this work.[26] Under the assumption that the difference in activity for the aerobic oxidation was attributed only to a size effect, the results presented here indicate that if the particle size was reduced to 0.5-1.5 nm the activity was reduced. This suggested a size-optimum somewhere between 0.5-3.5 nm however due to the width of the RuO_x size-distributions it was impossible to attribute the effect to size alone. In addition, the exact valence state, the level of hydration and crystallinity of the RuO_x was not determined for the incipient wetness deposited samples presented in literature,[26] and these factors could have significant effects. Further studies with well-controlled narrow size-distributions, crystallinity and hydration are needed to determine how these parameters affect the catalyst activity.

In this study it was observed that CeO_2 was by far the best support material for RuO_x. This was in accordance with what was observed in literature when comparing incipient wetness impregnated $Ru(OH)_x$ on CeO_2, spinel, and HT.[26] It is known from studies of the three-way catalysts that CeO_2 mixed with ZrO_2 supports have improved oxygen storage properties,[38,39] *i.e.* facilitates the oxidation of Ce to Ce^{3+} to occur at lower temperatures. Hence it was speculated that the redox active Ce^{3+}/Ce^{4+} properties of CeO_2 could be responsible for the increased acitivity of CeO_2 observed here for the oxidation of CH_3CH_2OH. To elucidate this RuO_x was loaded onto a mixed ZrO_2 and CeO_2 support, $Ce_{0.5}Zr_{0.5}O_2$ (50 mole % ZrO_2). This support composition is known from literature to allow the reversible reduction of CeO_2, for this type of oxide alloy, at the lowest reaction temperature.[38,39] Figure 6 show the results from the $RuO_x/Ce_{0.5}Zr_{0.5}O_2$ catalyst compared to the other CeO_2 supported catalysts. No positive effect was achieved by using the mixed oxide as support. Hence, we must tentatively conclude that the reduced temperature for oxidation/reduction was not the right descriptor to explain the increased activity of CeO_2. However, *in situ* spectroscopy techniques are needed to rule out the involvement of Ce^{3+}/Ce^{4+} in the reaction mechanism or more relevantly its involvement in the rate determining step.

To investigate the effect of dehydration a heat-treatment study on the RuO_x/CeO_2 catalyst was

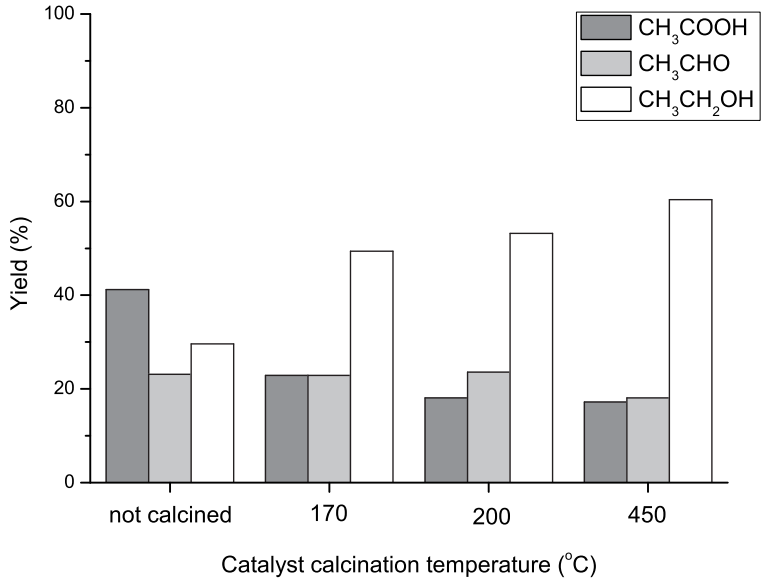

Figure 7: CH_3CH_2OH, CH_3CH_2HO, and CH_3COOH yields in the aerobic oxidation of CH_3CH_2OH with heat-treated 1.5 wt% RuO_2/CeO_2 catalysts (5 wt% aqueous CH_3CH_2OH solution, 10 bar O_2, 150°C, ca. 0.3 mol% Ru to CH_3CH_2OH, and 3 hours of reaction time).

conducted. In Figure 7 the effect on activity of the catalyst by heat-treatments at 170°C, 200°C, and 450°C are compared to the uncalcined sample. As the temperature was increased the yield of CH_3COOH, and CH_3CHO drops significantly, compared to the untreated sample. From our previous study[28] of the heat-treatment effect on RuO_x on TiO_2, above 250°C, it is know that this leads to a reduction of the Ru from a mixed oxide of Ru^{6+} and Ru^{3+} or hydrated Ru^{4+} into a mixed oxide of dehydrated RuO_2 and Ru^{3+} or hydrated Ru^{4+} (the XPS data did not allow for the distinction between Ru^{3+} and hydrated Ru^{4+}). This reduction was also accompanied by sintering into larger particles, as determined by TEM (data not shown). From literature it is known that reducing the amount of Ru^{6+},[30] and hydrated Ru^{4+}[31] decreases the oxidative dehydrogenation activity of CH_3OH. The results in Figure 7 suggests that the oxidation of CH_3CH_2OH to CH_3COOH also occurs much more readily on the mixed oxide containing: the Ru^{6+} and the hydrated Ru^{4+}. In the study by Gorbanev et al.[26] all the tested materials were heat-treated at 170°C before testing; further heating decreased the activity, likely due the dehydration described above. Deactivation through the simultaneous sintering could also have contributed to the loss in activity. The selective

oxidative dehydrogenation to CH_3CHO was not observed opposed to the case of crystalline RuO_2 on SnO_2.[32] From the observations in this study, we speculate that an optimal catalyst for the full and selective aerobic oxidation of CH_3CH_2OH to CH_3COOH, must consist of Ru oxide supported on CeO_2 having a high amount of the Ru^{6+} valence state and with a catalyst particle size between 0.5-3.5 nm supported on CeO_2. A higher loading of the active Ru^{6+} could potentially be achieved by increasing the degree of dopamine grafting onto the CeO_2 support.

Conclusions

In summary, we have demonstrated that the novel gas-phase synthesis for conformally coating Ru-oxide nanoparticles onto various metal oxides produced active catalysts for the selective aerobic oxidation of CH_3CH_2OH to CH_3COOH. Particles were deposited on P25 TiO_2, hydrotalcite (HT, $Mg_6Al_2(CO_3)(OH)_{16} \cdot 4\,H_2O$), spinel ($MgAl_2O_4$), sodium titanate nanotubes ($Na_2Ti_6O_{13}$-NTs), ZnO, γ-Al_2O_3 , WO_3, CeO_2 and $Ce_{0.5}Zr_{0.5}O_2$ mixed oxide supports. Of these, the CeO_2 yielded the most active catalyst, followed by the spinel, TiO_2, $Na_2Ti_6O_{13}$-NTs, γ-.Al2O3, WO_3, HT, and ZnO. To gain insight into the support influence we investigated the effect of a CeO_2 and ZrO_2 mixed oxide support. This mixed oxide is known to have increased redox activity in three-way catalysts but did not have any promoting effect on the present reaction. On this basis, it was concluded that the improved activity of CeO_2 supported RuO_x was not influenced by the increased redox activity of $Ce_{1-x}ZrxO_2$. By examining the effect of heat-treatment of the catalyst it was found that the performance of the active CeO_2 supported catalyst towards CH_3COOH decreased significantly as the calcination temperature was increased and the yield of CH_3CHO followed the same trend. We interpreted this as an effect of the decreased Ru valence state, and hydration level in the as-deposited Ru-oxide due to the heat-treatment. Most importantly, we have demonstrated that the loading of RuO_x, when deposited by this gas phase reaction did not effect the catalytic activity when normalized to the RuO_x content. This showed that the nanoparticles deposited by this synthesis is equally active on CeO_2 supports irrespectively of the support porosity and catalyst

loading. Hence, this type of catalyst may be produced with a very high loading allowing for the use of less catalyst material in a potential process, which could substancially decrease the overall size of an industrial reactor.

Acknowledgement

We gratefully acknowledge the assistance of Bodil Holten, CSC, with the BET measurements. This work was founded in part through the Catalysis for Sustainable Energy (CASE) research initiative, which is funded by the Danish Ministry of Science, Technology and Innovation. Center for Individual Nanoparticle Functionality is funded by The Danish National Research Foundation. A.K.S would like to thank the support from the Hans Christian Ørsted fellowship. The A. P. Møller and Chastine Mc-Kinney Møller Foundation is gratefully acknowledged for their contribution towards the establishment of the Center for Electron Nanoscopy at the Technical University of Denmark.

References

[1] Lancaster, M.; of Chemistry (Great Britain), R. S. *Green chemistry: an introductory text*; Royal Society of Chemistry paperbacks; Royal Society of Chemistry, 2002.

[2] Wagner, F. S. *Kirk-Othmer Encyclopedia of Chemical Technology*; John Wiley & Sons, Inc., 2000.

[3] Simpson, T. W.; Sharpley, A. N.; Howarth, R. W.; Paerl, H. W.; Mankin, K. R. *J. Environ. Qual.* **2006**, *37*, 318–324.

[4] Rass-Hansen, J.; Falsig, H.; Jørgensen, B.; Christensen, C. H. *J. Chem. Technol. Biot.* **2007**, *82*, 329–333.

[5] Bozell, J. J.; Petersen, G. R. *Green Chem.* **2010**, *12*, 539–554.

[6] Boisen, A.; Christensen, T. B.; Fu, W.; Gorbanev, Y. Y.; Hansen, T. S.; Jensen, J. S.; Klit-

gaard, S. K.; Pedersen, S.; Riisager, A.; Ståhlberg, T.; Woodley, J. M. *Chem. Eng. Res. Des.* **2009**, *87*, 1318–1327.

[7] Moreau, C.; Belgacem, M. N.; Gandini, A. *Top. Catal.* **2004**, *27*, 11–30.

[8] Gorbanev, Y. Y.; Klitgaard, S. K.; Woodley, J. M.; Christensen, C. H.; Riisager, A. *ChemSusChem* **2009**, *2*, 672–675.

[9] Mallat, T.; Baiker, A. *Chem. Rev.* **2004**, *104*, 3037–3058.

[10] ten Brink, G.-J.; Arends, I. W. C. E.; Sheldon, R. A. *Science* **2000**, *287*, 1636–1639.

[11] Christensen, C. H.; Jørgensen, B.; Rass-Hansen, J.; Egeblad, K.; Madsen, R.; Klitgaard, S. K.; Hansen, S. M.; Hansen, M. R.; Andersen, H. C.; Riisager, A. *Angew. Chem. Int. Ed.* **2006**, *45*, 4648.

[12] Marsden, C.; Taarning, E.; Hansen, D.; Johansen, L.; Klitgaard, S. K.; Egeblad, K.; Christensen, C. H. *Green Chem.* **2008**, *10*, 168–170.

[13] Kegnæs, S.; Mielby, J.; Mentzel, U. V.; Christensen, C. H.; Riisager, A. *Green Chem.* **2010**, *12*, 1437–1441.

[14] Vinke, P.; van der Poel, W.; van Bekkum, H. *Stud. Surf. Sci. Catal.* **1991**, *59*, 385–394.

[15] Jørgensen, B.; Egholm, S.; Thomsen, M. L.; Christensen, C. H. *J. Catal.* **2007**, *251*, 332–337.

[16] K´ockritz, A.; Sebek, M.; Dittmar, A.; Radnik, J.; Br´uckner, A.; Bentrup, U.; Pohl, M.-M.; Hugl, H.; M´agerlein, W. *J. Mol. Catal. A: Chem.* **2006**, *246*, 85–99.

[17] Trasatti, S. *Croa. Chem. Acta* **1990**, *63*, 313–329.

[18] Klerke, A.; Klitgaard, S. K.; Fehrmann, R. *Catal. Lett.* **2009**, *130*, 541–546.

[19] Schwab, P.; Grubbs, R. H.; Ziller, J. W. *J. Am. Chem. Soc.* **1996**, *118*, 100–110.

[20] Rovik, K.; Klitgaard, S. K.; Dahl, S.; Christensen, C. H.; Chorkendorff, I. *Appl. Catal. A* **2009**, *358*, 269–278.

[21] Pagliaro, M.; Campestrini, S.; Ciriminna, R. *Chem. Soc. Rev.* **2005**, *34*, 837–845.

[22] Ji, H.-B.; K. Ebitani, K.; Mizugaki, T.; Kaneda, K. *Catal. Commun.* **2002**, *3*, 511–517.

[23] Mori, K.; Kanai, S.; Hara, T.; Mizugaki, T.; Ebitani, K.; Jitsukawa, K.; Kaneda, K. *Chem. Mater.* **2007**, *19*, 1249–1256.

[24] Nikaidou, F.; Ushiyama, H.; Yamaguchi, K.; Yamashita, K.; Mizuno, N. *J. Phys. Chem. C* **2010**, *114*, 10873–10880.

[25] Mizuno, N.; Yamaguchi, K. *Catal. Today* **2008**, *132*, 18–26.

[26] Gorbanev, Y. Y.; Kegnæs, S.; Hanning, C. W.; Hansen, T. W.; Riisager, A. *submitted for publication* **2011**,

[27] Gorbanev, Y. Y.; Kegnæs, S.; Riisager, A. *Top. Catal* **2011**, *xx*, xx–xx.

[28] Kleiman-Shwarsctein, A.; Laursen, A. B.; Cavalca, F.; Tang, W.; Dahl, S.; Chorkendorff, I. *submitted for publication* **2011**,

[29] Miao, L.; Ina, Y.; Tanemura, S.; Jiang, T.; Tanemura, M.; Kaneko, K.; Toh, S.; Mori, Y. *Surface Science* **2007**, *601*, 2792–2799, International Conference on NANO-Structures Self-Assembling, International Conference on NANO-Structures Self-Assembling.

[30] Li, W.; Liu, H.; Iglesia, E. *J. Phys. Chem. B* **2006**, *110*, 23337–23342, PMID: 17107184.

[31] Yu, H.; Zeng, K.; Fu, X.; Zhang, Y.; Peng, F.; Wang, H.; Yang, J. *J. Phys. Chem. C* **2008**, *112*, 11875–11880.

[32] Liu, H.; Iglesia, E. *J. Phys. Chem. B* **2005**, *109*, 2155–2163, PMID: 16851207.

[33] Tojo, G.; Fernández, M. I. *Oxidation of Primary Alcohols to Carboxylic Acids*; Springer, New York, 2007.

[34] Tojo, G.; Fernández, M. I. *Oxidation of Alcohols to Aldehydes and Ketones*; Springer, New York, 2006.

[35] Haruta, M. *Chem. Rec.* **2003**, *3*, 75–87.

[36] Wolf, A.; Schüth, F. *Appl. Catal. A* **2002**, *226*, 1–13.

[37] Haider, P.; Kimmerle, B.; Krumeich, F.; Kleist, W.; Grunwaldt, J.-D.; Baiker, A. *Catal. Lett.* **2008**, *125*, 169–176.

[38] Monte, R. D.; Kašpar, J. *J. Mater. Chem.* **2005**, *15*, 633–648.

[39] Sugiura, M.; Ozawa, M.; Suda, A.; Suzuki, T.; Kanazawa, T. *Bull. Chem. Soc. Jpn.* **2005**, *78*, 752–767.